Faculty of Natural Science and Technology
Department of Physics

MASTER'S THESIS FOR

STUD. TECHN. KIRSTI KVANES

Thesis started: [01.19.2009]
Thesis submitted: [06.19.2009]

DISCIPLINE: APPLIED PHYSICS

Norsk tittel: *"Modellering av mellombåndsolceller"*

English title: *"Modeling of intermediate band solar cells"*

This work has been carried out at the Department of Physics, Faculty of Natural Sciences and Technology, Norwegian University of Science and Technology, Norway, under the supervision of Turid Worren Reenass.

Trondheim, June 19,2009

Turid Worren Reenaas

Responsible supervisor

Associate Professor at Department of Physics

Preface

This master thesis is written in the spring of 2009 as the tenth semester of the Master of Science degree in Applied Physics at the Norwegian University of Science and Technology, Trondheim. My supervisor has been Turid Worren Reenaas at the Department of Physics.

The objective for the master thesis was to develop a computer program in MATLAB to model intermediate band solar cells. In autumn 2008 a computer program used to model quantum well solar cells was developed as part of a project work. Some of the source code from MATLAB is used again in this master thesis. The theory of standard solar cells presented in section 2.1-2.5 is very similar to the theory presented in the project work, but is included here for completeness. Also some of the material parameters given in section 6.1 and 6.2 are similar to the ones used in the project work.

I would like to thank my supervisor Turid Worren Reenaas for many good advices and ideas throughout the semester and for reading through my master thesis several times. This has meant a lot. I would like to thank Antonio Martí at Universidad Politécnica de Madrid for helpfully answering my questions. I would also like to thank my brother Øyvind Kvanes and my parents Anna Torbjørg and Arvid Dan Kvanes for reading through my thesis. Finally I would like to thank Trine Mustorp Degnes for helping with graphics.

Abstract

To increase the efficiency beyond the theoretical limit for a single-junction solar cell the intermediate band solar cell is proposed. The intermediate band solar cell is made of a semiconductor with an intermediate band placed in the band gap between the conduction and valence band. This means that absorption of photons with energy below the band gap of the semiconductor is possible, and the photocurrent is thus increased. When the carrier concentrations in all three bands are described by their own quasi-Fermi level the intermediate band does not affect the voltage if carriers are extracted from the conduction band and the valence band. An increase of efficiency is therefore possible.

In this thesis a model of a single band gap reference p-i-n solar cell with anti-reflective coating, window, p^+-, p-, i-, n- and n^+-layers is presented along with a model of an intermediate band solar cell. The model of the intermediate band solar cell contains the same layers as the reference cell, but with the i-layer now having an intermediate energy band in the band gap. The intermediate band can be created by introducing quantum dots to the i-layer. The quantum dots should be placed in a flat band region to obtain a partially filled the intermediate band. If they are in a depleted region with an electric field all dots above the Fermi level will be empty and all below will be filled. Partial filling is needed so that both the transition of electrons from the valence band to the intermediate band and the transition from the intermediate band to the conduction band are possible at the same time. Existing models of p-i-n solar cells with no intermediate band only describes the behavior with a fully depleted i-layer since this is expected to give the highest efficiency. The i-layer is introduced to increase the width of the depleted layer where the carrier separation takes place. The quantum dots should be placed in a flat band region. A new model of a reference cell with a flat band i-layer is therefore developed in this thesis. This model is then extended to include the case of having an intermediate band material in the flat band region. Both radiative and non-radiative recombination are included in the model of the intermediate band solar cell.

The solar cells used in the modeling are made of GaAs or $Al_xGa_{1-x}As$ with InAs quantum dots embedded. The numerical results from the modeling show that the intermediate band solar cell has higher efficiency than the reference cell when only radiative recombination is included in the intermediate band material. By including non-radiative recombination and using numerical values for non-radiative lifetimes for InAs/GaAs quantum dot intermediate band solar cell samples, the reference cell is better than the quantum dot cell. These quantum dot solar cell samples are, however, known to be full of defects from the fabrication process. Also the quantum dot density is too low to form a real energy band. It is expected that fabrication of samples with few or no defects and with high enough quantum dot density will yield quantum dot intermediate band solar cells that are more efficient than the reference cell.

The models are used to obtain the current-voltage characteristics of samples made at the University of Glasgow and are compared with experimental data. The comparison shows that the models give too large values of both photocurrent and voltage. One reason for this is thought to be band gap narrowing in the heavily doped layers and that some reflection losses appear which is not included in the model. Another reason is the low density of the quantum dots used meaning that a real energy band is not formed.

Sammendrag

Mellombåndsolceller er et alternativ for å oppnå en høyere effektivitet enn det er teoretisk mulig å oppnå for solceller som kun benytter ett båndgap. En mellombåndsolcelle er laget av en halvleder som har et ekstra energibånd, kalt mellombånd, liggende i båndgapet mellom valensbåndet og ledningsbåndet. Mellombåndet gjør at det er mulig å absorbere fotoner med energi mindre enn båndgapet til halvlederen, og fotostrømmen øker. Når ladningskonsentrasjonene i de tre båndene kan beskrives med hvert sitt Ferminivå, vil ikke spenningen over solcellen reduseres så lenge kun ladninger fra valensbåndet og ledningsbåndet bidrar til solcellestrømmen. En økning i effektivitet er derfor mulig å oppnå ved bruk av mellombåndsolceller.

I denne masteroppgaven utvikles det en modell for en p-i-n referansecelle uten mellombånd. Referansecellen består av et anti-reflekterende lag, et vinduslag og p^+-, p-, i-, n- og n^+ lag. I tillegg presenteres en modell av en mellombåndsolcelle som består av de samme lagene som referansecellen, men hvor i-laget nå har et mellombånd i båndgapet. Mellombåndet kan dannes ved å introdusere kvanteprikker i i-laget. Kvanteprikkene må plasseres i et område uten elektrisk felt (dvs. med flate båndkanter) for å oppnå en delvis fylling av mellombåndet. Hvis de er i et deplesjonsområde med et elektrisk felt i en pn-overgang, vil alle kvanteprikkene over Ferminivået være tomme og de under Ferminivået vil være fylte. Delvis fylling er nødvendig for at elektronoverganger både til og fra mellombåndet kan skje på samme tid.

Eksisterende modeller av p-i-n solceller uten mellombånd beskriver kun oppførselen man får ved at hele i-laget ligger i deplesjonsområdet. Dette gir nemlig høyest effektivitet for slike solceller uten mellombånd. I-laget er da introdusert for å øke utbredelsen av deplesjonsområdet hvor landingsseppareringen finner sted.

Mellombåndsolceller er foreslått realisert ved bruk av kvanteprikker med mindre båndgap enn resten av solcellen. Denne forskjellen i båndgap, sammen med dimensjonene av kvanteprikkene vil gi opphav til (minst) ett mellombånd i materialer kvanteprikkene er introdusert i. For at kvanteprikkene skal gi et delvis fylt mellombånd, må de plasseres i et område med flate bånd. En ny modell for en p-i-n referansecelle med et flatt båndområde er derfor utviklet i denne oppgaven. Denne modellen utvides så til å inkludere tilfellet hvor vi har et mellombånd i flatt båndområdet. Både rekombinering ved stråling og rekombinering uten stråling er inkludert i modellen av mellombåndssolcellen. Strålingsrekombinering er uunngåelig, mens man i perfekte materialer skal kunne eliminere rekombinering uten stråling.

De modellerte solcellene er laget av InAs kvanteprikker plassert i GaAs eller $Al_xGa_{1-x}As$. De numeriske resultatene fra modelleringen viser at mellombåndssolcellen har en høyere effektivitet enn referansecellen når kun strålingsrekombinering er inkludert i mellombåndmaterialet. Ved å inkludere rekombinering uten stråling og bruke numeriske

(ideelle og målte) verdier for InAs/GaAs kvanteprikksolcelleprøver funnet i litteraturen, gir referansecellen høyere effektivitet enn mellombåndsolcellen. Disse kvanteprikksolcelleprøvene inneholder imidlertid defekter fra framstillingen og i tillegg er kvanteprikktettheten for lav til at et reelt energibånd dannes. Det er forventet at fabrikasjon av prøver med få eller ingen defekter og med en høy kvanteprikktetthet vil gi kvanteprikksolceller som har høyere effektivitet enn referansecellen.

De utviklede modellene blir brukt til å finne strøm-spenning karakteristikken til prøver laget ved Universitet i Glasgow. Resultatene fra modellene er sammenlignet med eksperimentelle data funnet i litteraturen- Sammenligningen viser at modellene gir for høye verdier for både fotostrøm og åpen-kretsspenning. En årsak til dette kan være båndgapkrymping i de høyt dopede lagene og noe refleksjonstap som ikke er inkludert i modellen. En annen årsak er den lave kvanteprikktettheten som betyr at et reelt energibånd ikke blir dannet dannet, og dette gjør at rekombinering uten stråling vil dominere.

Contents

1 Introduction **1**

2 The standard solar cell **3**
2.1 Carrier concentrations 4
2.2 Generation and recombination 5
2.3 The p-n junction 10
2.4 The p-n junction under bias and illumination 11
2.5 Current and voltage behavior for a solar cell 16
2.6 Detailed balance of a standard solar cell 19

3 Increasing the efficiency **21**
3.1 Strategies to increase the efficiency 21
3.2 Working principle for the intermediate band solar cell 23
3.3 The quantum dot based intermediate band solar cell 25
3.4 Detailed balance of the intermediate band solar cell 28

4 Model of the p-i-n reference cell **31**
4.1 Model of a reference cell with a depleted i-layer 32
4.1.1 Anti-reflective coating 32
4.1.2 i-layer 32
4.1.3 Front surface field 33
4.1.4 Window layer 36
4.1.5 Back surface field 36
4.1.6 Total current for a p-i-n reference cell with a depleted i-layer . . . 38
4.2 Model of a reference cell with a flat band i-layer 39

5 Model of the intermediate band solar cell **45**
5.1 Intermediate band solar cell design 45
5.2 Intermediate band solar cell with only radiative recombination in the flat band region 46
5.3 Modeled cases 51
5.4 Intermediate band solar cell including both radiative and non-radiative recombination in the flat band region 52

6 Material and sample parameters **55**
6.1 Material parameters 55
6.1.1 Band structure and effective density of states 55

6.1.2 Absorption coefficient and reflectivity 57
6.1.3 Mobilities, lifetimes and surface recombination velocities 60
6.2 Solar spectrum 67
6.3 Sample parameters 68

7 Numerical results and discussion 71
7.1 The simple p-i-n reference cell 72
7.1.1 The effect of varying the mobility 72
7.1.2 The effect of varying the lifetimes in the doped layers 75
7.1.3 The effect of varying the surface recombination velocities 78
7.1.4 The effect of varying the non-radiative lifetimes in the intrinsic region 80
7.1.5 Summary and discussion of the parameters in the model of the simple p-i-n solar cell 81
7.2 Complete reference cells 82
7.3 The simple model of the IB solar cell 90
7.3.1 Check of the simple model program 90
7.3.2 Black-body spectrum versus AM 1.5 spectrum 92
7.3.3 Mobility, effective density of states and absorption coefficient . . . 93
7.3.4 Variation of band gap 95
7.3.5 InAs/GaAs IB solar cells 96
7.4 The complete model of the IB solar cell 107
7.4.1 InAs/GaAs quantum dot intermediate band solar cell, X=1, fixed E_H and w_{IB} 107
7.4.2 InAs/GaAs quantum dot intermediate band solar cell, X=1000, fixed E_H and w_{IB} 111
7.4.3 Varying z_{IB} and E_H 112
7.5 Discussion of how to obtain an IB solar cell with high efficiency 123
7.6 Models used on real samples 123
7.6.1 Reference cell, sample A1677 124
7.6.2 Quantum dot intermediate band solar cell, sample A1681 126
7.7 $Al_{0.35}Ga_{0.65}As$ versus GaAs intermediate band solar cell 128
7.8 Discussion of the models 130
7.8.1 Reference cell 130
7.8.2 The simple model of the intermediate band solar cell 131
7.8.3 The complete model of the intermediate band solar cell 131

8 Summary and conclusion 133

9 Further work 135

Bibliography 137

A List of Symbols 141

B Source code from MATLAB **146**
B.1 Variables used for p-i-n reference cell with depleted i-layer 146
B.2 Photocurrent for p-i-n reference cell with depleted i-layer 154
B.3 Current-voltage characteristic p-i-n reference cell with depleted i-layer . . 181
B.4 Current-voltage characteristic p-i-n reference cell with undepleted i-layer . 185
B.5 Variables simple model of intermediate band solar cell 215
B.6 Radiative recombination coefficient in intermediate band solar cell 217
B.7 Current-voltage characteristic simple model of intermediate band solar cell 218
B.8 Variables complete model of intermediate band solar cell 232
B.9 Current-voltage characteristic complete model of intermediate band solar cell 244

Chapter 1

Introduction

The average worldwide power consumption was 1.6×10^{13} W in 2006 [1]. Every day the total solar radiation incident on earth at sea level is approximately 2×10^{17} W [2], which is over 12500 times the average worldwide power consumption in 2006. This shows the great potential solar energy has in supplying energy to the world. Solar cells are one way to utilize the energy of the sun.

Solar cells convert the incoming solar radiation into electricity by the photovoltaic effect discovered by Edmund Bequerel in 1839 [3]. In the 1950s after the development of the silicon electronic industry, solar cells with efficiencies over 5 % were made [3]. The applications of the cells were however limited due to the high costs of the cells. The energy crisis in the 1970s opened a new interest for research on solar cells, and many strategies to improve the efficiency were explored. Following the concern for global warming the interest in solar cells as an alternative to fossil fuels increased again in the 1990s, and the costs were also reduced. The photovoltaic power market expanded, and since 1998 installations of photovoltaic cells and modules have been growing at an average annual rate of more than 35 % [4].

In the competition between solar cells and other energy sources production cost and efficiency of the solar cells are important factors. The three generation of solar cells combine these factors in different ways. The first generation of solar cells is silicon wafer-based solar cells. Using the principle of detailed balance and assuming ideal solar cell properties one can calculate the theoretically maximum efficiency of Si equal to 27 % for 1 sun [5]. Production of crystalline wafers is expensive, and the second generation of solar cells is utilizing thin-film technology which reduces the material cost, but also lowers the efficiency [6]. The third generation of solar cells uses other concepts than the standard single junction solar cell of first and second generation photovoltaics in obtaining higher efficiencies than the theoretical maximum for a single-junction cell [5]. Sunlight can be converted to electricity at an efficiency close to 95 % [6]. Using third generation solar cells one can obtain efficiencies closer to this limit than possible with the first and second generation solar cells [6].

The strategies used in the third generation solar cells are [3]

1. Utilize more of the solar spectrum by increasing the number of band gaps; examples are tandem cells and intermediate band solar cells.

2. Increase the work per photon by utilizing some of the excess kinetic energy of the

photogenerated carriers before they relax; one example is hot carrier solar cells.

3. Increase the number of electron-hole pairs per photon,; one example is impact ionization solar cells.

In this thesis the intermediate band solar cell is studied. Intermediate band solar cells have a theoretical efficiency of 46.0 % using no concentration [7]. By having an intermediate band placed in the band gap of a single junction solar cell more of the photons from the sun are utilized which gives an increased photocurrent. When the carrier concentration in each of the bands can be described by their own quasi-Fermi level and carrers are extracted from the conduction band and valence band, the voltage of the cell is not reduced compared to a single junction solar cell made of the same material. The efficiency of an intermediate band solar cell may therefore be higher than the efficiency of a single junction standard solar cell.

One way of creating the intermediate band is through the use of quantum dots. This is a research topic at the Norwegian University of Science and Technology (NTNU). The quantum dot solar cells made at NTNU are made of InAs quantum dots in either GaAs or $Al_xGa_{1-x}As$. A computer program used in a modeling of these samples is useful. In this thesis models of both a single junction p-i-n reference cell and an intermediate band solar cell based on GaAs or $Al_xGa_{1-x}As$ are presented. The modeling is done using MATLAB.

Semiconductor theory is important in the understanding of solar cells and is given in chapter 2 along with a presentation of how the current-voltage characteristic of a standard p-n junction solar cell is derived. The theoretical expressions given here form the basis for the models presented in the rest of the thesis. Detailed balance calculations for the standard solar cell are also presented in this chapter.

In chapter 3 ways of improving the efficiency of solar cells are presented where the main emphasis is laid on the intermediate band solar cell. How quantum dots can be used to create an intermediate band is explained. Detailed balance calculations for the intermediate band solar cell are also presented in this chapter.

In chapter 4 a model of the single band gap p-i-n reference cell is presented. The reference cell consists of an anti-reflective coating and window, p^+-, p-, i- n- and n^+-layers. The function of each layer is described. Both a model of a solar cell with a fully depleted i-layer and a model of a solar cell with a flat band i-layer are presented. The models were developed combining theory from various sources and adjusting the expressions to the specific structure of the reference cell used in this thesis. Various models exist in literature for solar cells with fully depleted i-layers since this is commonly used in Si solar cells [3], but none was found for a flat band i-layer.

In chapter 4 two models of an intermediate band solar cell are presented. In the simple model, taken from literature, only contribution from the intermediate band material is taken into account. In the complete model, developed in this thesis, the contributions from all layers (anti-reflective coating, window-,p^+- ,p-, n and n^+-layer) are included.

The solar cells modeled are made of InAs, GaAs and $Al_xGa_{1-x}As$, and parameters for these materials necessary in the calculation of the current-voltage characteristic are given in chapter 6.

In chapter 7 results of the modeling of the solar cells are given along with a discussion of the results. A conclusion and summary are given in chapter 8, and proposals to further work are given in chapter 9. In the appendix the source code from MATLAB is given.

Chapter 2

The standard solar cell

Solar cells convert solar energy, in the form of electromagnetic radiation, into electrical energy. A standard solar cell is shown schematically in figure 2.1. Sunlight is incident on the surface covered by a metallic grid acting as an electrical contact. Between the grid lines photons are absorbed in a semiconductor which is covered by an anti-reflective coating to reduce reflection. Photons with energies larger than the band gap E_G of the semiconductor excite electrons from the valence band to the conduction band, resulting in free charge carriers; electrons and holes. The charge carriers are separated by either a gradient in the charge carrier density or an electric field. In figure 2.1 the charge carriers are separated by the electric field across the p-n junction and the electrons are transported through a load in the external circuit where they do work.

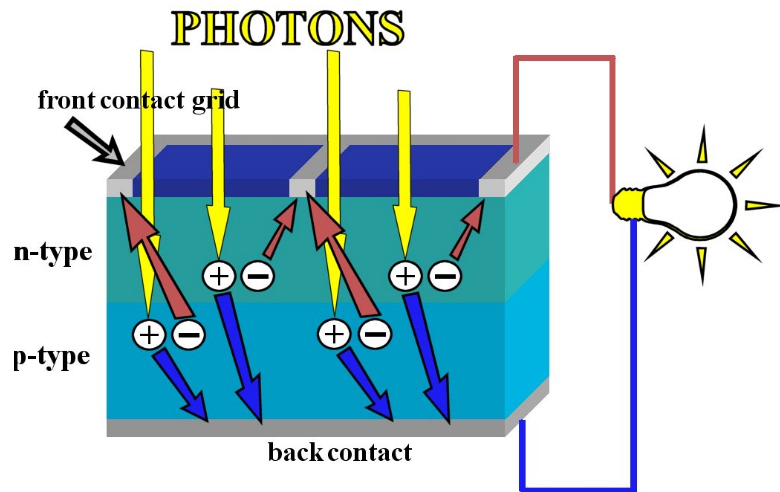

Figure 2.1: Structure of a standard solar cell shown schematically [8]. At the front surface there is a metallic grid (gray). Between the grid lines there is an anti-reflective layer (dark blue) covering a p-n junction (green/blue) made of a single semiconductor. The back surface of the cell is covered by a back contact (dark gray). Also shown is the external circuit where the electrons do work. The operation principle is described in the text.

Since solar cells are made of semiconductors, general properties dealing with semiconductors will be treated in section 2.1. Useful expressions for charge carrier concentrations will be presented, and the concept of Fermi levels will be introduced. In section 2.2 the

generation and recombination of charge carriers will be described. In a solar cell it is important to have high generation of free charge carriers and to have as low recombination as possible. Both unavoidable and avoidable recombination processes will be presented. The separation of photogenerated electrons and holes by the p-n junction is important to reduce recombination, and section 2.3 will explain how the p-n junction is formed and used to separate electrons and holes. A derivation of the current-voltage characteristic for solar cells under illumination will be presented in section 2.4, and important parameters describing the behavior of solar cells will be presented in section 2.5. The principle of detailed balance for a standard solar cell will be presented in section 2.6.

2.1 Carrier concentrations

This section is mainly based on [9].

The charge carriers in semiconductors are electrons and holes having concentrations n and p, respectively. In an intrinsic semiconductor at 0 K all states in the valence band are filled, and there are no electrons in the conduction band. An intrinsic material contains no impurities or lattice defects. At temperatures greater than 0 K, electrons in the valence band are thermally excited to the conduction band leaving holes behind, and the concentration of electron and holes is equal

$$n = p = n_i, \tag{2.1}$$

where i stands for intrinsic. The process takes place via thermal vibrations supplying energy equal or greater than the band gap E_G of the semiconductor and through absorption of thermal radiation from the ambient.

By introducing impurities in the lattice, i.e. the process of doping the material, new electron and hole concentrations are obtained. The impurities create new energy levels, usually in the band gap of the semiconductor. A n-doped material contains a concentration N_d of donors that introduces energy levels close to the conduction band edge. At 0 K these donor levels are filled with electrons. Only small amount of energy is required to excite these electrons to the conduction band, and at temperatures around 50-100 K almost all the donor electrons are excited by thermal energy. The conduction band electron concentration is increased, giving a new equilibrium concentration n_0, considerably larger than n_i for typical doping levels. The concentration of electrons is greater than the concentration of holes, and we call electrons majority carriers and holes minority carriers in the n-doped material. A p-doped material contains a concentration N_a of acceptors and is characterized by an acceptor level close to the valence band edge. The acceptor level is empty at 0 K, but at higher temperatures thermal energy excites electrons from the valence band into this level. The reduction of electron concentration in the valence band is equivalent with an increase of hole concentration, and a new equilibrium concentration p_0 of holes is obtained. In this case the majority carriers are holes and the minority carriers are electrons since the concentration of holes is much larger than the electron concentration.

To obtain expressions for the carrier concentrations in doped materials, the concept of Fermi energy, E_F, is useful. Electrons are fermions and therefore follow Fermi-Dirac statistics with the distribution function

$$f(E) = \frac{1}{1 + e^{(E-E_F)/k_BT}}, \tag{2.2}$$

where k_B is Boltzmann's constant and T is the absolute temperature. Equation (2.2) gives the probability that a state with energy E is occupied. From the equation we see that an energy state with energy equal to the Fermi energy has a probability 1/2 of being occupied. In an intrinsic material the Fermi energy is at the middle of the band gap and is denoted E_i. In a n-doped material the Fermi energy is close to the conduction band edge, while in a p-doped material it is close to the valence band edge. Useful expressions combining the equilibrium concentrations of electrons and holes in a doped material and in an intrinsic material are

$$n_0 = n_i e^{(E_F-E_i)/k_BT}, \tag{2.3}$$

$$p_0 = n_i e^{(E_i-E_F)/k_BT}. \tag{2.4}$$

From these expressions it is clear that

$$n_0 p_0 = n_i^2. \tag{2.5}$$

The Fermi-Dirac distribution is only valid in thermal equilibrium. If excess charge carriers are created optically, we are not in thermal equilibrium. Carriers in the conduction and valence band then form local thermal equilibriums with different chemical potentials, μ, also denoted quasi-Fermi levels. The concentration of electrons and holes in steady state can then be expressed as

$$n = n_i e^{(F_n-E_i)/k_BT}, \tag{2.6}$$

$$p = n_i e^{(E_i-F_p)/k_BT}, \tag{2.7}$$

where F_n and F_p are the quasi-Fermi levels for electrons and holes, respectively. The difference

$$\Delta\mu = F_n - F_p, \tag{2.8}$$

is equal to the difference in chemical potentials [3]. From equation (2.6), (2.7) and (2.8) it is seen that product of electron and hole concentration is given by

$$np = n_i^2 e^{\Delta\mu/k_BT}. \tag{2.9}$$

2.2 Generation and recombination

This section is based on [3].

The creation of free charge carriers in a semiconductor requires energy and is called generation. Recombination is the reverse event and releases energy. In solar cells the most important generation process is absorption of photons. In addition thermal generation is taking place as described in the previous section. Different recombination processes are shown in figure 2.2. The processes shown are radiative recombination,

non-radiative recombination via trap states and non-radiative Auger recombination. In general, each generation process is given its own generation rate G per unit time and unit volume. The recombination processes have different recombination rates, denoted U. The rates will in most cases take different values for electrons and holes. In thermal equilibrium the recombination and generation rates are equal. Since it is the disturbance from thermal equilibrium which is important, the excess (over the thermal) generation and recombination rates are used.

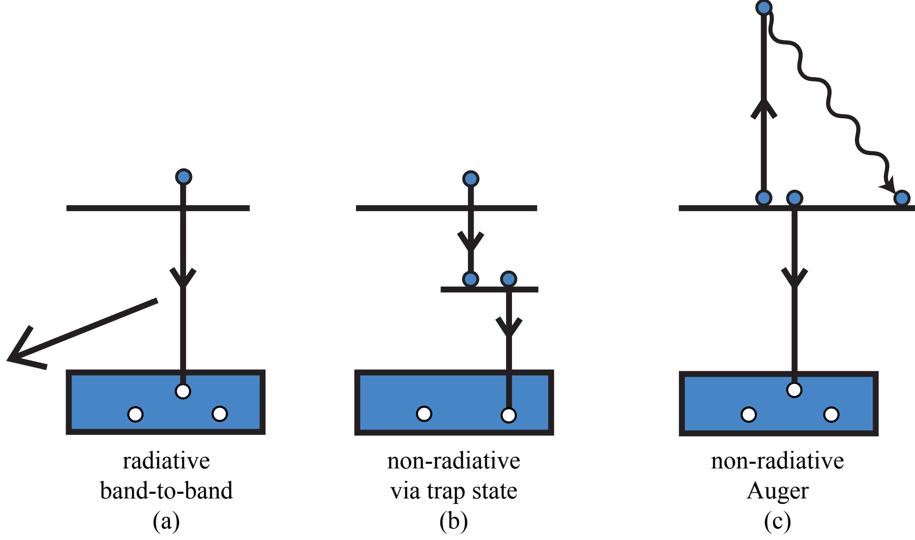

Figure 2.2: Recombination processes: (a) radiative, (b) non-radiative via trap states and (c) non-radiative Auger recombination.

The only generation process considered in this thesis is absorption of photons from sunlight. When the photon energy is larger than the band gap of the semiconductor, an electron-hole pair may be generated. The spectral rate of generation per unit volume of an electron-hole pair at a depth z below the surface of the solar cell is given by

$$g(E,z) = [1 - R(E)]\alpha(E)F(E)e^{-\int_0^z \alpha(E,z')dz'}, \tag{2.10}$$

where $R(E)$ is the reflectivity of the surface to normally incident light of energy E, $\alpha(E)$ is the absorption coefficient and $F(E)$ is the incident photon flux. We assume that all the absorbed photons generate one electron-hole pair each. To obtain the total generation rate $G(z)$ at a depth z, an integral over the photon energies has to be calculated

$$G(z) = \int_{E_G}^{\infty} g(E,z)dE. \tag{2.11}$$

The recombination processes can be divided into unavoidable and avoidable processes. Unavoidable processes can not be avoided through the use of perfect materials. They are related to physical processes in the material. Both radiative recombination and Auger recombination fall into this category. The third process arises because materials are not perfect and always contain some defects. Recombination may happen via defect

states in the forbidden gap, from now on referred to as trap states following the nomenclature in [3], and the process is known as non-radiative. In the following expressions for the recombination rates for all three processes are presented.

Radiative recombination takes place when an electron and hole recombine, emitting a photon. The excess radiative recombination rate is given as the total radiative recombination rate minus the rate at thermal equilibrium

$$\begin{aligned} U_{rad} &= U_{rad}(\text{total}) - U_{rad}(\text{thermal}) \\ &= \int_0^\infty r_{sp}(E, \Delta\mu)dE - \int_0^\infty r_{sp}(E, 0)dE, \end{aligned} \tag{2.12}$$

where r_{sp} is the rate of spontaneous transition between two energy states which considering the volume recombination rate, is given as

$$r_{sp}(E, \Delta\mu) = \frac{8\pi n_r^2}{h^3c^2} \frac{\alpha(E)E^2}{e^{(E-\Delta\mu)/k_BT} - 1}, \tag{2.13}$$

and is reduced by a factor 1/4 when considering recombination along a particular direction. Here n_r is the refractive index of the material. For $\Delta\mu = 0$ this corresponds to Planck's radiation formula.

It is useful to express the radiation rate in terms of electron and hole concentrations, and this can be done considering a non-degenerate semiconductor where $E - \Delta\mu >> k_BT$ for all energies where r_{sp} is non-negligible. The approximation

$$\frac{E^2}{e^{(E-\Delta\mu)/k_BT} - 1} \approx e^{-(E-\Delta\mu)/k_BT} E^2 \tag{2.14}$$

can then be used. Using equation (2.9) an approximate expression for the net radiative recombination rate is given as

$$U_{rad} = B_{rad}(np - n_i^2), \tag{2.15}$$

where the radiative recombination coefficient B_{rad} is given as

$$B_{rad} = \frac{1}{n_i^2} \frac{2\pi}{h^3c^2} \int_0^\infty n_r^2 \alpha(E) e^{-E/k_BT} E^2 dE \tag{2.16}$$

for recombination along one direction and is a property of the material.

In low level injection, meaning that the optically generated electron and hole densities Δn and Δp are much lower than the doping density of the material, equation (2.15) can be simplified. The electron and hole concentrations are given as

$$n = n_0 + \Delta n, \tag{2.17}$$

$$p = p_0 + \Delta n. \tag{2.18}$$

In a p-type material with acceptor concentration N_a we have that $n_0 << p_0$, and in low level injection $\Delta n << p_0$, giving

$$U_{rad_p} = \frac{\Delta n}{\tau_{n,rad}} \tag{2.19}$$

where $\tau_{n,rad} = \frac{1}{B_{rad}N_a}$ is the minority carrier radiative lifetime. In the same way for a n-type material with donor concentration N_d one obtains in low level injection

$$U_{rad_n} = \frac{\Delta p}{\tau_{p,rad}} \tag{2.20}$$

where $\tau_{p,rad} = \frac{1}{B_{rad}N_d}$. Radiative recombination dominates only in the limit of perfect materials.

Non-radiative recombination via trap states takes place when an electron moves from the conduction band to an energy state in the band gap without the emission of photons, as shown in figure 2.2b. These states appear because of defects or impurities in the crystal. The energy released is given up as heat to the lattice, i.e. phonons are emitted. Recombination through a single trap state has a recombination rate given by the Shockley Read Hall expression

$$U_{SRH} = \frac{np - n_i^2}{\tau_{n,SRH}(p + n_i e^{(E_i - E_t)/k_B T}) + \tau_{p,SRH}(n + n_i e^{(E_t - E_i)/k_B T})}, \tag{2.21}$$

where E_t is the energy of the traps in the band gap and $\tau_{n,SRH}$ and $\tau_{p,SRH}$ are the lifetimes for electron and hole capture by a trap state given as

$$\tau_{n,SRH} = \frac{1}{\sigma_n v_n N_t} \tag{2.22}$$

and

$$\tau_{p,SRH} = \frac{1}{\sigma_p v_p N_t}, \tag{2.23}$$

respectively. Here v_n and v_p are the thermal velocity of the electron and hole, respectively, σ_n and σ_p are the capture cross section of the trap for electrons and holes, respectively, and N_t is the density of traps at an energy E_t.

In a p-type or n-type material, equation (2.21) simplifies to respectively

$$U_{SRH_p} \approx \frac{\Delta n}{\tau_{n,SRH}} \tag{2.24}$$

and

$$U_{SRH_n} \approx \frac{\Delta p}{\tau_{p,SRH}}. \tag{2.25}$$

Recombination also happens through trap states at surfaces and interfaces in the material. Broken bonds, other defects and impurities are concentrated here giving a high density of trap states. Surfaces are two-dimensional, and the recombination rate is therefore given per unit area rather than per unit volume. The surface recombination flux at a surface containing N_s traps per unit area is within a layer δz given by

$$U_S \delta z = \frac{n_s p_s - n_i^2}{\frac{1}{S_n}(p_s + n_i e^{(E_i - E_t)/k_B T}) + \frac{1}{S_p}(n_s + n_i e^{(E_t - E_i)/k_B T})}, \tag{2.26}$$

where n_s and p_s are the electron and hole densities at the surface. S_n and S_p are the surface recombination velocity for electrons and holes equal to

$$S_n = v_n \sigma_n N_s \tag{2.27}$$

and

$$S_p = v_p \sigma_p N_s, \tag{2.28}$$

respectively. In a p-type or a n-type material, equation (2.26) simplifies to respectively

$$U_{Sp} \delta z \approx S_n(n_s - n_0) \tag{2.29}$$

and

$$U_{Sn} \delta z \approx S_p(p_s - p_0). \tag{2.30}$$

The second non-radiative recombination mechanism is Auger recombination which involves three charge carriers. An electron and hole recombine giving off the energy as kinetic energy to a third carrier. The third carrier soon looses the energy as heat to the lattice and relaxes to the band edge. This is in figure 2.2c shown for an electron and hole recombining loosing the energy as kinetic energy to an electron in the conduction band. Auger recombination can take place band-to-band or via trap states, and depends on the densities of the three carriers. For band-to-band Auger recombination the recombination rate is given as

$$U_{Aug} = A_p(n^2 p - n_0^2 p_0) \tag{2.31}$$

for a process where to electrons collide and

$$U_{Aug} = A_n(np^2 - n_0 p_0^2) \tag{2.32}$$

for a process where to holes collide. A_p and A_n are proportionality constants. The electron lifetime for band-to-band Auger recombination in a p-type material and hole lifetime in a n-type material are related to A_p and A_n as

$$\tau_{n,Aug} = \frac{1}{A_n N_a^2} \tag{2.33}$$

and

$$\tau_{p,Aug} = \frac{1}{A_p N_d^2}. \tag{2.34}$$

Auger recombination is important in low band gap materials with high carrier densities. Band-to-band Auger recombination conserves both momentum and energy and is therefore important in indirect band gap materials where radiative recombination is suppressed due to the need of phonons in the recombination process. In direct band gap materials the radiative recombination dominate however, and the Auger recombination process is not that important here.

2.3 The p-n junction

This section is based on [9] and [3].

As already mentioned, the first step to convert energy in solar cells is to generate electron-hole pairs by photon absorption, and the second step is to separate these carriers to prevent them from recombine. The separation process is essential in photovoltaic devices and requires a driving force. There are different ways to manage the separation process, and one way is to use an electric field since the resulting force drives the holes and electrons in opposite directions. In this thesis the only driving force considered will be the electrostatic force arising from a p-n junction.

The junction between a p-type and a n-type semiconductor is named a p-n junction and is shown in figure 2.3. When a p-type and n-type semiconductor are brought together, holes will diffuse from the p-type to the n-type, while electrons will diffuse in the opposite direction. The diffusive current is caused by the spatial variation in the concentration of electrons and holes. Expressions for the diffusive current density in the z-direction for electrons and holes are generally given as

$$J_n(\text{diff}) = qD_n \frac{dn(z)}{dz}, \tag{2.35}$$

$$J_p(\text{diff}) = -qD_p \frac{dp(z)}{dz}, \tag{2.36}$$

where D_n and D_p are the electron and hole diffusions coefficients respectively, and q is the electron charge.

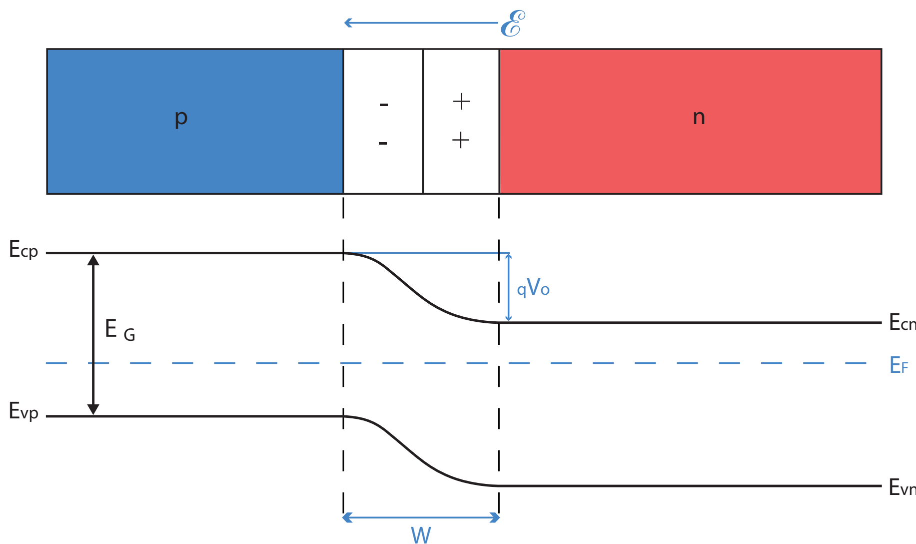

Figure 2.3: Schematic drawing of the p-n junction. The depletion region of width W is shown together with the electric field $\mathscr{E}$, the built-in potential V_0, the band gap E_G, the Fermi level E_F and the separation of the valence and conduction band edges in the p- and n-type material.

The movement of electrons from the n-type material to the p-type material and the opposite movement of holes, leaves the ionized doping atoms behind. A region depleted of free charge carriers named the depletion region arises. The depletion region has a

width W and is shown in figure 2.3. The static charges form an electric field $\mathscr{E}$ which causes a drift current in the opposite direction of the diffusion current. Expressions for the drift current density in the z-direction for electrons and holes are generally given as

$$J_n(\text{drift}) = q\mu_n n(z)\mathscr{E}(z), \tag{2.37}$$

$$J_p(\text{drift}) = q\mu_p p(z)\mathscr{E}(z), \tag{2.38}$$

where μ_n and μ_p are the mobilities of electrons and holes, respectively.

In thermal equilibrium the net current of each type of carrier has to be zero,

$$J_p(\text{drift}) + J_p(\text{diff}) = 0, \tag{2.39}$$

$$J_n(\text{drift}) + J_n(\text{diff}) = 0. \tag{2.40}$$

and the potential difference V_0 across the depletion region is given by

$$V_0 = \frac{k_B T}{q} \ln\left(\frac{N_a N_d}{n_i^2}\right). \tag{2.41}$$

Using the Einstein relation

$$\frac{D}{\mu} = \frac{k_B T}{q} \tag{2.42}$$

and the relation between electric field and potential V(z)

$$\mathscr{E}(z) = -\frac{dV(z)}{dz} = \frac{1}{q}\frac{dE_i}{dz} \tag{2.43}$$

the equilibrium conditions (2.39) and (2.40) give, together with equation (2.3) and (2.4), that the Fermi level has to be constant in equilibrium

$$\frac{dE_F}{dz} = 0 \tag{2.44}$$

as illustrated in figure 2.3.

2.4 The p-n junction under bias and illumination

This section is based upon [3].

When the p-n junction is illuminated, a current that depends on the incident light and properties of the p-n junction is generated. The aim of this section is to present an expression for the current as a function of voltage over the solar cell in the steady state. Steady state means that there is no time dependence, and for solar cells this is fulfilled when the illumination is constant. The derivation is based on the depletion approximation, and only recombination linear in the charge carrier densities in doped materials will be considered. The linear recombination approximation i.e. the recombination varies linearly with the minority charge carrier densities, is justified for low level injection when looking at equation (2.19), (2.20), (2.24) and (2.25).

In the depletion approximation we assume that there are no free charge carriers in

the depletion region. The electric field is only non-zero in the depletion region. In equilibrium the potential difference across the depletion region is, as mentioned, V_0. By applying a bias V across the junction, the potential changes to $(V_0 - V)$. V is positive when the p-side is forward biased relative to the n-side, as shown in figure 2.4. The lack of electric field outside the depletion region causes the current there to be only due to diffusion. Outside the depletion region the majority charge carriers are assumed to vary little from their equilibrium concentrations. This means that only the diffusion current of the minority carriers will determine the current.

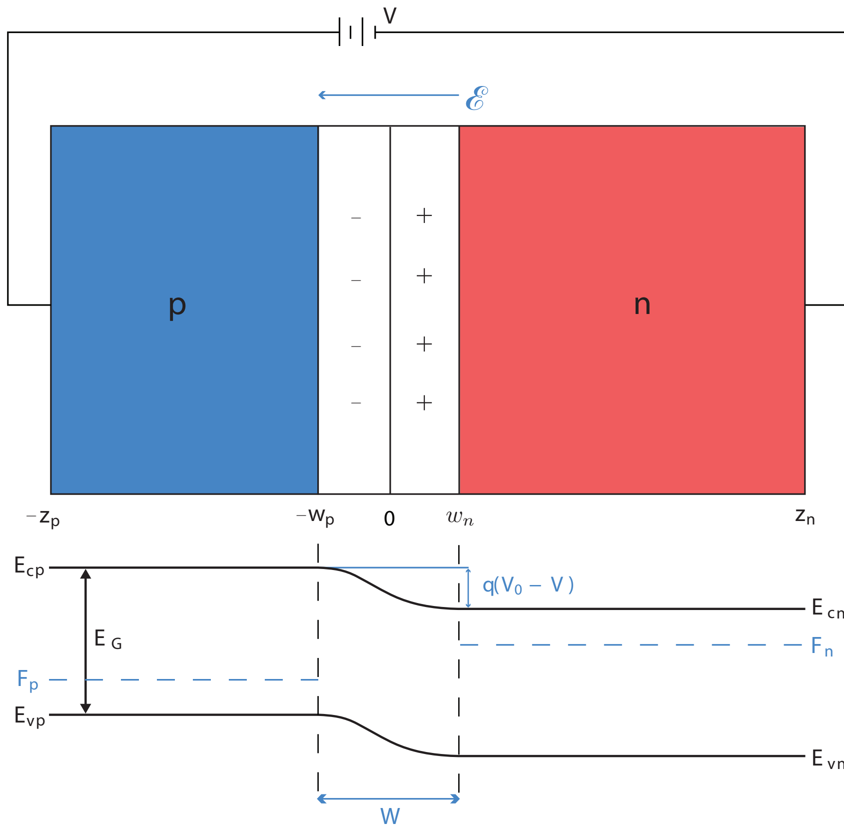

Figure 2.4: Schematic drawing of a forward biased p-n junction and its energy band diagram. The p-layer, depletion region and n-layer are shown together with the electric field. Also shown are the quasi-Fermi levels F_p and F_n on the p- and n-side, respectively.

The junction considered is the p-n junction shown in 2.4. The width of the p-layer is as shown equal to z_p, while the width of the n-layer is z_n. The width of the depletion region into the p-layer is w_p, and the width of the depletion region into the n-layer is w_n. The junction is illuminated by a photon flux $F(E)$, and the voltage over the junction is V. The current density of the minority charge carriers $J_n(z)$ and $J_p(z)$ are functions of depth z. To calculate the diffusion current from equation (2.35) and (2.36) the minority charge carrier concentration in the p- and n-layer are needed. These concentrations can be found using the continuity equations for electrons and holes together with appropriate

boundary conditions. The continuity equations for electrons and holes are

$$\frac{\partial \Delta n}{\partial t} = \frac{1}{q}\frac{\partial J_n}{\partial z} + (G_n - U_n) \tag{2.45}$$

and

$$\frac{\partial \Delta p}{\partial t} = -\frac{1}{q}\frac{\partial J_p}{\partial z} + (G_p - U_p), \tag{2.46}$$

respectively, where G is the generation rate and U is the recombination rate. In steady state when only diffusion current and linear recombination are considered, equation (2.45) and (2.46) can be written as

$$\frac{d^2\Delta n}{dz^2} - \frac{\Delta n}{L_n^2} + \frac{\int g(E,z)dE}{D_n} = 0 \quad \text{for} \quad z < -w_p \tag{2.47}$$

and

$$\frac{d^2\Delta p}{dz^2} - \frac{\Delta p}{L_p^2} + \frac{\int g(E,z)dE}{D_p} = 0 \quad \text{for} \quad z > w_n \tag{2.48}$$

in the p and n layer, respectively, where $L_n^2 \equiv D_n\tau_n$ and $L_p^2 \equiv D_p\tau_p$ are diffusion lengths and $g(E,z)$ is given in equation (2.10). τ_n and τ_p are electron and hole lifetimes. The equilibrium concentrations n_0 and p_0 are assumed constant in z. At the boundaries of the depletion region the electron and hole concentrations are given as

$$\Delta n = \frac{n_i^2}{N_a}(e^{qV/k_BT} - 1) \quad \text{for} \quad z = -w_p \tag{2.49}$$

and

$$\Delta p = \frac{n_i^2}{N_d}(e^{qV/k_BT} - 1) \quad \text{for} \quad z = w_n. \tag{2.50}$$

where it is utilized that the potential over the depletion region is given by $V_0 - V$ and that the majority charge carrier concentrations are approximately constant.

At the surfaces the recombination velocities S_n and S_p give the boundary conditions

$$D_n\frac{d\Delta n}{dz} = S_n\Delta n \quad \text{for} \quad z = -z_p, \tag{2.51}$$

$$-D_p\frac{d\Delta p}{dz} = S_p\Delta p \quad \text{for} \quad z = z_n, \tag{2.52}$$

using equation (2.29), (2.30), (2.37) and (2.38). Using the continuity equations together with the boundary conditions given in equation (2.49-2.52) the minority charge carriers concentrations are obtained leading to diffusion current densities

$$
\begin{aligned}
J_n(-w_p) = &-\int \left[\frac{q(1-R)F\alpha L_n}{(\alpha^2 L_n^2 - 1)}\right] \\
&\times \left\{ \frac{(K_n + \alpha L_n) - e^{-\alpha l_p}\left(K_n \cosh(\frac{l_p}{L_n}) + \sinh(\frac{l_p}{L_n})\right)}{K_n \sinh(\frac{l_p}{L_n}) + \cosh(\frac{l_p}{L_n})} - \alpha L_n e^{-\alpha l_p} \right\} dE \\
&+ \frac{qD_n n_0 (e^{qV/k_B T} - 1)}{L_n} \left\{ \frac{K_n \cosh(\frac{l_p}{L_n}) + \sinh(\frac{l_p}{L_n})}{K_n \sinh(\frac{l_p}{L_n}) + \cosh(\frac{l_p}{L_n})} \right\}
\end{aligned} \tag{2.53}
$$

and

$$
\begin{aligned}
J_p(w_n) = &-\int \left[\frac{q(1-R)F\alpha L_p}{(\alpha^2 L_p^2 - 1)} e^{-\alpha(z_p + w_n)}\right] \\
&\times \left\{ \frac{(K_p - \alpha L_p)e^{-\alpha l_n} - \left(K_p \cosh(\frac{l_n}{L_p}) + \sinh(\frac{l_n}{L_p})\right)}{K_p \sinh(\frac{l_n}{L_p}) + \cosh(\frac{l_n}{L_p})} + \alpha L_p \right\} dE \\
&+ \frac{qD_p p_0 (e^{qV/k_B T} - 1)}{L_p} \left\{ \frac{K_p \cosh(\frac{l_n}{L_p}) + \sinh(\frac{l_n}{L_p})}{K_p \sinh(\frac{l_n}{L_p}) + \cosh(\frac{l_n}{L_p})} \right\}
\end{aligned} \tag{2.54}
$$

for electrons and holes at the boundary of the depletion region. Here $K_n \equiv \frac{S_n L_n}{D_n}$, $K_p \equiv \frac{S_p L_p}{D_p}$, $l_p \equiv z_p - w_p$ and $l_n \equiv z_n - w_n$. The photon flux $F(E)$, absorption coefficient $\alpha(E)$ and reflectivity $R(E)$ are functions of energy. They are for brevity written here as F, α and R.

The total current density in the solar cell is given as the sum of the hole and electron current densities at a specific point in the cell and is given as

$$
\begin{aligned}
J &= -J_n(-w_p) - J_p(-w_p) \\
&= -J_n(-w_p) - J_p(w_n) - J_{dep}
\end{aligned} \tag{2.55}
$$

where the sign used gives a positive current when the current is flowing from p to n, meaning that the photocurrent is positive. J_{dep} is the net current density arising from generation and recombination in the depletion region. In the simples case this current density is assumed equal to zero.

The total current density contains terms dependent only on the incident light and terms dependent only on the applied voltage. These terms are independent due to the linear differential equations and boundary conditions determining the electron and hole concentrations given in equation (2.47-2.52). The current can be divided into a dark current $J_{dark}(V)$ dependent on the voltage and a photocurrent J_{light} dependent on the light

$$
J = J_{light} - J_{dark}(V). \tag{2.56}
$$

The photocurrent can be written in terms of the quantum efficiency $QE(E)$

$$J_{light} = q \int F(E) QE(E) dE \tag{2.57}$$

where $QE(E)$ is the probability that a photon of energy E will contribute with one electron to the current. The quantum efficiency is the sum of the quantum efficiency in the p-layer and n- layer given as

$$QE_p = \left[\frac{(1-R)\alpha L_n}{(\alpha^2 L_n^2 - 1)} \right] \left\{ \frac{(K_n + \alpha L_n) - e^{-\alpha l_p} \left(K_n \cosh(\frac{l_p}{L_n}) + \sinh(\frac{l_p}{L_n}) \right)}{K_n \sinh(\frac{l_p}{L_n}) + \cosh(\frac{l_p}{L_n})} - \alpha L_n e^{-\alpha l_p} \right\} \tag{2.58}$$

and

$$QE_n = \left[\frac{(1-R)\alpha L_p}{(\alpha^2 L_p^2 - 1)} \right] e^{-\alpha(z_p + w_n)} \left\{ \alpha L_p - \frac{K_p \left(\cosh(\frac{l_n}{L_p}) - e^{-\alpha l_n} \right) + \sinh(\frac{l_n}{L_p}) + \alpha L_p e^{-\alpha l_n}}{K_p \sinh(\frac{l_n}{L_p}) + \cosh(\frac{l_n}{L_p})} \right\}, \tag{2.59}$$

respectively, as can be seen from equation (2.53) and (2.54).

The net current density J_{dep} arising from generation and recombination in the depletion region is included in a more general case. The dominating recombination process is considered to be non-radiative recombination trough trap states given by the Shockley Read Hall expression in equation (2.21). The electron and hole concentrations are varying through the depletion region and may have similar magnitude. By assuming that the intrinsic Fermi energy level E_i varies linearly across the depletion region and that the difference between the quasi-Fermi levels F_n and F_p is constant and equal to qV, the recombination current density in the depletion region is taken as maximum

$$J_{SRH,dep} = \frac{q(w_n + w_p) n_i}{\sqrt{\tau_{n,SRH} \tau_{p,SRH}}} \frac{\pi \sinh(qV/2k_B T)}{q(V_0 - V)/k_B T}, \tag{2.60}$$

where V_0 is the built-in voltage of the p-n junction given in equation (2.41).

The generation current density in the depletion region is found by integrating the generation rate given in equation (2.10) over the depletion region with the result

$$J_{gen,dep} = \int q(1-R) F e^{-\alpha l_p} \left(1 - e^{-\alpha(w_p + w_n)} \right) dE. \tag{2.61}$$

Using equation (2.60) and (2.61) the net current density in the depletion region is

$$J_{dep} = J_{dep,0} \frac{\pi \sinh(qV/2k_B T)}{q(V_0 - V)/k_B T} - \int q(1-R) F e^{-\alpha l_p} \left(1 - e^{-\alpha(w_p + w_n)} \right) dE, \tag{2.62}$$

where

$$J_{dep,0} \equiv \frac{qn_i(w_n + w_p)}{\sqrt{\tau_{n,SRH}\tau_{p,SRH}}}. \tag{2.63}$$

The total current density in the solar cell may by including the net current density in the depletion region and using equation (2.53), (2.54), (2.62) and (2.55) be written as

$$J = J_{light} - J_0(e^{qV/k_BT} - 1) - J_{dep,0}(e^{qV/2k_BT} - 1), \tag{2.64}$$

where J_0 is the sum of the dark currents in the p- and n-layer. The recombination current density in the depletion region, given in equation (2.60), is approximated

$$J_{SRH,dep} \approx J_{dep,0}(e^{qV/2k_BT} - 1) \tag{2.65}$$

and the quantum efficiency in the depletion region is

$$QE_{dep} = (1 - R)\, e^{-\alpha l_p} \left\{1 - e^{-\alpha(w_p + w_n)}\right\}, \tag{2.66}$$

as can be seen from equation (2.62).

2.5 Current and voltage behavior for a solar cell

This section is mainly based on [3] and [10].

The general current-voltage characteristic for a solar cell under illumination is from section 2.4 given as

$$J = J_{light} - J_0(e^{qV/k_BT} - 1) - J_{dep,0}(e^{qV/2k_BT} - 1). \tag{2.67}$$

From this equation the solar cell can be modeled as a circuit consisting of an ideal current source with current density J_{light} and two diodes in parallel with ideality factors equal to 1 and 2 as can been seen in figure 2.5.

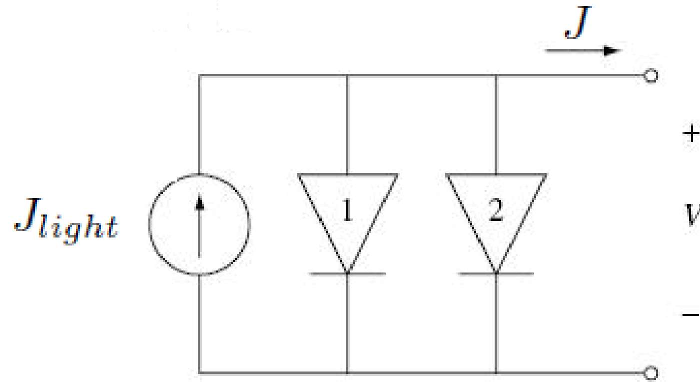

Figure 2.5: Modeling the solar cell as an circuit consisting of an ideal current source and two diodes in parallel with ideality factor 1 and 2 [10].

Equation (2.67) can be rewritten by introducing the diode ideality factor A_0

$$J = J_{light} - J_{dark}(e^{qV/A_0 k_B T} - 1). \tag{2.68}$$

A_0 has a value between 1 and 2 and varies with voltage and material quality. When non-radiative recombination in the depletion region dominates A_0 has a value approximately equal to 2, while when the recombination in the depletion region is not as important as the recombination in the p- and n-layers, A_0 has a value of 1.

Often only the diode in figure 2.5 with ideality factor equal to 1 is considered, meaning that recombination in the depletion region is not included. This gives the current-voltage behavior shown in figure 2.6. There three important points are identified, that is the short-circuit current density J_{sc}, the open circuit voltage V_{oc} and the current density J_m and voltage V_m that gives the maximum power density $P_m = J_m V_m$. The short-circuit current density can be found by setting V equal to 0 in equation (2.68) and is equal to the photocurrent density J_{light}. The open circuit voltage can be found by setting J equal to 0 in equation (2.68) and is equal to

$$V_{oc} = \frac{A_0 k_B T}{q} \ln\left(\frac{J_{light}}{J_{dark}} + 1\right) \tag{2.69}$$

The open circuit voltage varies dependent on the recombination in the solar cell which are again dependent on the band gap of the semiconductor. The open circuit voltage is expected to vary linearly with the band gap of the semiconductor [5].

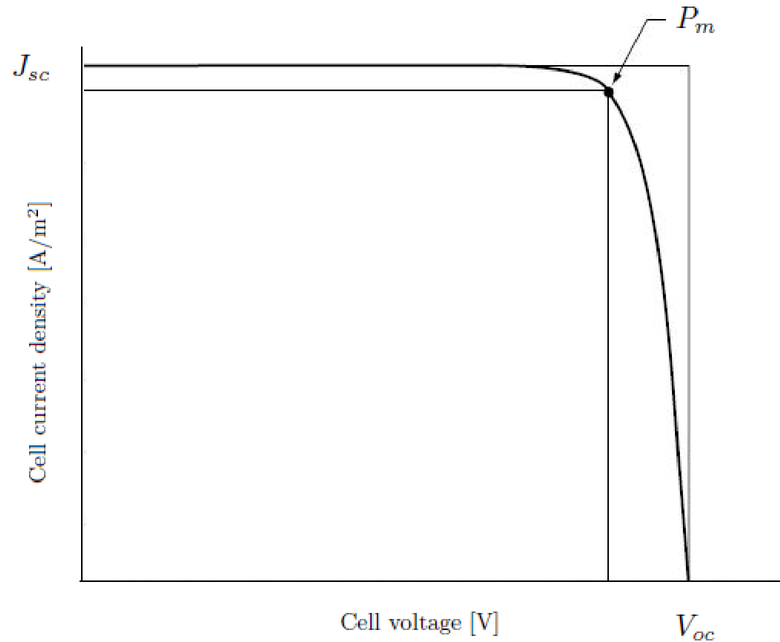

Figure 2.6: Current-voltage behavior for a solar cell showing the short-circuit current density J_{sc}, the open circuit voltage V_{oc} and the current density J_m and voltage V_m that gives the maximum power density $P_m = J_m V_m$. The inner rectangle has an area equal to $J_m V_m$, while the outer rectangle has an area equal to $J_{sc} V_{oc}$.

To obtain efficient solar cells, the main subject is to maximize the power. The ratio of maximum power density to the product of J_{sc} and V_{oc} is given the name fill factor, FF

$$FF = \frac{P_m}{V_{oc}J_{sc}}. \tag{2.70}$$

The fill factor is always less than one and describes the squareness of the JV-curve.

The most important term describing solar cells is the conversion efficiency, η, given as

$$\eta = \frac{P_m}{P_{in}}, \tag{2.71}$$

where P_{in} is the incident power density, a quantity determined by the incident light.

To consider the behavior of real solar cells series and shunt resistances have to be included, as shown in figure 2.7. The series resistance R_s is included due to the contact resistance to the front and back contact and the resistance of the cell material. The effect of series resistance is most important for high current densities and increases at high temperatures and high light intensities. Series resistance is always present in practical devices. It is more important in Si solar cells than in GaAs solar cells since the photocurrent is less in GaAs [11]. A shunt resistance R_{sh} represents current leakage through the cell and at its edges. Leakage through the cell can be due to dislocations, grain boundaries or crystal defects. Due to the higher output voltage of GaAs solar cells compared to Si solar cells, shunt resistance is more important in GaAs. Shunt resistance is usually not important in practical devices at common intensities, however [11]. The current density in the solar cell is by including resistances written

$$J = J_{light} - J_{dark}(V + JAR_s) - \frac{V + JAR_s}{AR_{sh}} \tag{2.72}$$

where A is the area of the cell.

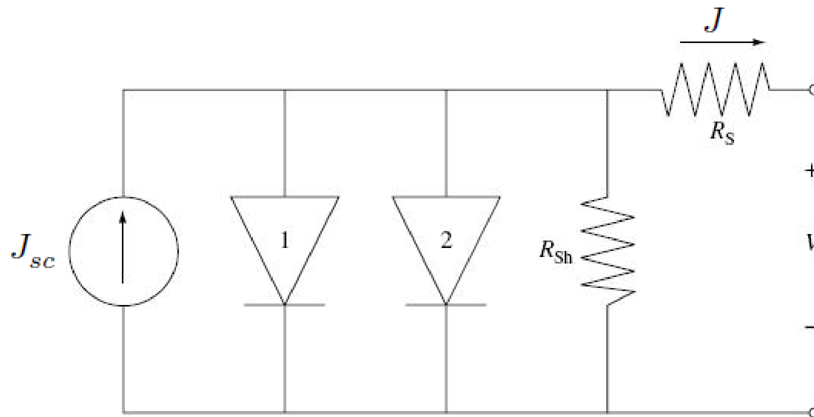

Figure 2.7: Modeling the solar cell as an circuit consisting of an ideal current source, two diodes in parallel with ideality factor 1 and 2 and a shunt and a series resistance [10].

2.6 Detailed balance of a standard solar cell

In this section based on [6] and [3] principle of detailed balance calculations are presented for the standard single junction solar cell. The limiting efficiencies for a solar cell under no concentration and maximum concentration are given.

Using the principle of detailed balance some idealistic assumptions are made. Carrier mobilities are assumed to be infinite, and the difference between the quasi-Fermi level F_n of the electrons on the n-side and the quasi-Fermi level F_p of the holes on the p-side of the p-n junction is assumed to be constant and equal to the voltage over the solar cell multiplied by the electron charge, $F_n - F_p = qV$. The contacts at each side of the cell are assumed to be ohmic, i.e. loss free. All incident light with $E > E_G$ is absorbed, and radiative recombination is the only recombination mechanism considered. This mechanism can not be avoided, even not by using defect free materials [3]. A perfect mirror is placed at the back of the cell meaning that radiation only escape by the front area.

The flux of photons over the energy range E_1 to E_2 emitted by the sun can be expressed as the spectrum of a black-body which normal to a solar cell surface, integrated over the whole hemisphere above it, is given as

$$F_{BB}(E_1, E_2, T) = \frac{2\pi}{h^3c^2} \int_{E_1}^{E_2} \frac{E^2}{e^{E/k_BT} - 1} dE, \tag{2.73}$$

where T is the temperature of the black-body (for the sun equal to $T_s = 5759$ K) and E is the photon energy. The principle of detailed balance says that in equilibrium the current density absorbed from the ambient is equal to the current emitted through the surface of the cell due to the radiative recombination. The solar cell has properties similar to a black-body and the flux emitted is thus given by equation (2.73) where T has to be taken as the temperature T_c of the solar cell. Under illumination the solar cell has developed a chemical potential $\Delta\mu$. The photons emitted from the solar cell are then given from a generalized form of Planck′s radiation law, which for emission normal to the solar cell is given as

$$F_B(E_1, E_2, \mu, T) = \frac{2\pi}{h^3c^2} \int_{E_1}^{E_2} \frac{E^2}{e^{(E-\mu)/k_BT} - 1} dE. \tag{2.74}$$

Equation (2.74) is equal to the black-body spectrum given in (2.73) for $\Delta\mu = 0$, $F_{BB}(E_1, E_2, T) \equiv F_B(F_B(E_1, E_2, 0, T)$. The photons are emitted from the solar cell with a chemical potential μ_{CV} equal to qV in an ideal cell.

The current-voltage characteristic of a standard solar cell using the principle of detailed balance is given as

$$J(V) = q\left[F_B(f_s, E_G, \infty, 0, T_s) + (f_c - f_s)F_B(E_G, \infty, 0, T_c) - f_cF_B(E_G, \infty, qV, T_c)\right] \tag{2.75}$$

where f_s and f_c are geometrical factors for the sun and the solar cell.

$$f_s = X \sin^2 \Theta_{sun} = X \times 2.1646 \times 10^{-5} \tag{2.76}$$

for the sun as seen from the earth, where X is a concentration factor ($1 \leq X \leq 46050$). How the solar cell performance is affected by X is described in section 3.1. By assuming that the radiation from the solar cell is emitted into a hemisphere we have that

$$f_c = 1. \tag{2.77}$$

Under maximum concentration $f_s = f_c = 1$. If T_s is taken as 5759 K and T_c as 300 K, equation (2.75) gives a maximum efficiency under no concentration equal to 30.5 % for a band gap equal to 1.26 eV. Under maximum concentration the maximum efficiency is 40.7% for a band gap equal to 1.06 eV. The solar cells considered in this thesis are made of GaAs which have a limiting efficiency of 30 % under no concentration and 38 % under maximum concentration [5]. The efficiency limits obtained for the ideal cells using detailed balance, as described above, are often referred to as the Shockley–Queisser limit after the authors of the first detailed balance paper [12].

Chapter 3

Increasing the efficiency

The third generation solar cells utilize different processes to increase the efficiency beyond the detailed balance limit of 30.5 % for a single-band gap material. The ways to obtain efficiencies beyond this limit are explained in section 3.1. The main emphasis of this chapter is the intermediate band solar cell. General theory concerning intermediate band solar cells is given in section 3.2. One way to create the intermediate band is to use quantum dots, and this is described in section 3.3. Detailed balance calculations on the intermediate band solar cell are presented in section 3.4.

3.1 Strategies to increase the efficiency

This section is based on [3].

As mentioned the limiting efficiency of a single-band gap solar cell is 30.5 % by using the principle of detailed balance. The two most important reasons for this rather low efficiency are that photons with energy lower than the band gap of the semiconductor are not absorbed and that carriers generated with $E > E_G$ lose kinetic energy by thermal dissipation. Different strategies are explored to increase the efficiency. One strategy is to use concentrator systems increasing the light intensity.

Concentration.
The solar cell absorbs sunlight only from a small angular range, and this can be increased by using concentrators based on lenses or mirrors. Light is thus collected over a large area and focused to a solar cell of a smaller area. By using a ratio X between the collector and cell area the incident flux density is increased by a concentration factor equal to X. The photocurrent is directly proportional to the photon flux F, see equation (2.57).The photocurrent is thus increased by a factor X, and the open-circuit voltage increases logarithmically to

$$V_{oc}(X) = \frac{A_0 k_B T}{q} \ln\left(\frac{X J_{light}}{J_{dark}} + 1\right). \tag{3.1}$$

By assuming a constant fill factor the efficiency $\eta(X)$ is increased by a factor equal to

$$\frac{\eta(X)}{\eta(1)} = 1 + \frac{A_0 k_B T}{q V_{oc}(1)} \ln X \tag{3.2}$$

where $\eta(1)$ and $V_{oc}(1)$ are the efficiency and open-circuit voltage using no concentration, respectively.

Concentration also increases the series resistance of the cell giving an increased voltage loss, and the temperature is raised leading to an increased dark-current. Both these effects lowers the open-circuit voltage and degrade the performance of the cell. Concentration may also give high injection conditions. This means that the photogenerated carrier densities are comparable to the doping densities in the doped layers. The radiative and Auger recombination rates then become non-linear with the carrier densities n and p, meaning that the total current can not be divided into an independent dark-current and a photocurrent. The increase of the open-circuit voltage is then less than given in equation (3.1). The concentration thus has an optimum value obtaining the highest efficiency for a solar cell.

Hot carrier and impact ionization solar cells.
One strategy to increase the efficiency is to reduce the dissipation of thermal energy by harnessing some of the kinetic energy of the carriers generated by photons of energy larger than E_G. The idea of hot carrier solar cells is to extract the carriers with the excess kinetic energy before they are slowed down. The extra kinetic energy is delivered to the electrical output of the cell. The limiting efficiency of an hot carrier solar cell is 85 % under maximum concentration.

The idea of impact ionization solar cells is that an energetic carrier can excite a second electron above the band gap by a collision process. This is process is the reverse of the Auger recombination shown in figure 2.2c. High energy photons with energy $E>E_G$ can then generate more than one electron-hole pair, and the quantum efficiency can thus be greater than one. The limiting efficiency of an impact ionization solar cell is 85 % under maximum concentration.

Multi-band solar cells.
The utilization of the energy from the photons is highest for photons with energy close to the band gap of the solar cell. When photons with energy close to the band gap are absorbed very little kinetic energy is lost. By using multiple band gaps in the solar cell, more of the photons are absorbed with energy close to one of the band gaps. The efficiency of the solar cell then increases.

In the tandem solar cell we have different band gap junctions placed on top of each other. The high energy photons are absorbed in the high band gap material, while the less energetic photons pass to the lower band gap material. By having more than one band gap the low energy photons which would be lost using a single low band gap material are absorbed, and the carriers generated have energy closer to the energy of the incident photon. For two band gaps the maximum efficiency is 55 % using maximum concentration.

Multi-band solar cells can also use one single junction. The intermediate band solar cell is an example of this, and this solar cell structure will be presented in detail in the rest of this chapter.

3.2 Working principle for the intermediate band solar cell

The intermediate band solar cell utilizes more of the incoming photons from the sun through the use of an intermediate band. In addition to the conduction band (CB) and the valence band (VB) the intermediate band solar cell contains an intermediate band (IB) placed in the band gap between the conduction and valence band. As seen in figure 3.1 the band gap of the semiconductor E_G is divided into two sub-band gaps E_L and E_H. $E_H \equiv E_I - E_v$ is the difference between the equilibrium Fermi energy of the intermediate band and the top of the valence band. $E_L \equiv E_c - E_I$ is the energy difference between the bottom of the conduction band and the equilibrium Fermi energy of the intermediate band, and we have that $E_G = E_H + E_L$. The width of the intermediate band is assumed to be negligible.

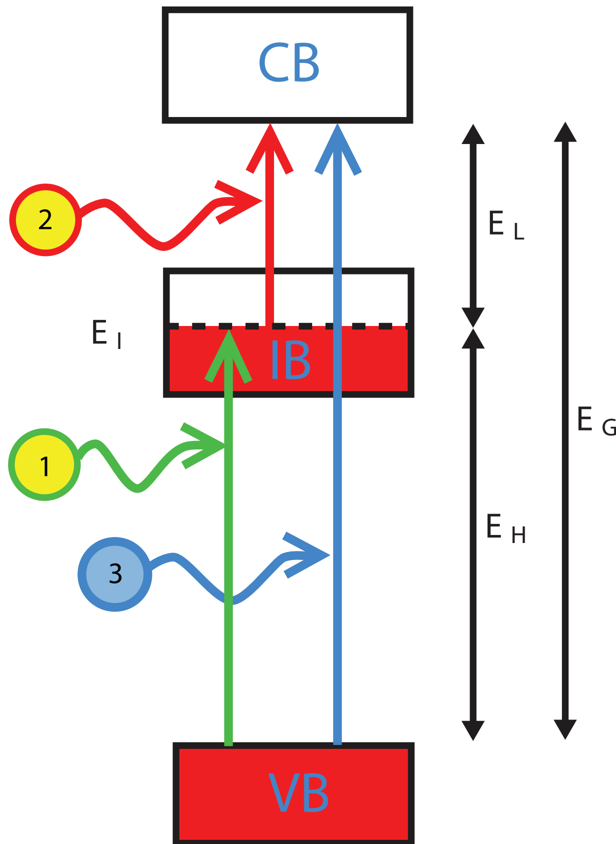

Figure 3.1: Band diagram of a material containing an intermediate band. The conduction band, valence band and intermediate band are shown along with the equilibrium Fermi energy of the intermediate band. By absorbing photons three transitions are possible. (1) an electron is transferred from the conduction band to the intermediate band. (2) an electron is transferred from the intermediate band to the conduction band. (3) an electron is transferred from the valence band to the conduction band. The symbols are explained in the text.

The division of the total band gap into two sub-band gaps makes absorption of photons with energies less than the total band gap possible, leading to an increased photocurrent. To create an electron-hole pair by absorption of photons with energies less than E_G, two transitions are necessary. In one of the transitions an electron is transferred from the valence band to the intermediate band leaving a hole behind in the valence band, visualized as transition (1) in figure 3.1. In the second transition the electron is transferred from the intermediate band to the conduction band, visualized as transition (2) in figure 3.1. In addition we have the "normal" creation of an electron-hole pair by absorption of a photon and the direct transfer of an electron from the valence band to the conduction band, visualized as transition (3) in figure 3.1.

The intermediate band has to be partially filled with electrons to make both transition (1) and (2) possible. A partially filled band contains both empty states to accommodate electrons being transfered from the valence band to the intermediate band and filled states to release electrons being pumped into the conduction band. The Fermi energy of the intermediate band has to be placed within the intermediate band to fulfill this condition.

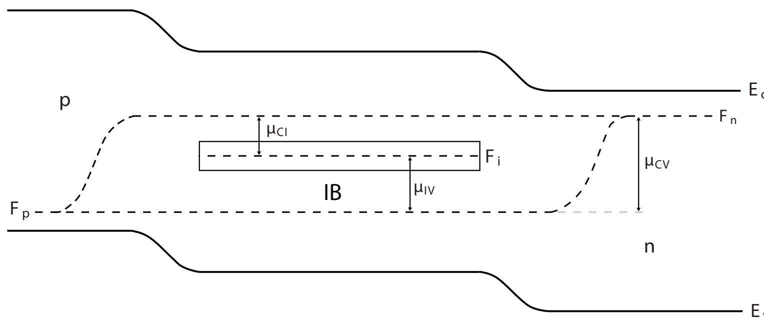

Figure 3.2: Quasi-Fermi levels and quasi-Fermi level splits in an intermediate band material placed between a p- and a n-layer. The symbols are explained in the text.

To obtain a high efficiency solar cell, not only the photocurrent, but also the voltage of the cell has to be optimized. A fundamental condition in the theory of intermediate band solar cells is that carrier concentration in each of the bands can be described by its own quasi-Fermi level; F_p for holes in the valence band, F_i for electrons in the intermediate band and F_c for electrons in the conduction band, as shown in figure 3.2. This condition is fulfilled when the carrier relaxation time within each band is much shorter than the carrier recombination time between bands [13]. One way of achieving this is to use quantum dots, which will be explained in section 3.3.

The quasi-Fermi level in the intermediate band is assumed to be fixed to its equilibrium position. This is an important assumption in the model of the quantum dot solar cell presented in section 5. No charge carriers are transported through the intermediate band, which is isolated from the external contacts by a p- and a n-layer placed on each side of the intermediate band material. The p-layer fixes the quasi-Fermi level for holes

in the valence band in the intermediate band material, while the n-layer fixes the quasi-Fermi level for electrons in the conduction band in the intermediate band material. The voltage V of the cell is given by [14]

$$qV = F_n - F_p \tag{3.3}$$

which has the same form as in a standard p-n solar cell. The voltage of the cell is thus unaffected by the intermediate band. The increase of the photocurrent in the intermediate band solar cell gives a higher efficiency.

3.3 The quantum dot based intermediate band solar cell

One way of creating the intermediate band is through the use of quantum dots and the resulting cell is called a quantum dot intermediate band solar cell. A quantum dot is confined in three dimensions and has a size limited by the de Broglie wavelength in all directions. Quantum dots placed in a barrier material with a larger band gap have discretely quantized energy levels dependent on the size of the quantum dot, the effective masses of the electrons and holes in the quantum dot and barrier materials and the band offset of the valence and conduction band [15]. The density of states of electron and holes in the quantum dot material is discrete and zero for energies not equal to the quantized energy levels as shown in figure 3.3. The physical properties of quantum dots resemble those of atoms [16].

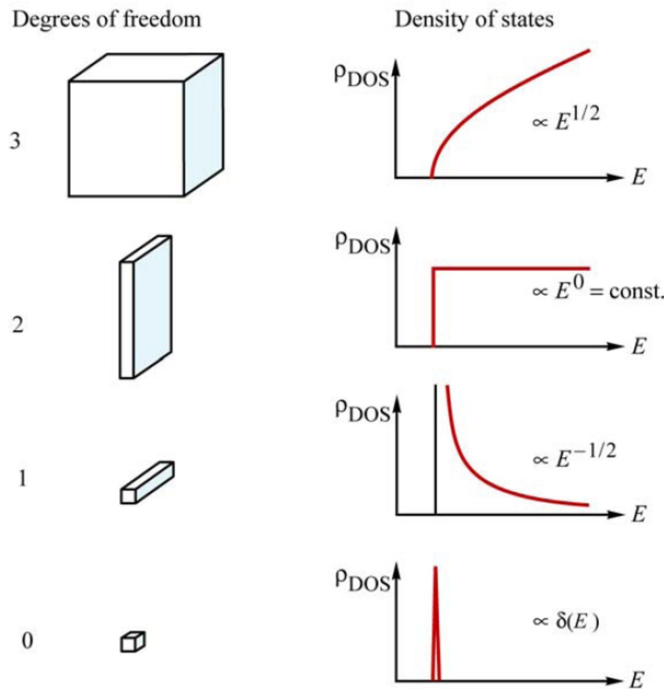

Figure 3.3: Density of states as function of energy in 3D/bulk material, 2D/quantum well, 1D/quantum wire, 0D/quantum dot [17]. The density of states is seen to be discrete in the case of quantum dot.

The energy levels in a single quantum dot is shown in figure 3.4. They arises due to the potential wells in the conduction and valence band obtained by having a quantum dot made of a material A placed in a material B with a higher band gap. The band offsets for the valence band ΔE_v and conduction band ΔE_c are shown in figure 3.4 and can be written as

$$\Delta E_v = E_{vB} - E_{vA} = (1-f)(E_B - E_A) = (1-f)\Delta E_G \quad (3.4)$$

and

$$\Delta E_c = E_{cB} - E_{cA} = f(E_B - E_A) = f\Delta E_G, \quad (3.5)$$

where $E_B > E_A$. E_A and E_B are the band gaps of material A and B respectively, E_{vA} and E_{cA} are respectively the valence and conduction band energy of material A, E_{vB} and E_{cB} are the valence and conduction band energy of material B. $f \equiv \frac{\Delta E_c}{\Delta E_g}$ is between 0 and 1 and depends on the materials [18]. The band offset in the conduction band forms the potential well for electrons. Similarly the band offset in the valence band forms the potential well for holes. In the case shown in figure 3.4 the band offset of the valence band is much lower than the band offset of the conduction band, meaning that the potential well is lower for the holes.

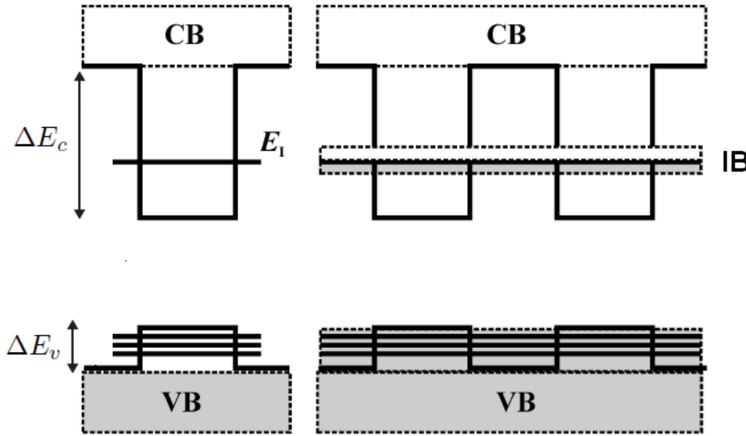

Figure 3.4: Electron and hole levels for a single quantum dot (left side) and for quantum dots placed in a periodic manner to create an intermediate band (right side) [19]. Only two of the quantum dots in the array of quantum dots are shown. The number of hole levels is seen to be much higher than the number of electron levels.

The number of quantized energy levels for the electron and holes increases with increasing effective mass. Most III-V semiconductors have a greater effective hole mass than effective electron mass, and thus the number of hole levels is higher than the number of electron levels. By using an appropriate quantum dot size it is possible to obtain a single electron level and several hole levels, as shown in figure 3.4 [20]. The shallowness of the hole well, combined with the many hole levels effectively connects the hole levels in the quantum dots with the hole levels in the valence band, i.e. thermal energy is enough to go from the dot to the valence band. This means one can not obtain a separate

quasi-Fermi level for the holes in the quantum dots. The electron levels in the quantum dot is, however, more than $k_B T$ away from the conduction band, and thus a separate Fermi level can be obtained.

The hole levels will extend the valence band and reduce the total band gap of the quantum dot solar cell. An array of quantum dots placed periodically will give an intermediate energy band due to the overlap of the electron states in the dot [20], shown in figure 3.4. In the figure only two quantum dots in the array of quantum dots are shown.

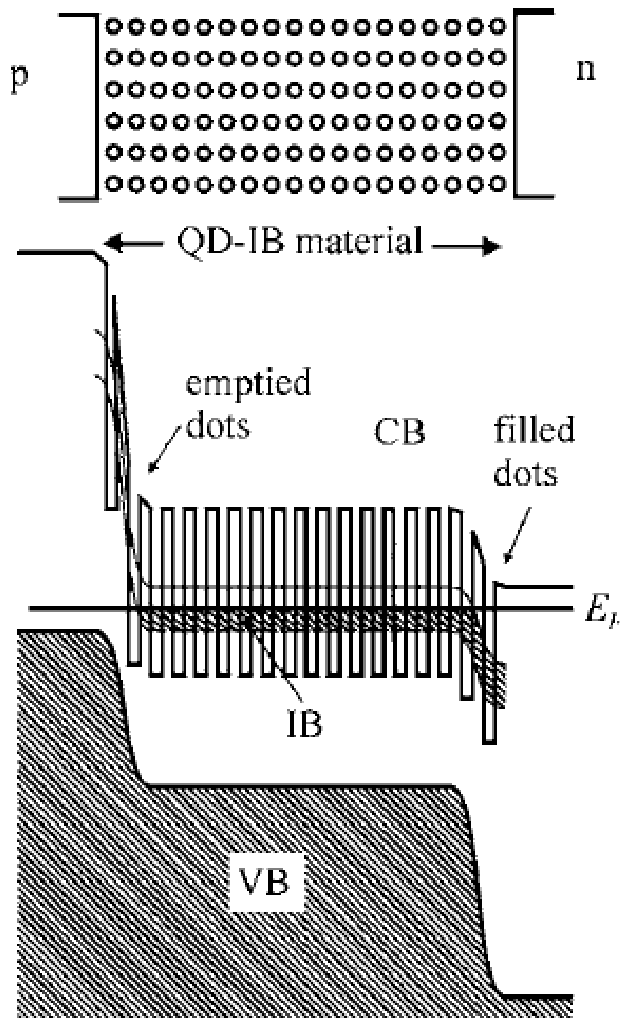

Figure 3.5: Band gap diagram of a quantum dot solar cell without all quantum dots placed in the flat band region. The quantum dots placed near the p-layer are empty of electrons, while the quantum dots placed near the n-layer are filled with electrons [13].

The zero density of states for energies not equal to the energy levels prevents the relaxation of electrons from the conduction band into the intermediate band through the phonon bottleneck effect. The released energy of an electron moving from the conduction band to the intermediate band has to be taken up by phonons [13]. Since the quantum

dots are periodically placed, they can not vibrate freely and should have vibrational modes as in a typical lattice. The phonons in a typical lattice have an energy of few tenths of meV, much lower than the energy difference between the conduction band and intermediate band. The energy of a single phonon is thus not sufficient to take up the released energy, and multiple phonon emission is unlikely. Non-radiative recombination between the conduction band and intermediate band is thus prevented [21]. The number of hole levels is high, and the holes quickly relax into the valence band, and the valence band extends upwards.

The quantum dot intermediate band solar cells can be made by placing quantum dots in the i-layer of a p-i-n solar cell. The p- and n-layers are present to separate the electron and holes generated in the intermediate band region. One important condition for maximizing the effect of the intermediate band solar cell is partial filling of the intermediate band. By doping the material where the quantum dots are placed with a density of donors equal to the number of quantum dots, and by placing the intermediate band in a flat band region, the intermediate band will be half-filled [13]. Quantum dots which are not placed in a flat band region will either be empty or completely filled with electrons. In figure 3.5 it is shown that the quantum dots placed in the depletion region near the p-layer is empty of electrons, while the quantum dots placed in the depletion region near the n-layer is filled with electrons [13]. By increasing the number of quantum dot layers the number of quantum dots in the flat band region increases. In the case of the much used InAs/GaAs system the number can not be too high. This is due to the fact that InAs/GaAs is a strained system and dislocations appear by increasing the number of quantum dot layers [14]. One can, however, compensate for the strain by introducing GaP or GaNAs layer in the structure or growing on a different substrate [22] and [23]. 100 strain-balanced quantum dot layers are in [24] reported grown on InP.

3.4 Detailed balance of the intermediate band solar cell

In the calculation of the limiting efficiency of the intermediate band solar cell using the theory of detailed balance the same assumptions are made as those for the reference cell, given in section 2.6. In addition one uses that when ideal behavior is considered no overlap exists between the absorption coefficients in the intermediate band region [25]. Absorption of photons with a specific energy will only give one possible transition where the photon energy is best utilized. Absorption of photons with energies greater than E_G will for instance only excite electrons from the valence band to the conduction and. Thus only one of the three absorption coefficients α_{CI}, α_{IV} and α_{CV} related to the transitions from the intermediate band to the conduction band, from the valence band to the intermediate band and from the valence band to the conduction band, respectively, will be non-zero for a given energy. In this way photons thermalization loss is minimal [6]. The solar cell is assumed to be thick enough that all photons with enough energy to induce one of the possible transitions are absorbed [26].

By assuming ideal behavior cell the current-voltage characteristic is given as [26]

$$\begin{aligned} J(V) = q\,[f_s F_B(E_G, \infty, 0, T_s) + (f_c - f_s) F_B(E_G, \infty, 0, T_c) - f_c F_B(E_G, \infty, \mu_{CV}, T_c)] \\ +q\,[f_s F_B(E_H, E_G, 0, T_s) + (f_c - f_s) F_B(E_H, E_G, 0, T_c) - f_c F_B(E_H, E_G, \mu_{IV}, T_c)] \end{aligned} \tag{3.6}$$

where $\mu_{IV} \equiv F_i - F_p$ and $\mu_{CV} \equiv F_n - F_p = qV$ are the quasi-Fermi level splits, F_B is the black-body spectrum given in equation (2.74) and f_s and f_c are geometrical factors of the sun and the cell given in equation (2.76) and (2.77), respectively. No carriers are assumed to be extracted from the intermediate band leading to

$$\begin{aligned} f_s F_B(E_L, E_H, 0, T_s) + (f_c - f_s) F_B(E_L, E_H, 0, T_c) - f_c F_B(E_L, E_H, \mu_{CI}, T_c) = \\ f_s F_B(E_H, E_G, 0, T_s) + (f_c - f_s) F_B(E_H, E_G, 0, T_c) - f_c F_B(E_H, E_G, \mu_{IV}, T_c) \end{aligned} \tag{3.7}$$

where $\mu_{CI} \equiv F_n - F_i$. The quasi-Fermi level splits are related through

$$\mu_{CI} + \mu_{IV} = \mu_{CV} \tag{3.8}$$

which together with equation (3.7) makes it possible to calculate all the variables in equation (3.6) giving the current-voltage characteristic of the intermediate band solar cell. The limiting efficiency using no concentration is 46.0% for the band gaps $E_L = 0.93$ eV and $E_H = 1.40$ eV [7]. Using maximum concentration the limiting efficiency is 63.2% for the band gaps $E_L = 0.71$ eV and $E_H = 1.24$ eV [7].

Under non-degenerate conditions, meaning that the quasi-Fermi level splits are lower than the band gap such that $E_G - \mu_{CV} >> k_B T$, one can use the approximation

$$\frac{1}{e^{(E-qV)/k_B T} - 1} \approx \frac{e^{qV/k_B T}}{e^{E/k_B T} - 1} \tag{3.9}$$

giving that

$$F_B(E_G, \infty, qV, T_c) \approx e^{qV/k_B T} F_B(E_G, \infty, 0, T_c). \tag{3.10}$$

Similarly one obtains

$$F_B(E_L, E_H, \mu_{CI}, T_c) \approx e^{\mu_{CI}/k_B T} F_B(E_L, E_H, 0, T_c) \tag{3.11}$$

and

$$F_B(E_H, E_G, \mu_{IV}, T_c) \approx e^{\mu_{IV}/k_B T} F_B(E_H, E_G, 0, T_c) \tag{3.12}$$

when $E_L - \mu_{CI} >> k_B T$ and $E_H - \mu_{IV} >> k_B T$.

The current-voltage characteristic for the intermediate band solar cell may then be written as

$$\begin{aligned} J(V) = q\left[f_s F_B(E_G, \infty, 0, T_s) + (f_c - f_s) F_B(E_G, \infty, 0, T_c) - f_c F_B(E_G, \infty, 0, T_c) e^{\mu_{CV}/k_B T_c}\right] \\ +q\left[f_s F_B(E_H, E_G, 0, T_s) + (f_c - f_s) F_B(E_H, E_G, 0, T_c) - f_c F_B(E_H, E_G, 0, T_c) e^{\mu_{IV}/k_B T_c}\right] \end{aligned} \tag{3.13}$$

and the solar cell may be modeled with three current generators JL_{CV}, JL_{IV} and JL_{CI} and three diodes D_{CV}, D_{IV} and D_{CI} as shown in figure 3.6. The currents through the

diodes D_{CI}, D_{IV} and D_{CV} are given as

$$J_{CI} = qf_c F_B(E_L, E_H, 0, T_c)\left(e^{\frac{\mu_{CI}}{k_B T_c}} - 1\right), \tag{3.14}$$

$$J_{IV} = qf_c F_B(E_H, E_G, 0, T_c)\left(e^{\frac{\mu_{IV}}{k_B T_c}} - 1\right), \tag{3.15}$$

$$J_{CV} = qf_c F_B(E_G, \infty, 0, T_c)\left(e^{\frac{\mu_{CV}}{k_B T_c}} - 1\right). \tag{3.16}$$

The photocurrent modeled by the current generators is given as

$$JL_{CI} = qf_s\left[F_B(E_L, E_H, 0, T_s) - F_B(E_L, E_H, 0, T_c)\right], \tag{3.17}$$

$$JL_{IV} = qf_s\left[F(E_H, E_G, 0, T_s) - F_B(E_H, E_G, 0, T_c)\right], \tag{3.18}$$

$$JL_{CV} = qf_s\left[F(E_G, \infty, 0, T_s) - F_B(E_G, \infty, 0, T_c)\right]. \tag{3.19}$$

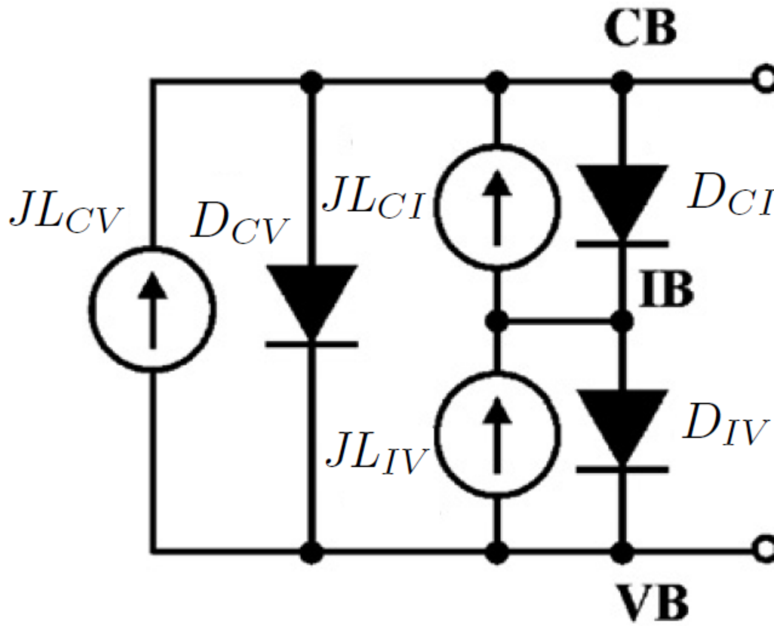

Figure 3.6: The intermediate band solar cell modeled as three current generators and three diodes [14].

Chapter 4

Model of the p-i-n reference cell

Practical solar cells have a complicated structure with several layers in addition to the p- and n-layer we find in the simplest p-n solar cell. The purpose of these layers is to reduce front and back surface recombination and surface reflection. A sketch of a p-i-n reference cell is shown in figure 4.1 showing all the layers (anti-reflective coating, window,p^+,p,i,n and n^+) included to obtain a high efficiency solar cell.

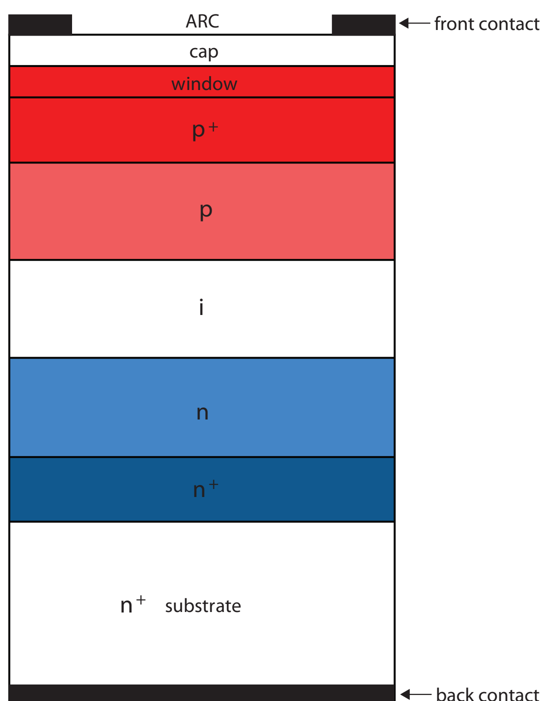

Figure 4.1: Structure of the p-i-n reference cell. It consists of an anti-reflective coating, a cap-, window-, p^+-, p-, i-, n- and n^+-layer placed on top of the substrate. The effect of using all these layers is described in the text.

In this thesis the aim is to model quantum dot intermediate band solar cells where the quantum dots are placed in an intrinsic layer between the p- and n-layers. As mentioned the quantum dots should be placed in a flat band region to obtain a partial filling of

the intermediate band. Amorphous Si solar cells are p-i-n solar cells with an depleted i-region placed to extend the thickness where the electric field, which separates the charge carriers, is present [3]. Models of p-i-n solar cells with a depleted i-layer is found in literature, but none with a flat band i-layer. In this chapter both a model of p-i-n solar cell with an undepleted i-layer and a depleted i-layer are developed. The p-i-n solar cell is called the reference cell and will be compared with the intermediate band solar cell.

In this thesis all the layers in the reference cell are made of GaAs or $Al_xGa_{1-x}As$ with properties as presented in chapter 6. At the top of the cell we find the front contacts and an anti-reflective coating minimizing the reflection losses. A GaAs-cap layer is then placed as a barrier against oxidation since the following $Al_xGa_{1-x}As$ window layer oxides easily. This high band gap window layer reduces the front surface recombination. Beneath the window layer we find a heavily doped p^+-layer which further reduces the front surface recombination. The p- and n-layers are then placed with an intrinsic (i) layer sandwiched in between. A heavily doped n^+-layer is placed beneath the n-layer to reduce the back surface recombination. At the bottom on the cell we find the substrate where the upper layers are deposited on and where the back contact is placed.

4.1 Model of a reference cell with a depleted i-layer

In chapter 2 the current-voltage characteristic of a solar cell made of only a p- and a n-layer is presented. In this and the next section a similar current-voltage characteristic for the solar cell structure shown in figure 4.1 will be derived. No complete model of the solar cell structure shown in figure 4.1 was found in literature and I therefore derived the current-voltage characteristic for such a solar cell structure using the continuity equations for electrons and holes, given in equation (2.45) and (2.46), together with the appropriate boundary conditions for this structure. Inspiration was found in [27] where the current-voltage characteristic of a n^+-n-p junction is derived.

4.1.1 Anti-reflective coating

By using an anti-reflective coating the reflectivity, R(E), is greatly reduced, and reflection losses may be as low as approximately 2 % [28]. The solar cells with anti-reflective coatings are in this thesis modeled by using a reflectivity equal to zero for all wavelenghts.

4.1.2 i-layer

The i-layer placed between the p- and n-layer is ideally undoped. In practice it has an background doping N_i much smaller than the doping of the p- and n-layer. The depletion region in a p-i-n junction extends furthest into the lightest doped region. In a p-i-n junction the depleted widths of the p- and n-layer are assumed to be very small [3]. A reasonable simplification is therefore to set them equal to zero, w_p and w_n in figure 2.4 are equal to zero. For narrow a i-layer with low background doping it is reasonable to consider the whole i-layer as depleted with an electric field present throughout the whole i-layer. This approximation is made in this section, while in section 4.2 a model where this approximation is not used and part of the i-layer is placed in a flat band region with a very small electric field, is presented.

By having the whole i-layer placed in the depletion region it is reasonable to set the width of the depletion region equal to the width z_i of the i-layer. The sum of w_p and w_n is the width of the depletion region. This sum is equal to $w_n + w_p = z_i$. The depleted widths of the p- and n-layers are zero, but we still have a depletion region which now is fully contained in a i-layer. The net current density J_i arising from generation and recombination in the i-layer is assumed to be of the same form as given for the p-n junction depletion region in equation (2.62) and is given by

$$J_i = J_{i,0} \frac{\pi \sinh(qV/2k_BT)}{q(V_0 - V)/k_BT} - \int q(1-R)Fe^{-[\alpha(z_p+z_p^+)+\alpha_w z_w]} \left(1 - e^{-\alpha z_i}\right) dE. \quad (4.1)$$

where

$$J_{i,0} \equiv \frac{q z_i n_i}{\sqrt{\tau_{n,i,SRH} \tau_{p,i,SRH}}} \quad (4.2)$$

and z_p^+ is the width of the p$^+$-layer, z_w is the width of the window layer, α_w is the absorption coefficient of the window material and $\tau_{n,i,SRH}$ and $\tau_{p,i,SRH}$ are the electron and hole non-radiative lifetimes in the i-layer, respectively.

The currents in the p- and n-layer are of the same form as obtained for the standard p-n junction solar cell given in equation (2.53) and (2.54). The expressions for the surface recombination velocities have to be changed however, due to the presence of the window layer and the heavily doped p$^+$- and n$^+$-layer. Generated currents in the p$^+$- and n$^+$-layer also have to be included in the model. Since the window layer is very narrow and is made of a high band gap material, the generated current in the window layer is not included.

4.1.3 Front surface field

The more heavily doped p$^+$-layer on top of the p-layer reduces the surface recombination velocity through a front surface field. The electrons in the p-layer meet a potential barrier dependent on the ratio of the doping concentrations in the p$^+$- and p-layer, when moving from the p-layer into the p$^+$ layer. This is called a front surface field [3]. Since the p$^+$-layer is placed near the front surface where the photon flux is highest, the carriers generated in the p$^+$-layer contribute considerably to the photocurrent [27].

The p$^+$-p junction considered is shown in figure 4.2 where the width of the p$^+$-layer is z_{p^+}, the width of the p-layer is z_p, and the width of the depletion region between the p$^+$- and p-layer is w_a. The width of this depletion region is $w_{a,p}$ into the p-layer and w_{a,p^+} into the p$^+$-layer. The total electron current at the edge of the undepleted p-layer, at $z = 0$ in figure 4.2, is the sum of the contributions from the p$^+$-layer, the p-layer and the depleted region between the p$^+$- and p-layer

$$J_{n,total}(0) = J_{n,p^+}(0) + J_{n,p}(0) + J_{n,dep}(0). \quad (4.3)$$

The contribution from the p-layer $J_{n,p}(0)$ is obtained using equation (2.53) after some modifications are made. One has to multiply with $e^{-[\alpha(z_p^+ + w_{a,p})+\alpha_w z_w]}$ due to the absorption in the window layer, p$^+$-layer and depletion region and due to the front surface

field use an effective surface recombination velocity

$$S_{n,pp^+,eff} = \frac{D_n^+}{L_n^+}\frac{N_a}{N_a^+}\left\{\frac{K_n^+ \cosh\left(\frac{l_p^+}{L_n^+}\right) + \sinh\left(\frac{l_p^+}{L_n^+}\right)}{K_n^+ \sinh\left(\frac{l_p^+}{L_n^+}\right) + \cosh\left(\frac{l_p^+}{L_n^+}\right)}\right\}, \tag{4.4}$$

replacing S_n. l_p in equation (2.53) is replaced with the width of the undepleted p-layer $l_p^{'} \equiv z_p - w_{a,p}$. In equation (4.4) $l_p^+ \equiv z_p^+ - w_{a,p^+}$, N_a^+ is the doping of the p$^+$-layer, $K_n^+ \equiv \frac{S_n^+ L_n^+}{D_n^+}$ where S_n^+ is the front surface recombination velocity of the p$^+$-layer and L_n^+ and D_n^+ are the diffusion length and diffusion coefficient in the p$^+$-layer, respectively. The equation which I obtained for the effective surface recombination velocity, equation (4.4), resembles the formula for effective surface recombination velocity given in [3].

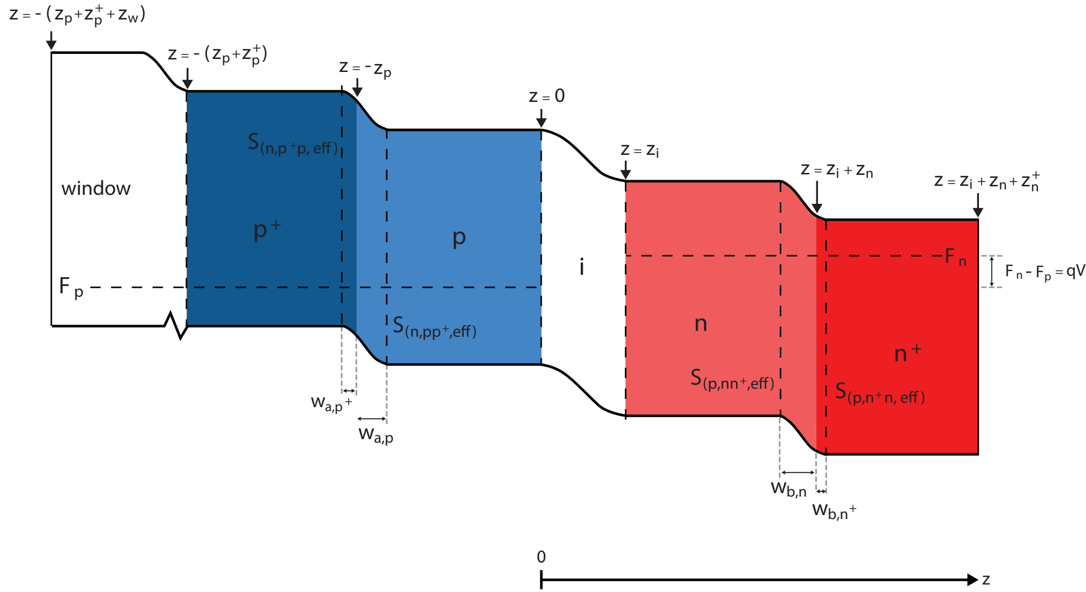

Figure 4.2: Structure of the reference cell with depleted i-layer. The p$^+$-layer is used as a front surface field reducing the front surface recombination velocity along with the window layer. The n$^+$-layer is used as a back surface field reducing the back surface recombination velocity. All the symbols are explained in the text.

The effective surface recombination velocity given in equation (4.4) arises from the fact that the built-in voltage of the p$^+$-p junction has the form [29]

$$V_{pp^+} = \frac{k_B T}{q} \ln\left(\frac{Na^+}{Na}\right) \tag{4.5}$$

in equilibrium. It is assumed that no additional voltage appears over the p$^+$-p junction

when we are out of equilibrium, meaning that the effective surface recombination velocity is constant for varying bias over the cell. Band gap narrowing in the heavily doped p$^+$-layer is neglected. Equation (4.4) expresses that as the ratio of the doping concentrations in the p- and p$^+$-layer is increased the potential barrier qV_{pp^+} between the p- and p$^+$-layer increases giving a lower effective surface recombination velocity. If the width of the p$^+$ layer is small the surface recombination velocity is proportional to the ratio of the doping in the p- and p$^+$ layer, $S_{n,pp^+,eff} \approx \frac{D_n^+}{L_n^+}\frac{N_a}{N_a^+}$.

The electron current at $z = -(z_p + w_{a,p^+})$ is found using the continuity equation for electrons when only diffusion current and linear recombination are considered, given in equation (2.47) and the boundary conditions

$$D_n^+ \frac{d\Delta n}{dz} = S_n^+ \Delta n \quad \text{for} \quad z = -(z_p + z_p^+), \tag{4.6}$$

and

$$\Delta n_{(z-)} = \Delta n_{(z+)} e^{-(qV_{pp^+}/k_B T)} \quad \text{for} \quad z = -(z_p - w_{a,p}) \tag{4.7}$$

where $z-$ expresses a small displacement from $z = -(z_p - w_{a,p})$ in the negative z-direction and $z+$ a small displacement in the positive z-direction. S_n^+ is the surface recombination velocity on top of the p^+-layer. The result obtained is

$$J_{n,p^+}(-z_p - w_{a,p^+}) = -F_{h-1} \int \left[\frac{q(1-R)F\alpha L_n^+}{(\alpha^2 (L_n^+)^2 - 1)} e^{-\alpha_w z_w} \right] \times \left\{ \frac{(K_n^+ + \alpha L_n^+) - e^{-\alpha l_p^+} \left(K_n^+ \cosh(\frac{l_p^+}{L_n^+}) + \sinh(\frac{l_p^+}{L_n^+}) \right)}{K_n^+ \sinh(\frac{l_p^+}{L_n^+}) + \cosh(\frac{l_p^+}{L_n^+})} - \alpha L_n^+ e^{-\alpha l_p^+} \right\} dE. \tag{4.8}$$

Here

$$F_{h-1} \equiv \frac{1}{1 + \frac{N_a^+ S_{n,pp^+,eff}}{N_a S_{n,p^+p,eff}}} \tag{4.9}$$

where

$$S_{n,p^+p,eff} \equiv \frac{D_n}{L_n} \frac{N_a^+}{N_a} \coth\left(\frac{l_p'}{L_n} \right). \tag{4.10}$$

$S_{n,p^+p,eff}$ is the effective surface recombination velocity at the edge of the undepleted p$^+$-layer ($z = -(z_p + w_{a,p^+})$) and reflects how light-generated electrons may be extracted from the p$^+$-layer [27].

The electron contribution from the p$^+$-layer at $z = 0$ in figure 4.2, is found including recombination in the p-layer while neglecting recombination in the depletion region between the p$^+$- and p-layer. This is justified since this depletion region is very narrow. The result is

$$J_{n,p^+}(0) = J_{n,p^+}[-(z_p + w_{a,p^+})] \cosh^{-1}\left(\frac{l_p'}{L_n} \right). \tag{4.11}$$

In the depletion region between the p$^+$- and p-layer all photons absorbed are generating

one electron-hole pair. The contribution at $z = 0$ is then given as

$$J_{n,dep}(0) = \int q(1-R)Fe^{-(\alpha l_p^+ + \alpha_w z_w)}\left(1 - e^{-\alpha w_a}\right) dE \cosh^{-1}\left(\frac{l_p'}{L_n}\right). \tag{4.12}$$

The depletion region goes mostly into the lightly doped p-region. The extension of the depletion region in the lightly doped region is taken from [30] and used as an approximation for w_a

$$w_a \approx \sqrt{\frac{2\epsilon k_B T}{q^2 N_a}} \arctan\left(\frac{qV_{pp^+}}{k_B T}\sqrt{\frac{N_a^+}{2N_a}}\right) \tag{4.13}$$

where ϵ is the permittivity of the material.

4.1.4 Window layer

By placing a window layer made of a higher band gap material above the p$^+$-layer the effective surface recombination velocity is further reduced. The window layer acts as a further potential barrier for the electrons in the p$^+$-layer. By assuming no recombination at the window-p$^+$ junction, linear recombination in the window layer and that the band bending of the conduction band equals the difference in band gaps of the two materials, the front surface recombination velocity of the p$^+$-layer S_n^+ can be replaced by an effective surface recombination velocity

$$S_{n,eff,window} = \frac{D_n^w}{L_n^w} e^{-\Delta E_G/k_B T} \left\{ \frac{K_n^w \cosh\left(\frac{z_w}{L_n^w}\right) + \sinh\left(\frac{z_w}{L_n^w}\right)}{K_n^w \sinh\left(\frac{z_w}{L_n^w}\right) + \cosh\left(\frac{z_w}{L_n^w}\right)} \right\}, \tag{4.14}$$

where ΔE_G is the difference in band gap between the window layer and the p$^+$-layer, $K_n^w \equiv \frac{S_n^w L_n^w}{D_n^w}$ where S_n^w is the front surface recombination velocity of the window layer and L_n^w and D_n^w are the diffusion length and diffusion coefficient in the window layer, respectively [3]. The samples used in the modeling in this thesis consist of a $Al_{0.85}Ga_{0.15}As$ window layer on GaAs. Equation (4.14) then gives a much lower surface recombination velocity than found experimentally in solar cell samples, due to the large band gap difference. The effective surface recombination velocity on top of a GaAs p$^+$-layer using a $Al_{0.85}Ga_{0.15}As$ window is therefore taken as 10^2 m/s, as is this is known to be a typically effective surface recombination velocity when window layers are used [11]. No generation or recombination currents in the window layer are included in the total current.

4.1.5 Back surface field

The more heavily doped n$^+$-layer layer placed beneath the n-layer gives a back surface field, reducing the effective rear surface recombination velocity in the same way as the front surface field. The derivation in this section is therefore very similar to the derivation in the previous section, but is included for completeness. The n-n$^+$ junction is shown in figure 4.2 where the width of n$^+$-layer is z_n^+, the width of the n-layer is z_n and the width of the depletion region between the n- and n$^+$-layer is w_b. The width of this depletion region is $w_{b,n}$ into the n-layer and w_{b,n^+} into the n$^+$-layer. The total hole current at the

edge of the undepleted n-layer is the sum of the contributions from the n^+-layer, the n-layer and the depleted region between the n^+- and n-layer

$$J_{p,total}(z_i) = J_{p,n^+}(z_i) + J_{p,n}(z_i) + J_{p,dep}(z_i). \tag{4.15}$$

If no recombination at the n-n^+ junction is assumed and recombination in the n^+-layer is linear, equation (2.54) may be used for the hole current at $z = z_i$ after some modifications. One has to multiply with $e^{-(\alpha(z_p^+ + z_i) + \alpha_w z_w)}$ and replace S_p with an effective surface recombination velocity given as

$$S_{p,nn^+,eff} = \frac{D_p^+}{L_p^+}\frac{N_d}{N_d^+}\left\{\frac{K_p^+\cosh\left(\frac{l_n^+}{L_p^+}\right) + \sinh\left(\frac{l_n^+}{L_p^+}\right)}{K_p^+\sinh\left(\frac{l_n^+}{L_p^+}\right) + \cosh\left(\frac{l_n^+}{L_p^+}\right)}\right\}, \tag{4.16}$$

due to the back surface field. l_n in equation (2.54) has to be replaced with the width of the undepleted n-layer $l_n^{'} \equiv z_n - w_{b,n}$. In equation (4.16) $l_n^+ \equiv z_n^+ - w_{b,n^+}$, N_d^+ is the doping of the n^+-layer, $K_p^+ \equiv \frac{S_p^+ L_p^+}{D_p^+}$ where S_p^+ is the rear surface recombination velocity of the n^+-layer and L_p^+ and D_p^+ are the diffusion length and diffusion coefficient in the n^+-layer, respectively [3]. The hole current at the edge of the undepleted n^+-layer ($z = z_i + z_n + w_{b,n^+}$) is found using the continuity equation for holes when only diffusion current and linear recombination are considered, given in equation (2.48) and the boundary conditions

$$D_p^+\frac{d\Delta p}{dz} = S_p^+\Delta p \quad \text{for} \quad z = (z_i + z_n + z_n^+), \tag{4.17}$$

and

$$\Delta p_{(z+)} = \Delta p_{(z-)}e^{-(qV_{nn^+}/k_BT)} \quad \text{for} \quad z = (z_i + z_n - w_{b,n}) \tag{4.18}$$

where $z-$ expresses a small displacement from $z = (z_i + z_n + z_n^+)$ in the negative z-direction and $z+$ a small displacement in the positive z-direction. V_{nn^+} is the built-in voltage of the n^+-n junction and has the form [29]

$$V_{nn^+} = \frac{k_BT}{q}\ln\left(\frac{N_d^+}{N_d}\right) \tag{4.19}$$

in equilibrium. It is assumed that no voltage appears over the n^+-n junction when we are out of equilibrium, meaning that the effective surface recombination velocity is constant for various voltages. Band gap narrowing in the heavily doped n^+-layer is neglected.

The result obtained is

$$J_{p,n^+}(z_i + z_n + w_{b,n^+}) = -F_{n-1}\int\left[\frac{q(1-R)F\alpha L_p^+}{(\alpha^2(L_p^+)^2 - 1)}e^{-(\alpha(z_p^+ + z_p + z_i + z_n + w_{b,n^+}) + \alpha_w z_w)}\right]\times \left\{\frac{(K_p^+ - \alpha L_p^+)e^{-\alpha l_n^+} - \left(K_p^+\cosh(\frac{l_n^+}{L_p^+}) + \sinh(\frac{l_n^+}{L_p^+})\right)}{K_p^+\sinh(\frac{l_n^+}{L_p^+}) + \cosh(\frac{l_n^+}{L_p^+})} + \alpha L_p^+\right\}dE \tag{4.20}$$

Here

$$F_{n-1} \equiv \frac{1}{1+\frac{N_d^+ S_{p,nn^+,eff}}{N_d S_{p,n^+n,eff}}} \tag{4.21}$$

where

$$S_{p,n^+n,eff} \equiv \frac{D_p}{L_p}\frac{N_d^+}{N_d}\coth\left(\frac{l_n'}{L_p}\right). \tag{4.22}$$

$S_{p,n^+n,eff}$ is the effective surface recombination velocity at the edge of the undepleted n^+-layer and reflects how light-generated holes may be extracted from the n^+ region [27].

Considering recombination in the n-layer and neglecting recombination in the depletion region between the n^+- and n-layer the hole contribution at $z = z_i$ is

$$J_{p,n^+}(z_i) = J_{p,n^+}(z_n + w_{b,n^+})\cosh^{-1}\left(\frac{l_n'}{L_p}\right). \tag{4.23}$$

In the depletion region between the n^+- and n-layer no recombination is assumed and all photons absorbed are expected to generate one electron-hole pair. The contribution at $z = z_i$ is taken as [27]

$$J_{p,dep}(z_i) = \int q(1-R)Fe^{-(\alpha(z_p^+ + z_p + z_i + z_n - w_{b,n}) + \alpha_w z_w)}\left(1-e^{-\alpha w_b}\right)dE\cosh^{-1}\left(\frac{l_n'}{L_p}\right). \tag{4.24}$$

The length of the depletion region into the lightly doped n-region is taken from [30] and used as an approximation for w_b

$$w_b \approx \sqrt{\frac{2\epsilon k_B T}{q^2 N_d}}\arctan\left(\frac{qV_{nn^+}}{k_B T}\sqrt{\frac{N_d^+}{2N_d}}\right). \tag{4.25}$$

Since the n^+-layer is placed near the rear surface where the photon concentration is small, the contribution from the n^+-layer to the total current is expected to be much smaller than the contribution from the p^+ layer.

4.1.6 Total current for a p-i-n reference cell with a depleted i-layer

The total current in the reference cell is given as

$$J_{ref} = -J_{n,total}(0) - J_{p,total}(z_i) - J_i \tag{4.26}$$

following the same sign convention as in chapter 2, and the current-voltage characteristic of the reference solar cell with a depleted i-layer is obtained. The current can be divided into a dark current $J_{dark,ref}$ dependent on the voltage and a photocurrent $J_{light,ref}$ dependent on the light where

$$J_{light,ref} = q\int F(E)(QE_{p^+} + QE_p + QE_{pp^+,dep} + QE_i + QE_n + QE_{n^+} + QE_{nn^+,dep})dE. \tag{4.27}$$

Here QE_{p^+} is the quantum efficiency of the p$^+$-layer given from equation (4.11), QE_p is the quantum efficiency of the p-layer given from equation (2.58) after multiplying with $e^{-[\alpha(z_p^+ + w_{a,p}) + \alpha_w z_w]}$ and replacing K_n with $K_n{}' \equiv \frac{S_{n,pp^+,eff} L_n}{D_n}$ and l_p with l_p', $QE_{pp^+,dep}$ is the quantum efficiency of the depletion region between the p$^+$-layer and the p-layer given from equation (4.12), QE_i is the quantum efficiency of the i-layer given from equation (4.1), QE_n is the quantum efficiency of the n-layer given from equation (2.59) after multiplying with $e^{-(\alpha(z_p^+ + z_i) + \alpha_w z_w)}$ and replacing K_p with $K_p{}' \equiv \frac{S_{p,nn^+,eff} L_p}{D_p}$ and l_n with l_n', QE_{n^+} is the quantum efficiency of the n$^+$-layer given from equation(4.23) and $QE_{nn^+,dep}$ is the quantum efficiency of the depletion region between the n$^+$- and n-layer given from equation (4.24).

The dark current is given as

$$J_{dark,ref} = J_{0,ref}(e^{qV/k_B T} - 1) + J_{i,0} \frac{\pi \sinh(qV/2k_B T)}{q(V_0 - V)/k_B T} \tag{4.28}$$

where

$$\begin{aligned} J_{0,ref} \equiv \frac{q D_p p_0}{L_p} &\left\{ \frac{K_p' \cosh(\frac{l_n'}{L_p}) + \sinh(\frac{l_n'}{L_p})}{K_p' \sinh(\frac{l_n'}{L_p}) + \cosh(\frac{l_n'}{L_p})} \right\} \\ + \frac{q D_n n_0}{L_n} &\left\{ \frac{K_n' \cosh(\frac{l_p'}{L_n}) + \sinh(\frac{l_p'}{L_n})}{K_n' \sinh(\frac{l_p'}{L_n}) + \cosh(\frac{l_p'}{L_n})} \right\}. \end{aligned} \tag{4.29}$$

4.2 Model of a reference cell with a flat band i-layer

The quantum dots in an intermediate band solar cell should, as explained, be placed in a flat band region between a p- and a n-layer. How to obtain a flat band region and how it affects the current-voltage characteristic of the reference cell are studied in this section. By having a model for both a reference cell with a flat band region and a quantum dot solar cell with quantum dots placed in the flat band region it is possible to see how the introduction of quantum dots affect the behavior of the solar cell.

The maximum width of a fully depleted i-layer depends on the background doping of the i-layer. For a i-layer thicker than the width of the depletion region a flat band of width w_F is obtained, as shown in figure 4.3. Here w_{ip} is the width of the depletion region between the p- and i-layer, and w_{in} is the width of the depletion region between the i- and n-layer. Both of these widths are dependent on voltage. The background doping in the i-layer is assumed p-type since this is typical for MBE grown GaAs.[31]. By assuming a p-type background doping the width of the depletion region between the i- and n-layer is given as [31]

$$w_{in}^2 = \frac{2\epsilon N_d}{q} \frac{(V_{ni} - V_n)}{N_i^2 + N_d N_i} \tag{4.30}$$

where V_{ni} is the built-in potential of the i-n junction equal to [3]

$$V_{ni} = \frac{k_B T}{q} \ln\left(\frac{N_d N_i}{n_i^2}\right) \tag{4.31}$$

and V_n is the part of the applied voltage V that appears over the i-n junction. The applied voltage V is the sum of the voltage V_p over the p-i junction and the voltage V_n over the i-n junction

$$V = V_p + V_n. \tag{4.32}$$

From equation (4.30) it is seen that the depletion region width decreases with applied voltage.

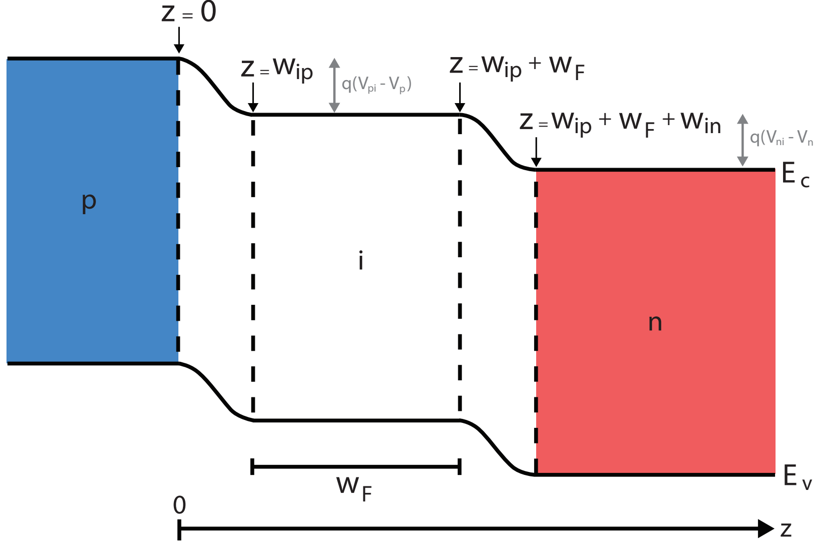

Figure 4.3: The p-i-n junction of the reference cell with parts of the i-layer placed in a flat band region. w_{ip} is the width of the depletion region between the p- and the i-layer, w_{in} is the width of the depletion region between the i- and the n-layer and w_F is the width of the flat band. All these widths are dependent on the voltage across the cell.

The width of the depletion region between the p- and i-layer is given as [30]

$$w_{ip} \approx \sqrt{\frac{2\epsilon k_B T}{q^2 N_i}} \arctan\left(\frac{q(V_{pi} - V_p)}{k_B T}\sqrt{\frac{N_a}{2N_i}}\right) \tag{4.33}$$

where V_{pi} is the built-in potential of the p-i junction equal to [29]

$$V_{pi} = \frac{k_B T}{q} \ln\left(\frac{N_a}{N_i}\right). \tag{4.34}$$

From equation (4.31) and (4.34) it is seen that the sum of the built-in voltages over the p-i- and i-n junction is equal to the built-in potential of the p-n junction given in equation (2.41).

Based on [32] and the Fletcher boundary conditions in [33] the electron and hole densities at $z = w_{ip} + w_F + w_{in} = z_i$, see figure 4.3, are given as

$$\Delta n(z_i) = \Delta p(z_i) = \frac{n_{0,i} + p_{0,n} e^{-q(V_{ni}-V_n)/k_B T}}{1 - e^{-2q(V_{ni}-V_n)/k_B T}} \left(e^{qV_n/k_B T} - 1 \right) \tag{4.35}$$

where $n_{0,i}$ is the equilibrium electron concentration in the i-layer and $p_{0,n}$ is the equilibrium hole concentration in the n-layer.

If we assume that there is no recombination in the depletion regions the electron and hole densities at $z = 0$ are given as

$$\Delta n(0) = \Delta p(0) = \frac{p_{0,i} + n_{0,p} e^{-q(V_{pi}-V_p)/k_B T}}{1 - e^{-2q(V_{pi}-V_p)/k_B T}} \left(e^{qV_p/k_B T} - 1 \right) \tag{4.36}$$

where $p_{0,i}$ is the equilibrium hole concentration in the i-layer and $n_{0,p}$ is the equilibrium electron concentration in the p-layer [32]. Since $p_{0,i} >> n_{0,p}$ for a p-type background doping equation (4.36) may be written

$$\Delta n(0) = \Delta p(0) = \frac{p_{0,i} \left(e^{qV_p/k_B T} - 1 \right)}{1 - e^{-2q(V_{pi}-V_p)/k_B T}}. \tag{4.37}$$

By assuming that the voltage over the i-n junction does not saturate when the i-layer is p-type background doped we have that $V_{ni} - V_n > \frac{k_B T}{q}$ and one can assume that $n_{0,i} >> p_{0,n} e^{-q(V_{ni}-V_n)/k_B T}$. Equation (4.35) may then be written

$$\Delta n(z_i) = \Delta p(z_i) = n_{0,i} e^{qV_n/k_B T} \tag{4.38}$$

for $qV_n/k_B T >> 1$.

By assuming a constant excess carrier concentration in the region $0 < z < w_{ip} + w_F + w_{in}$, meaning that the i-layer has to be so narrow that photons are absorbed throughout the whole i-layer, we have that

$$\Delta p(0) = \Delta p(z_i) \tag{4.39}$$

giving

$$n_{0,i} e^{q(V-V_p)/k_B T} = \frac{p_{0,i} \left(e^{qV_p/k_B T} - 1 \right)}{1 - e^{-2q(V_{pi}-V_p)/k_B T}} \tag{4.40}$$

using equation (4.32),(4.37) and (4.38). Solving the second order equation given in equation (4.40) gives

$$e^{-qV_p/k_B T} = \frac{1}{2} \left(-B + \sqrt{B^2 + 4C} \right) \tag{4.41}$$

where

$$B = \frac{p_{0,i}}{n_{0,i}} e^{-qV/k_B T} = \frac{N_i^2}{n_i^2} e^{-qV/k_B T} \tag{4.42}$$

and

$$C = B + e^{-2qV_{pi}/k_B T}. \tag{4.43}$$

V_p and V_n are then determined as function of applied voltage. The condition $qV_n/k_B T >>$

1 is not fulfilled for small voltages, but as a simplification equation (4.41) is used to determine V_p and V_n at all voltages.

When the i-layer is wider than the minimum depletion width $w_{ip_{min}}+w_{in_{min}}$, obtained for the maximum applied forward voltage which is equal to the open-circuit voltage, we obtain a flat band. The electric field in the flat band region is approximately equal to zero, meaning that the charge carriers have to diffuse across this part of the i-layer. This clearly affects the current-voltage characteristic of the reference cell, and will be studied below.

The charge carrier concentrations n and p in the flat band region are found using the continuity equations for electron and holes given in equation (2.45) and (2.46). The recombination in undoped regions is expected to be dominated by non-radiative Shockley Read Hall recombination given in equation (2.21), which may be written

$$U_{SRH} = \frac{p_0\Delta n + n_0\Delta p + \Delta n\Delta p}{\tau_{n,SRH}(p_0 + \Delta p) + \tau_{p,SRH}(n_0 + \Delta n)} \tag{4.44}$$

by assuming $p_0+\Delta p >> n_i e^{(E_i-E_t)/k_BT}$ and $n_0+\Delta n >> n_i e^{(E_t-E_i)/k_BT}$ in the flat band region. The equilibrium concentrations n_0 and p_0 in an intrinsic material are small and is therefore reasonable to assume that $\Delta n >> n_0$ and $\Delta p >> p_0$. Using this assumption and the condition that $\Delta p = \Delta n$, the excess non-radiative recombination rate in the intrinsic flat band region is obtained as

$$U_{SRH_i} = \frac{\Delta n}{\tau_{n,i,SRH} + \tau_{p,i,SRH}} = \frac{\Delta p}{\tau_{n,i,SRH} + \tau_{p,i,SRH}}, \tag{4.45}$$

In the numerical calculations the non-radiative lifetimes $\tau_{n,i,SRH}$ and $\tau_{p,i,SRH}$ are taken to be the same as for a fully depleted i-layer.

The excess radiative recombination rate in the intrinsic flat band region U_{rad_i} will from equation (2.15) and for $\Delta n >> n_0$ and $\Delta p >> p_0$ take the form

$$U_{rad_i} = B_{rad}\Delta n\Delta p = B_{rad}\Delta n^2 = B_{rad}\Delta p^2, \tag{4.46}$$

which is non-linear in Δn and Δp. The continuity equations for electrons and holes will by including the excess radiative recombination rate have to be solved numerically, which is beyond the scope of this thesis. An ideal reference cell where recombination is dominated by radiative processes can therefore not be modeled.

Considering only diffusion current in the flat band region, the electron and hole concentrations in the flat band region ($0<z<w_F$) are given as

$$\frac{d^2\Delta n}{dz^2} - \frac{\Delta n}{L_{n,i}^2} + \frac{\int g(E,z)dE}{D_{n,i}} = 0 \quad \text{for} \quad w_{ip} < z < w_F + w_{ip} \tag{4.47}$$

and

$$\frac{d^2\Delta p}{dz^2} - \frac{\Delta p}{L_{p,i}^2} + \frac{\int g(E,z)dE}{D_{p,i}} = 0 \quad \text{for} \quad w_{ip} < z < w_F + w_{ip}, \tag{4.48}$$

respectively, where $D_{n,i}$ and $D_{p,i}$ are the electron and hole diffusion coefficients in the i-layer, and $L_{n,i}^2 \equiv D_{n,i}(\tau_{n,i,SRH} + \tau_{p,i,SRH})$ and $L_{p,i}^2 \equiv D_{p,i}(\tau_{n,i,SRH} + \tau_{p,i,SRH})$ are the electron and hole diffusion lengths in the i-layer, respectively. $g(E,z)$ is given in equation

(2.10).

The boundary conditions for electrons and holes are using equation (2.3),(2.4), (2.35) and (2.36) taken as

$$\Delta n = n_0 \left\{ e^{[F_n(w_{ip}+w_F)-E_i]/k_BT} - 1 \right\} \quad \text{for} \quad z = w_{ip} + w_F \tag{4.49}$$

$$\Delta p = p_0 \left\{ e^{[E_i-F_p(w_{ip})]/k_BT} - 1 \right\} \quad \text{for} \quad z = w_{ip} \tag{4.50}$$

$$D_{n,i}\frac{d\Delta n}{dz} = \frac{1}{q}J_{np} \quad \text{for} \quad z = w_{ip}, \tag{4.51}$$

$$-D_{p,i}\frac{d\Delta p}{dz} = \frac{1}{q}J_{pn} \quad \text{for} \quad z = w_{ip} + w_F, \tag{4.52}$$

where J_{np} is the electron current from the p-layer and J_{pn} is the hole current from the n-layer. $[E_i - F_p(w_{ip})]$ is the difference between the intrinsic Fermi level and the quasi-Fermi level for holes at $z = w_{ip}$ and $[F_n(w_{ip} + w_F) - E_i]$ is the difference between the intrinsic Fermi level and the quasi-Fermi level for electrons at $z = w_{ip} + w_F$. The quasi-Fermi energy levels are related through

$$F_n(w_{ip} + w_F) - F_p(w_{ip}) = qV. \tag{4.53}$$

The total current density is given as the sum of the hole and electron current densities and is constant throughout the device. On the edge of the flat band close to the p-layer the current density is given by

$$J = -[J_{np}(w_{ip}) + J_p(w_{ip})], \tag{4.54}$$

and on the edge of the flat band close to the n-layer the current density is given by

$$J = -[J_{pn}(w_{ip} + w_F) + J_n(w_{ip} + w_F)] \tag{4.55}$$

following the same sign convention as used for the standard solar cell.

Using equation (4.47) and the boundary conditions given in equation (4.49) and (4.51) the electron current density at $z = w_{ip} + w_F$ is equal to

$$\begin{aligned} J_n(w_{ip} + w_F) = \int & \left[\frac{q(1-R)Fe^{-(\alpha(z_p^+ + z_p) + \alpha_w z_w)}\alpha L_{n,i}}{(\alpha^2 L_{n,i}^2 - 1)} \right] \\ & \times \left\{ \frac{e^{-\alpha w_F}\sinh(\frac{w_F}{L_{n,i}}) - \alpha L_{n,i}}{\cosh(\frac{w_F}{L_{n,i}})} + \alpha L_{n,i} e^{-\alpha w_F} \right\} dE \\ & + \frac{qD_{n,i}n_0(e^{(F_n(w_F)-E_i)/k_BT} - 1)}{L_{n,i}} \left\{ \frac{\sinh(\frac{w_F}{L_{n,i}})}{\cosh(\frac{w_F}{L_{n,i}})} \right\} + \frac{J_{np}}{\cosh\left(\frac{w_F}{L_{n,i}}\right)} \end{aligned} \tag{4.56}$$

which has the same form as the electron diffusion current in the p-layer given in equation (2.53) when the surface recombination velocity is set equal to zero. The hole current density at $z = w_{ip}$ is found using equation (4.48) and the boundary conditions in equation

(4.50) and (4.52) and is equal to

$$\begin{aligned} J_p(w_{ip}) = & \int \left[\frac{q(1-R)Fe^{-(\alpha(z_p^+ + z_p)+\alpha_w z_w)}\alpha L_{p,i}}{(\alpha^2 L_{p,i}^2 - 1)} \right] \\ & \times \left\{ \frac{\alpha L_{p,i} e^{-\alpha w_F} + \sinh(\frac{w_F}{L_{p,i}})}{\cosh(\frac{w_F}{L_{p,i}})} - \alpha L_{p,i} \right\} dE \\ & + \frac{q D_{p,i} p_0 (e^{(E_i - F_p(0))/k_B T} - 1)}{L_{p,i}} \left\{ \frac{\sinh(\frac{w_F}{L_{p,i}})}{\cosh(\frac{w_F}{L_{p,i}})} \right\} + \frac{J_{pn}}{\cosh\left(\frac{w_F}{L_{p,i}}\right)} \end{aligned} \tag{4.57}$$

which has the same form as the hole diffusion current in the n-layer given in equation (2.54) when the surface recombination velocity is set equal to zero.

The electron current density from the p-layer is given by

$$J_{np}(w_{ip}) = J_{n,total}(0) + J_{dep,pi}, \tag{4.58}$$

where $J_{n,total}(0)$ is the total electron current density from the p^+- and p-layer and the depletion region between the p$^+$- and p-layer, given in equation (4.3). $J_{dep,pi}$ is the net electron current density from the depletion region between the p-layer and the flat band region assumed to have the same form as in equation (2.62) for the standard solar cell and is given by

$$\begin{aligned} J_{dep,pi} = & -\int q(1-R)Fe^{-(\alpha(z_p^+ + z_p)+\alpha_w z_w)} \left(1 - e^{-\alpha w_{ip}}\right) \\ & + \frac{q n_i w_{ip}}{\sqrt{\tau_{n,i,SRH}\tau_{p,i,SRH}}} \frac{\pi \sinh(qV_p/2k_BT)}{q(V_{pi} - V_p)/k_BT}. \end{aligned} \tag{4.59}$$

The hole current density from the n-layer is given by

$$J_{pn}(w_{ip} + w_F) = J_{p,total}(z_i) + J_{dep,in}, \tag{4.60}$$

where $J_{p,total}(z_i)$ is the total hole current from the n^+- and n-layer and the depletion region between the n- and n$^+$-layer given in equation (4.15). $J_{dep,in}$ is the net hole current density from the depletion region between the n-layer and the flat band region given by

$$\begin{aligned} J_{dep,in} = & -\int q(1-R)Fe^{-(\alpha(z_p^+ + z_p + z_i)+\alpha_w z_w)} \left(1 - e^{-\alpha w_{in}}\right) \\ & + \frac{q n_i w_{in}}{\sqrt{\tau_{n,i,SRH}\tau_{p,i,SRH}}} \frac{\pi \sinh(qV_n/2k_BT)}{q(V_{ni} - V_n)/k_BT}. \end{aligned} \tag{4.61}$$

The current-voltage characteristic of the reference cell with a flat band region is obtained by simultaneous solving of equation (4.54) and (4.55) for the current density together with the relation between the quasi-Fermi levels given in equation (4.53). Since the width of the flat band and the depletion regions are dependent on voltage the photocurrent is dependent on voltage, and the total current density can not be divided into an independent photocurrent and dark-current as in section 4.1.

Chapter 5

Model of the intermediate band solar cell

The intermediate band solar cell structure is the same as the structure of the p-i-n reference cell shown in figure 4.1 with quantum dots placed in the i-layer. In this chapter two models of the intermediate band solar cell are presented. The simple model is based on [34]. It only includes the contribution from the intermediate band layer and the width of the flat band region is assumed equal to the thickness of the intermediate band layer for all voltages. The complete model takes all layers (ARC, window, p^+, p, i, IB, n and n^+) into account and includes the voltage dependency of the width of the flat band region. The complete model is developed in this thesis. In section 5.2 only radiative recombination is included in the flat band region of the intermediate band layer. In section 5.4 non-radiative recombination is also included.

5.1 Intermediate band solar cell design

The p- and n-layers in the intermediate band solar cell studied in this thesis are in figure 5.1 shown together with the region in between where the intermediate band layer is placed. The upper p-layer is followed by an intrinsic layer of width $w_{ip,min}$. $w_{ip,min}$ is the minimum width of the depletion region between the p-layer and the intrinsic layer found from equation (4.33) by setting V_p equal to a voltage $V_{max,p}$ equal to the open-circuit voltage over the p-i junction. This intrinsic layer is included since we want most of the intermediate band layer to be contained in a flat band region. For all voltages the width $w_{ip,min}$ close to the p-layer is depleted, and it is then not necessary to have an intermediate band layer here.

After the intrinsic layer of width $w_{ip,min}$ follows an intermediate band material of width w_{IB}, and we then have a second intrinsic layer of width $w_{in,min}$. $w_{in,min}$ is the minimum width of the depletion region between the n-layer and the i-layer found from equation (4.30) by setting V_n equal to a voltage $V_{max,n}$ equal to the open-circuit voltage over the i-n junction. Finally the n-layer is placed below the intrinsic material.

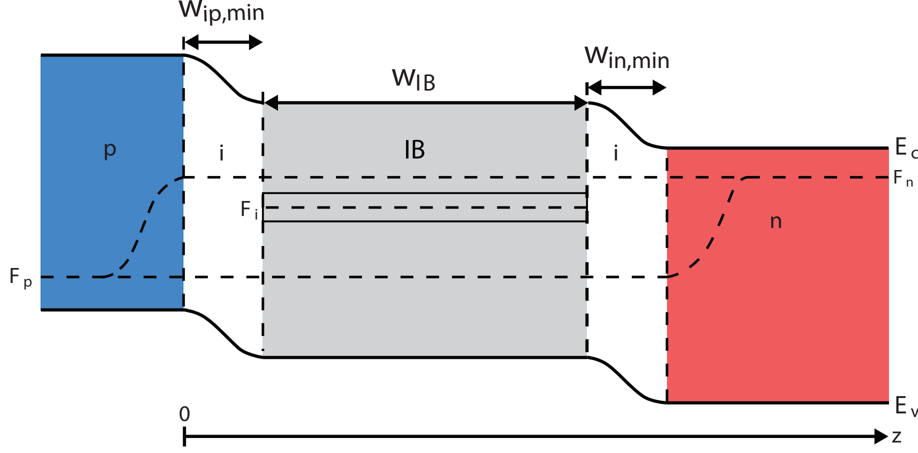

Figure 5.1: The structure of the forward biased intermediate band solar cell used in the modeling. Also shown are the quasi-Fermi level F_c of the electrons in the conduction band, the quasi-Fermi level F_i of the electrons in the intermediate band and the quasi-Fermi level F_p of the holes in the valence band.

The widths of the depleted regions of the p-i and i-n junction, w_{ip} and w_{in}, are dependent on voltage and is taken from from equation (4.33) and (4.30) neglecting any effect the intermediate band material may have on these widths. When the thicknesses of the i-layers are equal to $w_{ip,min}$ and $w_{in,min}$ the i-layers on the p- and n-side are depleted at all voltages. The part of the intermediate band material contained in the depleted regions near the p-layer and the n-layer is in the models assumed to behave like an intrinsic material with no quantum dots since the quantum dots in these regions are completely full or empty of electrons. Only the part of the intermediate band material that is in the flat band region is taken to follow the behavior of an intermediate band material, i.e. as presented below.

5.2 Intermediate band solar cell with only radiative recombination in the flat band region

The electron and hole concentrations in the conduction band and valence band are influenced by the presence of an intermediate band. The electron concentration in the conduction band in an intermediate band material equals $n = \Delta n + n_{0,IB}$, where $n_{0,IB}$ is the equilibrium electron concentration in the conduction band and Δn is the optically generated electron concentration. n can be expressed as

$$\begin{aligned} n &= N_C e^{-[(E_c - F_i)/k_B T]} e^{(F_n - F_i)/k_B T} \\ &= n_{0,\mathrm{IB}} e^{\mu_{CI}/k_B T}, \end{aligned} \tag{5.1}$$

where the last equality only holds if the quasi-Fermi level F_i of the intermediate band is pinned to its equilibrium position E_I [7]. N_C is the effective density of states in the conduction band and

$$n_{0,\mathrm{IB}} \equiv N_C e^{-E_L/k_B T}. \tag{5.2}$$

In the same way the hole concentration in the valence band in an intermediate band material equals $p = \Delta p + p_{0,IB}$, where $p_{0,IB}$ is the equilibrium hole concentration in the valence band and Δp is the optically generated hole concentration. p can be expressed as

$$\begin{aligned} p &= N_V e^{-[(F_i - E_v)/k_B T]} e^{(F_i - F_p)/k_B T} \\ &= p_{0,\mathrm{IB}} e^{\mu_{IV}/k_B T}, \end{aligned} \tag{5.3}$$

where N_V is the effective density of states in the valence band and

$$p_{0,\mathrm{IB}} \equiv N_V e^{-E_H/k_B T}. \tag{5.4}$$

The introduction of an intermediate band makes it necessary to consider the generation rates for both valence band to conduction band transitions $G_{CV}(z)$, intermediate band to conduction band transitions $G_{CI}(z)$ and valence band to intermediate band transitions $G_{IV}(z)$. The generation rates depend on the absorption coefficient for the specific transition through the relations

$$G_{CV}(z) = \int_{E_G}^{\infty} [1 - R(E)] \alpha_{CV}(E) F(E) e^{-\alpha_{CV}(E) z} dE, \tag{5.5}$$

$$G_{CI}(z) = \gamma \int_{E_L}^{E_H} [1 - R(E)] \alpha_{CI}(E) F(E) e^{-\alpha_{CI}(E) z} dE \tag{5.6}$$

and

$$G_{IV}(z) = \gamma \int_{E_H}^{E_G} [1 - R(E)] \alpha_{IV}(E) F(E) e^{-\alpha_{IV}(E) z} dE. \tag{5.7}$$

F(E) is the flux of photons which may be taken as the black-body spectrum of the sun or as the Air Mass 1.5 spectrum, given in section 6.2. The absorption coefficients for the different transitions are taken to be non-overlapping which gives the integration limits in equation (5.5-5.7). This is the same assumption used in section 3.4 describing ideal behavior. The γ factor in equation (5.6) and (5.7) is a number describing to what extent electrons are confined at the quantum dots. When the electron wave functions in the quantum dots do not penetrate into the barrier region it is given by

$$\gamma = \frac{3}{4}\pi \left(\frac{r_d}{d}\right)^3 \tag{5.8}$$

where r_d is the radius of the quantum dot and d is the distance between the dots [35]. When the wave functions do penetrate into the barrier and it is equally likely to find an electron in the quantum dots as in the barriers $\gamma = 1$. The ideal situation is encountered when $\gamma = 1$ and this is assumed in this model.

The generation of charge carriers due to photon recycling is omitted in the model. Photon recycling is the process where photons generated by radiative recombination are reabsorbed in the material to generate charge carriers. This process is omitted in the model of the reference cell and is also omitted here.

In the limiting case the only recombination process included is radiative recombination. By having an intermediate band three radiative recombination processes are possible:

- Recombination between the conduction band and the valence band
- Recombination between the conduction band and the intermediate band
- Recombination between the intermediate band and the valence band

The excess radiative recombination rate between the conduction band and the intermediate band is from equation (2.12) and (2.13) for $n_r = 1$ equal to

$$\begin{aligned} U_{rad,CI} &= \int_{E_L}^{E_H} r_{sp}(E, \mu_{CI})dE - \int_{E_L}^{E_H} r_{sp}(E, 0)dE \\ &= \frac{8\pi}{h^3 c^2} \int \alpha_{CI}(E) \left[\frac{E^2}{e^{(E-\mu_{CI})/k_B T} - 1} - \frac{E^2}{e^{E/k_B T} - 1} \right] dE. \end{aligned} \tag{5.9}$$

By considering the Fermi level of the intermediate band F_i clamped to its equilibrium position E_I and using the approximation

$$\frac{E^2}{e^{(E-\mu_{CI})/k_B T} - 1} \approx e^{-(E-\mu_{CI})/k_B T} E^2 \tag{5.10}$$

valid when $E_L - \mu_{CI} >> k_B T$ one obtains

$$\begin{aligned} U_{rad,CI} &= \frac{8\pi}{h^3 c^2} \int \alpha_{CI}(E) e^{-E/k_B T} E^2 \left(e^{\mu_{CI}/k_B T} - 1 \right) dE \\ &= \frac{8\pi}{h^3 c^2} \frac{\Delta n}{n_{0,IB}} \int \alpha_{CI}(E) e^{-E/k_B T} E^2 dE \\ &= B_{rad,CI} N_{Dp} \Delta n \end{aligned} \tag{5.11}$$

using equation (5.1), and $n_{0,IB}$ is given by equation (5.2). $B_{rad,CI}$ is the radiative recombination coefficient for conduction band to intermediate band transitions and N_{Dp} is the density of empty states in the intermediate band. Their product is defined as

$$B_{rad,CI} N_{Dp} \equiv \frac{1}{n_{0,\mathrm{IB}}} \frac{8\pi}{h^3 c^2} \int_{E_L}^{E_H} \alpha_{CI}(E) E^2 e^{-E/k_B T} dE. \tag{5.12}$$

In the same way the excess radiative recombination rate between the conduction band and the valence band and between the intermediate band and the valence band are

$$U_{rad,CV} = B_{rad,CV} \Delta n \Delta p \tag{5.13}$$

and

$$U_{rad,IV} = B_{rad,IV} N_{Dn} \Delta p, \tag{5.14}$$

where N_{Dn} is the density of occupied states in the intermediate band and $B_{rad,CV}$ and $B_{rad,IV}$ are the radiative recombination coefficients for the different recombination processes. The products are defined as

$$B_{rad,CV} \equiv \frac{1}{p_{0,\mathrm{IB}} n_{0,\mathrm{IB}}} \frac{8\pi}{h^3 c^2} \int_{E_G}^{\infty} \alpha_{CV}(E) E^2 e^{-E/k_B T} dE \tag{5.15}$$

and

$$B_{rad,IV}N_{Dn} \equiv \frac{1}{p_{0,\mathrm{IB}}}\frac{8\pi}{h^3c^2}\int_{E_H}^{E_G} \alpha_{IV}(E)E^2e^{-E/k_BT}dE. \tag{5.16}$$

Equation (5.12) and (5.16) are valid only when the quasi-Fermi energy level F_i of the intermediate band is pinned to its equilibrium position E_I. The assumption of pinning of the intermediate band quasi-Fermi energy level together with the assumption that the quasi-Fermi energy levels of the valence and conduction bands do not penetrate their respective bands, i.e. they are in the band gap, give absorption coefficients independent of z. This gives radiative recombination rates independent of position z.

Including only diffusion current in the flat band region where the intermediate band material is placed the electron and hole concentrations in the flat band region ($w_{ip} < z < w_F + w_{ip}$) are given as

$$D_{n,f}\frac{d^2\Delta n}{dz^2} - B_{rad,CI}N_{Dp}\Delta n - B_{rad,CV}\Delta n\Delta p + G_{CV} + G_{CI} = 0 \quad \text{for} \quad w_{ip} < z < w_F + w_{ip} \tag{5.17}$$

and

$$D_{p,f}\frac{d^2\Delta p}{dz^2} - B_{rad,IV}N_{Dn}\Delta p - B_{rad,CV}\Delta n\Delta p + G_{CV} + G_{IV} = 0 \quad \text{for} \quad w_{ip} < z < w_F + w_{ip}, \tag{5.18}$$

respectively, where $D_{n,f}$ is the electron diffusion coefficient for electrons in the conduction band and $D_{p,f}$ is the hole diffusion coefficient for holes in the valence band in the intermediate band material. The validity of the approximation of only including diffusion current in the intermediate band material may be checked [34] looking the current density of carriers in the intermediate band J_{ib} given by

$$\frac{1}{q}J_{ib} = G_{CI} - G_{IV} - U_{rad,CI} + U_{rad,IV} \tag{5.19}$$

which is zero only on the edges of the intermediate band material, at $z = w_{ip}$ and $z = w_{ip} + w_F$. This current density is related to an electric field $\mathscr{E}(z)$ by the relation

$$J_{ib} = q\mu_{ib}N_D\mathscr{E}(z) \tag{5.20}$$

where μ_{ib} is the mobility in the intermediate band and N_D is the density of dots. To be able to ignore the drift current of electrons in the conduction band and holes in the valence band the electric field has to be small. As can be seen from equation (5.20) this implies that the product of the density of dots and the mobility of the intermediate band has to be large. The model used in this thesis is thus only valid when this product is large or when the generation and recombination rates are uniform with z which makes J_{ib} very small.

The boundary conditions for the electron and hole concentration in the intermediate band material at the edge of the flat band region are

$$\Delta n = n_{0,\mathrm{IB}}(e^{\mu_{CI}(w_{ip}+w_F)/k_BT} - 1) \quad \text{for} \quad z = w_{ip} + w_F, \tag{5.21}$$

$$\Delta p = p_{0,\mathrm{IB}}(e^{(\mu_{IV}(w_{ip})/k_BT} - 1) \quad \text{for} \quad z = w_{ip}, \tag{5.22}$$

$$D_{n,f}\frac{d\Delta n}{dz} = \frac{1}{q}J_{np} \quad \text{for} \quad z = w_{ip} \tag{5.23}$$

and

$$-D_{p,f}\frac{d\Delta p}{dz} = \frac{1}{q}J_{pn} \quad \text{for} \quad z = w_{ip} + w_F, \tag{5.24}$$

see figure 4.3. As in section 4.2 J_{np} is the electron current coming from the p-layer and J_{pn} is the hole current coming from the n-layer. In the simplest model J_{np} and J_{pn} are set equal to zero, meaning that the generation and recombination in these layers are set equal to zero. The boundary conditions for the electron and holes in the flat band region in the intermediate band material are almost identical to the boundary conditions for the electron and hole concentration in the flat band region in the i-layer of the p-i-n reference cell given in equation (4.49-4.52), but when an intermediate band is present it is the Fermi level of the intermediate band that determines the concentration of electron and holes.

The difference between the quasi-Fermi energy level of the intermediate band and the valence band μ_{IV} at $z = w_{ip}$ and the difference between the quasi-Fermi energy level of the conduction band and the intermediate band μ_{CI} at $z = w_{ip} + w_F$ are related through

$$\mu_{IV}(w_{ip}) + \mu_{CI}(w_{ip} + w_F) = qV. \tag{5.25}$$

Equation (5.17) and (5.18) may be solved analytically if $B_{rad,CV}\Delta n\Delta p$ is much lower than $B_{rad,CI}N_{Dp}\Delta n$ and $B_{rad,IV}N_{Dn}\Delta p$. Then the non-linear term $B_{rad,CV}\Delta n\Delta p$ may be omitted. It is found that $B_{rad,CV}\Delta n\Delta p << B_{rad,IV}N_{Dn}\Delta p, B_{rad,CI}N_{Dp}\Delta n$ in cases relevant for obtaining the maximum efficiency [34], and it is assumed that this holds in all cases used in the modeling in this thesis.

The electron and hole concentrations then follow the same behavior as in the flat band region in reference cell, and the hole current density $J_{p,IB}$ at $z = w_{ip}$ is given by

$$\begin{aligned} J_{p,IB}(w_{ip}) = &\int_{E_H}^{E_G} \left[\frac{q(1-R)Fe^{-(\alpha(z_p^+ + z_p)+\alpha_w z_w)}\alpha_{IV}L_{p,IB}}{(\alpha_{IV}^2 L_{p,IB}^2 - 1)}\right] \\ &\times \left\{\frac{\alpha_{IV}L_{p,IB}e^{-\alpha_{IV}w_F} + \sinh(\frac{w_F}{L_{p,IB}})}{\cosh(\frac{w_F}{L_{p,IB}})} - \alpha_{IV}L_{p,IB}\right\} dE \\ &+ \int_{E_G}^{\infty} \left[\frac{q(1-R)Fe^{-(\alpha(z_p^+ + z_p)+\alpha_w z_w)}\alpha_{CV}L_{p,IB}}{(\alpha_{CV}^2 L_{p,IB}^2 - 1)}\right] \\ &\times \left\{\frac{\alpha_{CV}L_{p,IB}e^{-\alpha_{CV}w_F} + \sinh(\frac{w_F}{L_{p,IB}})}{\cosh(\frac{w_F}{L_{p,IB}})} - \alpha_{CV}L_{p,IB}\right\} dE \\ &+ \frac{qD_{p,i}p_0(e^{\mu_{IV}/k_BT} - 1)}{L_{p,IB}}\left\{\frac{\sinh(\frac{w_F}{L_{p,IB}})}{\cosh(\frac{w_F}{L_{p,IB}})}\right\} + \frac{J_{pn}}{\cosh\left(\frac{w_F}{L_{p,i}}\right)} \end{aligned} \tag{5.26}$$

where $L_{p,IB}^2 \equiv \frac{D_{p,f}}{B_p N_{Dn}}$. The electron current density $J_{n,IB}$ at $z = w_{ip} + w_F$ is given by

$$\begin{aligned}
J_{n,IB}(w_{ip} + w_F) = & \int_{E_L}^{E_H} \left[\frac{q(1-R)Fe^{-(\alpha(z_p^+ + z_p) + \alpha_w z_w)} \alpha_{CI} L_{n,IB}}{(\alpha_{CI}^2 L_{n,IB}^2 - 1)} \right] \\
& \times \left\{ \frac{e^{-\alpha_{CI} w_F} \sinh(\frac{w_F}{L_{n,IB}}) - \alpha_{CI} L_{n,IB}}{\cosh(\frac{w_F}{L_{n,IB}})} + \alpha_{CI} L_{n,IB} e^{-\alpha_{CI} w_F} \right\} dE \\
& + \int_{E_G}^{\infty} \left[\frac{q(1-R)Fe^{-(\alpha(z_p^+ + z_p) + \alpha_w z_w)} \alpha_{CV} L_{n,IB}}{(\alpha_{CV}^2 L_{n,IB}^2 - 1)} \right] \\
& \times \left\{ \frac{e^{-\alpha_{CV} w_F} \sinh(\frac{w_F}{L_{n,IB}}) - \alpha_{CV} L_{n,IB}}{\cosh(\frac{w_F}{L_{n,IB}})} + \alpha_{CV} L_{n,IB} e^{-\alpha_{CV} w_F} \right\} dE \\
& + \frac{q D_{n,i} n_0 (e^{\mu_{CI}/k_B T} - 1)}{L_{n,IB}} \left\{ \frac{\sinh(\frac{w_F}{L_{n,IB}})}{\cosh(\frac{w_F}{L_{n,IB}})} \right\} + \frac{J_{np}}{\cosh\left(\frac{w_F}{L_{n,IB}}\right)}
\end{aligned} \tag{5.27}$$

where $L_{n,IB}^2 \equiv \frac{D_{n,f}}{B_n N_{Dp}}$.

The current-voltage characteristic of the solar cell is found by simultaneous solving

$$J = -(J_{np}(w_{ip}) + J_{p,IB}(w_{ip})) \tag{5.28}$$

and

$$J = -(J_{pn}(w_{ip} + w_F) + J_{n,IB}(w_{ip} + w_F)) \tag{5.29}$$

for the current density together with the relation between the quasi-Fermi level splits given in equation (5.25). $J_{np}(w_{ip})$ and $J_{pn}(w_{ip} + w_F)$ are given in equation (4.58) and (4.60), respectively.

5.3 Modeled cases

As mentioned two different models of the intermediate band solar cell are used. In the simple model, the width of the flat band does not depend on voltage and is always equal to w_{IB}, and J_{pn} and J_{np} are set equal to zero. The p- and n-layer are then present only to separate the electrons and holes to avoid recombination. The window-, p^+- and n^+-layer used in the reference cell to maximize the currents from the p- and n-layer are then not important. In the complete model J_{pn} and J_{np} is calculated, and all the layers of the reference cell are important. In the complete model the variation of the flat band width with voltage is included.

5.4 Intermediate band solar cell including both radiative and non-radiative recombination in the flat band region

In the limiting case only radiative recombination is included in the intermediate band material. Non-radiative recombination is present unless in the limit of perfect materials [3], and it has to be included in a more realistic model. Data for quantum dot solar cell prototypes grown by molecular beam epitaxy indicates that recombination is dominated by non-radiative processes possibly caused by defects at the interfaces between the dot and barrier material [36]. In this section non-radiative recombination is included in the model of the intermediate band solar cell.

The non-radiative recombination processes present in an intermediate band material are:

- Non-radiative recombination between the conduction band and the valence band
- Non-radiative recombination between the conduction band and the intermediate band
- Non-radiative recombination between the intermediate band and the valence band

The excess non-radiative recombination rate between the conduction band and the valence band is in the intermediate band material having the rate

$$U_{SRH,CV} = \frac{\Delta n \Delta p}{\tau_{n,CV,SRH}\Delta p + \tau_{p,CV,SRH}\Delta n} \tag{5.30}$$

where $\tau_{n,CV,SRH}$ and $\tau_{p,CV,SRH}$ are the electron and hole non-radiative lifetimes for conduction band to valence band transitions. Equation (5.30) is obtained by using (2.21) and that $\Delta n >> n_{0,IB}$, $\Delta p >> p_{0,IB}$, $p_{0,IB} + \Delta p >> n_i e^{(E_i - E_t)/k_B T}$ and $n_{0,IB} + \Delta n >> n_i e^{(E_t - E_i)/k_B T}$ in the flat band region. The excess non-radiative recombination rate between the conduction band and the intermediate band is from equation (2.21) given by

$$U_{SRH,CI} = \frac{nN_{Dp} - n_{0,IB}N_{Dp0}}{\tau_{n,CI,SRH}(N_{Dp} + n_i e^{(E_i - E_t)/k_B T}) + \tau_{p,CI,SRH}(n + n_i e^{(E_t - E_i)/k_B T})} \tag{5.31}$$

using $N_{Dp} = N_{Dp0} + \Delta N_{Dp}$, where N_{Dp0} is the density of empty states in the intermediate band at equilibrium and ΔN_{Dp} is the change in the density of empty states in the intermediate band when the solar cell is illuminated. $\tau_{n,CI,SRH}$ and $\tau_{p,CI,SRH}$ are the electron and hole non-radiative lifetimes for conduction band to intermediate band transitions.

N_{Dp0} is a very large number when the intermediate band is half-filled with electrons, and it is therefore reasonable to assume $N_{Dp0} >> \Delta N_{Dp}$. This assumption is fulfilled when the Fermi level in the intermediate band is equal to the equilibrium Fermi-level, an assumption used throughout the whole derivation of the model. Using this assumption together with $\Delta n >> n_{0,IB}$, $N_{Dp} >> n_i e^{(E_i - E_t)/k_B T}$ and $n >> n_i e^{(E_t - E_i)/k_B T}$, the

excess non-radiative recombination rate may be written

$$U_{SRH,CI} = \frac{\Delta n N_{Dp0}}{\tau_{n,CI,SRH} N_{Dp0} + \tau_{p,CI,SRH} \Delta n} \tag{5.32}$$

By assuming a high density of states in the intermediate band in such a way that $N_{Dp0} > \Delta n$ the non-radiative recombination rate may be simplified further giving

$$U_{SRH,CI} = \frac{\Delta n}{\tau_{n,CI,SRH}}. \tag{5.33}$$

By having a half-filled intermediate band the density of filled states in the intermediate band at equilibrium is equal to the density of quantum dots. The last equation is therefore valid only for a high density of quantum dots. The excess non-radiative recombination rate between the intermediate band and the valence band is given by

$$U_{SRH,IV} = \frac{N_{Dn} p - N_{Dn0} p_{0,IB}}{\tau_{n,IV,SRH}(p + n_i e^{(E_i - E_t)/k_B T}) + \tau_{p,IV,SRH}(N_{Dn} + n_i e^{(E_t - E_i)/k_B T})} \tag{5.34}$$

using $N_{Dn} = N_{Dn0} + \Delta N_{Dn}$, where N_{Dn0} is the density of filled states in the intermediate band at equilibrium and ΔN_{Dn} is the change in the density of filled states in the intermediate band when the solar cell is illuminated. $\tau_{n,IV,SRH}$ and $\tau_{p,IV,SRH}$ are the electron and hole non-radiative lifetimes for intermediate band to valence band transitions, N_{Dn0} is the density of filled states in the intermediate band at equilibrium and ΔN_{Dn} is the change in the density of filled states in the intermediate band when the solar cell is illuminated. By assuming $N_{Dn0} >> \Delta N_{Dn}$, $\Delta p >> p_{0,IB}$, $p >> n_i e^{(E_i - E_t)/k_B T}$, $N_{Dn} >> n_i e^{(E_t - E_i)/k_B T}$ and $N_{Dn0} > \Delta p$ the excess non-radiative recombination rate between the intermediate band and the valence band may be written

$$U_{SRH,IV} = \frac{\Delta p}{\tau_{p,IV,SRH}} \tag{5.35}$$

The excess non-radiative recombination rate between the conduction band and the valence band given in equation (5.30) is non-linear in Δn and Δp. When the non-radiative lifetimes for conduction band to valence band transitions are much larger than non-radiative lifetimes for the conduction band to intermediate band and intermediate band to valence band transitions, the non-radiative recombination rate between the conduction band and the valence band may be neglected. Analytical solutions of equation (5.17) and (5.18) may then be obtained. Since the lifetimes for conduction band to intermediate band transitions and for intermediate band to valence band transitions are in experiments found to be very small [13], the non-radiative recombination rate between the conduction band and the valence band is neglected in this model.

The hole current density at $z = w_{ip}$ is given by (5.26) and the electron current density at $z = w_{ip} + w_F$ by (5.27), by using $L^2_{p,IB'} = \frac{D_{p,f}}{B_{rad,IV} N_{Dn} + \frac{1}{\tau_{p,IV,SRH}}}$ and $L^2_{n,IB'} = \frac{D_{n,f}}{B_{rad,CI} N_{Dp} + \frac{1}{\tau_{n,CI,SRH}}}$ instead of $L^2_{p,IB}$ and $L^2_{n,IB}$. The same form of the current-voltage characteristic as when only radiative recombination is considered is then obtained, just with other numerical factors.

Chapter 6

Material and sample parameters

As is clear from the preceding chapters several material parameters are involved in the expressions determining the current-voltage charactersitc of a solar cell. To obtain the current-voltage characteristic for a specific solar cell numerical values for all these parameters must be known. The numerical values can either be measured for the solar cell in question or data has to be taken from litterature. In this thesis data from literature is used, and in this chapter material parameters are given. In section 6.1 parameters for GaAs and $Al_xGa_{1-x}As$ are given, and in section 6.2 the solar spectrum used in the modeling is presented. The thicknesses and doping concentrations of the layers in the solar cell samples used in the modeling are given in section 6.3.

6.1 Material parameters

The solar cells considered in this thesis are made of InAs, GaAs and $Al_xGa_{1-x}As$. In this section material parameters like band gap, carrier concentration, mobility, lifetime etc. of these materials are given.

6.1.1 Band structure and effective density of states

Both $Al_xGa_{1-x}As$ and GaAs crystallize in the zinc blende structure with similar lattice constants, the lattice mismatch is only 0.12 % [18]. This means that $Al_xGa_{1-x}As$ can be grown on GaAs without strain, an important fact because we then avoid formation of dislocations which would increase the recombination [9].

The band structure of GaAs is shown in figure 6.1, showing that the top of the Γ_8 valence band and the bottom of the Γ_6 conduction band are at the same position in k-space, at the Γ point. This means that GaAs is a direct band gap semiconductor and phonons are not necessary in the absorption process. The temperature dependent band gap of GaAs is given as [37]

$$E_{GaAs}(T) = \left[1.519 - \frac{5.405 \times 10^{-4} T^2}{T + 204}\right] eV. \qquad (6.1)$$

The temperature used in this thesis is 300 K.

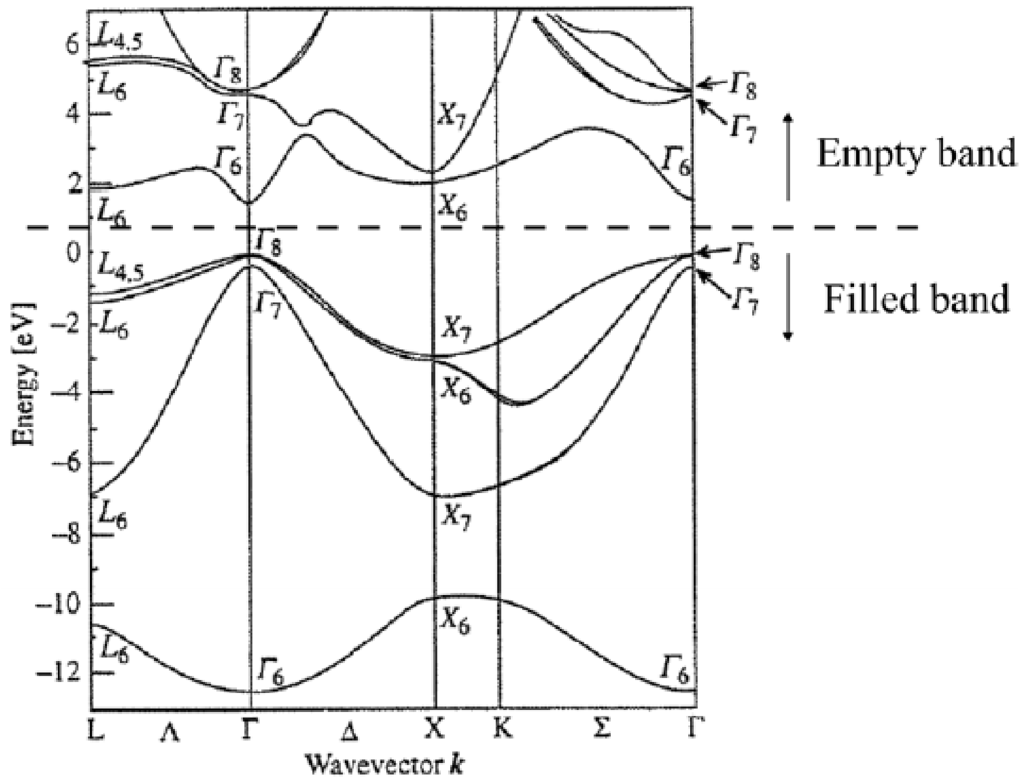

Figure 6.1: Band structure of GaAs plotted as function of wave vector.

For $Al_xGa_{1-x}As$ the positions of the lowest conduction bands, the Γ, L and X bands are dependent on x, and $Al_xGa_{1-x}As$ is a direct band gap semiconductor for $x < 0.45$. The band gap for $x < 0.45$ is given as [38]

$$E_{Al_xGa_{1-x}As} = E_{GaAs} + 1.247x. \tag{6.2}$$

$Al_xGa_{1-x}As$ is an indirect band gap semiconductor for $x \geq 0.45$ with a band gap given as

$$E_{Al_xGa_{1-x}As} = 1.911 + 0.005x + 0.245x^2 \tag{6.3}$$

at room temperature [38].

The effective densities of states in the conduction and valence band in GaAs are given as $N_C = 4.7 \times 10^{17}$ cm^{-3} and $N_V = 7.0 \times 10^{18}$ cm^{-3}, respectively [39]. The intrinsic carrier concentration n_i of GaAs is at 300 K equal to 1.79×10^6 cm^{-3} [39].

The effective densities of states in the conduction band N_C and valence band N_V in $Al_xGa_{1-x}As$ is as function of x given as [9]

$$N_C(x) = 2\left[\frac{2\pi m_e^*(x)k_BT}{h^2}\right]^{3/2} \tag{6.4}$$

$$N_V(x) = 2\left[\frac{2\pi\left\{m_{hh}^*(x)^{3/2} + m_{lh}^*(x)^{3/2}\right\}^{2/3} k_BT}{h^2}\right]^{3/2} \tag{6.5}$$

where m_e^*, m_{lh}^* and m_{hh}^* are the effective electron mass, light hole mass and heavy hole mass for $Al_xGa_{1-x}As$ given as [37]

$$m_e^*(x) = (0.0632 + 0.0856x + 0.0231x^2)m_0 \tag{6.6}$$

$$m_{hh}^*(x) = (0.50 + 0.2x)m_0 \tag{6.7}$$

$$m_{lh}^*(x) = (0.088 + 0.0372x + 0.0163x^2)m_0 \tag{6.8}$$

for x<0.45, where m_0 is the electron mass. The intrinsic carrier concentration of $Al_xGa_{1-x}As$ is as function of x given as [9]

$$n_i(x) = \sqrt{N_C(x)N_V(x)}e^{-E_{Al_xGa_{1-x}As}/2k_BT}. \tag{6.9}$$

The permittivity of GaAs has a temperature dependence given by

$$\epsilon = \left[12.79(1 + 1.0 \times 10^{-4}T)\right]\epsilon_0 \tag{6.10}$$

where ϵ_0 is the permittivity of free space [40]. The permittivity of $Al_xGa_{1-x}As$ is given as [37]

$$\epsilon = (13.1 - 2.2x)\epsilon_0. \tag{6.11}$$

at 300 K.

6.1.2 Absorption coefficient and reflectivity

Data for the absorption coefficient of GaAs are taken from [41], which gives measured data for single crystal GaAs at room temperature for various photon energies. To obtain the absorption coefficient for photon energies different than the ones given in [41], the absorption coefficient values are interpolated using piecewise polynomial interpolation since the absorption coefficient is expected to vary as $\sqrt{E - E_G}$ for direct transitions. Higher transitions involving other bands and points in k-space are possible for energies higher than their characteristic band gaps. This will contribute with peaks in the absorption function [42]. The data together with the interpolated curve are shown in figure 6.2.

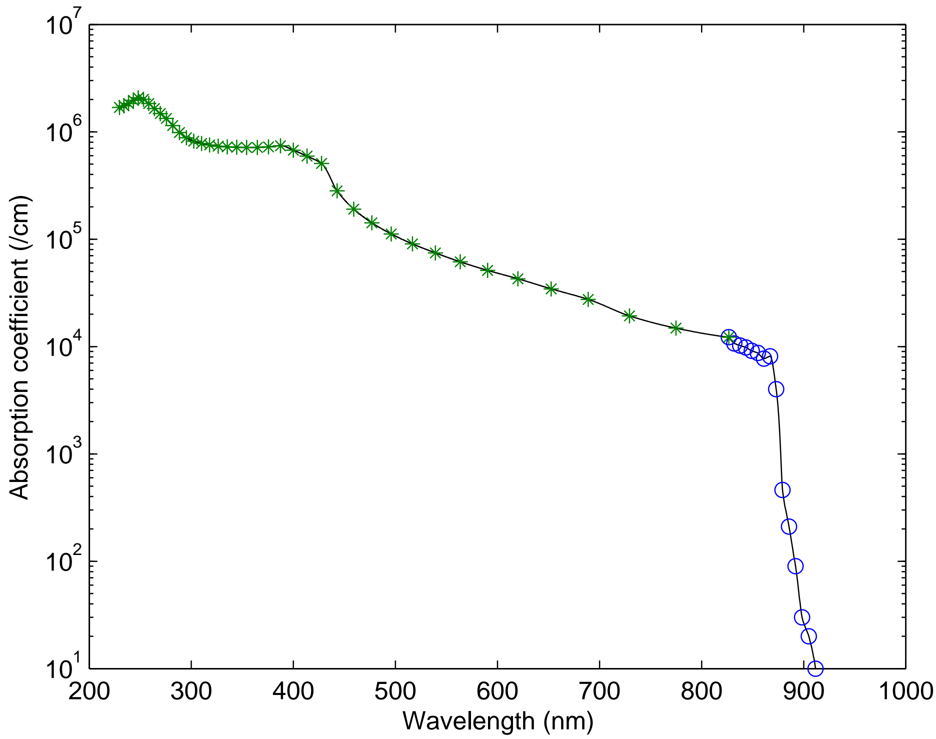

Figure 6.2: Interpolated absorption coefficient (solid line) of GaAs plotted together with measured data (stars,circles) from [41].

Data for the absorption coefficient for $Al_xGa_{1-x}As$ are given for a limited number of aluminum contents x and are not accurate enough around the band edge. Different methods can be used to approximate the absorption coefficient and they are discussed in [43]. I used the same method preferred in [43], which is to use the values for the absorption coefficient for GaAs, but with a non-linear shift of the energy axis decreasing with increasing energy. This is a reasonable method since the absorption spectrum of $Al_xGa_{1-x}As$ for $x < 0.45$ is expected to resemble that of GaAs, but shifted because of the different band gap. At high energies, $E > 3.5$ eV, the absorption should be nearly independent of x which explains the use of a decreasing energy shift [44]. The absorption coefficient $\alpha_x(E_x)$ of $Al_xGa_{1-x}As$ is then given from the absorption coefficient $\alpha_0(E_{GaAs})$ of GaAs as

$$\alpha_x(E_x) \approx \alpha_0(E_{GaAs}) \tag{6.12}$$

where

$$E_x = E_{GaAs} + 1.247x - Ax(E_{GaAs} - E_{g(GaAs)})^n \left(\frac{1}{e^{-B(E_{GaAs} - E_{g(GaAs)})} + 1} \right) \tag{6.13}$$

using equation (6.2). The values used for A, n and B are 0.62, 0.5 and 10 respectively [43]. The resulting form of the absorption coefficient is showed in figure 6.3 for $x = 0.35$ showing that the absorption coefficient for GaAs is greater than the absorption coefficient for $Al_{0.35}Ga_{0.65}As$ at the wavelengths considered here.

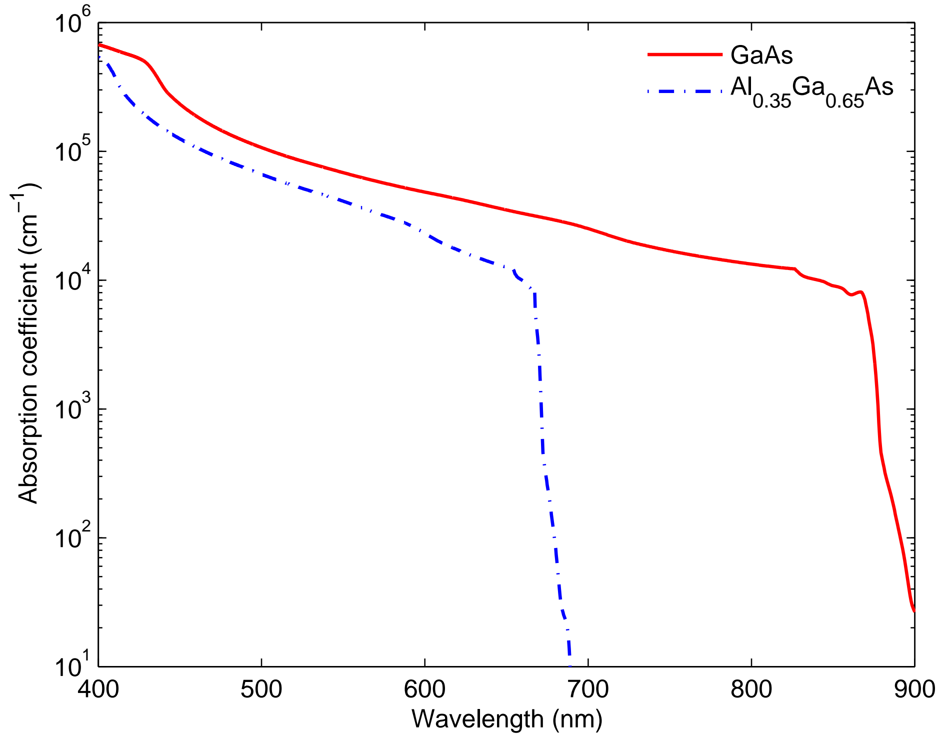

Figure 6.3: The absorption coefficient of $Al_{0.35}Ga_{0.65}As$ (solid line) using a non-linear energy shift together with the absorption coefficient of GaAs (dash-dot line).

The absorption coefficient of the $Al_{0.85}Ga_{0.15}As$ window layer α_{window} can not be found using equation (6.12) since $Al_{0.85}Ga_{0.15}As$ is an indirect band gap semiconductor in contrast to GaAs. The absorption coefficient of the window layer is taken as the average of the absorption coefficients $\alpha_y(E_y)$ of $Al_{0.804}Ga_{0.196}As$ and $Al_{0.900}Ga_{0.100}As$, $y = 0.804$ or $y = 0.900$, after using a linear shift on the energy axis

$$\alpha_{window}(E_w) = \alpha_y(E_y) \tag{6.14}$$

where

$$E_w = E_y + (0.005 \times 0.85) + (0.245 \times 0.85^2) - (0.005y + 0.245y^2). \tag{6.15}$$

using equation (6.3). The values of the absorption coefficients of $Al_{0.804}Ga_{0.196}As$ and $Al_{0.900}Ga_{0.100}As$ are given in [38] which gives measured data for the absorption coefficient at room temperature for various photon energies. The absorption coefficient values are interpolated in the same way as the absorption coefficient of GaAs. The resulting absorption coefficient is shown in figure 6.4, which shows that the window layer absorbs at wavelengths equal to 550 nm and shorter.

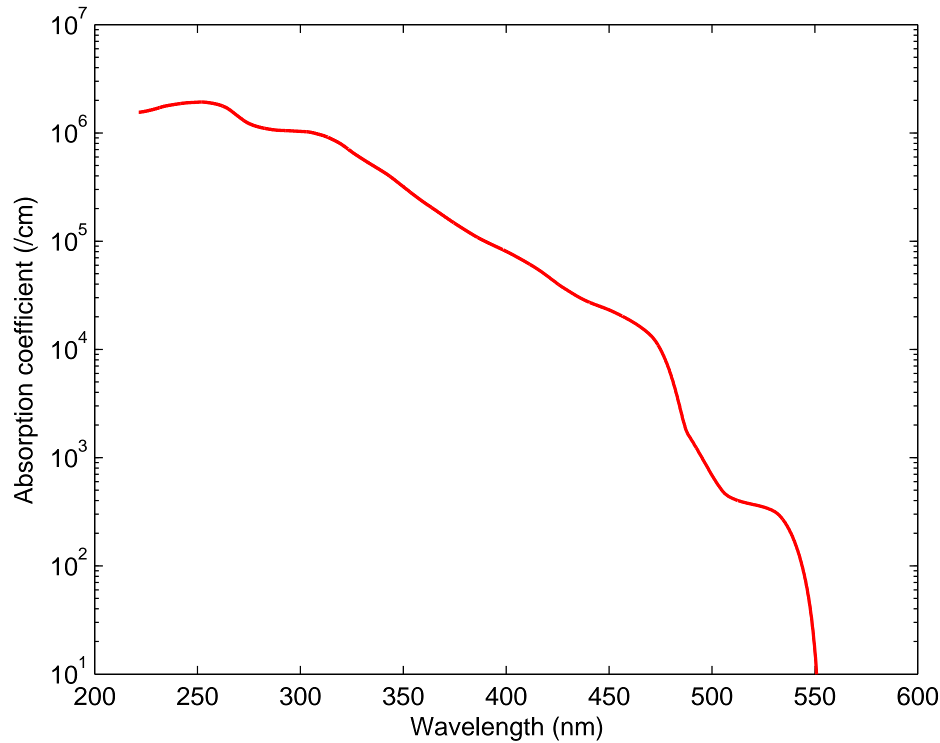

Figure 6.4: The absorption coefficient of the $Al_{0.85}Ga_{0.15}As$ window layer.

The reflectivity of the GaAs cap when no anti-reflective coating is present are taken from [41].

6.1.3 Mobilities, lifetimes and surface recombination velocities

The diffusion coefficients are found using the Einstein relation for the diffusion coefficient and mobility given in equation (2.42). The mobilities depend on the doping concentration of the material. A plot of the theoretical minority and majority electron mobility in doped GaAs is shown in figure 6.5 as a function of doping concentration together with experimental data. Here it is seen that the minority and majority mobility are not equal. For doping concentrations lower than $2 \times 10^{19}\text{cm}^{-3}$ the majority carrier mobility is higher than the minority carrier mobility, while for greater concentrations the roles are reversed [40].

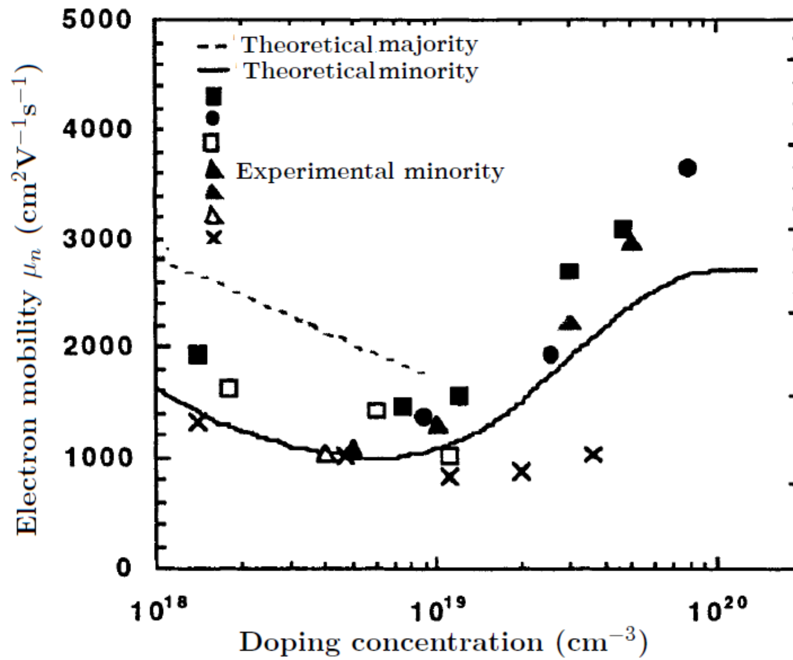

Figure 6.5: Electron mobility as function of doping concentration at 300 K. The solid line is the theoretical minority carrier mobility. The dashed line is the theoretical majority carrier mobility. The circles, squares, crosses and triangles are experimental minority carrier mobility [40].

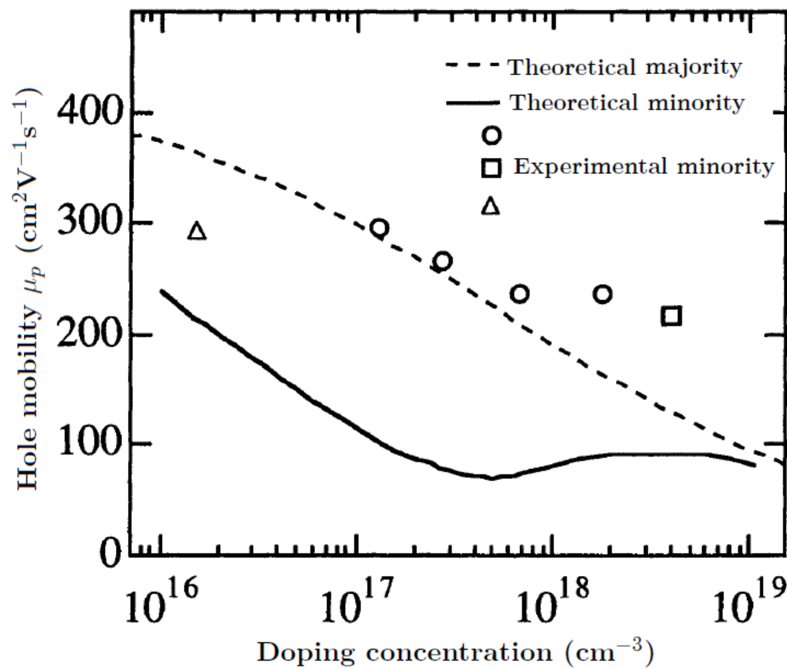

Figure 6.6: Hole mobility as function of doping concentration at 300 K. The dashed line is the theoretical majority carrier mobility. The solid line is the theoretical minority carrier mobility. The circles, squares and triangles are experimental minority carrier mobility [40].

A plot of the theoretical majority and minority hole mobility in doped GaAs as function of doping concentration is shown in figure 6.6 together with experimental data. The experimental data show that the minority hole mobility is greater than the majority hole mobility for doping concentrations greater than $1.5 \times 10^{17}\text{cm}^{-3}$.

The minority carrier mobilities for the given doping concentrations are found using the experimental data given in figure 6.5 and 6.6. The electron mobility in undoped GaAs is given as 8000 $\text{cm}^2/(\text{Vs})$ and the hole mobility in undoped GaAs as 400 $\text{cm}^2/(\text{Vs})$ [45].

The majority hole mobility of $\text{Al}_x\text{Ga}_{1-x}\text{As}$ is shown in figure 6.7 as function of the aluminium content x for doping concentrations 1.5×10^{17} to 2.5×10^{17} cm^{-3} and 1.5×10^{18} to 2.5×10^{18} cm^{-3}. The majority electron mobility for various doping concentrations and aluminium contents is shown in figure 6.8.

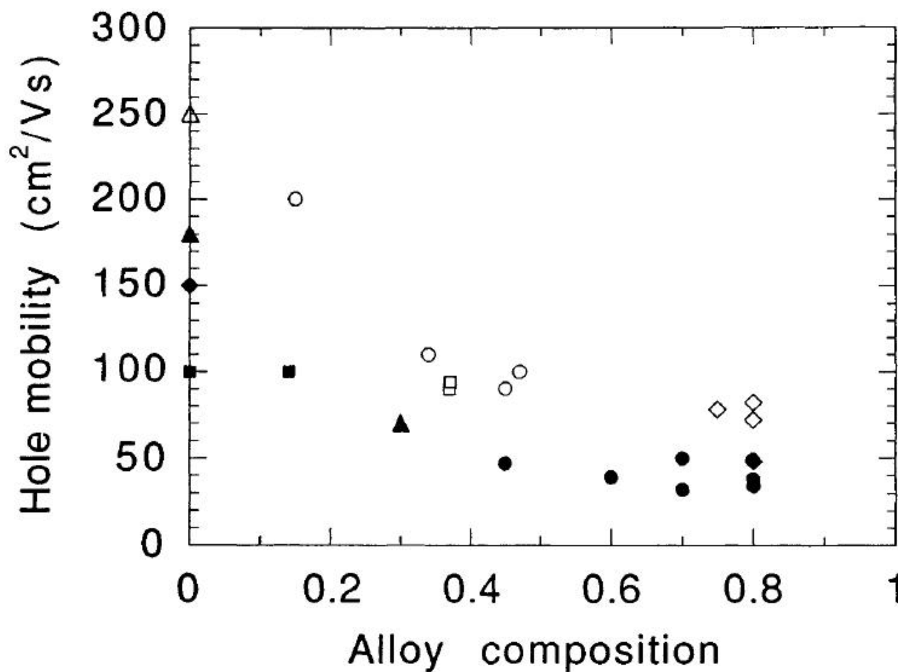

Figure 6.7: Experimental majority hole mobilities as function of aluminiuim content for two different doping concentration ranges: $1.5 \times 10^{17} \rightarrow 2.5 \times 10^{17}$ cm^{-3} open symbols, $1.5 \times 10^{18} \rightarrow 2.5 \times 10^{18}$ cm^{-3} filled symbols [38].

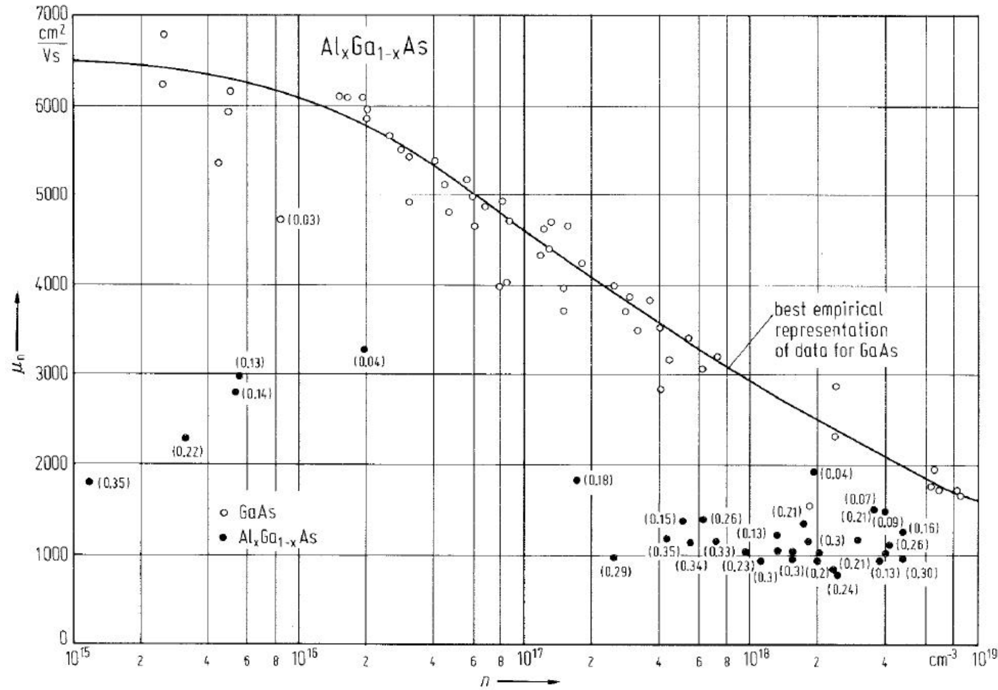

Figure 6.8: Majority electron mobility for various aluminum contents as function of doping concentration [46].

The minority carrier mobilities for the given doping concentrations are taken as equal to the majority carrier mobilities given in figure 6.7 and 6.8 due to the difficulty of finding values for the minority carrier mobility in $Al_xGa_{1-x}As$. The mobility in undoped $Al_xGa_{1-x}As$ is found from figure 6.7 and 6.8 from the lowest doping concentrations given there.

The diffusion lengths are found from the electron and hole diffusion coefficients and their lifetimes using the relation $L = D\tau$. The electron and hole lifetimes in GaAs are dependent on the lifetimes for radiative recombination, Shockely Read Hall recombination and Auger recombination [40]

$$\frac{1}{\tau} = \frac{1}{\tau_{rad}} + \frac{1}{\tau_{SRH}} + \frac{1}{\tau_{Aug}}. \tag{6.16}$$

The electron lifetime in p-doped GaAs is shown in figure 6.9 as function of doping concentration. The experimental data are the resulting lifetime for all the mentioned recombination mechanisms, while the solid line shows the theoretical radiative limit. The electron lifetimes are generally given by

$$\tau_n = \frac{1}{BN_a} \tag{6.17}$$

where in the radiative limit B is equal to 1.0×10^{-10} cm^3/s. The growth technique of the material is not important for the electron lifetime [40].

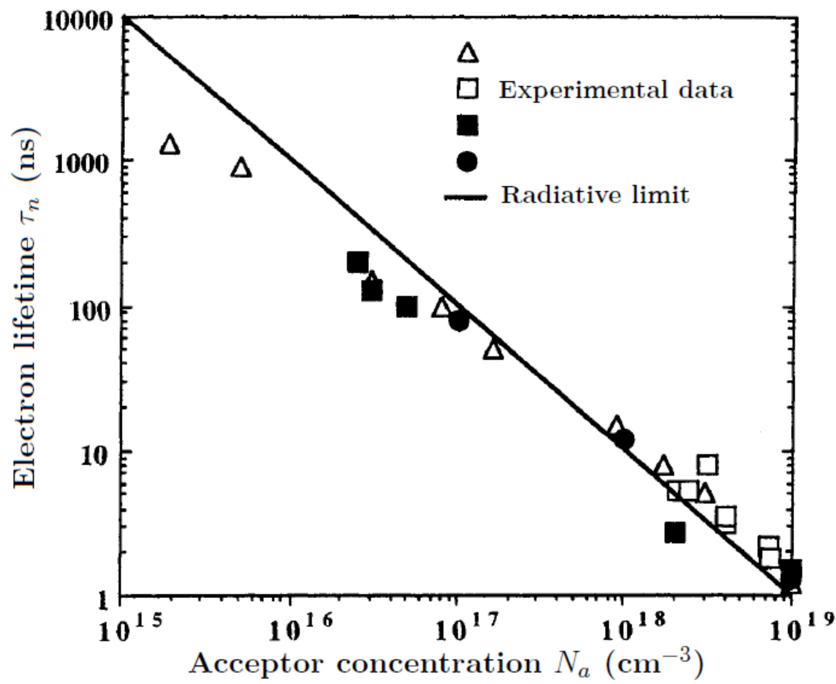

Figure 6.9: Electron lifetime in p-doped GaAs. The solid line is the radiative limit. The squares, circles and triangles are experimental data [40].

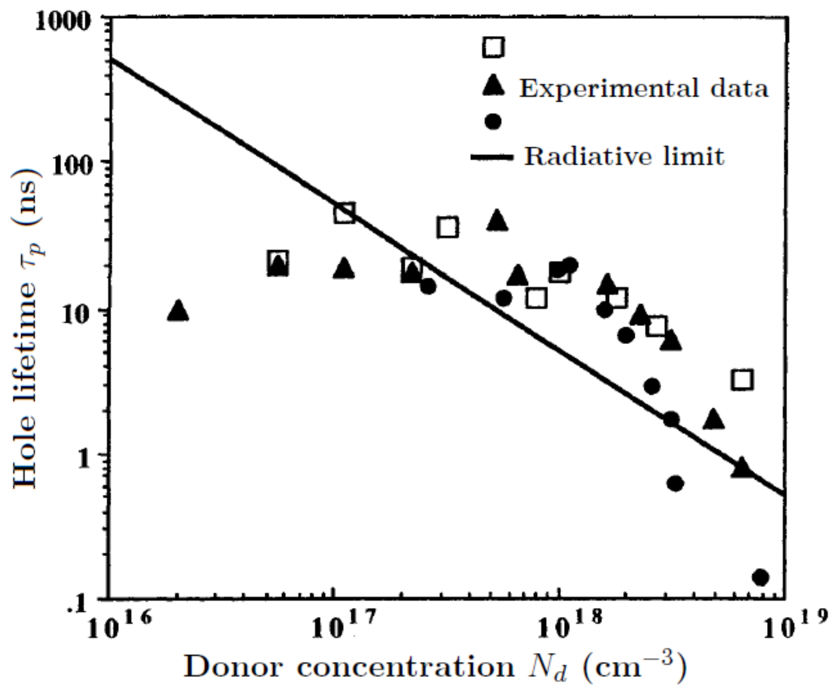

Figure 6.10: Hole lifetime in n-doped GaAs grown by LPE. The solid line is the radiative limit. The squares, circles and triangles are experimental data [40].

In figure 6.10 the hole lifetime in n-doped GaAs grown by liquid phase epitaxy (LPE) is shown as function of donor concentration. The theoretical radiative limit is shown by the straight line obtained from

$$\tau_p = \frac{1}{BN_d} \tag{6.18}$$

for B equal to 2.0×10^{-10} cm^3/s [40]. The lifetimes should not exceed this radiative limit. As shown in figure 6.10 this happens in n-doped GaAs for doping levels higher than 10^{18} cm^{-3}. One explanation is that B changes with doping concentration and is not well known for n-type GaAs. Another explanation is photon recycling which gives longer lifetimes.

In figure 6.11 the hole lifetime in n-doped GaAs grown by metal-organic chemical vapor deposition (MOCVD) is shown as function of donor concentration. The radiative limit line is the same as in figure 6.10. In figure 6.11 all the experimental lifetimes are larger than those given from the radiative limit. This indicates photon recycling. As can be seen from figure 6.10 and 6.11 the hole lifetime is not equal for the two growth methods. The samples used in the modeling in this thesis are grown by molecular beam epitaxy, and the lifetimes are expected to fall between the lifetimes of materials grown by (LPE) and (MOCVD) [40]. The hole lifetime is therefore taken as the average of the values in figure 6.10 and 6.11 for the specific donor concentrations.

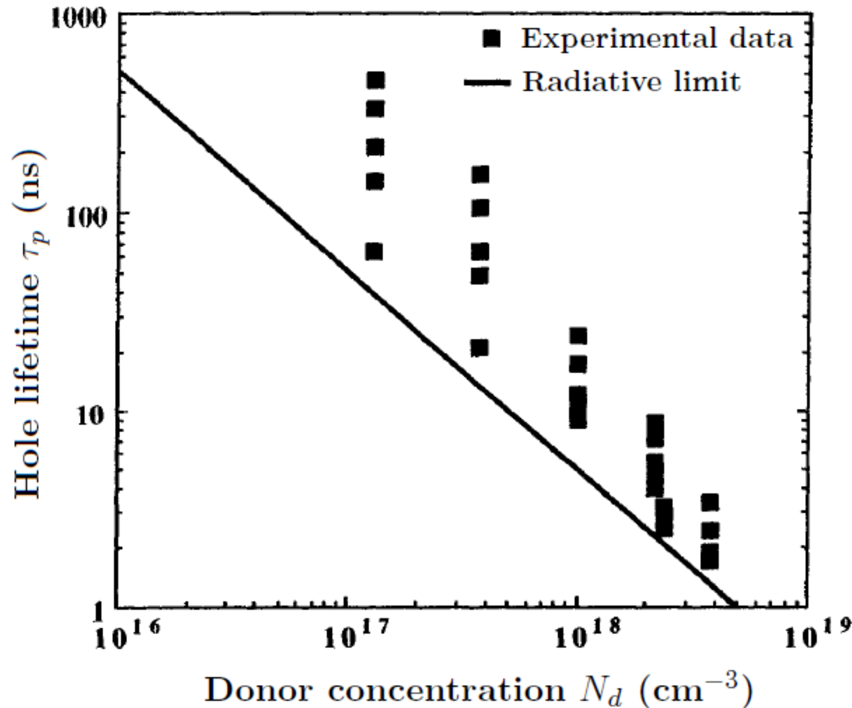

Figure 6.11: Hole lifetime in n-doped GaAs grown by MOCVD. The solid line is the radiative limit. The squares are experimental data when all the recombination mechanisms are present [40].

The electron and hole lifetimes for $Al_xGa_{1-x}As$ are for some doping concentrations given in [38]. They are lower than the lifetimes for GaAs for the same doping concen-

trations. For the doping concentrations needed in this thesis, but not given in [38], the lifetimes are in this thesis obtained from the lifetimes of GaAs after multiplying them by a factor equal to the ratio between the lifetimes of $Al_xGa_{1-x}As$ and GaAs for the doping concentrations where both lifetimes are known.

The electron and hole lifetimes in the i-layer are of the order of ns. The product of the electron and hole lifetime in the i-layer $\sqrt{\tau_{n,i}\tau_{p,i}}$ is taken as 7 ns since this is the value used in the modeling in [5].

The values of mobility and lifetime in the conduction band and valence band when an intermediate band is present are taken equal to the values of an intrinsic material. This choice is discussed in section 7.3.3. The lifetimes for conduction band to intermediate band transitions $\tau_{n,CI,SRH}$ and for intermediate band to valence band transitions $\tau_{p,IV,SRH}$ when non-radiative recombination is included, are taken as 0.5 ps and 40 ps, respectively. These values are experimentally obtained lifetimes for conduction band to intermediate band transitions and for intermediate band to valence band transitions given in [13] for the intermediate band solar cell sample A1681 described in table 6.3. Since few data exist for these lifetimes they are used generally as the lifetimes when non-radiative recombination is included. They are much lower than the lifetimes for conduction band to valence band transitions.

The recombination velocities on GaAs surfaces are of the order of 10^6 cm/s [11], and the values of the front and rear surface recombination velocity are taken as 10^6 cm/s for both GaAs and $Al_xGa_{1-x}As$.

6.2 Solar spectrum

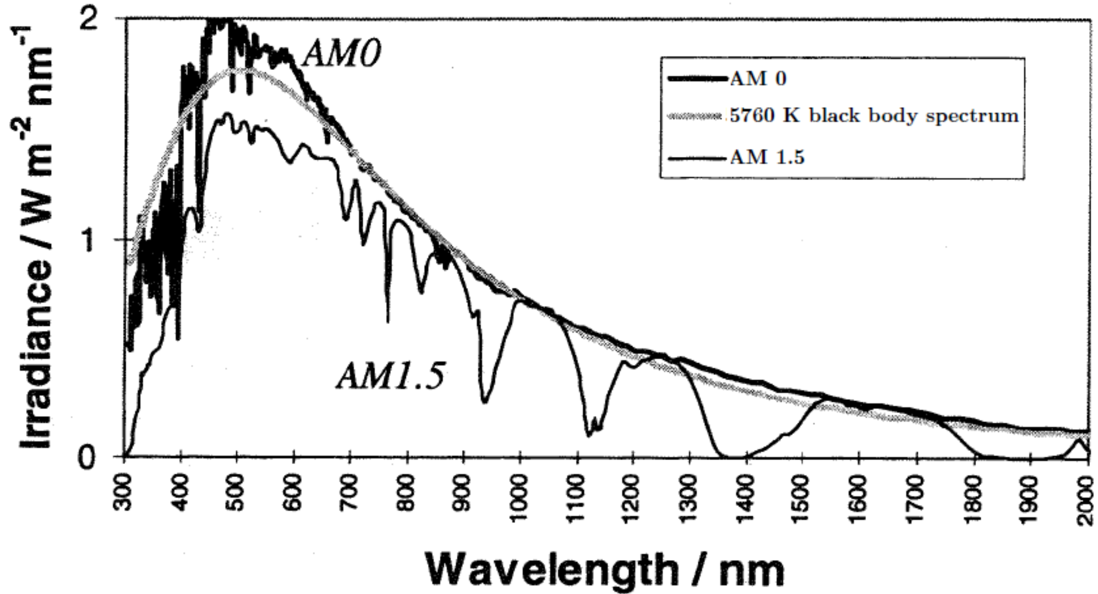

Figure 6.12: Air Mass 0 solar spectrum, 5760 K black body spectrum reduced by the geometrical factor of the sun and Air Mass 1.5 spectrum [3].

The solar spectrum resembles as mentioned the spectrum of a black body with temperature 5760 K, and this spectrum is shown in figure 6.12. The emitted light is distributed over wavelengths from the ultraviolet to the visible and infrared part of the spectrum. Light is absorbed and scattered as it passes through the atmosphere. The attenuation of the light is quantized using the Air Mass. The Air Mass is the ratio between the optical length from the earth to the sun when the sun is placed at an angle γ_s and when the sun is placed directly overhead [3]

$$AM = \frac{1}{cos\gamma_s}. \tag{6.19}$$

The extraterrestrial spectrum is referred to as the Air Mass 0, where $\gamma_s = 0^o$. The standard spectrum used to test solar cell is the Air Mass 1.5 spectrum, where $\gamma_s = 42^o$, shown in figure 6.12 as the thin line. In my modeling the normalised Air Mass 1.5 spectrum is used giving an incident power density of 1000 W/m^2. Tabulated measured data for the Air Mass 1.5 are taken from [47].

6.3 Sample parameters

The reference cells that are used in the modeling have thicknesses and doping concentrations as given in table 6.1. A table with the values needed for the mobility and lifetime in GaAs for these doping concentrations, found from the experimental data shown in figure 6.5, 6.6, 6.9, 6.10 and 6.11, are given in table 6.2

Table 6.1: Parameters for the p-i-n reference cell, sample A1677

Layer	Al (%)	Thickness (nm)	Doping (cm^{-3})
Window	85	5	2×10^{19}
p^+-layer	0	100	2×10^{19}
p-layer	0	200	2×10^{18}
i-layer	0	100	1×10^{14}
n-layer	0	300	2×10^{17}
n^+-layer	0	100	2×10^{18}
substrate	0	-	2×10^{17}

Table 6.2: Values of mobility and lifetimes in GaAs.

Doping (cm^{-3})	μ_p (cm^2/Vs)	μ_n (cm^2/Vs)	τ_p(ns)	τ_n(ns)
2×10^{19} (p^+)	-	1400	-	0.5
2×10^{18} (p)	-	1250	-	3
1×10^{14} (i)	400	8000	$\sqrt{7}$	$\sqrt{7}$
2×10^{17} (n)	278	-	32.5	-
2×10^{18} (n^+)	238	-	7	-

The thicknesses and doping concentrations used for the reference cell are the same as the values for sample A1677 made by molecular beam epitaxy at the University of Glasgow. The parameters for sample A1677 are found from [48], [49], [50] and [36]. The background doping of the i-layer is not given in these references. The value used is $N_i = 1 \times 10^{14}$ cm^{-3} as this is a typical value for GaAs solar cells [43]. The p-doped GaAs layer is doped with Be, while the n-doped GaAs layer is doped with Si [49].

The thicknesses and doping concentrations of the intermediate band solar cell samples used in the modeling are the same as in table 6.1, except the width of the i-layer which varies. The parameters for the intermediate band solar cell sample A1681 made at the University of Glasgow, with InAs quantum dots in the i-layer, are given in table 6.3 obtained from parameters given in [48], [49], [50] and [36].

Table 6.3: Parameters for the quantum dot intermediate band solar cell, sample A1681.

Layer	Al (%)	Thickness (nm)	Doping (cm^{-3})
Window	85	5	2×10^{19}
p^+-layer	0	100	2×10^{19}
p-layer	0	200	2×10^{18}
IB-layer	0	100	δ doping 4.0×10^{10} (cm^{-2})
n-layer	0	300	2×10^{17}
n^+-layer	0	100	2×10^{18}
substrate	0	-	2×10^{17}

The InAs quantum dots in sample A1681 are formed in the Stranski-Krastanov growth mode. Ten layers of InAs quantum dots with the same density of quantum dots as the δ doping are placed on top of each other with an GaAs layer in between giving the total width of 100 nm of the intermediate band region [48]. The values of the band gaps E_G and E_H are from photoluminescence reported as $E_G = 1.38$ eV and $E_H = 1.12$ eV [48].

The thicknesses and doping concentrations for the intermediate band solar cell made of InAs quantum dots in $Al_0.35Ga_{0.65}As$ are given in table 6.4. The mobility and lifetimes in $Al_0.35Ga_{0.65}As$ for these doping concentrations are given in table 6.5.

Table 6.4: Parameters for $Al_0.35Ga_{0.65}As$ sample

Layer	Al (%)	Thickness (nm)	Doping (cm^{-3})
Window	85	5	2×10^{19}
p^+-layer	0.35	100	2×10^{19}
p-layer	0.35	200	2×10^{18}
IB-layer	0.35	1300	δ doping 4.0×10^{10} (cm^{-2})
n-layer	0.35	300	2×10^{17}
n^+-layer	0.35	100	2×10^{18}
substrate	0.35	-	2×10^{17}

Table 6.5: Values of mobility and lifetimes in $Al_0.35Ga_{0.65}As$

Doping (cm^{-3})	μ_p (cm^2/Vs)	μ_n (cm^2/Vs)	τ_p (ns)	τ_n(ns)
2×10^{19} (p^+)	-	830	-	0.4
2×10^{18} (p)	-	1000	-	2.3
2×10^{17} (n)	100	-	3.1	-
2×10^{18} (n^+)	65	-	0.7	-

Chapter 7

Numerical results and discussion

In this chapter results from the modeling of p-i-n reference cells and intermediate band solar cells are given. For both the reference cell and the intermediate band solar cell two models are used, a simple model with only a few layers included and a complete model with anti-reflective coating, window and front and back surface field layers included. Only the simple model of the intermediate band solar cell was found in literature, the three others were developed in this thesis work, in chapter 4 and 5.

As described in chapter 6 the parameters needed in the modeling are selected material parameters form literature. The influence of these parameters on the quantum efficiency and the current-voltage characteristic of a simple p-i-n reference cell is studied in section 7.1. In section 7.2 the effect of adding an anti-reflective coating, a window layer and heavily doped back and front layers are discussed showing the importance of these additional layers.

The simple model of the intermediate band solar cell, where we only consider the contribution form the intermediate band layer, i.e. even omitting the p- and n-layers, is studied in section 7.3. For this model the results obtained using the black-body spectrum are compared with the results obtained using the AM 1.5 spectrum, and the material parameters used for the intermediate band layer are discussed. Next the simple model is used to calculate solar cell properties for the InAs/GaAs quantum dot intermediate band solar cell. The optimum size of the band gap E_H is found for different thicknesses of the intermediate band layer.

In section 7.4 the complete model of the intermediate band solar cell is studied. The complete model takes all layers (ARC, window, p^+, p, i, IB, n and n^+) into account. The importance of having the quantum dots placed in a flat band layer is discussed. The band gaps and width of the intermediate band layer are studied to obtain the highest efficiency. How to obtain the intermediate band solar cell with the highest efficiency is discussed in section 7.5 based on the preceding sections.

The models given in chapter 4 and 5 are used in section 7.6 on real samples and compared with experimental data from literature. In section 7.7 a GaAs intermediate band solar cell is compared with a $Al_{0.35}Ga_{0.65}As$ solar cell for values of band gap E_H reported from photoluminescence of such materials made at NTNU. In section 7.8 the models of the reference cell and the intermediate band solar cell are discussed. The AM 1.5 spectrum is used for all calculations except in section 7.3.1 and 7.3.2.

7.1 The simple p-i-n reference cell

The simple p-i-n solar cell modeled in this section consists of a p-layer, an i-layer and a n-layer is shown in figure 7.1 with doping concentrations and thicknesses given in table 6.1. The thicknesses of the other layers given in table 6.1 (ARC, window, p^+, n^+) are set equal to zero. The aim of this section is to study how material parameters like the minority carrier mobilities and lifetimes in the doped layers, the non-radiative carrier lifetime in the intrinsic layer and the surface recombination velocities affect the quantum efficiency and current-voltage characteristic of the p-i-n solar cell. Only one parameter is changed at a time while the other parameters are held constant and equal to the values listed in table 6.2. In this way the effect of varying each of the parameters is shown. The solar spectrum used in this section is the AM 1.5 spectrum and X=1.

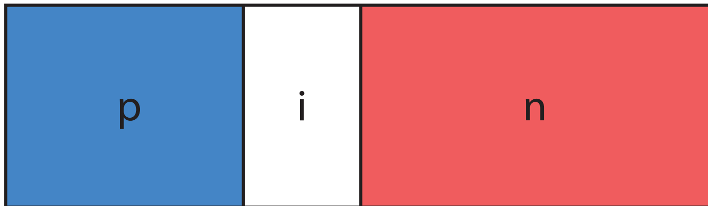

Figure 7.1: Structure simple p-i-n solar cell.

7.1.1 The effect of varying the mobility

The mobilities of the electrons in the p-layer doped to 2×10^{18} cm^{-3} and the holes in the n-layer doped to 2×10^{17} cm^{-3} are given in table 6.2 as $\mu_n = 1250$cm^2/Vs and $\mu_p = 278$cm^2/Vs obtained from the experimental data given in figure 6.5 and 6.6. The effect on the quantum efficiency of the p-layer by varying the electron mobility is shown in figure 7.2 and the effect on the quantum efficiency of the n-layer by varying the hole mobility is shown in figure 7.3. The effect on the current-voltage characteristic by varying both of the mobilities is shown in figure 7.4.

The quantum efficiency of the p-layer is clearly affected by varying the mobility as shown in figure 7.2. The mobility of the p-layer is found in the experimental data in figure 6.5 to be $1000 < \mu_n < 1500$cm^2/Vs. Using the lowest mobility in this interval of 100cm^2/Vs gives a maximum quantum efficiency of 0.44, while the highest mobility of 1500cm^2/Vs gives a maximum of 0.49. As can been seen the difference in quantum efficiency is less for longer wavelengths. The reason for this may be that for long wavelengths the absorption coefficient is small and has a larger effect on the quantum efficiency than the mobility. The mobilities of 125cm^2/Vs and 12500cm^2/Vs are included to show how the effect of varying the mobility of a factor 10. These are not realistic values. As can been seen the quantum efficiency obtained for the mobility of 125cm^2/Vs is much smaller for all wavelengths than the quantum efficiency obtained for the mobility of 12500cm^2/Vs. This gives a much smaller photocurrent.

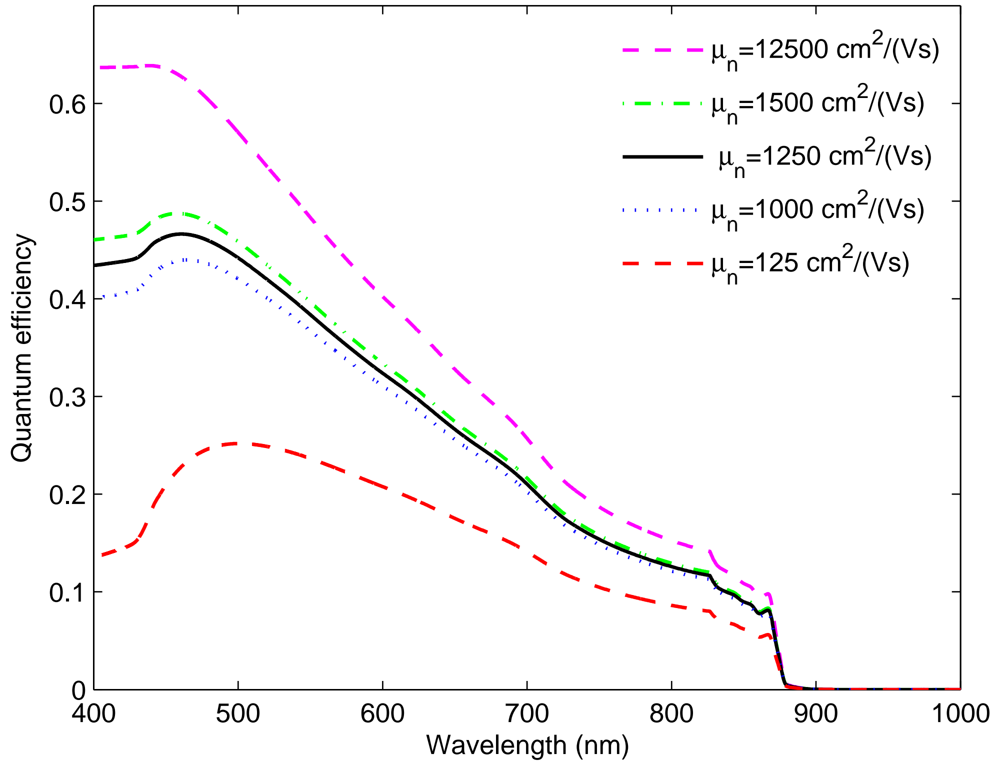

Figure 7.2: Quantum efficiency of p-layer using different values for the electron mobility while holding all other parameters constant. The value for the mobility used throughout the rest of the modeling is $\mu_p = 0.125\text{m}^2/(\text{Vs})$

The effect on the quantum efficiency of the n-layer by varying the mobility of the holes is shown in figure 7.3, where it is seen that it has not the same significance as varying the mobility in the p-layer. Since much of the photons are absorbed in the preceding layers, the quantum efficiency in the n-layer is in any case low. The mobility of the n-layer is found from the experimental data in figure 6.6 to be $250 < \mu_p < 300\text{cm}^2/\text{Vs}$. The lowest mobility in this interval gives a maximum of quantum efficiency of 0.107 and the highest mobility a maximum of quantum efficiency of 0.109. By increasing the mobility by a factor 10 (from $\mu_p = 278\text{cm}^2/\text{Vs}$ to $\mu_p = 278\text{cm}^2/\text{Vs}$) the maximum of the quantum efficiency increases from 0.108 to 0.146. While the relative change might be comparable with the change of quantum efficiency in the p-layer by varying the mobility by a factor of 10, the corresponding change in total photocurrent is small since the n-layer quantum efficiencies are small. The conclusion is that a high mobility of electrons in the p-layer is more important than the mobility of the holes in the n-layer. In contrast to the case for the p-layer, the effect of varying the mobility in the n-layer increases for longer wavelengths. This is because the absorption in the n-layer is larger for the longest wavelengths because less of these photons are absorbed in the preceding layers, and thus the importance of the hole mobility of the n-layer increases with wavelength.

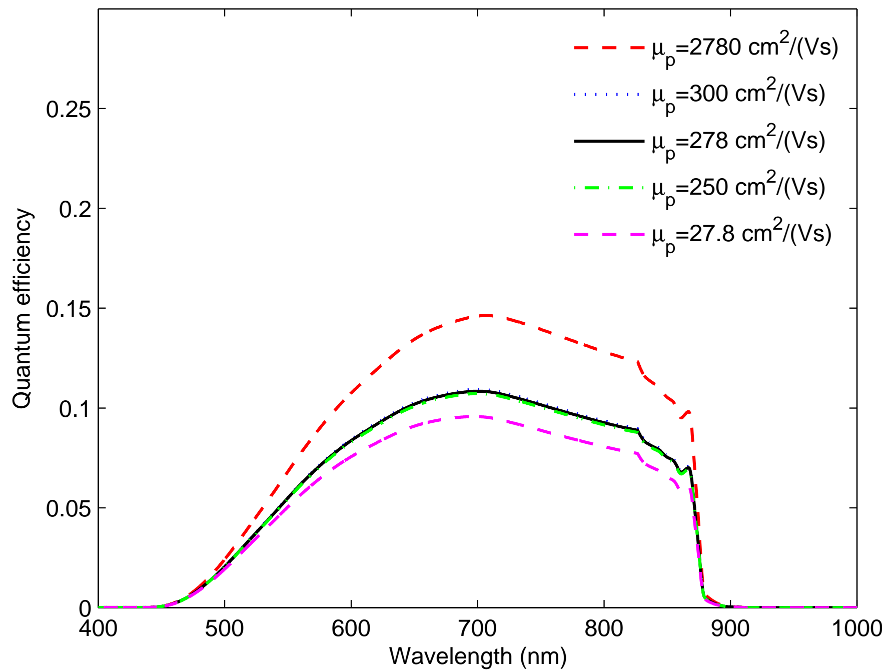

Figure 7.3: Quantum efficiency of n-layer using different values for the hole mobility while holding all other parameters constant. The value for the hole mobility used throughout the rest of the modeling is $\mu_n = 278\text{cm}^2/(\text{Vs})$

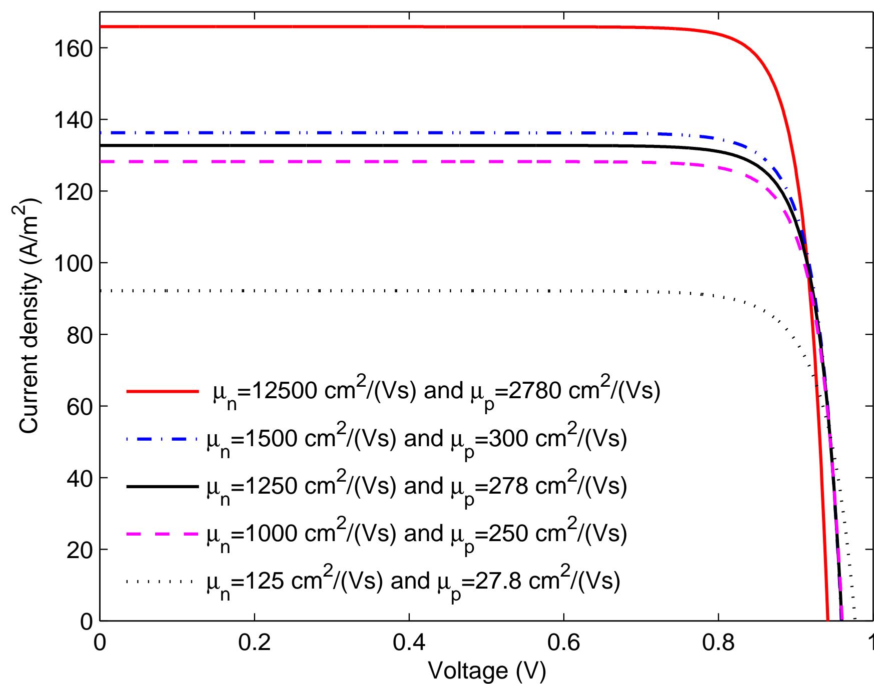

Figure 7.4: Current-voltage characteristic of simple p-i-n solar cell for various mobilities while holding all other material parameters constant.

In figure 7.4 the current-voltage characteristics of the simple p-i-n solar cell for various mobilities are shown. As expected the photocurrent increases with increasing mobilities since this increase was seen for the quantum efficiencies. The open circuit voltage is however reduced with increasing mobilities, as the dark current increases. The reason for this can be seen in the equations for the dark current given in equation (2.53) and (2.54). In table 7.1 the short-circuit current, the dark current, the open-circuit voltage and the resulting efficiencies for various mobilites are liseted. As can be seen from the table the effect of varying the mobilities is that the efficiency increases with increasing mobilities.

Table 7.1: Effects of varying the mobilities in the simple p-i-n solar cell

μ_n(cm^2/Vs)	μ_h (cm^2/Vs)	J_{sc}(A/m^2)	J_{dark}(0.8V) (A/m^2)	V_{oc} (V)	η(%)
125	27.8	92.1	1.54	0.977	7.44
1000	250	128.2	1.68	0.960	10.43
1250	278	132.7	1.70	0.960	10.80
1500	300	136.2	1.71	0.959	11.10
12500	2780	165.8	2.08	0.942	13.41

7.1.2 The effect of varying the lifetimes in the doped layers

The minority carrier lifetimes for electrons in the p-layer and holes in the n-layer are given in table 6.2 as τ_n = 3.0 ns and τ_p = 32.5 ns, respectively. They are obtained from the experimental data given in figure 6.9, 6.10 and 6.11. The effect of varying the lifetimes in the p-layer and in the n-layer by a factor of 10^3 is shown in figure 7.5 and 7.6. The lifetimes had to be varied this much to see an effect in the quantum efficiency. By increasing the lifetimes by a factor 10^3 the quantum efficiency is almost unchanged, while decreasing the lifetimes by a factor 10^3 the quantum efficiency in both the p- and n-layer clearly changes. The reason for this is that by using τ_n = 3.0 ns and τ_p = 32.5 ns and μ_n = 1250cm^2/Vs and μ_p = 278cm^2/Vs the values for the diffusion lengths are L_n = 3114 nm and L_p = 4833 nm which is larger than the widths of the p- and n-layer of 200 nm and 300 nm, respectively. The actual value of the diffusion length is not that important when it is larger than the p- and n-layer widths [3]. By decreasing the lifetimes in the p- and n-layer by a factor 10^3 the diffusion lengths are less than the widths of the p- and n-layer and thus the quantum efficiency dependency of the diffusion lengths is seen, see figure 7.5. When the p-layer is much thicker than the diffusion length the quantum efficiency is reduced. In that case part of the p-layer, called the dead layer, absorbs light, but does not contribute to the photocurrent [3]. The reduction in quantum efficiency in the n-layer, shown in figure 7.6,by decreasing the lifetime by a factor 10^3 is clearly seen. Since the quantum in the n-layer is quite small the change in photocurrent by changing the lifetime in the n-layer is much smaller than than by changing the lifetime in the p-layer. Since the n-layer is placed on the bottom of the solar cell where most of the photons are already absorbed, the 'dead' layer problem is not encountered.

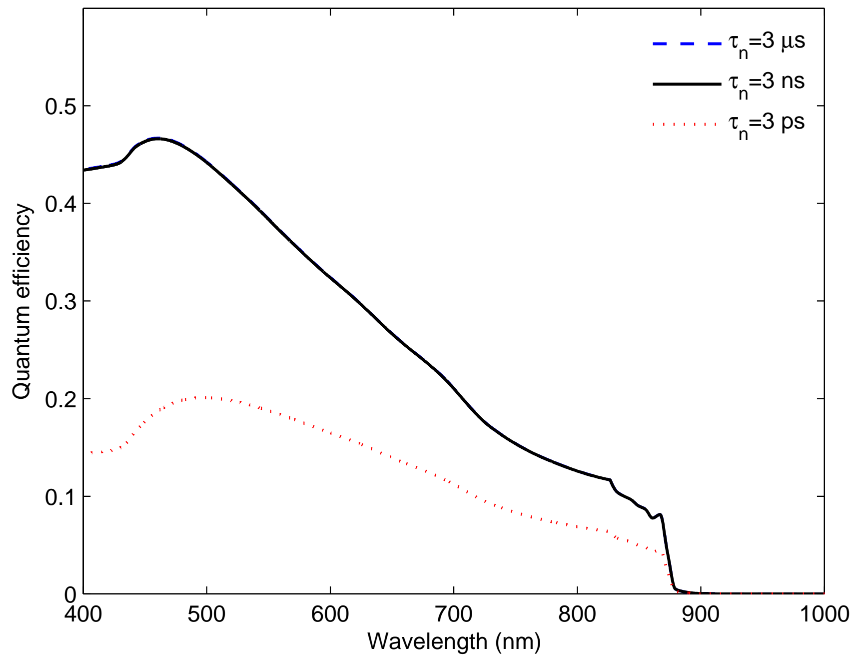

Figure 7.5: Quantum efficiency of p-layer using different values for the electron lifetime while holding all other parameters constant. The value used for electron lifetime in p-layer is $\tau_n = 3.0$ ns throughout the rest of the modeling.

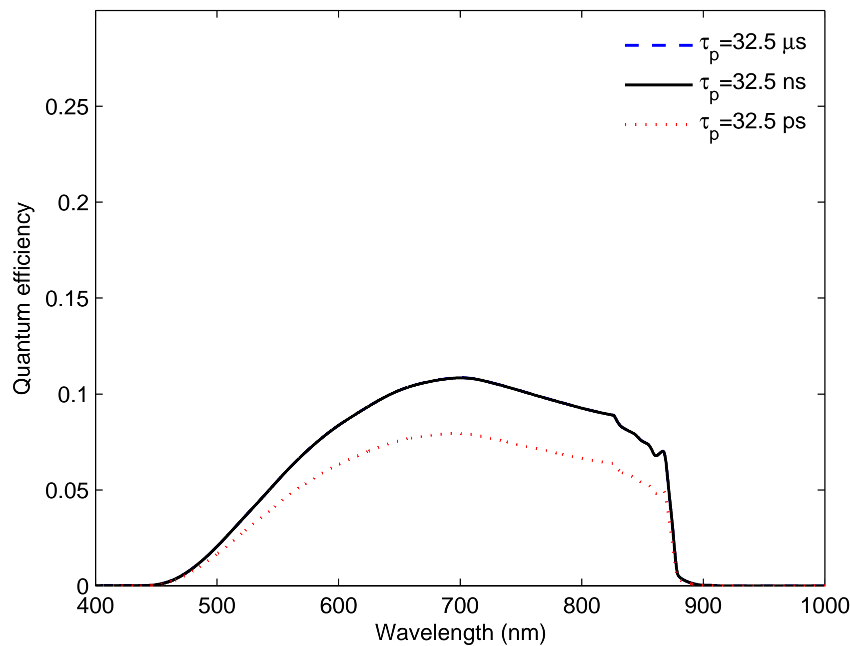

Figure 7.6: Quantum efficiency of n-layer using different values for the hole lifetime while holding all other parameters constant. The value used for hole lifetime in n-layer is $\tau_p = 32.5$ ns throughout the rest of the modeling.

The effect on the current-voltage characteristics by varying the lifetimes is shown in figure 7.7. The same effect can be observed in the current-voltage characteristics as in the quantum efficiency curves. By increasing the lifetimes, the change in the current-voltage curve is not seen, while decreasing the lifetime by a factor 10^3 the change in the current-voltage curve is clearly visible. The reason for this is the same as mentioned for the quantum efficiencies, when the diffusion lengths are much longer than the widths of the p- and n-layer they do not affect the dark-current much. When they are shorter than the widths of the p- and n-layer they clearly affect the dark-current. For diffusion lengths shorter than the widths of the layers, the dark-current increases with decreasing lifetimes, and as a result the open-circuit voltage reduces. The open-circuit voltage, photocurrent and efficiency for the various values of the electron and hole lifetimes are listed in table 7.2.

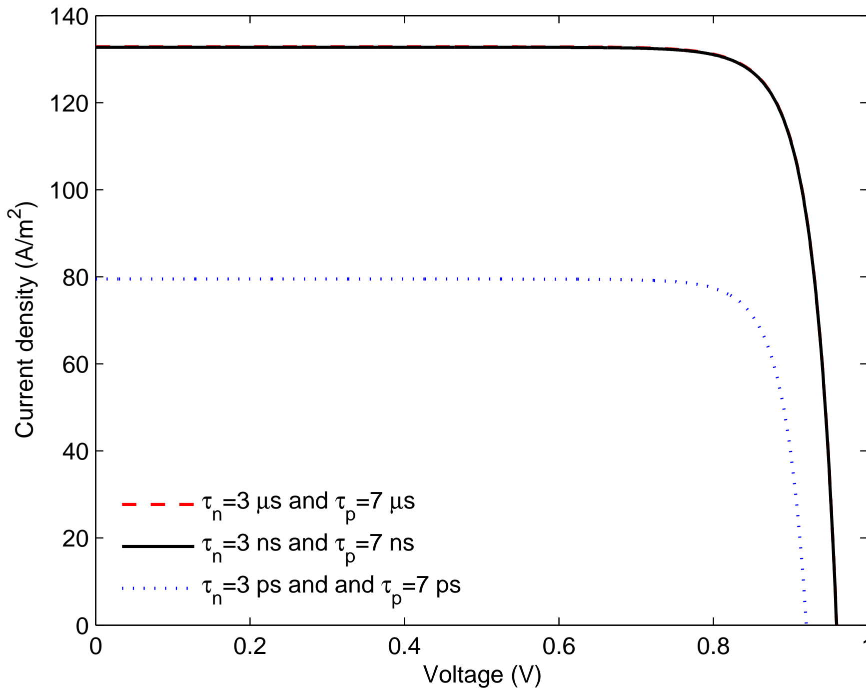

Figure 7.7: Current-voltage characteristic of simple p-i-n solar cell for various lifetimes of the minority carriers in the p- and n-layers while holding all other parameters constant.

Table 7.2: Effects of varying the lifetimes in the simple p-i-n solar cell

τ_n(ns)	τ_p (ns)	J_{sc}(A/m^2)	J_{dark}(0.8V) (A/m^2)	V_{oc} (V)	η(%)
3×10^{-3}	7×10^{-3}	79.5	2.08	0.921	6.23
3	7	132.7	1.70	0.960	10.80
3×10^3	7×10^3	132.8	1.70	0.9602	10.81

The conclusion drawn from the current-voltage and quantum efficiency curves is that the uncertainties in the lifetimes for electrons and holes are not important in the modeling, as long as the width of the p- and n-layer are smaller than the corresponding diffusion lengths.

7.1.3 The effect of varying the surface recombination velocities

The surface recombination velocities at the edge of the p- and n-layer are as mentioned in chapter 6 taken as $S_n = S_p = 10^4$ m/s typical for GaAs solar cells. The effect on the quantum efficiency by varying the surface recombination velocity by at the edge of the p-layer by a factor 10 is shown in figure 7.8, and the effect on the quantum efficiency by varying the surface recombination velocity at the edge of the n-layer by a factor 10 is show in figure 7.9. The maximum of the quantum efficiency in the p-layer takes the value 0.64 for $S_n = 10^3$ m/s and decreases to 0.47 when $S_n = 10^4$ m/s and 0.25 when $S_n = 10^5$ m/s showing that the value of the surface recombination velocity is an important parameter in determining the photocurrent. Looking at the quantum efficiency in the p-layer it is seen that the value of the surface recombination velocity is most important for the shortest wavelengths where the absorption near the surface is highest. This is the same dependence as was seen by varying the mobility in the same layer. Similarly, the behavior of the quantum efficiency of the n-layer shows that the surface recombination velocity here is more important for longer wavelength. This is as expected since the long wavelength absorption is highest here. As for the mobilities and the lifetimes the value of the surface recombination velocity in the p-layer is more important than in the n-layer since the quantum efficiency is larger there.

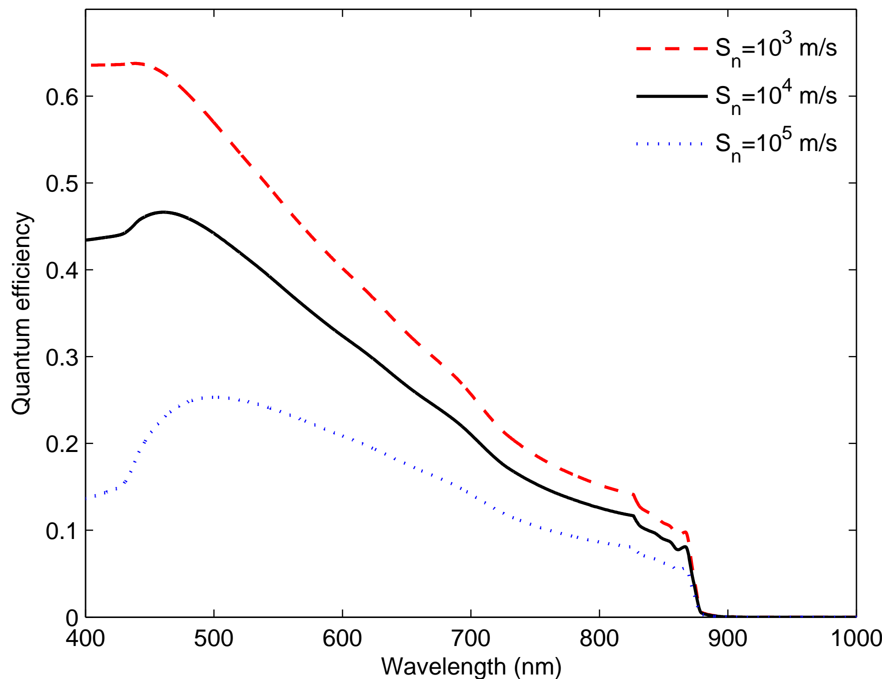

Figure 7.8: Quantum efficiency of p-layer using different values for front surface recombination velocity while holding all other parameters constant. The value used for front surface recombination velocity is $S_n = 10^4$ m/s throughout the rest of the modeling.

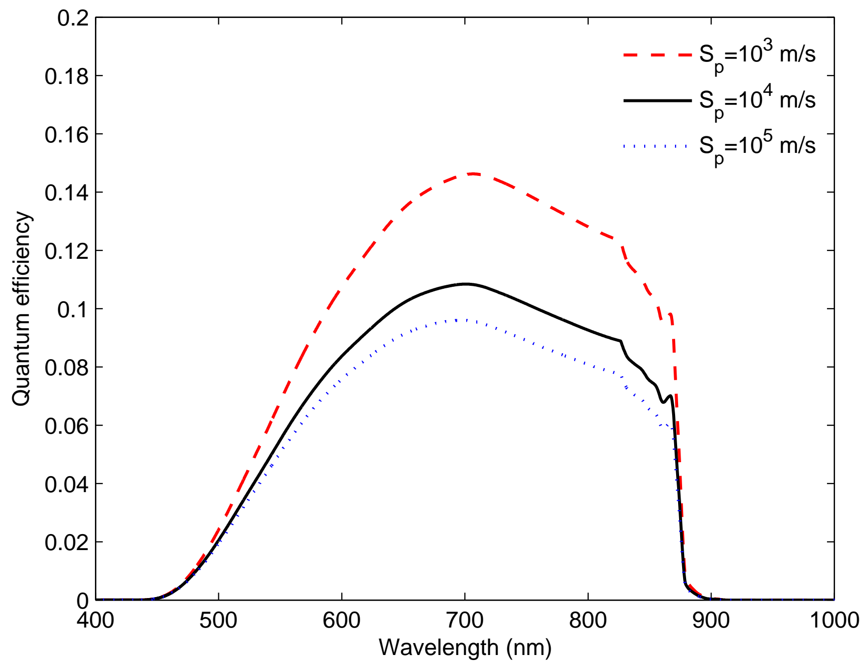

Figure 7.9: Quantum efficiency of n-layer using different values for rear surface recombination velocity while holding all other parameters constant. The value used for rear surface recombination velocity is $S_p = 10^4$ m/s throughout the rest of the modeling.

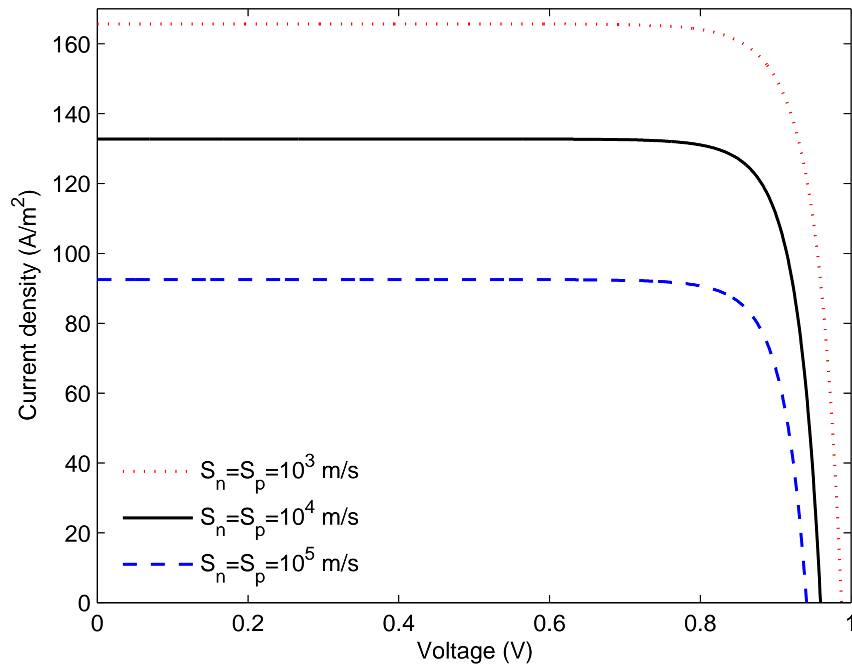

Figure 7.10: Current-voltage characteristic of simple p-i-n solar cell for various surface recombination velocities of the front and rear surface while holding all other parameters constant.

The dark current increases with increasing surface recombination velocities resulting in lower open-circuit voltages for higher surface recombination velocities, as shown in figure 7.10. A high surface recombination velocity gives both a low photocurrent and a low open-circuit voltage which both lead to a low efficiency. The photocurrents, open-circuit voltages and efficiencies for various recombination velocities are listed in table 7.3 showing how important the surface recombination velocities are. As mentioned the front surface recombination velocity is the most important however, and this may be reduced using a heavily doped front surface layer or a window layers which will be considered in the next section.

Table 7.3: Effects of varying the surface recombination velocities in the simple p-i-n solar cell

S_n(m/s)	S_p (m/s)	J_{sc} (A/m^2)	J_{dark}(0.8V) (A/m^2)	V_{oc}(V)	η(%)
10^3	10^3	165.6	1.58	0.988	13.75
10^4	10^4	132.7	1.70	0.960	10.80
10^5	10^5	92.4	1.78	0.941	7.37

7.1.4 The effect of varying the non-radiative lifetimes in the intrinsic region

The non-radiative lifetimes of the electrons and holes in the intrinsic region affects the dark current in the intrinsic region given by equation (2.60). They do not affect the photocurrent. Current-voltage characteristics for various values of the product of the lifetimes of the electron and holes $\tau_{n,i}\tau_{p,i}$ are shown in figure 7.11. The corresponding photocurrent, open-circuit voltages and efficiencies are listed in table 7.4.

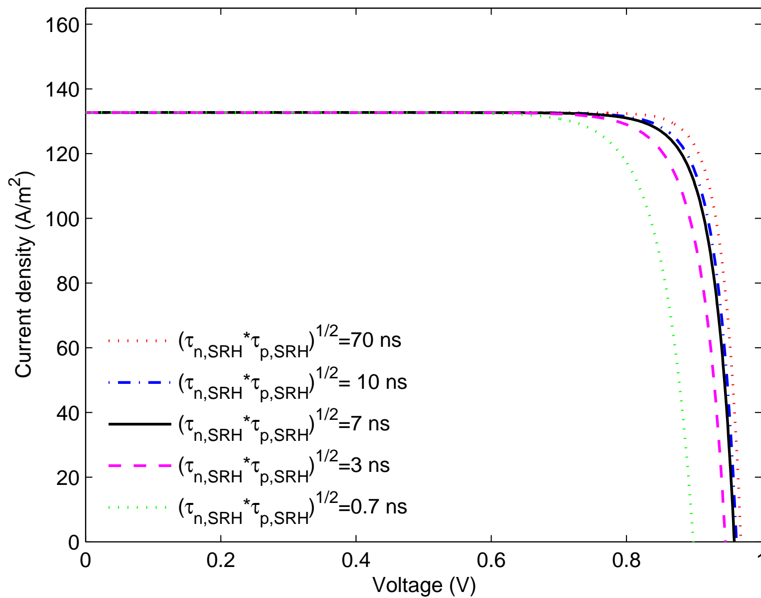

Figure 7.11: Current-voltage characteristic using different values for electron and hole non-radiative lifetimes in undoped GaAs while holding all other parameters constant. The value used for $\sqrt{\tau_{n,i}\tau_{p,i}}$ is 7 ns throughout the rest of the modeling.

Few values of non-radiative lifetime in undoped GaAs exist. The values used for the non-radiative lifetime is $\sqrt{\tau_{n,i}\tau_{p,i}} = 7$ ns which for a voltage equal to 0.8 V gives a dark current of 1.70 A/m^2. The non-radiative lifetimes are varied to a value as great as $\sqrt{\tau_{n,i}\tau_{p,i}} = 10$ and as small as $\sqrt{\tau_{n,i}\tau_{p,i}} = 3$ ns which for a voltage of 0.8 V gives dark currents equal to 1.24 A/m^2 and 3.72 A/m^2 respectively. As seen in table 7.4 this affects the open circuit voltage and the efficiency of the p-i-n solar cell. By decreasing the non-radiative lifetime from $\sqrt{\tau_{n,i}\tau_{p,i}} = 7$ ns to $\sqrt{\tau_{n,i}\tau_{p,i}} = 3$ ns the efficiency decreases from 10.80 % to 10.41 % as seen from table 7.4. Here open-circuit voltages and efficiencies are also given for various non-radiative lifetimes, showing how increasing the non-radiative lifetime gives a larger open-circuit voltage and efficiency.

Table 7.4: Effects of varying the non-radiative lifetimes in the intrinsic layer in the simple p-i-n solar cell

$\sqrt{\tau_{n,i}\tau_{p,i}}$ (ns)	$J_{sc}(A/m^2)$	J_{dark}(0.8V) (A/m^2)	V_{oc} (V)	η(%)
70	132.7	0.33	0.970	11.26
10	132.7	1.24	0.963	10.93
7	132.7	1.70	0.960	10.80
3	132.7	3.72	0.946	10.41
0.7	132.7	15.36	0.899	9.59

7.1.5 Summary and discussion of the parameters in the model of the simple p-i-n solar cell

In the preceding sections various parameters used in the modeling of solar cells have been varied and the effect on the quantum efficiency and current-voltage characteristic has been presented. From these sections we see that the parameters most important in determining the quantum efficiency are the mobility of the electrons in the p-layer and the surface recombination velocity at the front surface. A high mobility and a low surface recombination velocity give a large photocurrent. Variations in the magnitude of mobility and surface recombination velocity affect the photocurrent, and the photocurrent obtained by modeling is connected with some uncertainty if the parameters are not known.

The mobility and surface recombination velocity also affect the dark current together with the non-radiative lifetime in the i-layer. The non-radiative lifetime is the most important parameter determining the dark current. Values for the non-radiative lifetime in the i-layer were difficult to find and is a reason for some uncertainty in dark current. Since the non-radiative lifetime does not affect the photocurrent, the mobility and surface recombination velocity have the same importance in determining the open circuit voltage and efficiency of the solar cell. The lifetimes of the minority carriers in the doped layers are not important as long as the width of the layers are smaller than the diffusion lengths.

7.2 Complete reference cells

The structure of the complete reference cell is shown in figure 7.12, showing the ARC, window, p^+, p, i, n and n^+-layer needed to obtain a high efficiency.

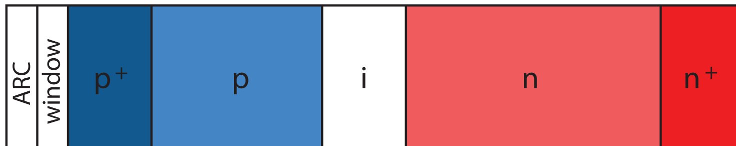

Figure 7.12: Structure of the complete reference cell.

The quantum efficiency of the simple p-i-n solar cell with material parameters given in table 6.1 and 6.2 is shown in figure 7.13 and has a maximum value of 0.52. As mentioned, one way to obtain higher quantum efficiency is to reduce the reflection losses from the front surface by adding an anti-reflective layer. By adding an anti-reflective layer the reflection may be reduced to 2%, in this thesis it is set equal to zero [28]. The quantum efficiency of the p-i-n solar cell with a 100 % anti-reflective layer is shown in figure 7.14 with a maximum value of 0.78. The anti-reflective layer thus results in a higher photocurrent, while the dark current is not affected. The result is an increased efficiency from 10.80 % without an anti-reflective layer to 16.34 % with an anti-reflective layer, an increase of 51 %!

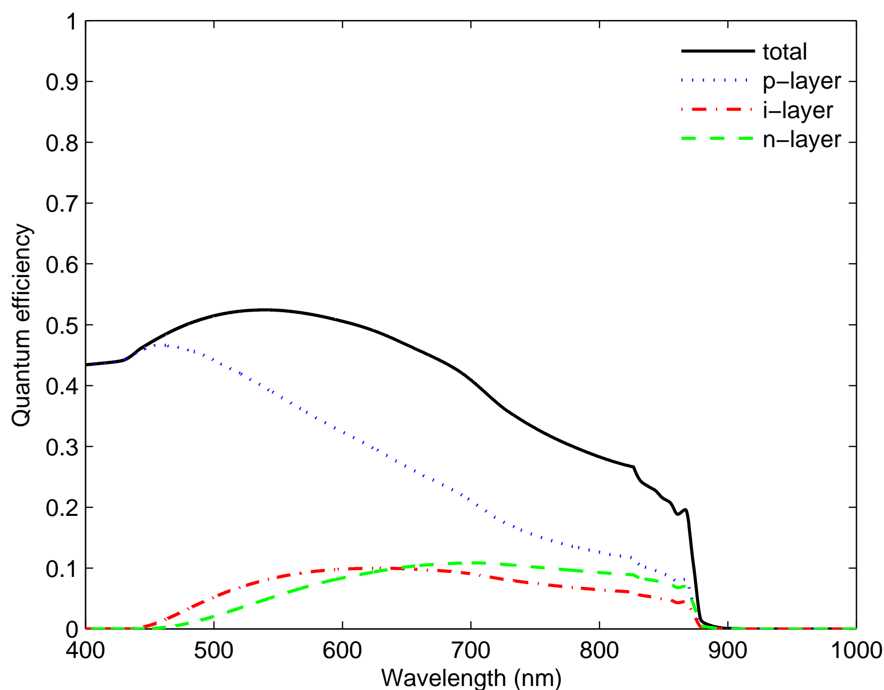

Figure 7.13: Quantum efficiency in p-i-n solar cell without anti-reflective coating.

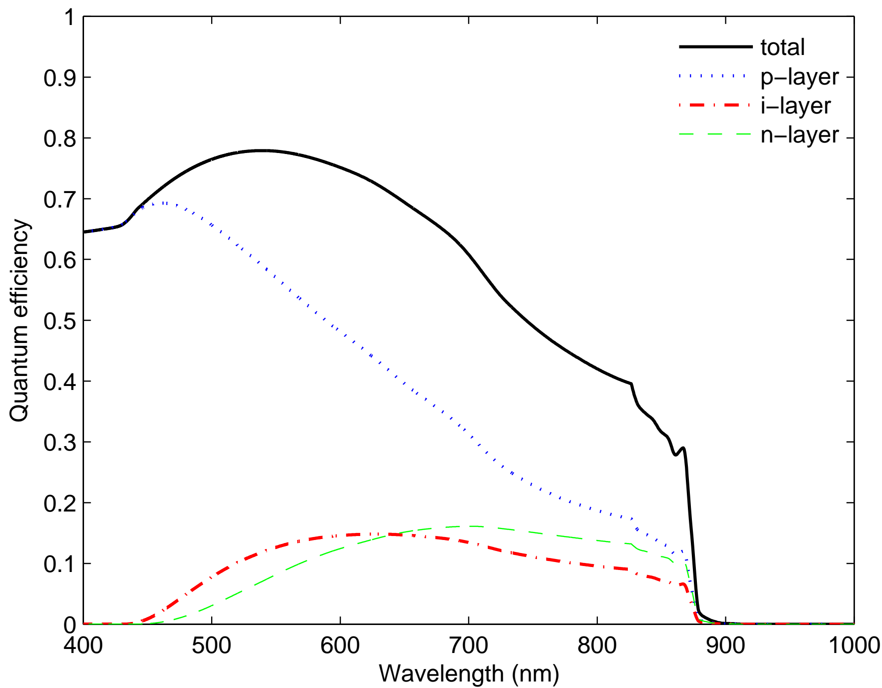

Figure 7.14: Quantum efficiency in p-i-n solar cell with anti-reflective coating.

As discussed in section 7.1.3 the front surface recombination velocity is a parameter which greatly influences the quantum efficiency. By including a heavily doped p^+-layer on top of the p-layer the front surface recombination velocity is reduced and we get a higher quantum efficiency as shown in figure 7.15. Here it is seen that for the shortest wavelengths the largest contribution to quantum efficiency comes from the p^+-layer. This is reasonable since the p^+-layer lays closest to the surface and absorbs the high energy photons. The p^+-layer has a higher mobility than the p-layer, which as discussed in section 7.1.1 results in a higher quantum efficiency. The width of the p-layer is two times the width of the p^+-layer, and for wavelengths longer than about 575 nm the quantum efficiency of the p-layer is greater than the quantum efficiency of the p^+-layer. Since the depletion layer between the p- and p^+-layer is very narrow (4.7 nm), the quantum efficiency of this depletion layer is very small with a maximum of 0.017.

As discussed in section 7.1.3 a reduction in surface recombination velocities gives a lower dark-current. Thus including a p^+-layer results in a higher quantum efficiency and lower dark current and an increased efficiency, for the p^+-p-i-n solar cell equal to 19.31 % for the chosen material parameters. This is an increase of 18 % compared to the solar cell without the heavily doped p^+-layer.

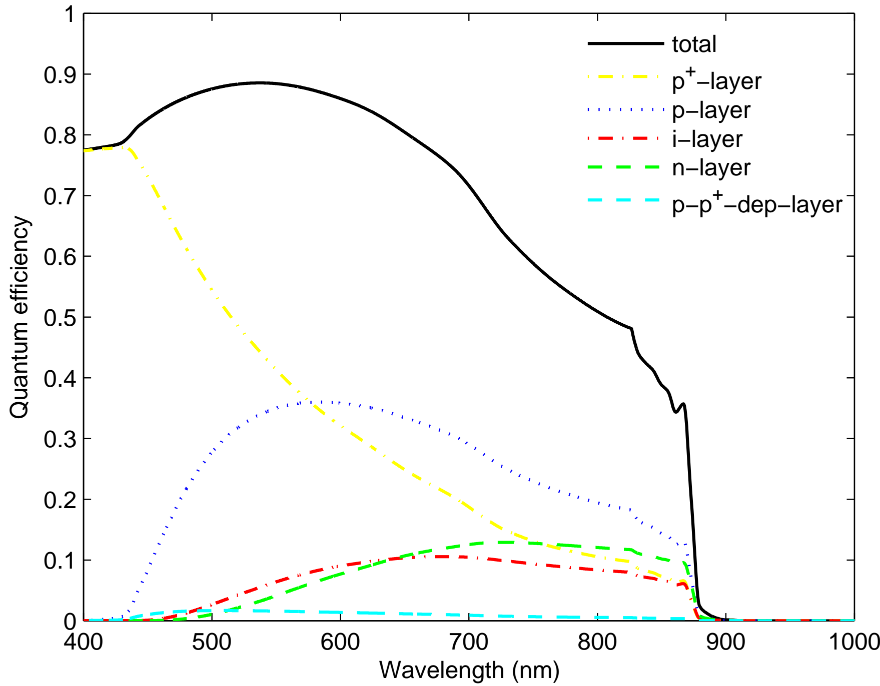

Figure 7.15: Quantum efficiency in p^+-p-i-n solar cell with ARC.

In a similar manner, to reduce the back surface recombination velocity a heavily doped n^+-layer is placed beneath the n-layer. The resulting quantum efficiency is showed in figure 7.16. Comparing figure 7.15 and 7.16 it is seen that the quantum efficiency of the n-layer is increased by including a n^+-layer. In the model we add a contribution from the n^+-layer and the depletion layer between the n- and n^+-layer. Since these layers are placed near the rear surface where the flux is very low, the contribution from these layers is very low. The maximum of the quantum efficiency of the n^+-layer is 0.030.

The effect of a heavily doped front surface layer and a heavily doped back surface layer is in both cases to reduce the surface recombination velocities. In the case of a front surface field the contribution to photocurrent from the heavily doped p^+-layer has to be included since many high energy photons are absorbed here. In the case of a back surface field the contribution from the heavily doped layer is not so important however, and may be omitted since very few photons are absorbed here.

The reduction of the back surface recombination velocity further decreases the dark current, and the efficiency of the p^+-p-i-n-n^+ solar cell is 20.94 %, compared to 19.31 % without the n^+-layer, an increase of 8.4 %.

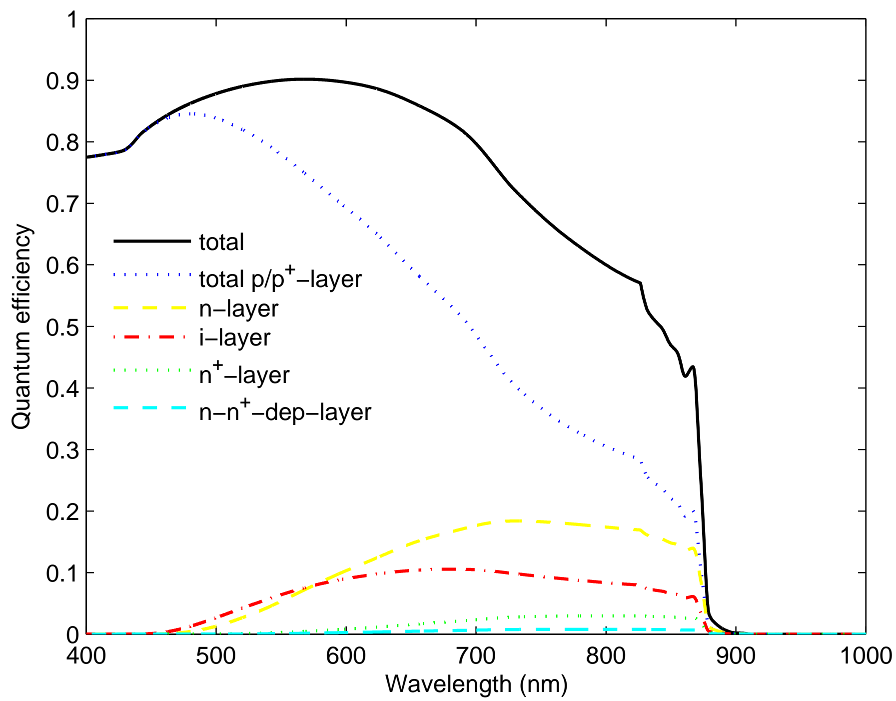

Figure 7.16: Quantum efficiency in p^+-p-i-n-n^+ solar cell with ARC.

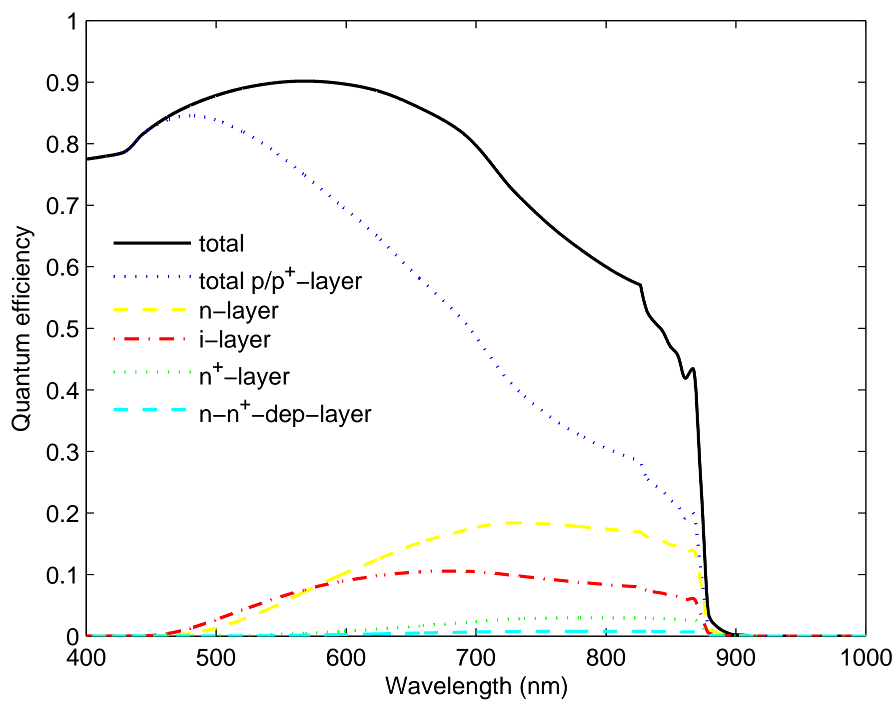

Figure 7.17: Quantum efficiency in p^+-p-i-n-n^+ solar cell with ARC and window.

As mentioned in section 7.1.3 the front surface recombination velocity is the most important to reduce. A further reduction in the surface recombination velocity is obtained by placing a window layer on top of the p$^+$- and p-layer with a resulting increased quantum efficiency as shown in figure 7.17 with a maximum of 0.993. The increased quantum efficiency is mostly due to the increased quantum efficiency in the p$^+$-layer as can be seen from figure 7.18 where quantum efficiencies of the p$^+$- and p-layer are shown with and without a window layer. The ARC and window are assumed not to contribute to the photocurrent, but the window absorbs some photons and is therefore included as a "dead layer".

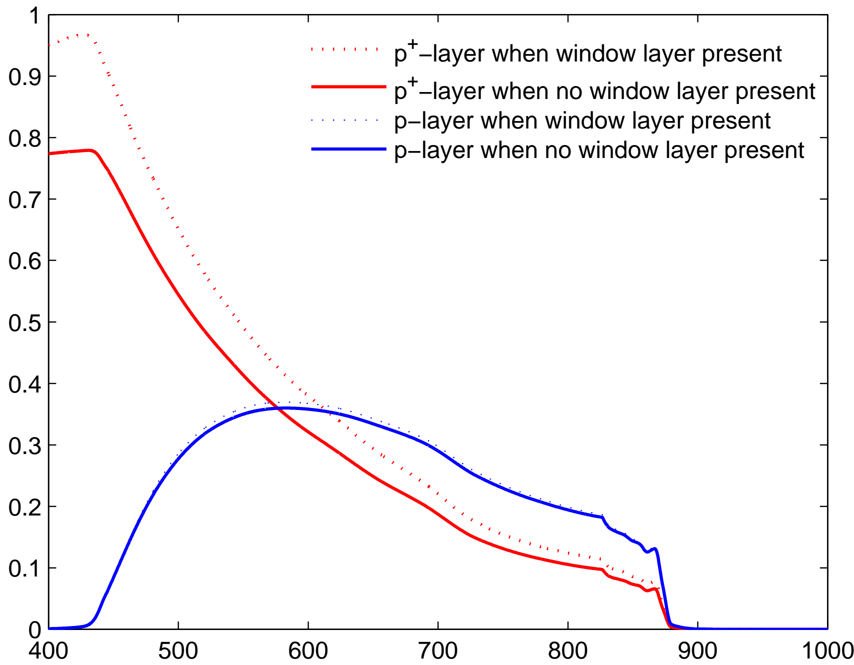

Figure 7.18: Quantum efficiency of p^+- and p-layer with a window layer present and without a window layer.

To study the effect of the window layer and the heavily doped layer on the quantum efficiency and current-voltage characteristic of window-p-i-n-n$^+$, window-p$^+$-i-n-n$^+$ and window-p$^+$-p-i-n-n$^+$ solar cells are obtained where the total thickness of the p$^+$ and p-layers is set equal to 300 nm. All other widths are fixed. The quantum efficiencies in figure 7.19 show us a higher quantum efficiency when only a p-layer or a p$^+$-layer is used than when both are used. The current-voltage characteristics of the three cases are shown in figure 7.20. The dark currents are larger when we do not have the p$^+$-layer and the highest efficiency is obtained using the window-p$^+$-p-i-n-n$^+$ solar cell, equal to 22.90 % which is an increase of 9 % compared to the solar cell without the window layer.

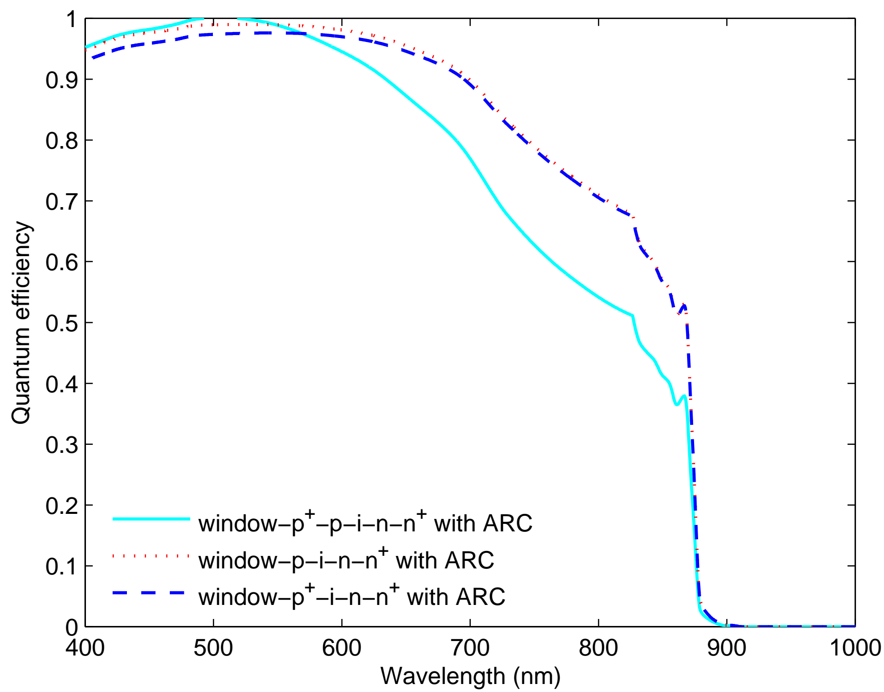

Figure 7.19: Quantum efficiency in a window-p-i-n-n$^+$, window-p$^+$-i-n-n$^+$ and window-p$^+$-p-i-n-n$^+$ solar cell.

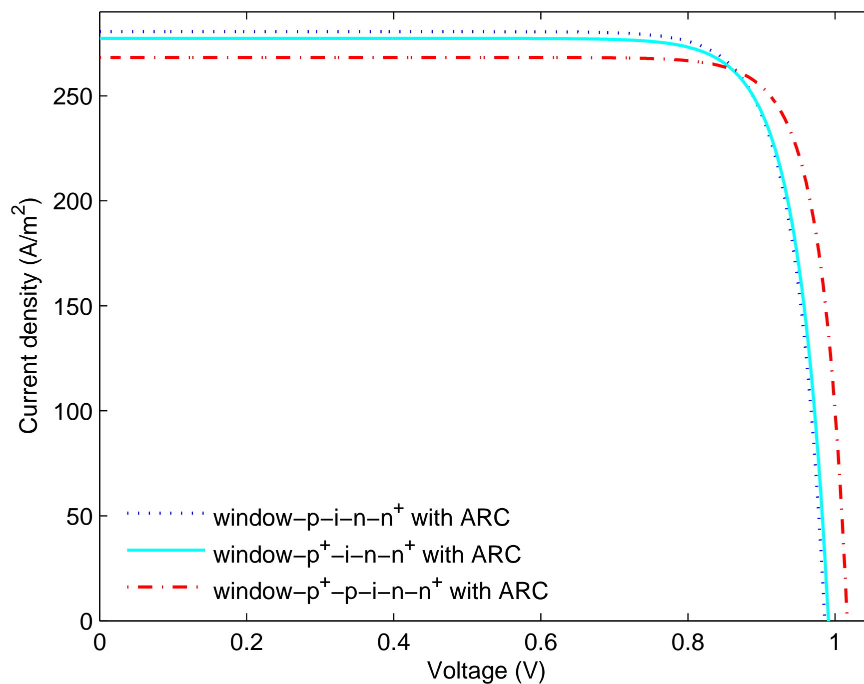

Figure 7.20: Current-voltage characteristics of a window-p-i-n-n$^+$, window-p$^+$-i-n-n$^+$ and window-p$^+$-p-i-n-n$^+$ solar cell.

The effect on quantum efficiency by adding additional layers to the p-i-n solar cell is shown in figure 7.21, and the effect on the current-voltage characteristic is shown in figure 7.22. The various photocurrents, dark currents by an applied voltage 0.8 V, open circuit voltages and efficiencies are given in table 7.5 showing how important the front surface field, back surface field, anti-reflective coating and window are in obtaining large photocurrent, little dark current and large efficiency.

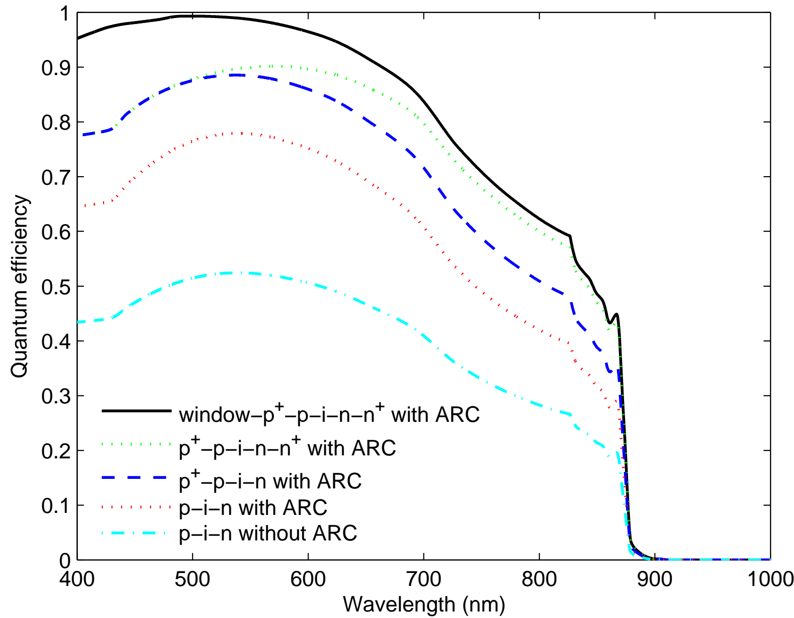

Figure 7.21: Comparison of quantum efficiency of p-i-n solar cells with different additional layers.

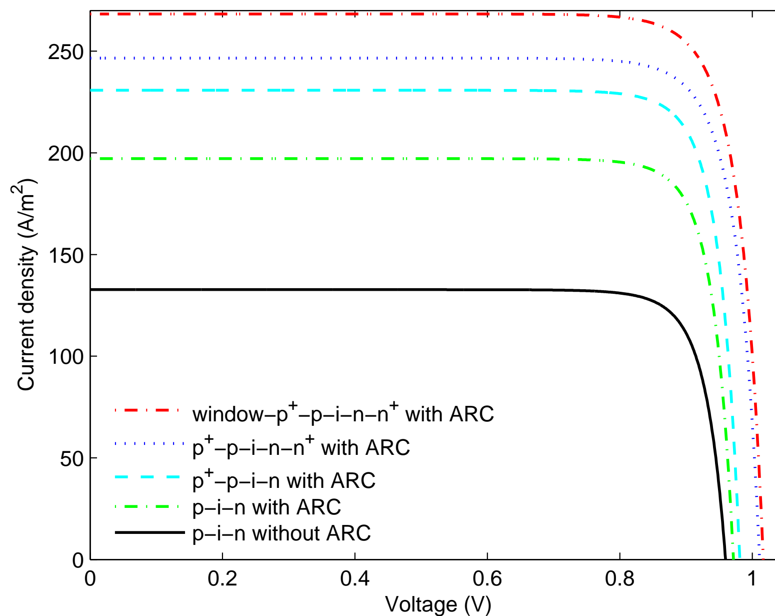

Figure 7.22: Current-voltage characteristic of p-i-n solar cells with different additional layers.

Table 7.5: Reference cells with multiple layers. Window is shortened as w.

Layers	J_{sc} (A/m^2)	J_{dark}(0.8V) (A/m^2)	V_{oc} (V)	η(%)	Abs. $\Delta\eta$(%)
p-i-n	132.7	1.70	0.960	10.80	-
ARC-p-i-n	197.1	1.70	0.972	16.34	5.5
ARC-p$^+$-p-i-n	230.8	1.66	0.981	19.31	3.0
ARC-p$^+$-p-i-n-n$^+$	246.6	1.55	1.011	20.94	1.6
ARC-w-p$^+$-p-i-n-n$^+$	268.3	1.54	1.017	22.90	2.0

Summary and discussion for the complete reference cell

The largest efficiency obtained by the modeling is 22.9 % for the window-p$^+$-p-i-n-n$^+$ solar cell. This is 76 % of the theoretical detailed balance maximum which is 30 % for the bandgap of GaAs [5]. In obtaining the theoretical detailed balance maximum only radiative recombination is included and infinite mobilities are assumed. This is not the case using real materials and is one reason why the obtained efficiency is lower than the theoretical. Other doping concentrations and thicknesses than the ones given in table 6.1 will change the efficiency and might result in a higher value. By including series and shunt resistances the efficiency is reduced, as described in section 2.5.

7.3 The simple model of the IB solar cell

In the preceding sections reference solar cells which only contain one band gap are modeled. In this section intermediate band solar cells with three band gaps E_G, E_H and E_L are modeled using the simple model presented in chapter 5. In the simple model the electron current from the p-layer J_{np} and the hole current from the n-layer J_{pn} are not included in the current-voltage characteristics. The p- and n-layers are required to separate the electrons and holes to avoid recombination. Generation and recombination in these layers are set equal to zero in the simple model. The width of the flat band region is held constant with voltage and equal to the thickness of the intermediate band layer $w_F = w_{IB}$. Both radiative recombination and non-radiative recombination in the intermediate band layer are included.

7.3.1 Check of the simple model program

The simple model is based on [34]. To check the correctness of my modeling program all material parameters are in this section taken directly from [34], except the absorption coefficients. The absorption coefficients in [34] contain a typing error, and the correct values of the absorption coefficients are 4×10^4 cm^{-1} [35]. The spectrum used is the black-body spectrum given in equation (2.74), and the material parameters used are given in table 7.6.

Table 7.6: Material parameters taken from [34] and [35] for α.

Band gap	$E_L = 0.57$ eV $E_H = 1.10$ eV $E_G = 1.67$ eV
Thickness	$w_{IB} = 1.3$ μm
Mobility	$\mu_{n,f} = \mu_{p,f} = 2000$ cm^2/(Vs)
Absorption coefficient	$\alpha_{CI} = 4 \times 10^4$ cm^{-1} for $E_L < E < E_H$, else 0 $\alpha_{IV} = 4 \times 10^4$ cm^{-1} for $E_H < E < E_G$, else 0 $\alpha_{CV} = 4 \times 10^4$ cm^{-1} for $E_G < E$, else 0
Sun temperature	$T_s = 6000$ K
Cell temperature	$T_c = 300$ K
Concentration factor	X=1000
Geometrical factor for the sun	$f_s = \frac{1}{46050}$
Effective densities of states	$N_C = N_V = 5 \times 10^{18}$ cm^{-3}

The thickness $w_{IB} = 1.3$ μm is the thickness of the intermediate band layer giving the maximum efficiency for maximum concentration [35]. This thickness is varied later to find the optimum thickness for the concentration X=1 and X=1000. The values of the band gaps $E_L = 0.57$ eV, $E_H = 1.10$ eV and $E_G = 1.67$ eV are the values giving the maximum efficiency for a concentration X=1000 [35]. The mobility and effective density of states in table 7.6 are the values used for mobility and effective density of states in the valence band and conduction band in the intermediate band layer.

The current-voltage characteristic obtained from my modeling by using these parameters is shown in figure 7.23 which resembles the form of the current-voltage characteristic

obtained in [34], here reproduced in figure 7.24. The parameters describing the behavior of the solar cell are given in table 7.7.

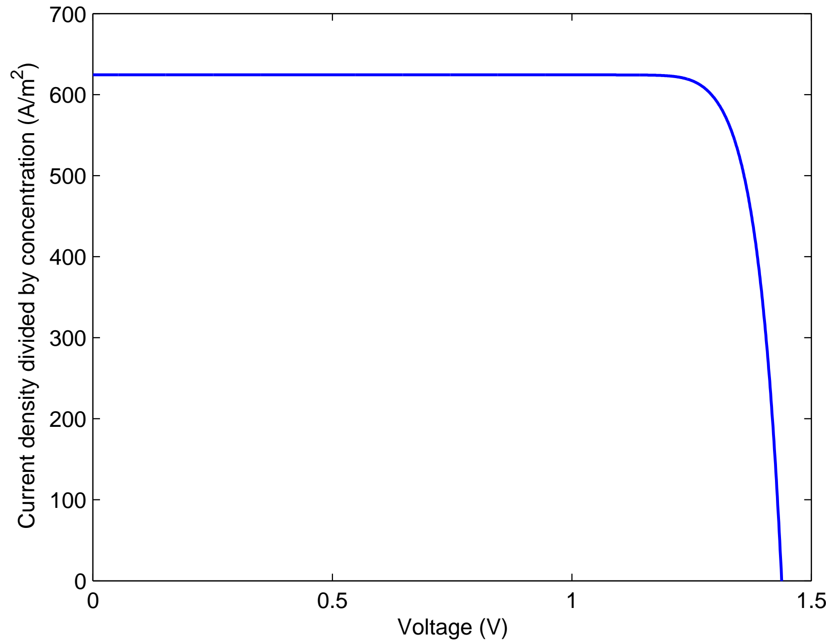

Figure 7.23: Current-voltage characteristic of an intermediate band solar cell obtained from my modeling using all the parameters from [34], a black-body spectrum and X=1000. The current-density is divided by the concentration factor X.

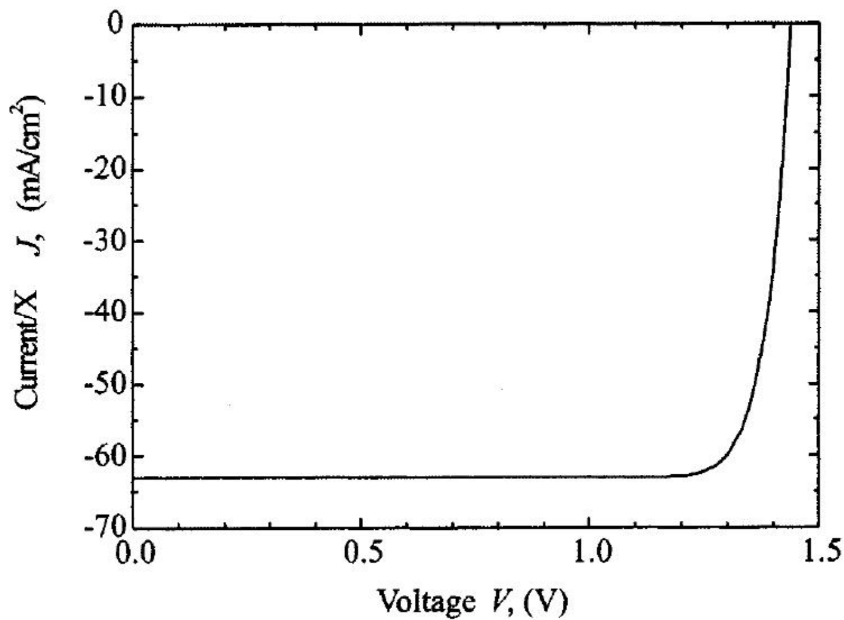

Figure 7.24: The current-voltage characteristic given in [34] of an intermediate band solar cell. Here the photocurrent is taken as negative in opposite to the sign convention used in this thesis. The current-density is divided by the concentration factor.

Table 7.7: Parameters describing the behavior of an intermediate band solar cell obtained in [34] and obtained from my modeling using the same parameters as in [34], listed in table 7.6.

Where obtained	$\frac{J_{sc}}{X}$(A/m^2)	V_{oc}(V)	η(%)
Taken from [34]	630	1.439	49.1
Taken from my modeling	624.3	1.438	48.66

Discussion

The small differences in the short-circuit current density and open-circuit voltage given in table 7.7 are probably due to different rounding off procedures. The simple model used in this thesis is therefore expected to give the correct results.

7.3.2 Black-body spectrum versus AM 1.5 spectrum

The AM 1.5 spectrum is shown in figure 6.12. As this spectrum better resembles the solar spectrum illuminating the solar cells placed on earth, the results obtained using this spectrum should be more realistic than using the black-body spectrum. In this section I therefore compare the results using the simple model for the same cell, but with different spectra.

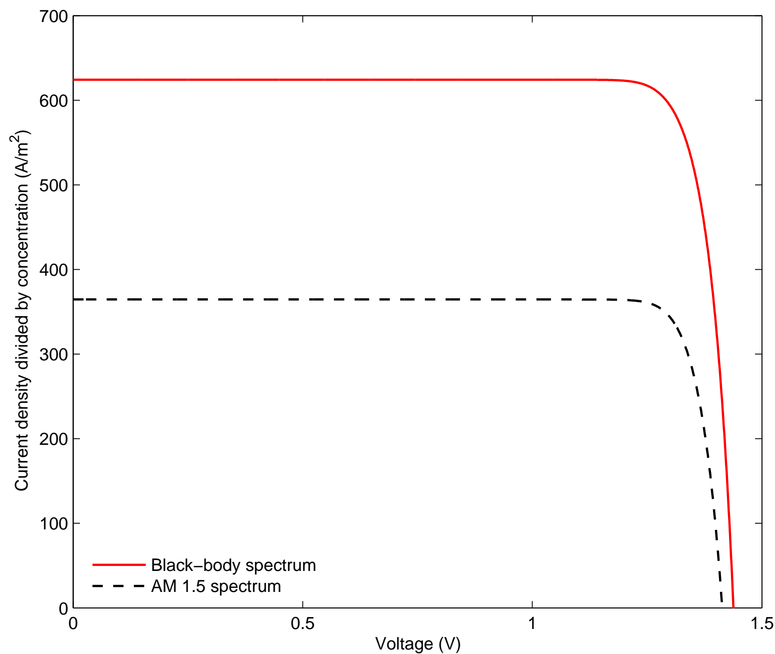

Figure 7.25: Current-voltage characteristic for a concentration X=1000 obtained by using black-body spectrum (solid, red line) and AM 1.5 spectrum (dashed, black line). All material parameters are taken from [34].

The current-voltage characteristic obtained by using the AM 1.5 spectrum is shown in figure 7.25 together with the current-voltage characteristic obtained by using the black-body spectrum. The material parameters used are the ones from [34] given in the previous section. Important parameters describing the behavior of the solar cell are listed in table 7.8.

Table 7.8: Parameters describing the behavior of an intermediate band solar cell for a concentration X=1000 obtained using the black-body spectrum and the AM 1.5 spectrum.

Spectrum	$\frac{J_{sc}}{X}$(A/m^2)	V_{oc}(V)	η(%)
Black-body	624.3	1.438	48.66
AM 1.5	364.6	1.414	45.32

As seen from figure 7.25 the short-circuit current obtained from the modeling is much smaller by using the AM 1.5 spectrum than by using the black-body spectrum. This is reasonable since the black-body spectrum has a larger intensity. The open-circuit voltage is of the same order. The efficiency is 48.66 % using the black-body spectrum which has an incoming flux of 1596 W/m^2 and 45.32 % using the normalized AM 1.5 spectrum which has an incoming flux of 1000 W/m^2.

Discussion
Using the AM 1.5 spectrum the limiting efficiency under no concentration of a standard solar cell is 31 %, while it is 30.5 % using the black-body spectrum [5]. The limiting efficiency of an intermediate band under no concentration is 49.4 % using the AM 1.5 spectrum [51] and 46.0 % using the black-body spectrum [7]. The difference in efficiency using the two spectras is,however, dependent on the band gap in the solar cell [52]. The band gaps $E_G = 1.67$ eV and $E_H = 1.10$ eV suit the black-body spectrum better than the AM 1.5 spectrum. The efficiency is therefore higher using the black-body spectrum. Through the rest of this thesis the AM 1.5 spectrum is used.

7.3.3 Mobility, effective density of states and absorption coefficient

Another set of values for the mobility and the effective density of states than the ones given in table 7.6 are used to see how this affects the current-voltage characteristic. The new parameters used are the effective density of states and mobility of intrinsic GaAs, given in section 6.1. Using these values the current-voltage characteristic shown in figure 7.26 [1][2] is obtained which is almost identical to the one obtained by using the parameters from [34], shown in the same figure. As can be seen from figure 7.26 and the values of short-circuit current density, open-circuit voltage and efficiency given in table 7.9, the effect of using another set of parameters is small.

[1] a: from [34]
[2] b: from section 6.1, (for intrinsic GaAs)

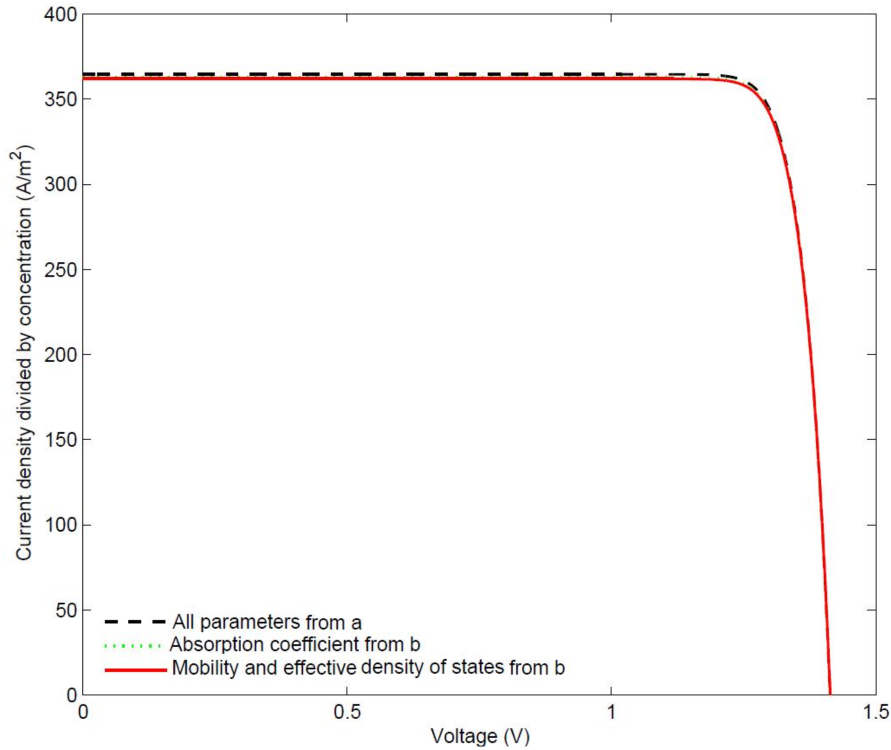

Figure 7.26: The resulting current-voltage characteristic of an intermediate band solar cell for three different cases: 1) All parameters are taken from [34] , 2) The mobility and effective density of states of intrinsic GaAs are used from section 6.1 , all other parameters are taken from [34]. 3) The absorption coefficient for valence band to conduction band transitions is taken as the absorption coefficient for GaAs from section 6.1, all other parameters are taken from [34].

Table 7.9: Parameters describing the behavior of an intermediate band solar cell obtained using the parameters from [34] and by changing some of these parameters.

N_C & N_V (10^{18}cm^{-3})	$\mu_{n,f}$ & $\mu_{p,f}$(cm^2/Vs)	α_{CV} (cm^{-1})	$\frac{J_{sc}}{X}$(A/m^2)	V_{oc}(V)	η(%)
5^a & 5^a	2000^a & 2000^a	4×10^{4a}	364.6	1.414	45.32
0.47^b & 7.0^b	8000^b & 400^b	4×10^{4a}	361.9	1.415	44.98
5^a & 5^a	2000^a & 2000^a	$\alpha_{GaAs}(E)^b$	362.8	1.414	45.11

When InAs/GaAs quantum dot solar cells are modeled, the mobility and density of states of intrinsic GaAs are used. By using the parameters for intrinsic GaAs we do not take into account that the mobility and the effective density of states may change by having quantum dots placed in the intrinsic region. Since the effect of changing these parameters in the case of $E_G = 1.67$, i.e not GaAs as intrinsic material, is small the simplification of using the intrinsic values is not expected to affect the results much.

To see the effect of having an absorption coefficient α_{CV} for valence band to conduction band transitions varying with energy instead of independent of energy as in [34], α_{CV} is taken to be the absorption coefficient of GaAs $\alpha_{GaAs}(E)$. The resulting current-voltage characteristic of the intermediate band solar cell is shown in figure 7.26 together with the current-voltage characteristic obtained by holding all parameters fixed

to the ones given in [34]. The open-circuit voltage, short circuit current density and efficiency obtained for the two cases are given in table 7.9. By using a constant value of $\alpha_{CV} = 4 \times 10^4$ cm^{-1} the efficiency obtained is 45.32 %, while by using a absorption coefficient equal to the absorption coefficient of GaAs, $\alpha_{CV} = \alpha_{GaAs}(E)$, the efficiency obtained is 45.11 %. The efficiency is thus almost unchanged.

Discussion

In intermediate band solar cells all the absorption coefficients α_{CI}, α_{IV} and α_{CV} may vary with energy [7]. The effect of varying α_{CV} with energy is seen not to affect the current-voltage characteristic much, and the simplification of using constant α_{CI} and α_{IV} values is thus not expected to be a drawback in the model. When InAs/GaAs quantum dot solar cells are modeled α_{CV} is set equal to $\alpha_{GaAs}(E)$ and $\alpha_{IV} = \alpha_{CI} = 4 \times 10^4$ cm^{-1}.

7.3.4 Variation of band gap

In this section the value of the band gap between the valence band and the intermediate band E_H is varied. E_G is taken from [34] as 1.67 eV while E_L is given from the relation $E_L = E_G - E_H$. All other parameters are taken from table 7.6. The efficiency as function of E_H is shown in figure 7.27 which shows that the maximum efficiency is 49.49 % obtained for a band gap E_H equal to 1.17 eV. The current-voltage characteristic using this value of the band gap E_H is shown in figure 7.28. The short-circuit current density obtained is 408.78 A/m^2 and the open-circuit voltage is equal to 1.419 V.

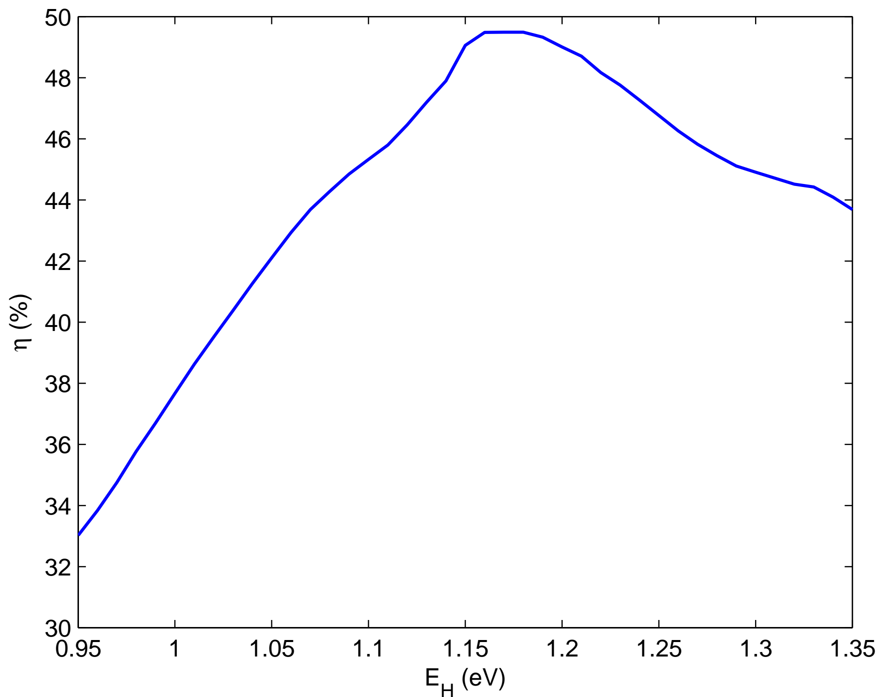

Figure 7.27: Efficiency of an intermediate band solar cell as function of the band gap E_H. All other parameters are given in table 7.9

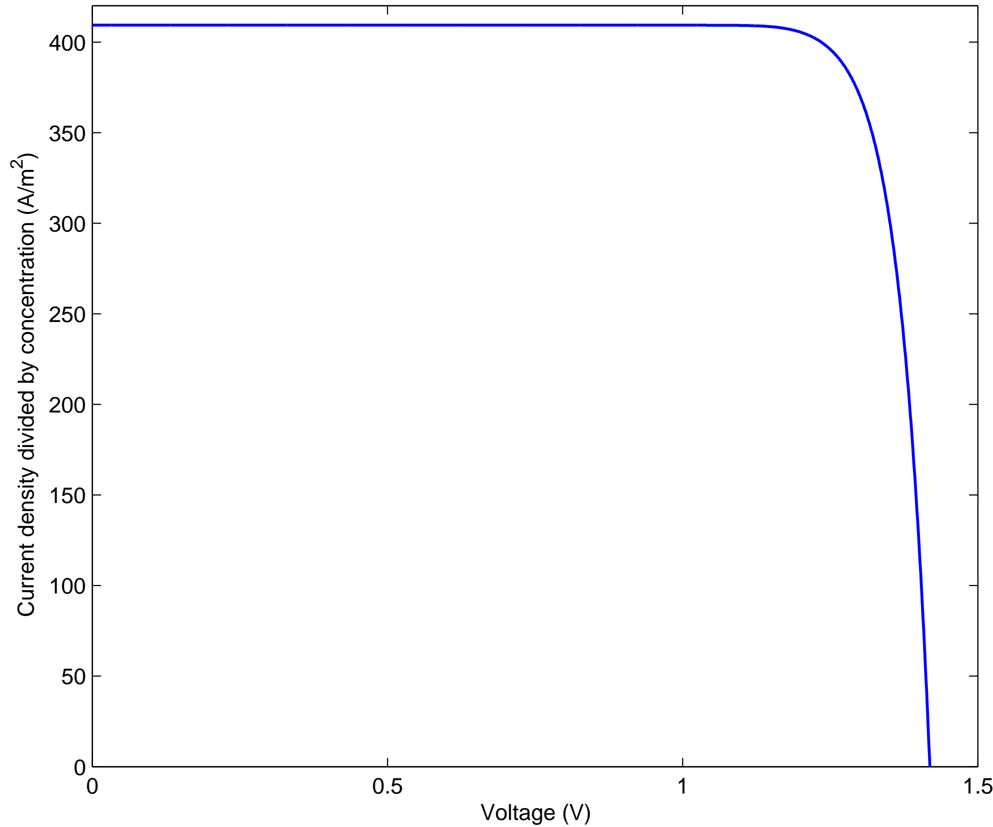

Figure 7.28: Current-voltage characteristic of an intermediate band solar cell using a value of $E_H = 1.17$ eV which gives the maximum efficiency. All other parameters are given in table 7.9

Discussion

As seen from figure 7.27 the value of the band gap E_H is clearly something to consider in the intermediate band solar cell. The efficiency is 33.02 % for $E_H = 0.95$ eV and is raised to 49.49 % for $E_H = 1.17$ eV. This is the value of E_H that gives the maximum efficiency. The value of the band gap E_H is dependent on the barrier and quantum dot material as well as the size of the quantum dots [15]. One common way to create quantum dots solar cells is to use GaAs as the barrier layers and InAs as the quantum dot material. These materials will be considered in the next section, where the optimum band gap E_H will be found for this system.

7.3.5 InAs/GaAs IB solar cells

Intermediate band solar cell samples made at NTNU are made of InAs quantum dots placed in GaAs, and this system will be studied in this section. The solar cell parameters are equal to the parameters for the solar cell sample A1681, given in table 6.3, except the thickness of the intermediate band layer which is taken as $w_{IB} = 1.3$ μm. This is the optimum value for maximum concentration [35].

By using GaAs as the barrier layers, the band gap E_G is set equal to the band gap of GaAs, approximately equal to 1.42 eV at 300 K. The mobilities and effective densities of states are taken as the values of intrinsic GaAs given in section 6.1. The absorption

coefficients are taken as $\alpha_{CV} = \alpha_{GaAs}(E)$ and $\alpha_{IV} = \alpha_{CI} = 4 \times 10^4$ cm^{-1}.

The band gap E_H is varied between 0.9 and 1.2 eV, while holding E_G constant. The value of E_L is given from $E_L = E_G - E_H$. The efficiency as function of E_H is shown in figure 7.29 for a concentration X=1 and X=1000. Only radiative recombination in the intermediate band layer is included. The current-voltage characteristic using the optimum band gaps from figure 7.29 are shown in figure 7.30. Important parameters describing the behavior of the solar cell are listed in table 7.10.

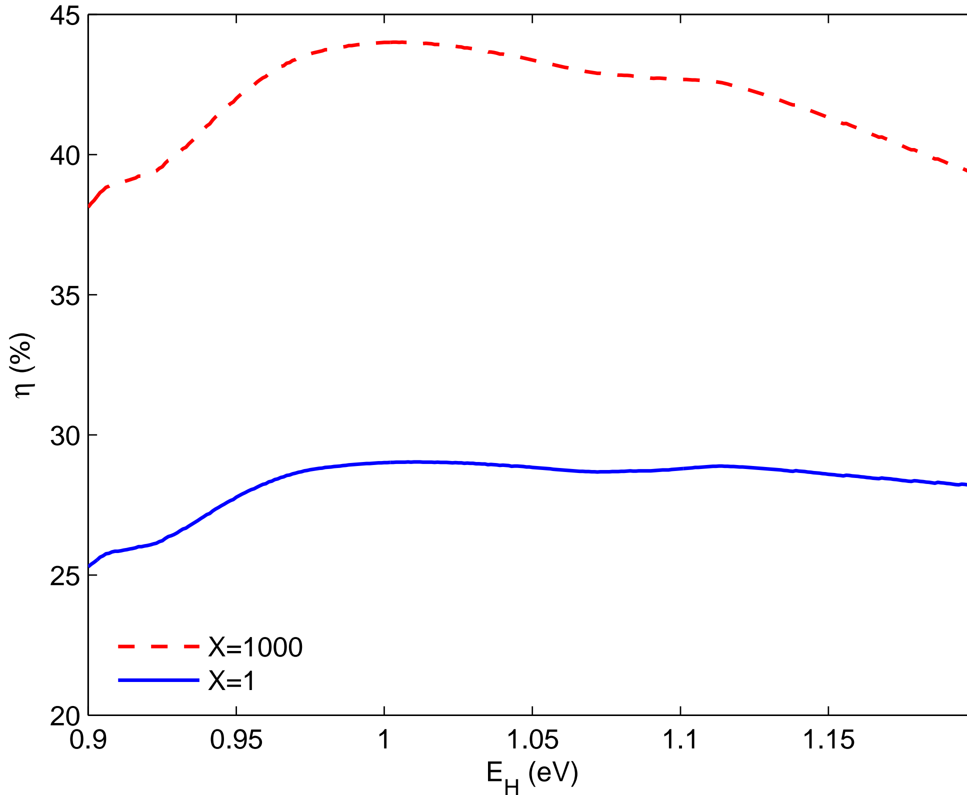

Figure 7.29: The efficiency of an intermediate band solar cell as function of E_H using concentration factors X=1 (solid, blue line) and X=1000 (dashed, red line). The maximum efficiency for X=1 is 29.03 % for E_H = 1.010 eV. The maximum efficiency for X=1000 is 44.01 % for $E_H = 1.004$ eV.

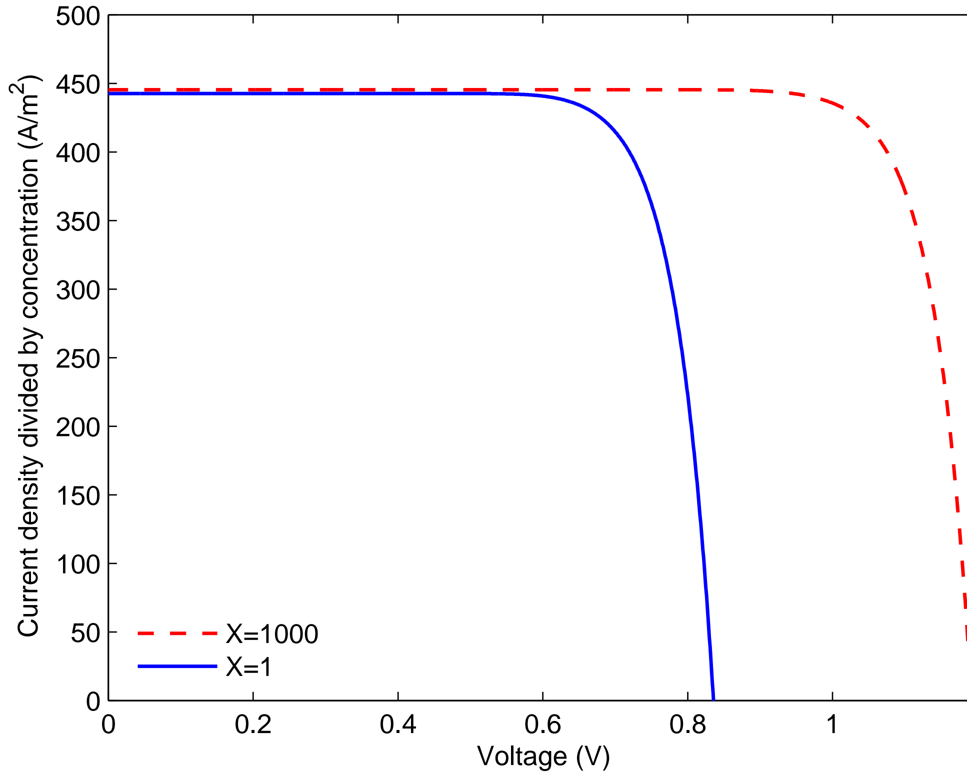

Figure 7.30: The current-voltage characteristic of an intermediate band solar cell for X=1 and the optimum band gap $E_H = 1.010$ eV (solid, blue line) and for X=1000 and the optimum band gap $E_H = 1.004$ eV (dashed, red line).

Table 7.10: Parameters describing the behavior of a InAs/GaAs quantum dot solar cell for X=1 and X=1000 using the optimum values of E_H.

Concentration factor X	E_H (eV)	$\frac{J_{sc}}{X}$(A/m^2)	V_{oc}(V)	η(%)
1	1.010	442.63	0.836	29.03
1000	1.004	445.33	1.193	44.01

A concentration X=1000 gives the highest efficiency for all band gaps E_H as expected from section 3.1. The variation of efficiency as function of band gap is having the same form for both concentration factors with a maximum efficiency 29.03 % for a band gap $E_H = 1.010$ eV for X=1 and 44.01 % for a band gap $E_H = 1.004$ eV for X=1000.

Discussion

The efficiencies obtained for $E_G = E_{GaAs}$ are as expected lower than for $E_G = 1.67$ eV which is the optimum band gap for 1000 suns [35]. To increase E_G one can replace GaAs with $Al_xGa_{1-x}As$. Some NTNU solar cell samples, optimized for concentrations larger than X=1000, are made of $Al_{0.35}Ga_{0.65}As$ with $E_G = 1.86$ eV. In section section 7.7 both InAs/$Al_{0.35}Ga_{0.65}As$ and InAs/GaAs intermediate band solar cells are modeled, and the effect of increasing E_G from $E_{GaAs} = 1.42$ eV to $E_{Al_{0.35}Ga_{0.65}As}$=1.86 eV is seen.

Varying thickness of intermediate band layer z_{IB} and band gap E_H.
Photon recycling is as mentioned not included in the models used in this thesis. This means that the thickness of the intermediate band layer has to be optimized [35]. The effect of varying the thickness of the intermediate band layer is now studied. Four different values of the thickness of the intermediate band layer are used: $w_{IB} = 0.65$ μm, $w_{IB} = 1.30$ μm, $w_{IB} = 2.60$ μm and $w_{IB} = 5.20$ μm. For each of the cases the value of the band gap E_H is varied to obtain the highest efficiency. Both radiative and non-radiative recombination in the intermediate band layer are included, and concentration factors X=1 and X=1000 are used.

i) Radiative recombination, X=1
For X=1 and only including radiative recombination, the efficiency for the four thicknesses varies as function of band gap as shown in figure 7.31. The current-voltage characteristic using the optimum band gaps for each of the four thicknesses is shown in figure 7.32. Important parameters describing the behavior of the solar cells are listed in table 7.11.

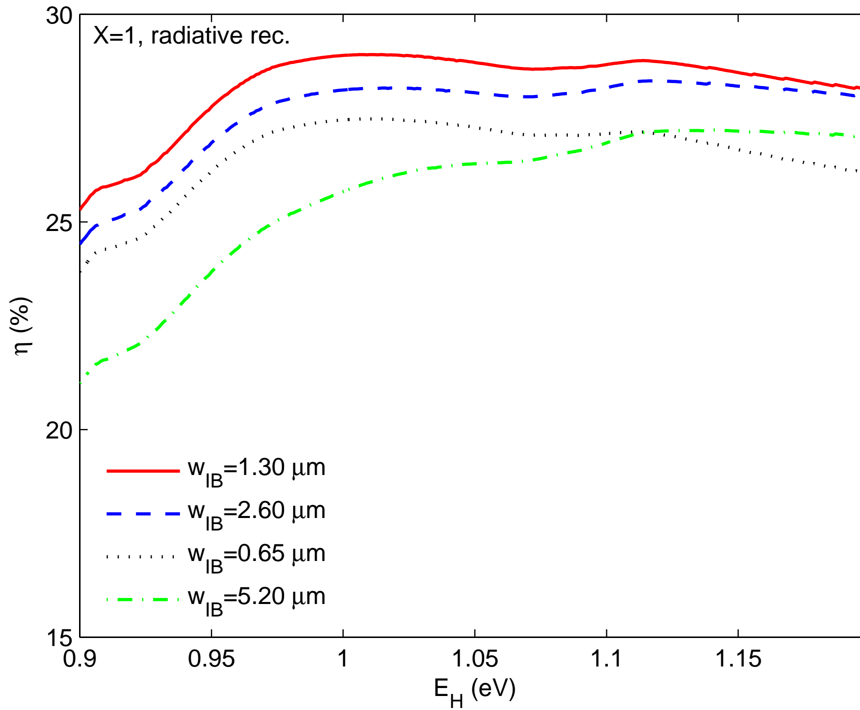

Figure 7.31: Efficiency as function of band gap E_H using four different thicknesses of intermediate band layer. Only radiative recombination is included.

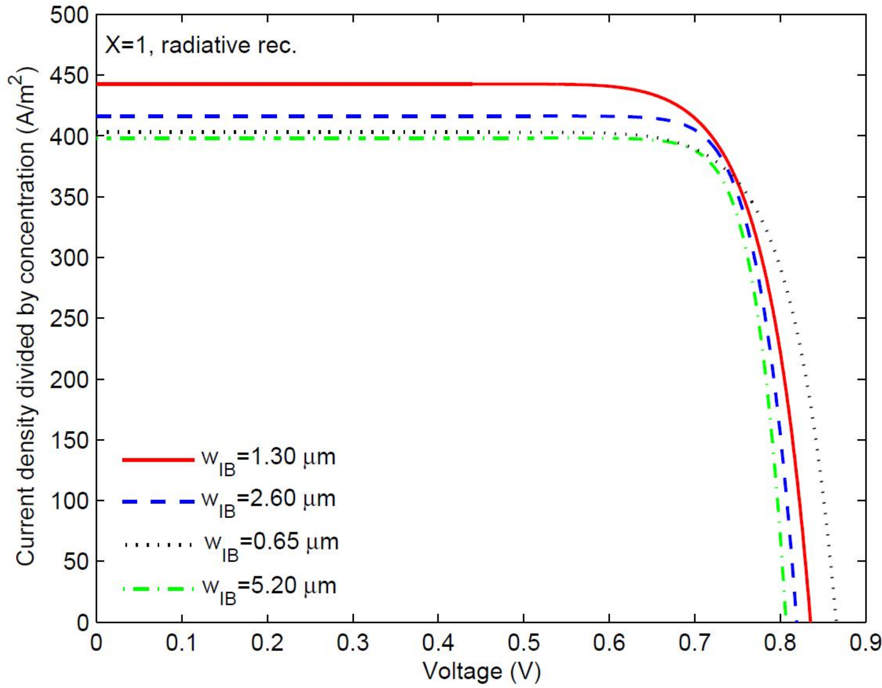

Figure 7.32: Current-voltage characteristic of an intermediate band solar cell using four different thicknesses of the intermediate band layer. The optimum band gaps E_H=1.010 eV for $w_{IB} = 0.65$ μm, E_H=1.010 eV for $w_{IB} = 1.30$ μm, $E_H = 1.116$ eV for $w_{IB} = 2.60$ μm and $E_H = 1.139$ eV for$w_{IB} = 5.20$ μm are used. Only radiative recombination is included.

Table 7.11: Parameters describing the behavior of an intermediate band solar cell for four different thicknesses of the intermediate band layer using the optimum value of E_H and X=1. Only radiative recombination is included.

Width of IB material w_{IB} (μm)	E_H (eV)	$\frac{J_{sc}}{X}$(A/m^2)	V_{oc}(V)	η(%)
0.65	1.010	402.83	0.866	27.48
1.30	1.010	442.63	0.836	29.03
2.60	1.116	416.24	0.820	28.40
5.20	1.139	398.10	0.807	27.22

Discussion

The highest efficiency 29.03 % is obtained for the width w_{IB} equal to 1.30 μm. The intermediate band layer is then wide enough to absorb lots of of photons and at the same time narrower than the electron and hole diffusion lenghts, equal to $L_{n,IB} = 11.1$ μm and $L_{p,IB} = 4.1$ μm for $E_H = 1.010$ eV. This gives a high photocurrent. The dark-current increases with increasing thickness of the intermediate band layer, as can be seen from equation (5.26) and (5.27). This is the reason for the decreasing open-circuit voltage with increasing thickness of the intermediate band layer. The increase of photocurrent is, however, higher than the increase of dark-current increasing w_{IB} from 0.65 μm to 1.30 μm. This gives a higher efficiency for w_{IB} equal to 1.30 μm than for w_{IB} equal to 0.65 μm. The decrease in photocurrent by increasing the thickness of the intermediate band layer further than 1.30 μm is due to a higher increase of recombination than gen-

eration. This gives a lower efficiency for the thicknesses 2.60 μm and 5.20 μm than for $w_{IB} = 1.30 \mu m$.

ii) Radiative and non-radiative recombination, X=1

By including non-radiative recombination in the intermediate band layer the efficiency is reduced. The efficiency as function of the band gap E_H for four different thicknesses of the intermediate band layer is shown in figure 7.33. The current-voltage characteristic using the optimum band gaps for each of the four thicknesses is shown in figure 7.34. Important parameters describing the behavior of the solar cells are listed in table 7.12.

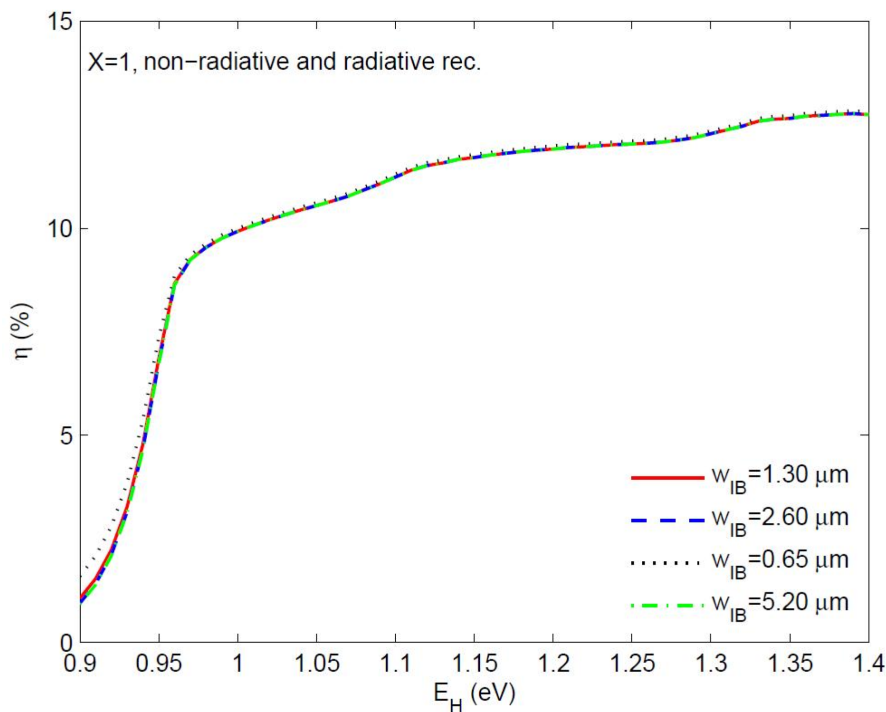

Figure 7.33: Efficiency as function of band gap E_H using four different thicknesses of intermediate band layer. Both radiative and non-radiative recombination are included.

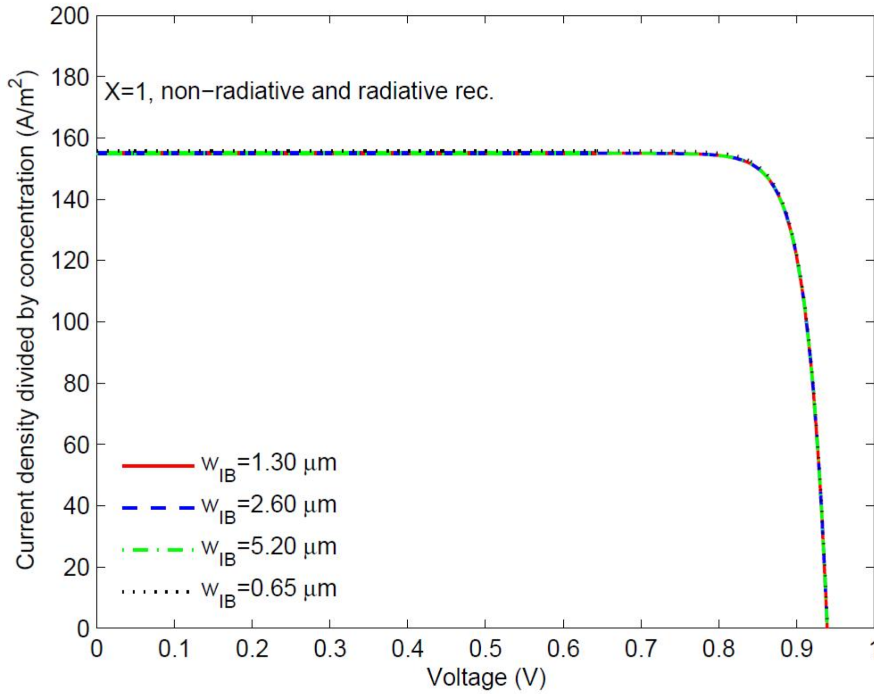

Figure 7.34: Current-voltage characteristic of an intermediate band solar cell using four different thicknesses of the intermediate band layer. The optimum band gaps are E_H=1.390 eV for all the thicknesses. Radiative and non-radiative recombination are included.

Table 7.12: Parameters describing the behavior of an intermediate band solar cell for four different thicknesses of the intermediate band layer using the optimum value of E_H and X=1. Radiative and non-radiative recombination are included.

Width of IB material w_{IB} (μm)	E_H (eV)	$\frac{J_{sc}}{X}$(A/m^2)	V_{oc}(V)	η(%)
0.65	1.390	155.77	0.941	12.83
1.30	1.390	155.00	0.941	12.76
2.60	1.390	155.00	0.941	12.76
5.20	1.390	155.00	0.941	12.76

Discussion

The maximum efficiency is 12.83 % when non-radiative recombination is included in the intermediate band layer. The thickness of the intermediate band layer is then 0.65 μm and the band gap is E_H = 1.390 eV. By having such a great value for E_H the intermediate band is placed very close to the conduction band. The assumption of having three distinct quasi-Fermi levels in the intermediate band layer is probably not fulfilled by having the intermediate band placed very close to the conduction band, and the simple model is then not valid.

The diffusion lengths of electrons and holes when non-radiative recombination is included are $L_{n,IB'}$ = 100 nm and $L_{p,IB'}$ = 200 nm for a band gap E_H = 1.39 eV. All the thicknesses used for the intermediate band layer are larger than the diffusion lengths, see table 7.12. The narrowest solar cell has the highest short-circuit current density and the highest efficiency, see table 7.12. The open-circuit voltage is equal for all the cases

considered. The reason for this is that the dark-current saturates when the thickness of the intermediate band layer is much wider than the diffusion lengths. The efficiency is expected to increase using thicknesses of the intermediate band layers smaller than the diffusion lengths.

iii) Radiative recombination, X=1000

For a concentration factor X=1000 and only including radiative recombination the efficiency varies as function of band gap E_H as shown in figure 7.35 for four thicknesses of the intermediate band layer. The current-voltage characteristic by using the optimum band gaps for each of the thicknesses is shown in figure 7.36. Important parameters describing the behavior of the solar cells are listed in table 7.13.

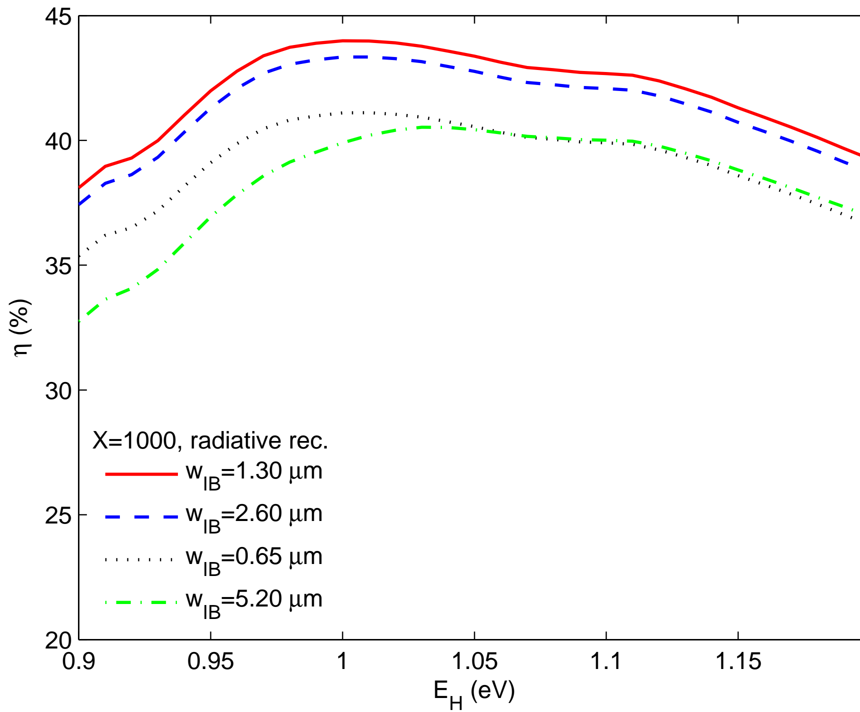

Figure 7.35: Efficiency as function of band gap E_H using four different thicknesses of the intermediate band layer. Only radiative recombination is included.

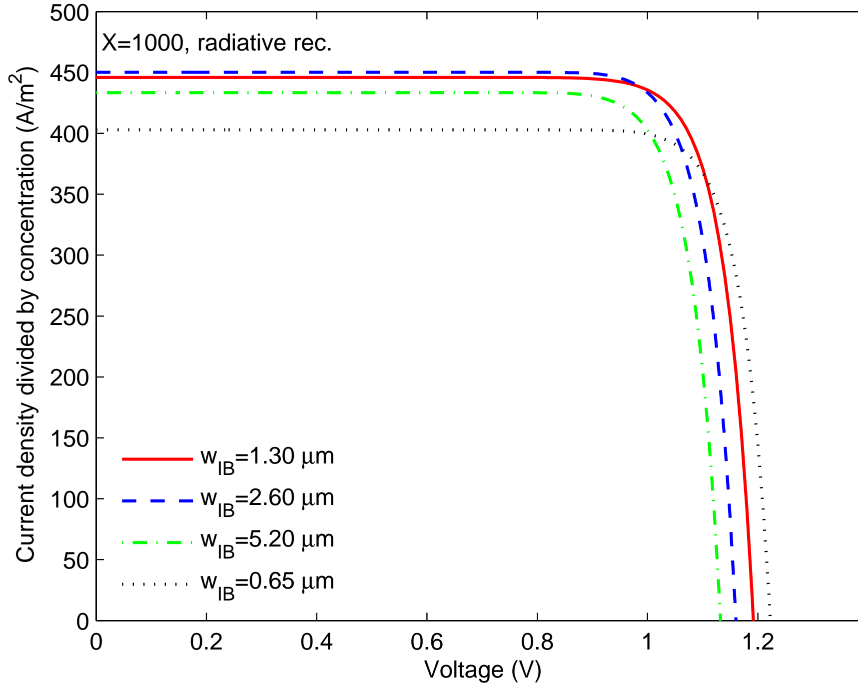

Figure 7.36: Current-voltage characteristic of an intermediate band solar cell using four different thicknesses of the intermediate band layer. The optimum band gaps E_H=1.010 eV for $w_{IB} = 0.65$ μm, E_H=1.000 eV for $w_{IB} = 1.30$ μm, $E_H = 1.010$ eV for $w_{IB} = 2.60$ μm and $E_H = 1.030$ eV for $w_{IB} = 5.20$ μm are used. Only radiative recombination is included.

Table 7.13: Parameters describing the behavior of an intermediate band solar cell for four different thicknesses of the intermediate band layer using the optimum value of E_H and X=1000. Only radiative recombination is included.

Width of IB material w_{IB} (μm)	E_H (eV)	$\frac{J_{sc}}{X}$(A/m^2)	V_{oc}(V)	η(%)
0.65	1.010	402.83	1.226	41.11
1.30	1.000	445.88	1.195	44.00
2.60	1.010	450.09	1.160	43.34
5.20	1.030	433.40	1.134	40.52

The efficiency shows the same trend as for X=1. The highest efficiency 44.00 % is obtained for $w_{IB} = 1.30$ μm and the band gap $E_H = 1.000$ eV. As expected the open-circuit voltage is higher for a concentration factor X=1000 than for X=1. The short-circuit current density divided by X is equal for the concentration factors X=1 and X=1000 when the same band gap E_H is used. This is the case for $w_{IB} = 0.65$ μm. By using different band gap the current density is different, as expected. For X=1000 the short-circuit current density is largest for $w_{IB} = 2.60$ μm. This is in contrast to for X=1 where the short-circuit current density is largest for $w_{IB} = 1.30$ μm. The reason why the wider layer gives a higher current density for X=1000 is that for a higher concentration more photons are available for absorption and the layers can be wider. The decrease of open-circuit voltage leads, however, to a maximum efficiency for $w_{IB} = 1.30$ μm rather than for $w_{IB} = 2.60$ μm.

iv) Radiative and non-radiative recombination, X=1000
By also including non-radiative recombination the efficiency for X=1000 varies as function of band gap E_H as shown in figure 7.37. The current-voltage characteristic for the optimum band gaps for each of the thicknesses is shown in figure 7.38. Important parameters describing the behavior of the solar cells are listed in table 7.14.

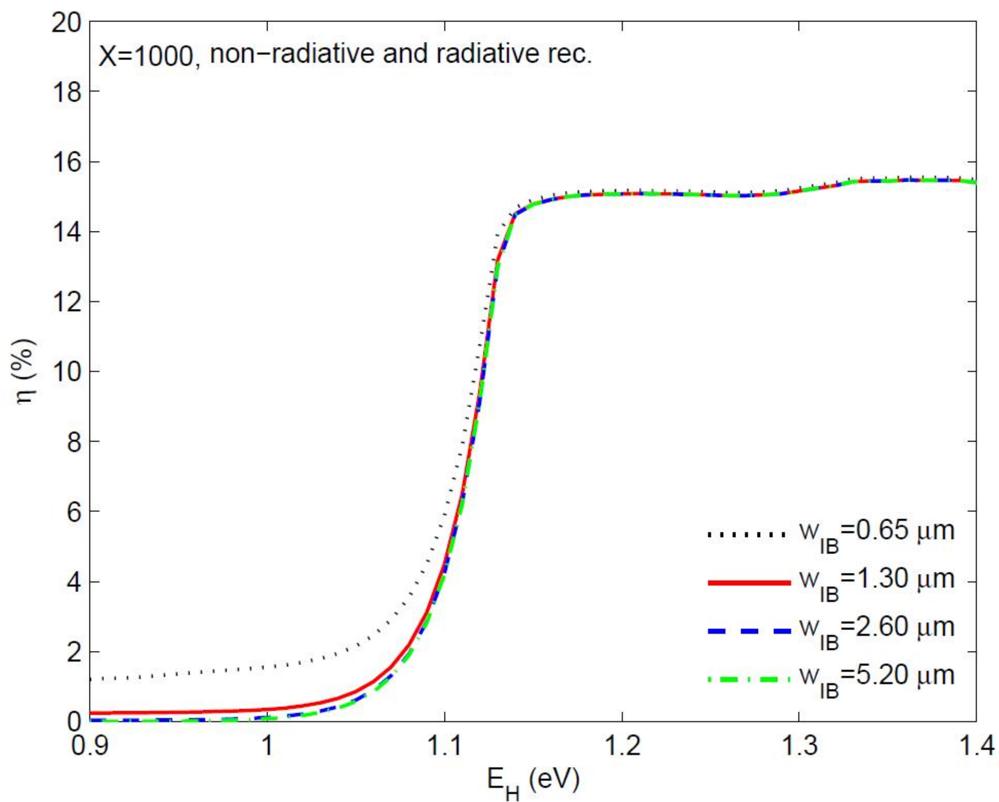

Figure 7.37: Efficiency as function of band gap E_H using four different thicknesses of intermediate band layer. Both radiative and non-radiative recombination are included.

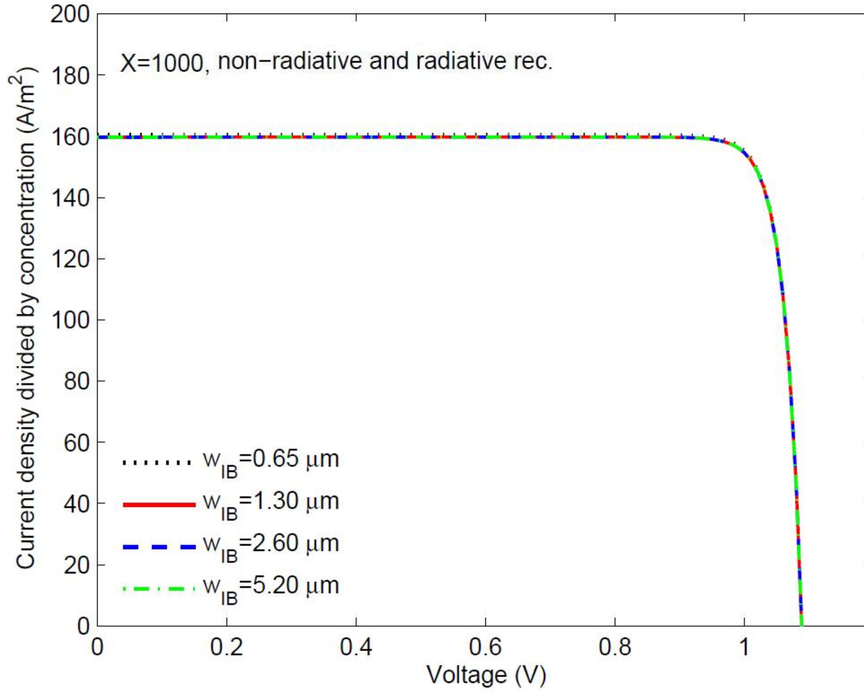

Figure 7.38: Current-voltage characteristic of an intermediate band solar cell using four different thicknesses of the intermediate band layer. The optimum band gaps are E_H=1.360 eV for all the thicknesses. Both radiative and non-radiative recombination are included.

Table 7.14: Parameters describing the behavior of an intermediate band solar cell for four different thicknesses of the intermediate band layer using the optimum value of E_H and X=1. Radiative and non-radiative recombination are included.

Width of IB material w_{IB} (μm)	E_H (eV)	$\frac{J_{sc}}{X}$(A/m^2)	V_{oc}(V)	η(%)
0.65	1.360	160.53	1.090	15.55
1.30	1.360	159.71	1.090	15.47
2.60	1.360	159.70	1.090	15.47
5.20	1.360	159.70	1.090	15.47

The maximum efficiency 15.55 % is obtained for the smallest thickness of the intermediate band layer. Comparing table 7.12 and 7.14 we see that when radiative and non-radiative recombination are included the maximum efficiency is 21.2 % higher for X=1000 than for X=1. When only radiative recombination is included the maximum efficiency is 51.6 % higher for X=1000, see table 7.11 and 7.13. The use of concentrators is thus more important when radiative recombination is dominating the recombination in the solar cell.

7.4 The complete model of the IB solar cell

In this section the complete model described in chapter 5 is used in the modeling of intermediate band solar cells. In the complete model the electron current from the p-layer J_{np} and the hole current from the n-layer J_{pn} are included. All the layers of the solar cell; the anti-reflective coating, window-, p$^+$-, p-, i-, n-, n$^+$- and the intermediate band layer, are included in obtaining the current-voltage characteristic. The width of the flat band region w_F varies with voltage and is not equal to the thickness of the intermediate band layer w_{IB} as assumed in the simple model.

The quantum dot solar cells modeled in this section are made of GaAs and are having the same structure as shown in figure 4.1 with doping and thicknesses of all layers, except the i-layer, given in table 6.1. InAs quantum dots are placed in a part of the i-layer. Reference cells made of GaAs are modeled to be able to compare the intermediate band solar cells with the reference cells having the same thicknesses and doping concentrations. The most of the material parameters are taken for GaAs, given in table 6.2. The band gap E_G is equal to the band gap of GaAs. In the section 7.4.1 and 7.4.2 the value used for E_H is 1.14 eV. The value of 1.14 eV for E_H is obtained from a value of E_H equal to 1.22 eV at 2 K. This value is taken from reported experimental values from photoluminescence for InAs quantum dots in GaAs. The temperature dependence of E_H is assumed to be the same as the temperature dependence of the band gap of GaAs, given in equation (6.1). In section 7.4.3 E_H is varied.

The absorption coefficients α_{IV} and α_{CI} are set equal to 4×10^4 cm^{-1} as in the previous sections. The thickness of the intermediate band layer is 1.3 μm. The thicknesses of the i-layers, $w_{ip,min}$ and $w_{in,min}$, see figure 5.1, depend on the concentration X. The total thickness of the i-layers and the intermediate band layer is $z_i = w_{ip,min} + w_{IB} + w_{in,min}$. As mentioned in chapter 5, $w_{ip,min}$ and $w_{in,min}$ are the depletion widths between the p- and the i-layer and between the i- and the n-layer obtained for a voltage V_{max} approximately equal to the open-circuit voltage. For X=1 the open-circuit voltage is approximately equal to 0.85 V, see figure 7.39. $V_{max} = 0.85$ V gives a total thickness of the i-layers and the intermediate band layer equal to $z_i = 4.246$ μm and this thickness is used for all solar cell samples for X=1. For X=1000 the open-circuit voltage is approximately equal to 1.2 V, see figure 7.42. $V_{max} = 1.2$ V gives a total thickness of the i-layers and the intermediate band layer equal to $z_i = 3.179$ μm, and this thickness is used for all solar cell samples for X=1000.

7.4.1 InAs/GaAs quantum dot intermediate band solar cell, X=1, fixed E_H and w_{IB}

The current-voltage characteristic for an intermediate band solar cell for X=1 and $E_H = 1.14$ eV is shown in figure 7.39 together with the current-voltage characteristic of the reference cell. Two cases are shown for the quantum dot solar cell, one where only radiative recombination in the flat band region of the intermediate band layer is included and one where also non-radiative recombination is included. Only non-radiative recombination is included in the i-layers. The reason why radiative recombination in the i-layers is omitted is because the current can not be determined analytically in this case, and as mentioned numerical modeling is out of the scope of this thesis. Important parameters describing the behavior of the solar cells are listed in table 7.15

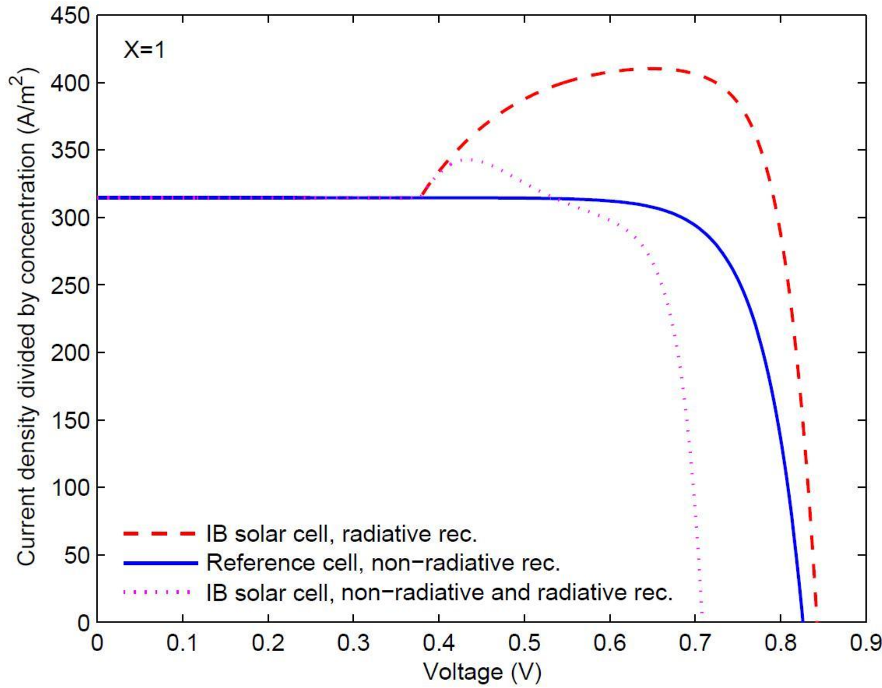

Figure 7.39: Current-voltage characteristic of an InAs/GaAs quantum dot solar cell when only radiative and both radiative and non-radiative recombination are included in the flat band region of the intermediate band layer. Also shown is the current-voltage characteristic of the reference cell without quantum dots. The concentration factor is X=1 and the total thickness of the i-layers and the intermediate band layer is $z_i = 4.246\ \mu$m. The band gap E_H is 1.14 eV.

Table 7.15: Parameters describing the behavior of an InAs/GaAs quantum dot solar cell and a GaAs reference cell when only radiative recombination and both radiative recombination and non-radiative recombination are included. The concentration factor is X=1. The band gap E_H is 1.14 eV.

Cell	Recombination	$\frac{J_{sc}}{X}$(A/m^2)	V_{oc}(V)	η(%)
Reference	Non-radiative	314.55	0.831	20.59
Intermediate band	Radiative	314.55	0.846	29.03
Intermediate band	Radiative and non-radiative	314.55	0.711	18.01

Discussion of the importance of having a flat band

As seen from figure 7.39 the current density in the quantum dot solar cell starts to rise for voltages greater than 0.37 V. The reason for this is that the width of the flat band increases for increasing voltages. The width is zero for voltages less than 0.37 V, as shown in figure 7.40. The intermediate band is fully depleted for V<0.37 V.

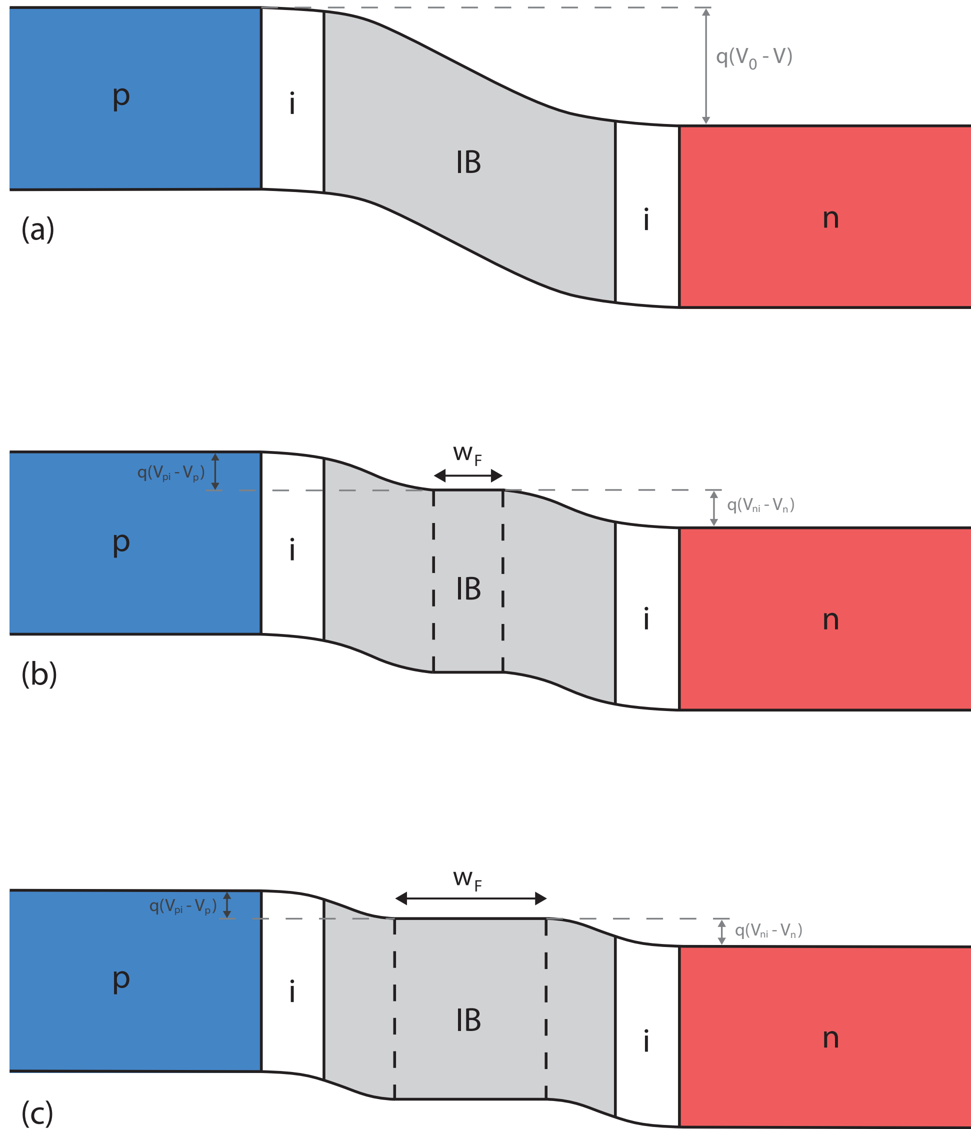

Figure 7.40: Drawing showing how the width of the flat band increases as function of voltage. (a) V<0.37 V and intermediate band layer is fully depleted. (b) V>0.37 V and some of the intermediate band layer is contained in a flat band region. (c) V»0.37 V and more of the intermediate band layer than in case (b) is contained in a flat band region. V_0 is the built-in potential of the p-n junction, V_{pi} is the built-in potential of the p-i junction and V_{ni} is the built-in potential of the i-n junction. V_p is the part of the voltage V that appears over the p-i junction. V_n is the part of the voltage V that appears over the i-n junction.

The intermediate band, formed by quantum dots, placed in a depletion region is either filled or empty of electrons as shown in figure 3.5. Then only two of the three needed transitions are possible in the intermediate band layer, as shown in figure 7.41a and b, in contrast to when the intermediate band is partially filled with electrons and three transitions are possible, see figure 7.41c. Two transitions via the intermediate band are necessary to create an electron in the conduction band and a hole in the valence

band. When only one of these transitions is possible at the same time, the value of the photocurrent depends heavily on the lifetimes of electrons/holes in the intermediate band. If the intermediate band is empty, an electron may be transferred from the valence band to the intermediate band. If the lifetime for the electron in the intermediate band is long enough it may be transferred from the intermediate band to the conduction band by absorption of a second photon, and an electron-hole pair is created. If the lifetime is short, however, the electron will recombine before being transferred to the conduction band. The current from the intermediate band layer should be no greater than from a material without an intermediate band. Short lifetimes are assumed in my model. This is the reason for the behavior of the current as function of voltage as shown in figure 7.39. In the flat band with a partially filled intermediate band both the transition from the valence band to the intermediate band and the transition from the intermediate band to the conduction band are possible at the same time, and the intermediate band contributes to the photocurrent. Until now quantum dot solar cells have only been made with quantum dots placed in the depletion region, and measurements show an increased quantum efficiency of the quantum dot solar cell compared with the quantum efficiency of the reference cell, but lower open-circuit voltage [13]. A further development of the complete model should take the quantum dots in the depletion region into account.

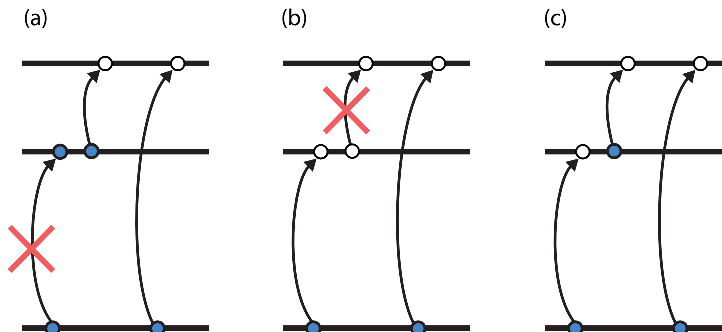

Figure 7.41: Transitions possible in (a) a filled intermediate band, (b) an empty intermediate band and (c) a partially filled intermediate band

Discussion of the importance of the recombination

The current-voltage characteristic is greatly influenced by the type of recombination included. When only radiative recombination in the flat band region of the intermediate band layer is included the current increases for voltages in the interval between 0.37 V and 0.70 V, see figure 7.39. This is due to the increasing flat band region. For voltages higher than 0.70 V the increase of generation caused by the increasing flat band region is smaller than the increase of recombination, and the current decreases. When non-radiative recombination is included, the current increases for voltages between 0.37 V and 0.43 V, see figure 7.39. This narrow interval gives a low efficiency. By assuming that radiative

recombination dominates the efficiency is 29.04 %. The efficiency is reduced to 18.01 % by including non-radiative recombination. When non-radiative recombination is included, the reference cell has a greater efficiency (20.59 %) than the intermediate band solar cell (18.01%), see table 7.15. 20.59 % is 69 % of the theoretical maximum of GaAs that is 30 % [5]. The values used for the non-radiative lifetimes are taken for a specific solar cell in [13] and are thought to be very pessimistic values. The efficiency obtained by considering only radiative recombination is too optimisitic, however. The real efficiency is thought to lay between the value obtained when only radiative recombination is included, and the value obtained when both radiative and non-radiative recombination are included.

7.4.2 InAs/GaAs quantum dot intermediate band solar cell, X=1000, fixed E_H and w_{IB}

The current-voltage characteristic for the quantum dot solar cell for X=1000 and $E_H = 1.14$ eV is shown in figure 7.42 together with the current-voltage characteristic of the reference cell. Two cases are shown for the quantum dot solar cell, one where only radiative recombination in flat band region of the intermediate band layer is included and one where also non-radiative recombination is included. Important parameters describing the behavior of the solar cell are listed in table 7.16.

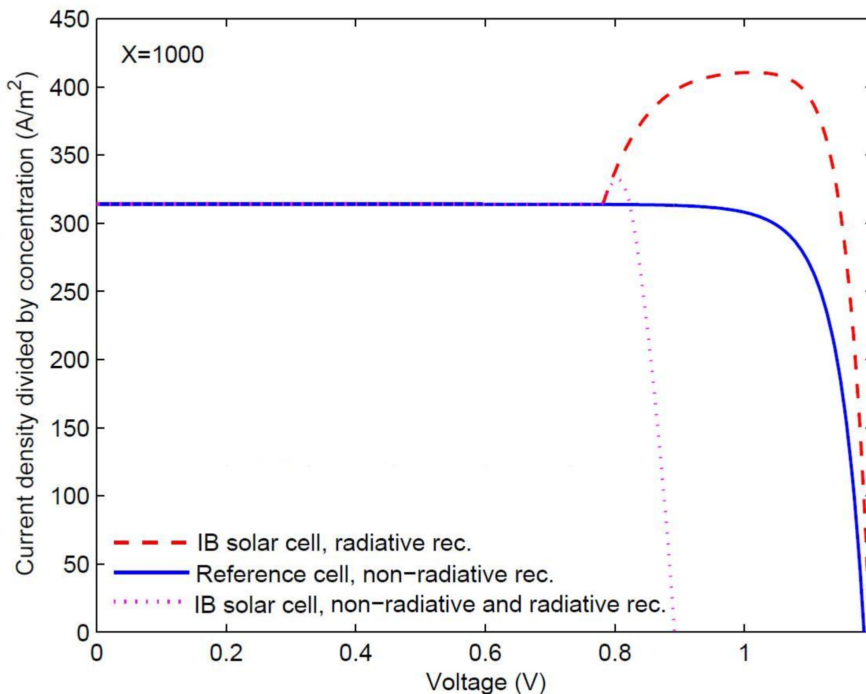

Figure 7.42: Current-voltage characteristic of an InAs/GaAs quantum dot solar cell when only radiative and both radiative and non-radiative recombination are included in the flat band region of the intermediate band layer. Also shown is the current-voltage characteristic of the reference cell without quantum dots. The concentration factor is X=1000 and the width of the intrinsic layer is 3.179 μm. The band gap E_H is 1.14 eV.

Table 7.16: Parameters describing the behavior of an InAs/GaAs quantum dot solar cell and a GaAs reference cell when only radiative recombination and both radiative recombination and non-radiative recombination are included in the flat band region of the intermediate band layer. The concentration factor is X=1000. The band gap E_H is 1.14 eV.

Cell	Recombination	$\frac{J_{sc}}{X}$(A/m^2)	V_{oc}(V)	η(%)
Reference	Non-radiative	313.74	1.184	31.36
Intermediate band	Radiative	313.73	1.197	43.50
Intermediate band	Non-radiative and radiative	313.74	0.897	26.80

Discussion
Using a concentration factor X=1000 the voltage giving a flat band region is 0.77 V. This is the voltage where the current in the quantum dot solar cell starts to rise with increasing voltage. Only including radiative recombination the current rises for voltages between 0.77 V and 1.08 V. Also including non-radiative recombination the current rises for voltages between 0.77 V and 0.80 V. The highest efficiency is 43.50 % for the quantum dot solar cell when only radiative recombination is included. By including non-radiative recombination the efficiency is lower for the quantum dot solar cell than the reference cell. This is the same behavior as for X=1. The efficiency value of the reference cell 31.36 % is near the theoretical maximum of GaAs solar cells of 36-37 % for a concentration factor X=1000 [3]. For a concentration factor equal to 1000 high-injection conditions might appear and this is in the complete model not taken into account in other layers than in the i-layer. In the i-layer high injection is assumed for all concentrations since the doping densty is very low here. The complete model may therefore give too optimistic values for the efficiency when the concentration factor X=1000 is used.

7.4.3 Varying z_{IB} and E_H

The value of the band gap E_H is in this section varied for four different thicknesses of the intermediate band layer (w_{IB} = 0.65 μm, w_{IB} = 1.30 μm, w_{IB} = 2.60 μm and w_{IB} = 5.20 μm). E_G is the band gap of GaAs equal to 1.42 eV at 300 K. The maximum efficiency is found for all of the thicknesses for X=1 and X=1000. Two cases are studied; one with only radiative recombination in the flat band region of the intermediate band layer and one with both radiative and non-radiative recombination in the flat band region of the intermediate band layer. The efficiency of the reference cell for four different thicknesses of the i-layer is also calculated. As in the previous section only non-radiative recombination is included in the i-layer.

i) IB cell, radiative recombination, X=1
The efficiency of the quantum dot solar cell as function of band gap E_H for X=1 and only including radiative recombination in the flat band region of the intermediate band layer is shown in figure 7.43 for four different thicknesses of the intermediate band layer. The efficiency shows the same E_H dependence for all the thicknesses of the intermediate band layer. The efficiency is highest for all values of E_H for w_{IB} = 1.30 μm. The same result is found using the simple model.

Discussion

When photons are reaching the intermediate band layer, meaning that the window-, p^+ and p-layer are narrow, the efficiency is expected to have the same thickness dependence in the complete model as in the simple model. The highest efficiency obtained for w_{IB}=1.30 μm in both of the models is therefore as expected.

The current-voltage characteristic using the values of E_H giving the maximum efficiency for each of the thicknesses of the intermediate band layer is shown in figure 7.44, and important parameters describing the behavior of the solar cell are listed in table 7.17.

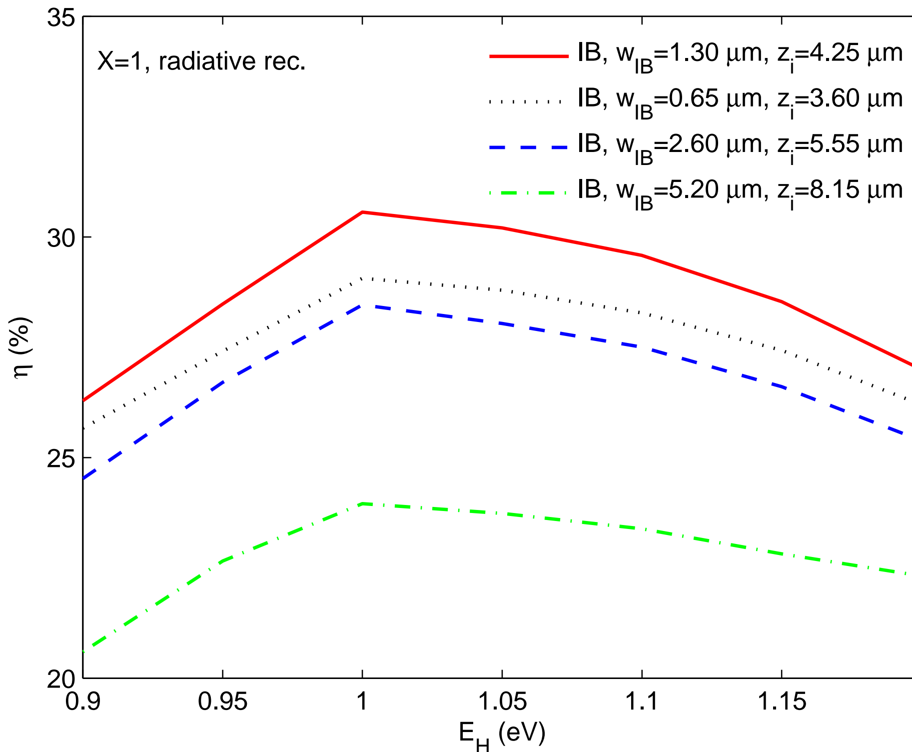

Figure 7.43: Efficiency as function of band gap E_H using four different thicknesses of the intermediate band layer. The complete model is used for X=1 and only radiative recombination is included in the flat band region of the intermediate band layer.

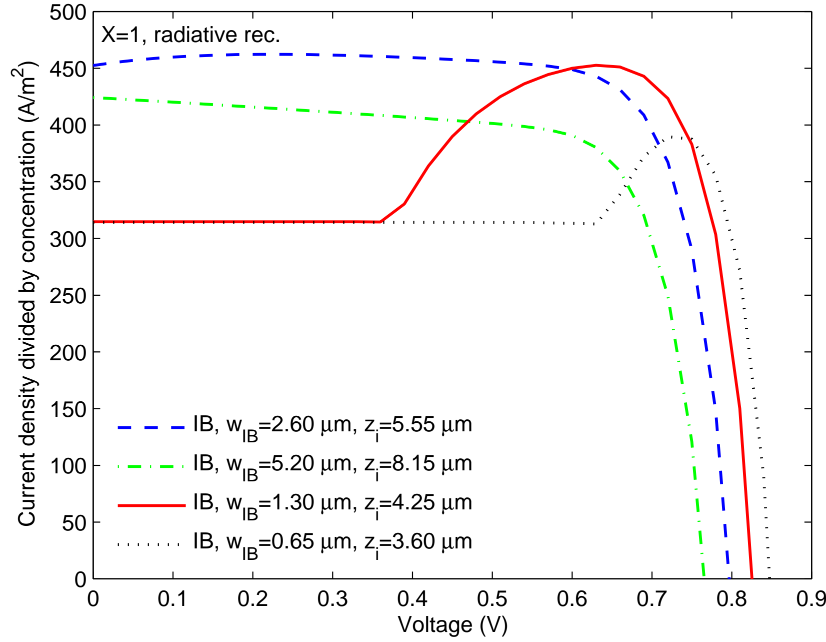

Figure 7.44: Current-voltage characteristic of an intermediate band solar cell using four different thicknesses of the intermediate band layer. The optimum band gaps are E_H=1.0 eV for all the cases. The complete model is used for X=1 and only radiative recombination is included in the flat band region of the intermediate band layer.

Table 7.17: Parameters describing the behavior of an intermediate band solar cell using the complete model and X=1. Only radiative recombination is included in the flat band region of the intermediate band layer.

Width of IB material w_{IB} (μm)	E_H (eV)	$\frac{J_{sc}}{X}$(A/m^2)	V_{oc}(V)	η(%)
0.65	1.0	314.16	0.85	29.06
1.30	1.0	314.55	0.83	30.56
2.60	1.0	452.36	0.80	28.46
5.20	1.0	424.12	0.75	23.95

Discussion

The highest efficiency 30.56 % is obtained for the width w_{IB} = 1.30 μm for the band gap E_H = 1.0 eV. By using this thickness of the intermediate band layer a flat band is obtained for voltages larger than 0.37 V. This explains the rise of the current for V=0.37 V. For voltages greater than 0.66 V the increase of the recombination is greater than the increase of the generation, and the current decreases. By using a thickness w_{IB} = 0.65 μm, the voltage where a flat band is obtained is higher than 0.37 V. The width of the flat band for w_{IB} = 0.65 μm is for all voltages less than the width of the flat band for w_{IB} = 1.30 μm. This gives a lower current. Since the dark-current rises with the width of the intermediate band layer, the open-circuit voltage is greater for w_{IB} = 0.65 μm than for w_{IB} = 1.30 μm.

A flat band is obtained for all voltages having w_{IB} = 2.60 μm and w_{IB} = 5.20 μm. An intermediate band layer of width 5.20 μm means that the total thickness of the

intermediate band layer and the i-layers on both side of the intermediate band layer is 8.15 μm. For this thickness the recombination increases more than the generation for all voltages, and the current decreases. Having a thickness of the intermediate band layer equal to $w_{IB} = 2.60$ μm and a total thickness $z_i = 5.55$ μm the current rises at the smallest voltages. The recombination is larger than the generation for voltages higher than 0.13 V, and the current decreases for voltages higher than 0.13 V.

A total thickness of 5.55 μm and 8.15 μm means that almost all photons are absorbed before reaching the bottom of the i-layer. When the voltage drop over the p-i and i-n junctions are derived, it is assumed that optically generated electron and hole concentrations are equal at the beginning and end of the i-layer at $z = 0$ and $z = z_i$, see equation (4.39), this assumption is not valid when almost no photons reach the bottom of the i-layer, meaning that the model is not valid for the widest layers.

ii) IB cell, radiative and non-radiative recombination, X=1

By also including non-radiative recombination in the flat band region of the intermediate band layer the efficiency decreases. The efficiency as function of band gap E_H is shown in figure 7.45. The current-voltage characteristic using the optimum band gaps is shown in figure 7.46, and important parameters describing the behavior of the solar cell are listed in table 7.18.

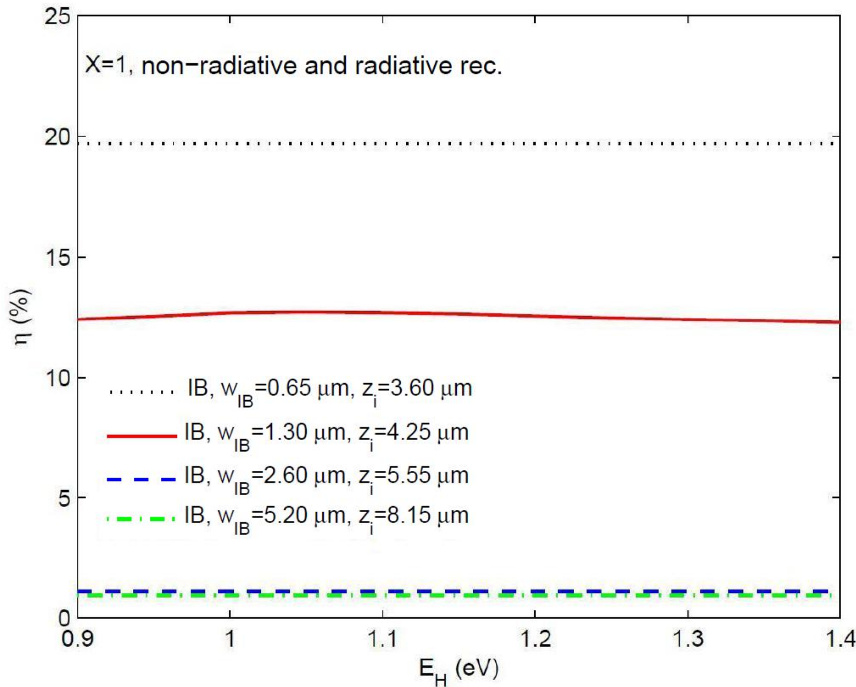

Figure 7.45: Efficiency as function of band gap E_H using four different thicknesses of the intermediate band layer. The complete model is used for X=1 and both radiative and non-radiative recombination are included in the flat band region of the intermediate band layer.

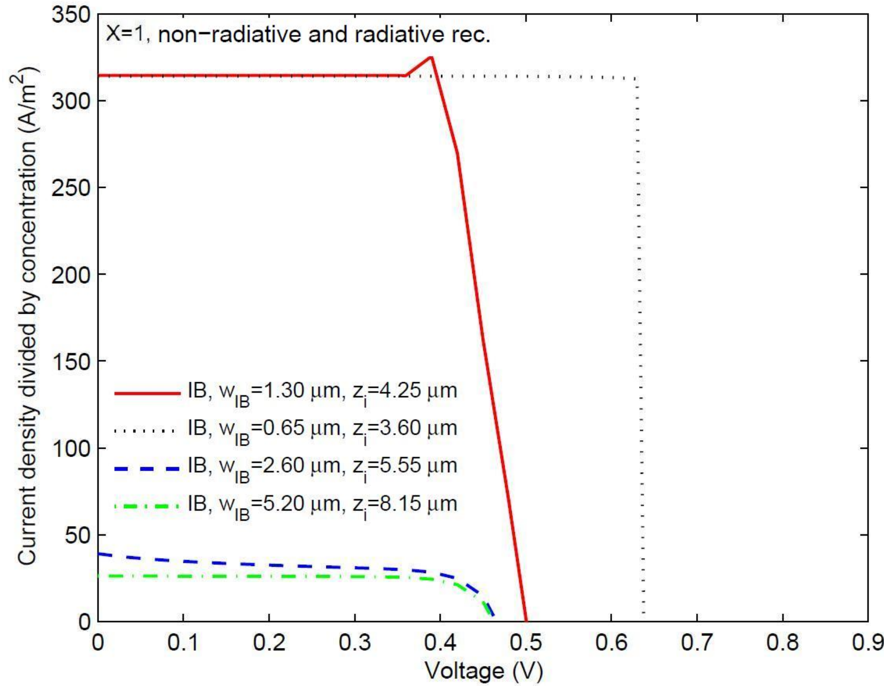

Figure 7.46: Current-voltage characteristic of an intermediate band solar cell using four different thicknesses of the intermediate band layer. The optimum band gaps are E_H=0.9 eV for w_{IB} = 0.65 μm, w_{IB} = 2.60 μm and w_{IB} = 5.20 μm and E_H = 1.5 eV for w_{IB} = 1.30 μm. The complete model is used for X=1 and both radiative and non-radiative recombination are included in the flat band region of the intermediate band layer.

Table 7.18: Parameters describing the behavior of an intermediate band solar cell using the complete model and X=1. Both radiative and non-radiative recombination are included in the flat band region of the intermediate band layer.

Width of IB material w_{IB} (μm)	E_H (eV)	$\frac{J_{sc}}{X}$(A/m^2)	V_{oc}(V)	η(%)
0.65	0.9	314.16	0.64	19.69
1.30	1.5	314.55	0.50	12.70
2.60	0.9	39.08	0.47	1.11
5.20	0.9	26.29	0.46	0.95

Discussion

As seen from figure 7.45 the efficiency is not changing much with the value of the band gap E_H when non-radiative recombination is included. This is in contrast to when only radiative recombination is included. The non-radiative lifetimes are very small. This means that the intermediate band layer should be narrow to decrease the recombination. The highest efficiency is obtained for the smallest thickness of the intermediate band layer, 0.65 μm. This thickness gives a square shaped current-voltage characteristic, shown in figure 7.46. The reason for this form is the size of the flat band layer. The width of the flat band is zero for voltages smaller than 0.63 V. When the width of the flat band is greater than zero, the recombination in this part of the intermediate band layer is very large giving a very steep fall in the current. For w_{IB} = 1.30 μm the width

of the flat band is greater than zero for V>0.37 V. The fall in the current is not as steep as for $w_{IB} = 0.65$ μm. This is because the voltage giving a flat band is smaller, and this gives a lower dark-current. The dark-current increases with voltage. For the thicknesses $w_{IB} = 2.60$ μm and $w_{IB} = 5.20$ μm the flat band is obtained for all voltages. The recombination in this layer is the reason for the low current.

iii) Reference cell, X=1

To compare the intermediate band solar cell with the reference cell the reference cell is modeled using a thickness of the i-layer, z_i shown in figure 4.1, equal to the total thickness of the i-layers and intermediate band layer in the intermediate band solar cell, $w_{ip,min} + w_{IB} + w_{in,min}$ shown in figure 5.1. In figure 7.47 the current-voltage characteristic of the reference cell is shown for four thicknesses of the i-layer. Important parameters describing the behavior of the reference cell are given in table 7.19

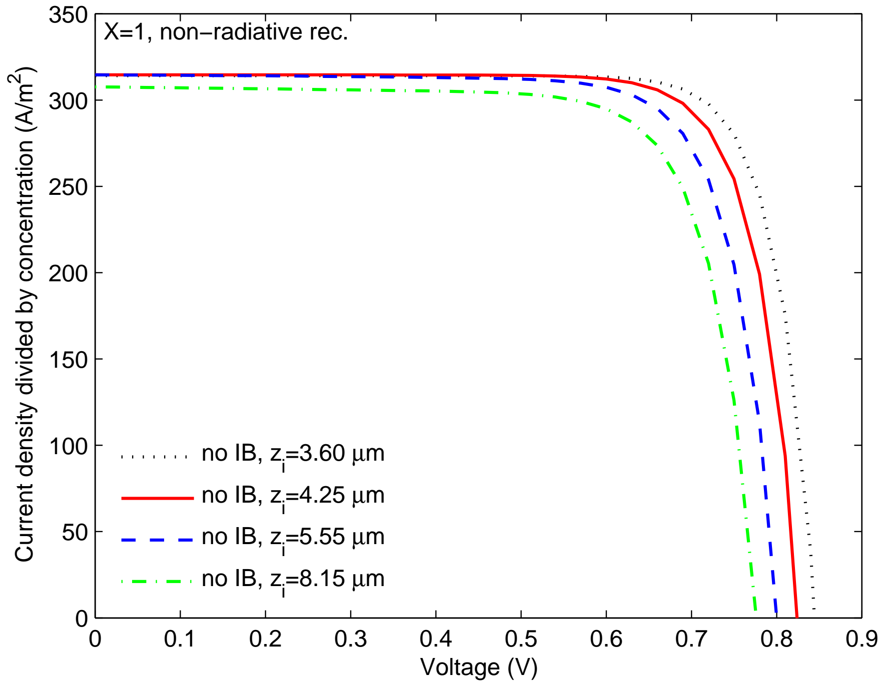

Figure 7.47: Current-voltage characteristic of a GaAs reference cell using four different thicknesses of the i-layer. The complete model is used for X=1.

Table 7.19: Parameters describing the behavior of reference solar cell using the complete model and X=1.

Width of intrinsic material z_i (μm)	$\frac{J_{sc}}{X}$(A/m^2)	V_{oc}(V)	η(%)
3.60	314.16	0.83	21.44
4.25	314.55	0.81	20.60
5.55	314.58	0.80	19.48
8.15	307.66	0.77	18.10

Discussion

The highest efficiency 21.44 % is obtained for the smallest thickness of the i-layer. This is as expected since a flat band layer in a intrinsic material is expected to reduce the efficiency [43]. The reference cell gives higher efficiency than the quantum dot solar cell when non-radiative recombination is included in the flat band region of the intermediate band layer. The lifetimes used when non-radiative recombination is included are quite pessimistic. The material quality determines if the quantum dot solar cell or the reference cell has the highest efficiency.

iv) IB cell, radiative recombination, X=1000

The efficiency of the quantum dot solar cell as function of band gap E_H for X=1000 and only including radiative recombination in the flat band region of the intermediate band layer is shown in figure 7.48 for four different thicknesses of the intermediate band layer. The efficiency shows the same behavior as function of band gap E_H as for X=1, with the maximum efficiency obtained for E_H = 1.0 eV for all thicknesses. The thickness w_{IB} = 1.30 μm gives the highest efficiency for all values of the band gap E_H. The current-voltage characteristic using the optimum value of the band gap E_H is in figure 7.49 shown for the four thicknesses of the intermediate band layer. Important parameters describing the behavior of the solar cell are listed in table 7.20.

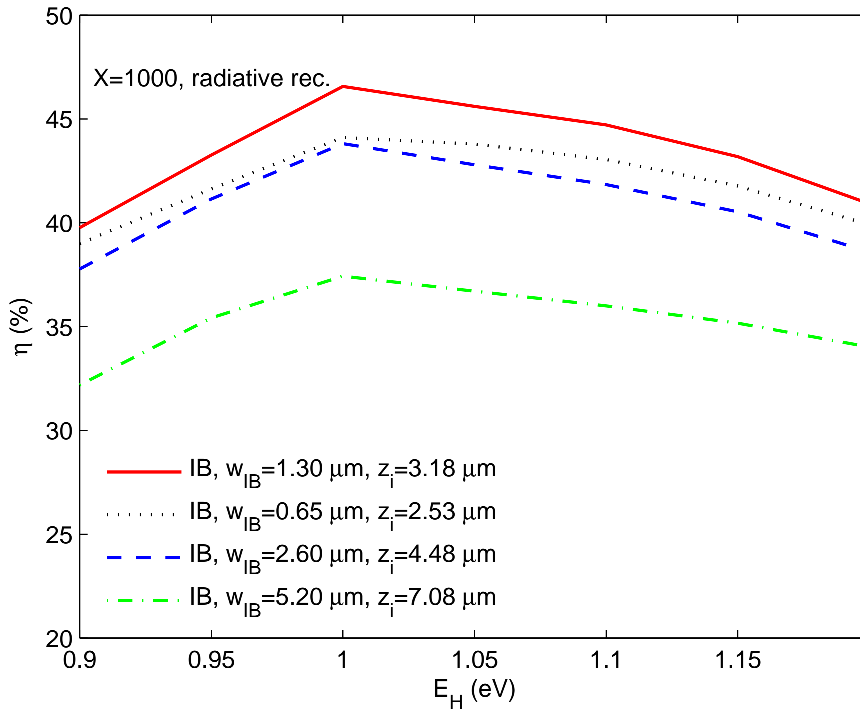

Figure 7.48: Efficiency as function of band gap E_H using four different thicknesses of the intermediate band layer. The complete model is used for X=1000 and only radiative recombination is included in the flat band region of the intermediate band layer.

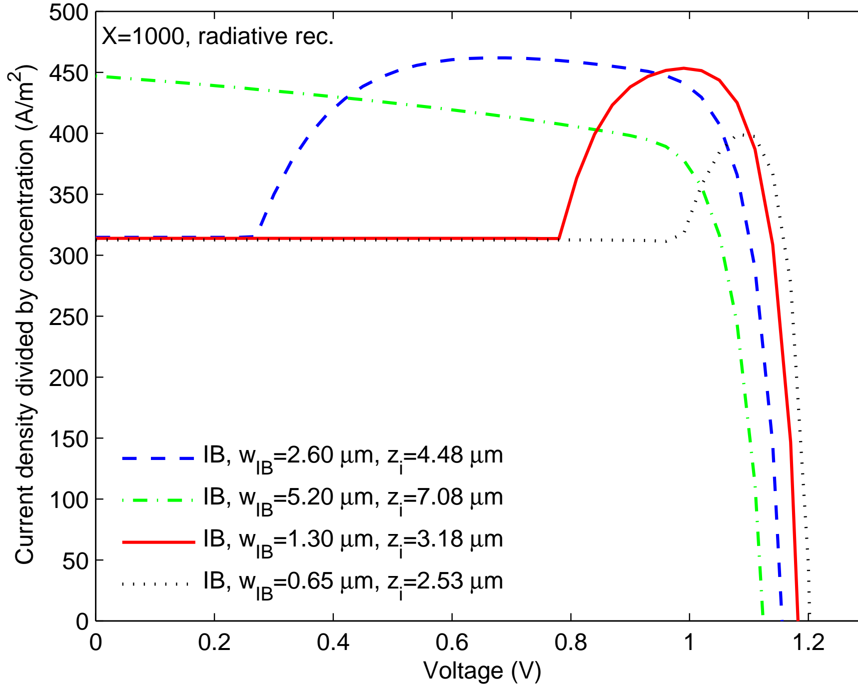

Figure 7.49: Current-voltage characteristic of an intermediate band solar cell for four different thicknesses of the intermediate band layer. The optimum band gaps are E_H=1.0 eV for all the cases. The complete model is used for X=1000 and only radiative recombination is included in the flat band region of the intermediate band layer.

Table 7.20: Parameters describing the behavior of an intermediate band solar cell using the complete model and X=1000. Only radiative recombination is included in the flat band region of the intermediate band layer.

Width of IB material w_{IB} (μm)	E_H (eV)	$\frac{J_{sc}}{X}$(A/m^2)	V_{oc}(V)	η(%)
0.65	1.0	312.56	1.20	44.10
1.30	1.0	313.74	1.18	46.56
2.60	1.0	314.64	1.15	43.81
5.20	1.0	446.91	1.12	37.43

Comparing X=1 and X=1000, radiative recombination only.

As seen from the current-voltage characteristic in figure 7.49 and 7.44 the flat band is obtained for higher voltages for X=1000 than for X=1. The reason for this is that the i-layer thicknesses $w_{ip,min}$ and $w_{in,min}$ placed on both sides of both the intermediate band layer, shown in figure 5.1, are wider for a concentration factor X=1. The reason for this is that for X=1000 the open-circuit voltage is higher. The voltage used to find the minimum widths of the depletion is then higher for X=1000. A higher voltage gives smaller values of the minimum depletion widths. By having a narrower i-layer more of the intermediate band layer is contained in the depletion layer, and the flat band is obtained for higher voltages. For X=1 both the solar cells with w_{IB} = 2.60 μm and w_{IB} = 5.20 μm have a flat band region at all voltages. For X=1000 a flat band region is obtained for all voltages only for the width w_{IB} = 5.20 μm.

The short-circuit currents for X=1 and X=1000 given in table 7.17 and 7.20 are not equal. The short-circuit currents are less for X=1000 for the thicknesses $w_{IB} = 0.65$ μm, $w_{IB} = 1.30$ μm and $w_{IB} = 2.60$ μm. This is explained by the higher voltage necessary to obtain the flat band for X=1000. The open-circuit voltage and efficiency are larger for X=1000. The short-circuit current density for the thickness $w_{IB} = 5.20$ μm is larger for X=1000 than for X=1. Using this thickness a flat band region is obtained when the voltage is equal to zero. Since the thicknesses of the i-layers are less for X=1000, the short-circuit current is larger for X=1000 in this case. The percentual increase of efficiency changing X=1 to X=1000 is thus greatest for the width $w_{IB} = 5.20$ μm.

v) IB cell, radiative and non-radiative recombination, X=1000

The efficiency of the intermediate band solar cell as function of band gap E_H for X=1000 and both radiative and non-radiative recombination are included in the flat band region of the intermediate band layer is shown in figure 7.50. Four thicknesses of the intermediate band layer are used. The efficiency varies very little with voltage. The optimum band gaps are E_H=0.9 eV for $w_{IB} = 0.65$ μm, $w_{IB} = 2.60$ μm and $w_{IB} = 5.20$ μm and $E_H = 1.35$ eV for $w_{IB} = 1.30$ μm. They are obtained from numerical values. Since the variation in efficiency is very little, the exact value of the band gap giving the highest efficiency is uncertain. The current-voltage characteristics using these optimum band gaps are shown in figure 7.50, and important parameters describing the behavior of the solar cell are listed in table 7.21.

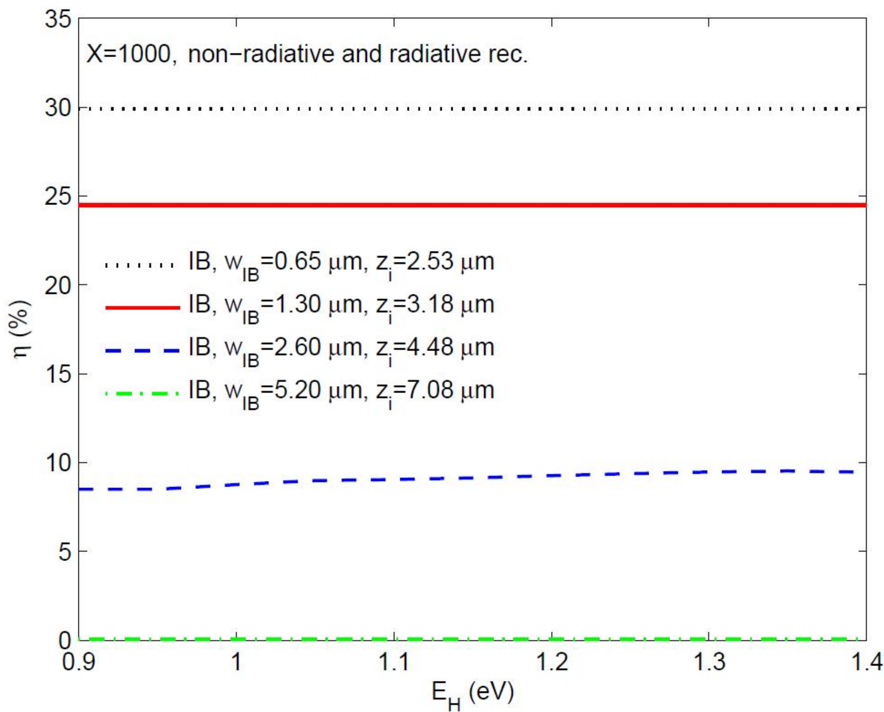

Figure 7.50: Efficiency as function of band gap E_H for four different thicknesses of the intermediate band layer. The complete model is used for X=1000 and both radiative non-radiative radiative recombination are included in the flat band region of the intermediate band layer.

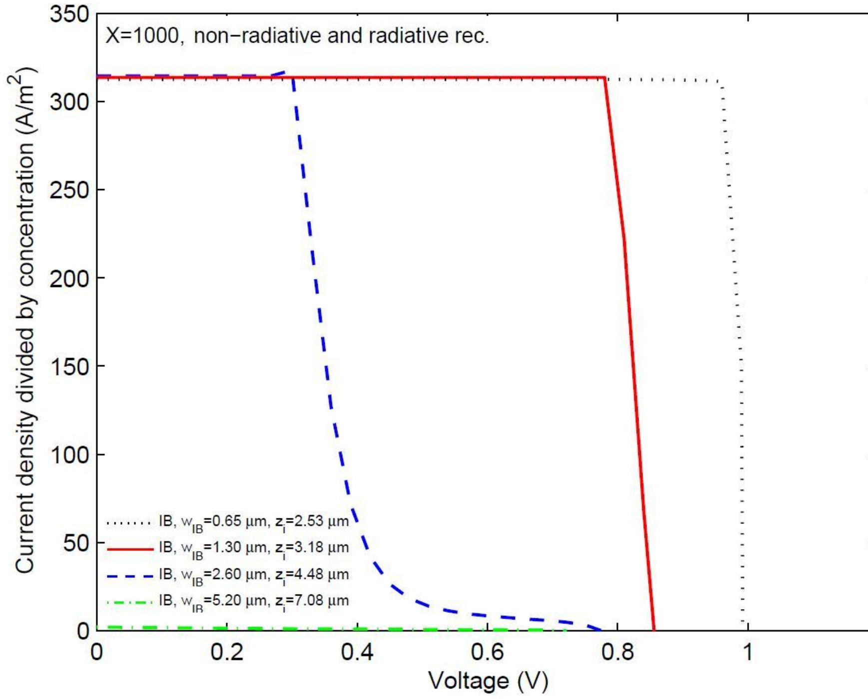

Figure 7.51: Current-voltage characteristic of an intermediate band solar cell using four different thicknesses of the intermediate band layer. The optimum band gaps are E_H=0.9 eV for w_{IB} = 0.65 μm, w_{IB} = 2.60 μm and w_{IB} = 5.20 μm and E_H = 1.35 eV for w_{IB} = 1.30 μm. The complete model is used for X=1000 and both radiative and non-radiative recombination are included in the flat band region of the intermediate band layer.

Table 7.21: Parameters describing the behavior of an intermediate band solar cell using the complete model and X=1000. Both non-radiative and radiative recombination are included in the flat band region of the intermediate band layer.

Width of IB material w_{IB} (μm)	E_H (eV)	$\frac{J_{sc}}{X}$(A/m^2)	V_{oc}(V)	η(%)
0.65	0.90	312.56	0.99	29.89
1.30	0.90	313.74	0.86	24.47
2.60	1.35	314.64	0.77	9.53
5.20	0.90	2.04	0.72	0.04

Discussion

The efficiency is as expected reduced when non-radiative recombination is included. The largest reduction in efficiency is found for w_{IB} = 5.20 μm. The intermediate band solar cell with this thickness has only an efficiency equal to 0.04 %. The short-circuit current density for this thickness is 2.04 A/m^2. A flat band region where we have a lot of recombination is obtained for all voltages using this thickness. This explains the low efficiency.

When non-radiative recombination is included, the recombination increases with the thickness of the flat band region, meaning that the intermediate band solar cell with the minimum thickness w_{IB} = 0.65 μm gives the highest efficiency. In contrast to when only radiative recombination is included, the efficiency is for the width w_{IB} = 5.20 μm

lower for X=1000 than for X=1. When non-radiative recombination dominates, using higher concentration only reduces the current. The reason why this is not seen for the other thicknesses is that the flat band for X=1000 is obtained for voltages higher than the voltages giving a flat band for X=1. The recombination for the lowest voltages is then less for X=1000, and the efficiency is increased.

vi) Reference cell, X=1000

To compare the intermediate band solar cell with the reference cell for X=1000, the reference cell is modeled for X=1000. The current-voltage characteristic of the reference cell for X=1000 and four thicknesses of the i-layers is shown in figure 7.52. Important parameters describing the behavior of the solar cells are given in table 7.22.

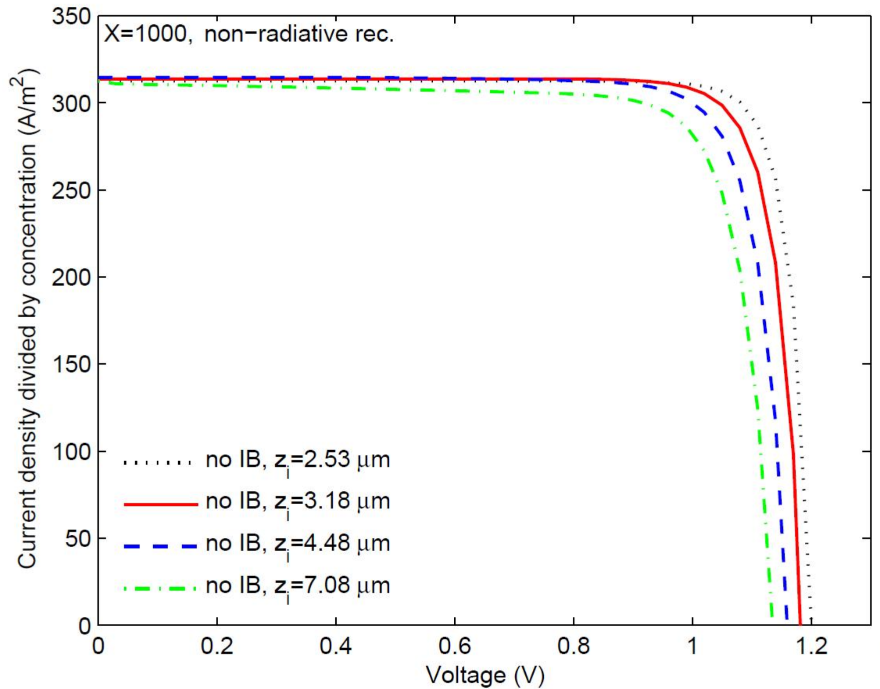

Figure 7.52: Current-voltage characteristic of a GaAs reference cell using four different thicknesses of the i-layer. The complete model is used for X=1000.

Table 7.22: Parameters describing the behavior of the reference solar cell using the complete model and X=1000.

Width of intrinsic material z_i (μm)	$\frac{J_{sc}}{X}$(A/m^2)	V_{oc}(V)	η(%)
2.53	312.56	1.20	32.45
3.18	313.74	1.18	31.35
4.48	314.64	1.16	30.05
7.08	312.53	1.14	28.34

The maximum efficiency 32.45 % is obtained for the narrowest i-layer. As is the case for X=1, the reference cell has a higher efficiency than the intermediate band solar cell when non-radiative recombination is included.

7.5 Discussion of how to obtain an IB solar cell with high efficiency

From the results obtained from the modeling in the previous sections a conclusion can be drawn of what is important in obtaining a solar cell with a high efficiency. This is looked into in this section.

High current density in the p- and n-layers are obtained when a window layer and heavily doped p^+- and n^+-layers are used. These layers result in a low effective surface recombination velocity. The thicknesses and doping concentrations of all the layers in the solar cell should be optimized. An anti-reflective layer is important to reduce the reflectivity. This is important for both the reference cell and the intermediate band solar ell.

The intermediate band layer used in the intermediate band solar cell should be placed in a flat band region to obtain a high efficiency. The intermediate band is then partially filled. Both the valence band to intermediate band transition and the intermediate band to the conduction band transition are then present at the same time. The thickness of the intermediate band layer should be thick to be contained in the flat band region. To avoid the increased recombination in a wider layer, the thickness of the intermediate band layer has to be optimized. The band gaps E_H and E_G have to be optimized to obtain the highest efficiency for the given thickness of the intermediate band layer. The band gap E_G is dependent on the barrier material used; a greater band gap gives less photocurrent, but a higher open-circuit voltage. The band gap E_H may be optimized via the quantum dot material and the size of the quantum dots.

The type of recombination in the intermediate band layer is important. In all the cases studied only the intermediate band solar cells where only radiative recombination is included have a higher efficiency than the reference solar cell. The values used for the non-radiative lifetimes are, as mentioned, quite pessimistic, but they show how important the material quality is. If the increase of recombination is greater than the increase of generation using quantum dot material, no positive effect is obtained.

The positive effect of using light concentration is also shown. Using the optimum thicknesses and band gaps the efficiencies obtained for the solar cells for X=1000 are much higher than for X=1. One has to remember however, that series resistance increases for high concentrations and high injection conditions may arise. This is not included in the models, except in the i-layers.

7.6 Models used on real samples

In this section the complete model is used to calculate the current-voltage characteristic of the GaAs reference cell sample A1677 and compared with the current-voltage characteristic obtained from experiments reported in [48] and [13]. The thicknesses of the layers and the doping concentration in sample A1677 are given in table 6.1. The current-voltage characteristic of the InAs/GaAs quantum dot solar cell sample A1681 is calculated using the simple model and the complete model. The doping concentrations and thicknesses of sample A1681 are given in table 6.3. The band gaps are $E_G = 1.38$ eV and $E_H = 1.12$ eV. The results from the modeling are then compared with the current-voltage characteristic obtained from experiments reported in [48] and [13]. The

experiment was performed under no concentration, i.e. X=1.

7.6.1 Reference cell, sample A1677

The current-voltage characteristic of the reference cell, sample A1677, obtained from the complete model is shown in 7.53. The experimental current-voltage characteristic is shown in figure 7.54. Important parameters describing the behavior of sample A1677 are given in table 7.23.

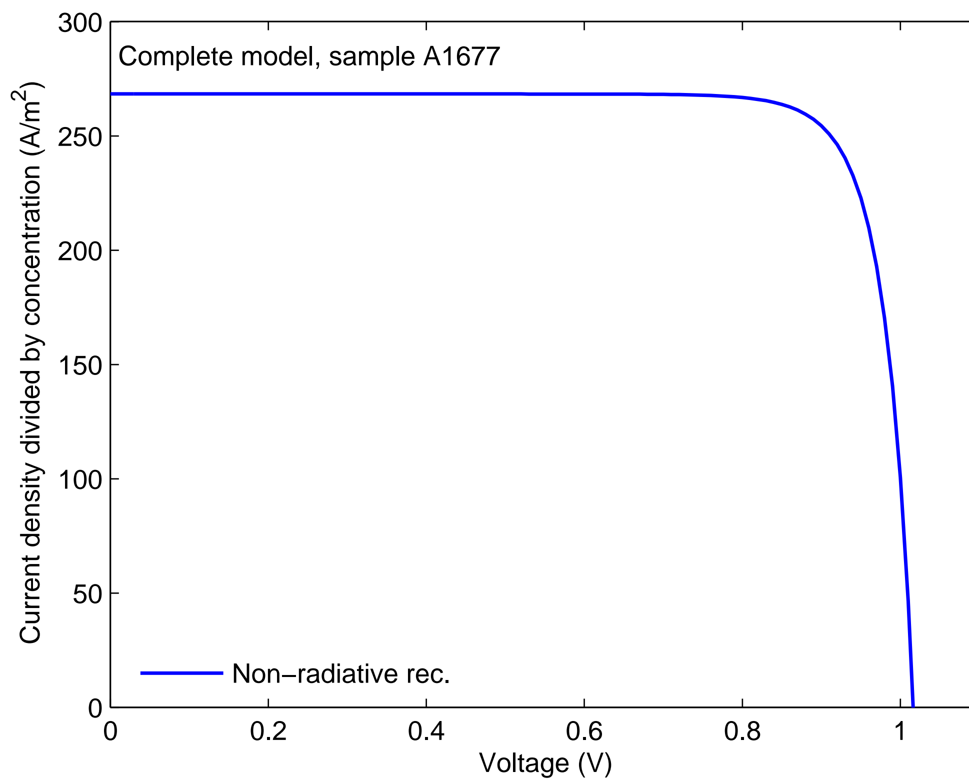

Figure 7.53: Current-voltage characteristic of sample A1677 (referenc cell) obtained using the complete model.

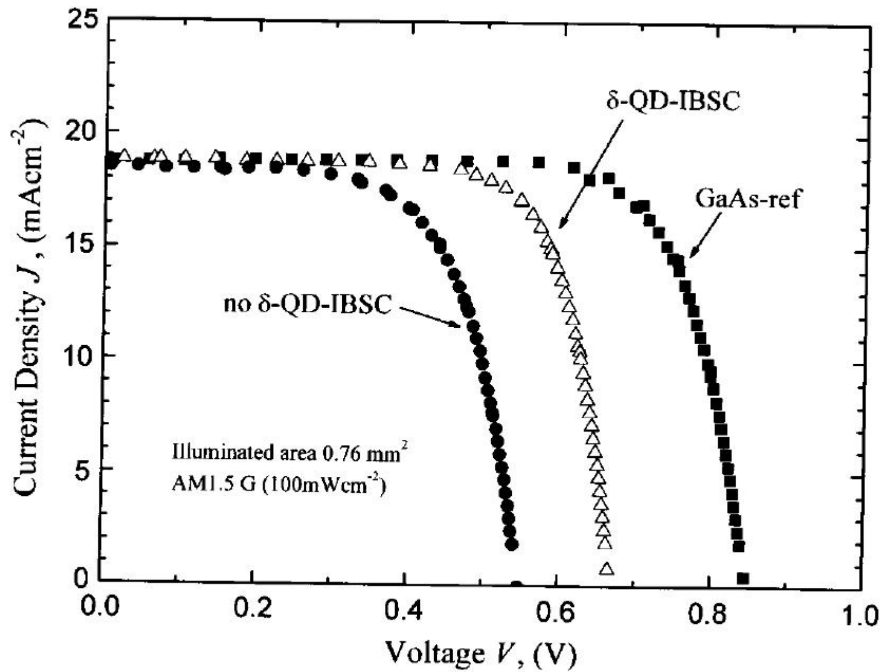

Figure 7.54: Experimental current-voltage characteristics of sample A1677 (GaAs-ref) and sample A1681 (δ-QD-IBSC) reported in [13]. The sample without δ-doping (no δ-QD-IBSC) is not studied in this thesis.

Table 7.23: Parameters describing the behavior of the reference cell sample A1677 found using the complete model and experimentally measured values reported in [48].

Model	Recombination	$\frac{J_{sc}}{X}$(A/m^2)	V_{oc}(V)	η(%)
Complete	Radiative and non-radiative	268.34	1.03	22.90
Experimental	Radiative and non-radiative	188.4	0.84	12.0

Discussion

Comparing the experimental current-voltage characteristic of the reference cell shown in figure 7.54 with the current-voltage characteristic obtained from the complete model, shows that the complete model gives a higher short-circuit current density and a higher open-circuit voltage. A reason for the high photocurrent obtained from the model is that the reflectivity is set equal to zero for a solar cell with an anti-reflective coating. Using a higher value of the reflectivity the value of the current decreases. Since there are not given any details about the anti-reflective layer in the description of the solar cells samples, it is difficult to estimate how well the anti-reflective layer of these specific samples performs. An anti-reflective coating may result in reflectivity as low as 2 % [28], and the effect of neglicing this reflection loss can not be the only explanation of the high current.

The recombination at the interfaces between different layers in the reference cell is assumed equal to zero which may be another explanation of the higher current obtained from the complete model than from the experimental values. The approximation of

neglecting band gap narrowing in the heavily doped layers also influence the current-voltage characteristic. This is discussed in section 7.8.

Series resistance is not included in the complete model. Since the series resistance in [36] is estimated to be $1.026 \times 10^{-5}\Omega$, the higher open-circuit voltage obtained from the complete model can not be explained by this low series resistance.

7.6.2 Quantum dot intermediate band solar cell, sample A1681

The current-voltage characteristic of the quantum dot solar cell sample A1681 obtained using the simple model is shown in figure 7.55. In figure 7.56 the current-voltage characteristic of sample A1681 obtained using the complete model is shown. Two cases are shown, one where only radiative recombination is included in the flat band region of the intermediate band layer and one where both radiative and non-radiative recombination are included. The experimental current-voltage characteristic of sample A1681 is shown in figure 7.54. A table with parameters describing the behavior of sample A1681 using the simple model and the complete model is given in table 7.24. Here also the experimental values are given.

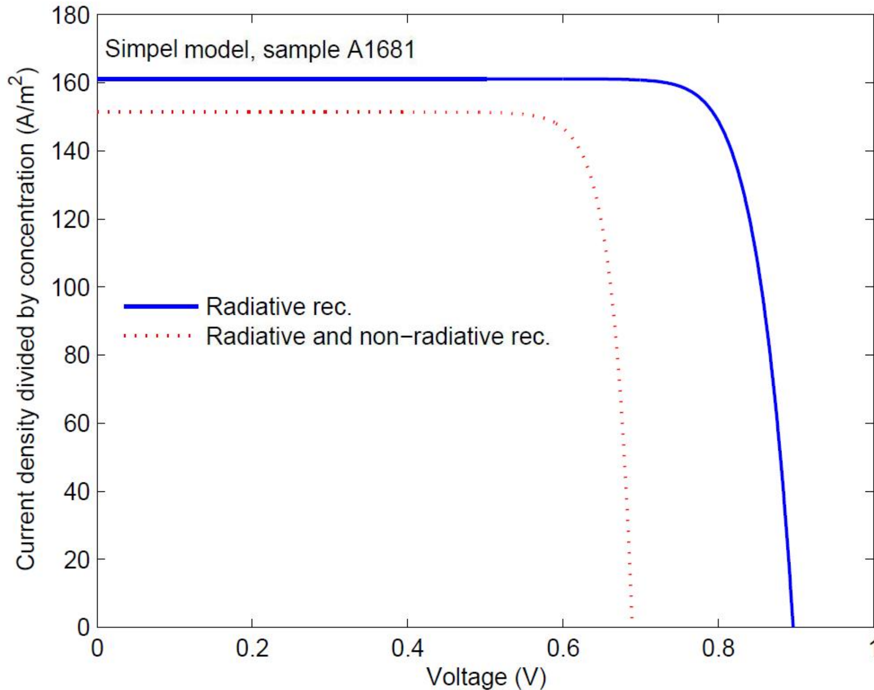

Figure 7.55: Current-voltage characteristic of quantum dots solar cell sample A1681 using the simple model.

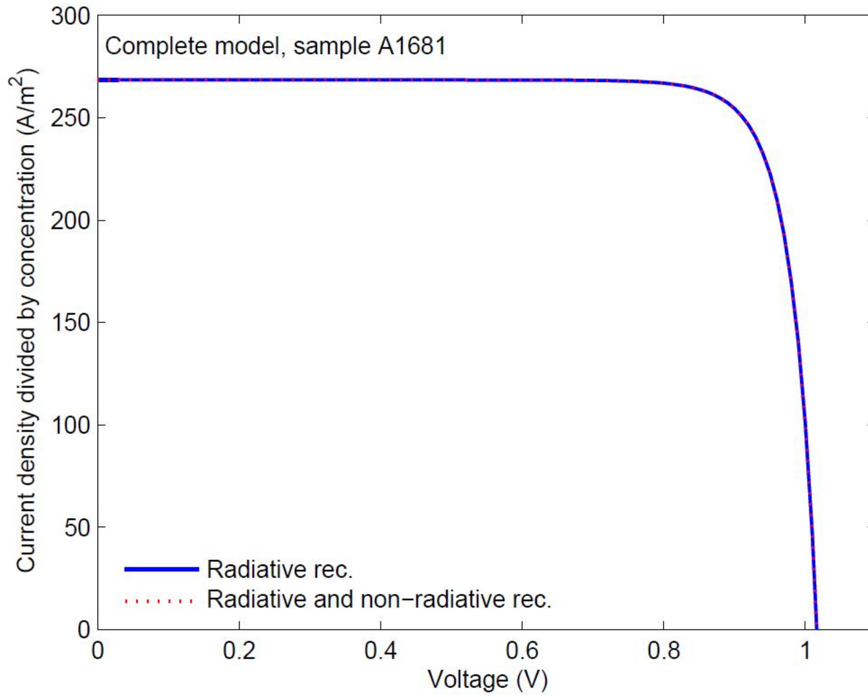

Figure 7.56: Current voltage characteristic of quantum dot solar cell sample A1681 using the complete model

Table 7.24: Parameters describing the behavior of the quantum dot solar cell sample A1681 found using the simple model and the complete model and experimentally measured values reported in [48].

Model	Recombination	$\frac{J_{sc}}{X}$(A/m^2)	V_{oc}(V)	η(%)
Simple	Radiative	161.06	0.90	12.07
Simple	Radiative and non-radiative	151.37	0.70	8.81
Complete	Radiative	268.34	1.03	22.90
Complete	Radiative and non-radiative	268.34	1.03	22.90
Experimental	Radiative and non-radiative	189.1	0.67	9.4

Discussion

The simple model gives lower values for the short-circuit current density than the experimental values. Using the simple model only generation and recombination in the intermediate band layer are included. The p- and n-layers are only required to separate the electron and holes. When these layers are thick as in sample A1681 where they are thicker than the intermediate band layer, omitting this current gives a too low value of the short-circuit current density. Using the simple model the dark-current density from the other layers than the intermediate band layer is omitted, which explains the higher open-circuit voltages obtained.

The quantum dot density in sample A1681 4.0×10^{10} cm^{-2} may be too low to form an energy band, which is assumed in the models. A condition for neglecting the diffusion current in the intermediate band material is that the density of quantum dots are high,

see chapter 5. This condition is not fulfilled for sample A1681. This is one explanation why the experimental data do not fit with the results from the modeling.

The complete model gives higher values for both the short-circuit current density and the open-circuit voltage compared to experimental values. The current-voltage characteristic is equal for the cases with and without non-radiative recombination in the flat band region. The reason for this is that the thickness of the intermediate band layer is only 100 nm. The intermediate band layer is depleted at all voltages and no flat band region is obtained. Since the complete model only takes into account the intermediate band layer placed in a flat band region, the model gives the same current density when only radiative and when both radiative and non-radiative recombination are included in the flat band region of intermediate band layer. When the intermediate band layer is as narrow as 100 nm, the complete model gives the same current-voltage characteristic for the intermediate band solar cell and the reference cell. A new model has to be developed to model the behavior of the quantum dots placed in the depletion region.

7.7 $Al_{0.35}Ga_{0.65}As$ versus GaAs intermediate band solar cell

The value of the band gap E_G is increased by using $Al_{0.35}Ga_{0.65}As$ instead of GaAs as the barrier material. In this section the complete model is used to find the current-voltage characteristic for $E_G = E_{GaAs}$ and $E_G = E_{Al_{0.35}Ga_{0.65}As}$ for both an intermediate band solar cell and a reference cell. The samples parameters used for the samples modeled in this section are the same used in the intermediate band solar cell samples made at NTNU, except the thickness of the intermediate band layer. The thickness of the intermediate band layer is taken as the optimum thickness for X=1000 equal to $w_{IB} = 1.3$ μm. This is done since the complete model then clearly show the effect of using quantum dots.

The doping concentrations and thicknesses of the layers in the GaAs cell, except the thickness of the i-layer, are given in table 6.1. Material parameters for these doping concentrations are given in table 6.2. The doping concentrations and thicknesses of the layers in the $Al_{0.35}Ga_{0.65}As$ cell, except the thickness of the i-layer, are given in table 6.4. Material parameters for these doping concentrations are given in table 6.5. E_H is taken as values reported from photoluminescence measurements at Linköping University. For GaAs E_H is measured as 1.22 eV at 2 K. This value is 1.14 eV at 300 K by assuming the same temperature dependence of this band gap as the value of the band gap of GaAs given in equation (6.1). For $Al_{0.35}Ga_{0.65}As$ E_H is measured as 1.12 eV at 300 K. The thickness of the intermediate band layer is taken as 1.30 μm, and only radiative recombination in the flat band region of the intermediate band layer is included. The total thickness of the i-layers and the intermediate band layer $w_{ip,min} + w_{IB} + w_{in,min}$, see figure 5.1, is 4.25 μm for X=1 and 3.18 μm for X=1000.

The current-voltage characteristics of the reference cell and intermediate band solar cell are shown in figure 7.57 for X=1 and in figure 7.58 for X=1000. Important parameters describing the behavior of the solar cell are listed in table 7.25.

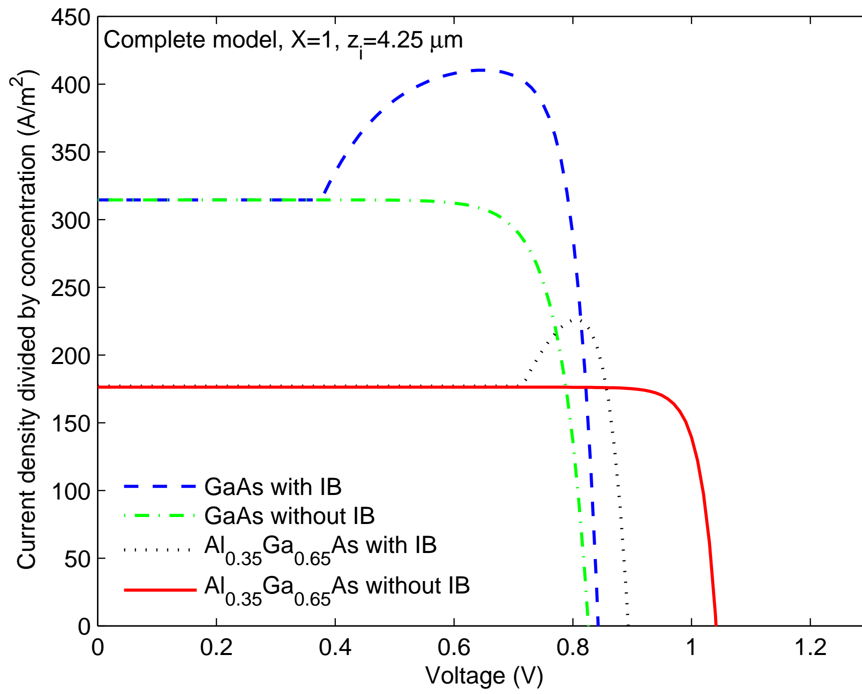

Figure 7.57: Current-voltage characteristic for the reference cell and intermediate band solar cell for X=1 and $E_G = E_{GaAs}$ and $E_G = E_{Al_{0.35}Ga_{0.65}As}$.

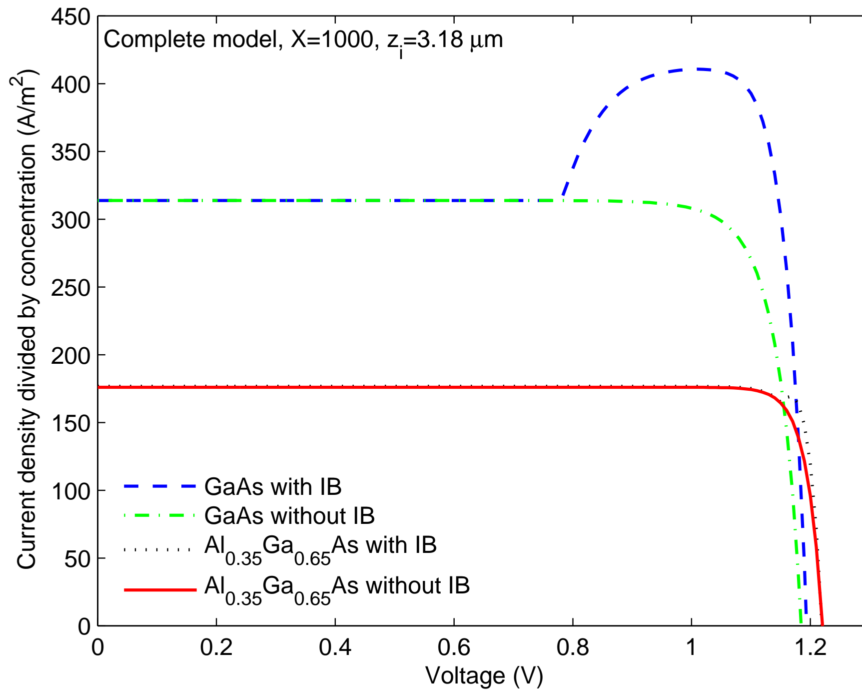

Figure 7.58: Current-voltage characteristic for the reference cell and intermediate band solar cell for X=1000 and $E_G = E_{GaAs}$ and $E_G = E_{Al_{0.35}Ga_{0.65}As}$.

Table 7.25: Parameters describing the behavior of a reference solar cell and an intermediate band solar cell using the complete model and $E_G = E_{GaAs}$ and $E_G = E_{Al_{0.35}Ga_{0.65}As}$.

Cell	Material	Concentration	$\frac{J_{sc}}{X}$(A/m^2)	V_{oc}(V)	η(%)
Intermediate	GaAs	1	314.55	0.85	29.03
Reference	GaAs	1	314.55	0.83	20.59
Intermediate	$Al_{0.35}Ga_{0.65}As$	1	177.00	0.90	18.31
Reference	$Al_{0.35}Ga_{0.65}As$	1	176.24	1.04	16.17
Intermediate	GaAs	1000	313.73	1.20	43.50
Reference	GaAs	1000	313.73	1.19	31.35
Intermediate	$Al_{0.35}Ga_{0.65}As$	1000	176.69	1.23	19.80
Reference	$Al_{0.35}Ga_{0.65}As$	1000	175.97	1.22	19.30

Discussion
As seen from figure 7.57 and 7.58 the photocurrent is higher using GaAs than $Al_{0.35}Ga_{0.65}As$, while the open-circuit voltage is higher using $Al_{0.35}Ga_{0.65}As$ than GaAs. The reason for the increased photocurrent using GaAs is that the lower band gap of GaAs makes it possible to absorb photons with less energy than in $Al_{0.35}Ga_{0.65}As$. The higher band gap of $Al_{0.35}Ga_{0.65}As$ gives the higher open-circuit voltage. The efficiency is higher using GaAs than $Al_{0.35}Ga_{0.65}As$. The values of the band gap E_H are not optimized in the cells. By having optimized values of the band gap E_H the $Al_{0.35}Ga_{0.65}As$ cell can give higher efficiency.

7.8 Discussion of the models

In this thesis reference cells and intermediate band solar cells are modeled. The validity and drawbacks of the models used are discussed in this section.

7.8.1 Reference cell

As mentioned in the previous section the model of the reference cell gives a higher photocurrent and open-circuit voltage as compared with experimental values. Band gap narrowing is one of the reasons for this. It is found that band gap narrowing is more important in the heavily doped p$^+$-layers than in the heavily doped n$^+$-layers [53]. Band gap narrowing gives an increased dark-current and also affects the front surface field, giving a higher effective surface recombination velocity [53]. The surface recombination velocity of the p-layer is in section 7.1.3 shown to have a large influence on the quantum efficiency of the p-layer. An increased effective surface recombination velocity of the p-layer will therefore give a great reduction in the photocurrent. An increased dark-current will give a lower open-circuit voltage. A more accurate model of the reference cell should take the band gap narrowing of the p$^+$-layer into account.

When an anti-reflective layer is present with a known reflectivity value this reflectivity values should be used in the model instead of assuming a reflectivity equal to zero for all anti-reflective coatings.

Low-injection is assumed in all layers except in the i-layer. This may not be fulfilled under high concentration, which means that the model of the reference cell is not valid under high concentration. This drawback of the model may only be solved by numerical

methods since the equations given for the current density can not be solved analytically under high-injection. The model of the reference cell is not valid when the optically generated electron and hole concentrations are not equal throughout the whole i-layer, as assumed in equation (4.39). This means that the model is not valid in such cases.

More realistic values of the current may be obtained by measuring the mobilities and lifetimes in the solar cell material. Then more accurate values of the mobilities and lifetimes can be included which is expected to improve the results from the modeling.

7.8.2 The simple model of the intermediate band solar cell

The simple model of the intermediate band solar cell shows how the intermediate band may give a larger current due to the intermediate band, if the increased generation by having the intermediate band is greater than the extra recombination. The importance of having materials of good quality is shown through the large difference in efficiency obtained for the cases with and without non-radiative recombination in the flat band region of the intermediate band layer. How the flat band region width is dependent on voltage is not taken into account using the simple model. It is assumed that the whole intermediate band is contained in the flat band region. This is not realistic, and is also not found to be the case in experiments [13]. The contribution of the other layers in the solar cell is also not taken into account in the simple model. This gives a too low current when these layers are of the same size as the intermediate band layer. The simple model works in describing what takes place in an intermediate band, but is too simple to use on real samples which contains many layers.

7.8.3 The complete model of the intermediate band solar cell

Using the complete model all layers in the solar cell are taken into account, and the width of the flat band is dependent on the voltage. In addition to the drawbacks mentioned for the model of the reference cell, a drawback of the complete model is that the intermediate band layer placed in the depleted regions is assumed to behave in the same way as an intrinsic material. Experiments where the intermediate band solar cell is placed in a depleted region show an increased absorption giving a larger photocurrent in the intermediate band solar cells. They also show an increased recombination giving a smaller photocurrent [13]. This indicates that the intermediate band layer placed in the depleted region does not behave as an intrinsic material even though the intermediate band in this region is full or empty of electrons. By assuming that the intermediate band layer placed in the depletion region behaves as an intrinsic material, we see no difference in the modeling of a reference cell and an intermediate band solar cell when the intermediate band layer is depleted at all voltages.

Chapter 8

Summary and conclusion

In this master thesis intermediate band solar cells and suitable reference cells have been modeled for two different values of concentration, X=1 and X=1000. The modeling of the reference cells shows the importance of using a window layer and heavily doped p^+- and n^+-layers to obtain a low effective surface recombination velocity together with an anti-reflective coating minimizing the reflection losses. By using these layers a high quantum efficiency is obtained.

Due to the non-existence of a model of a p-i-n solar cell with parts of the intrinsic material placed in a flat band region, a model of such a solar cell was developed. A similar model with an intermediate band material placed in the flat band region was also developed. A simple model of an intermediate band solar cell where only the intermediate band material is taken into account was taken from literature. Both radiative and non-radiative recombination were included in the flat band region of the intermediate band material in the models of the intermediate band solar cell.

The results from the modeling show that when the recombination in the intermediate band solar cell is dominated by non-radiative recombination with very short lifetimes, the reference cell with a flat band layer gives a higher efficiency than the corresponding intermediate band solar cell. When radiative recombination dominates the efficiency is higher using an intermediate band material. The current is increased and the open-circuit voltage is almost unchanged.

The modeling of the intermediate band solar cell shows how the thickness of the intermediate band material and the values of the band gaps E_G, E_H and E_L are affecting the current-voltage characteristic. Optimum band gaps were found for different thicknesses of the intermediate band material. By using the complete model, only including radiative recombination and using GaAs as the barrier layer the maximum efficiency for X=1 is found to be 30.6 % for a thickness of the intermediate band material equal to 1.30 μm and E_H equal to 1.0 eV. For X=1000 the efficiency is found to be 46.6 %, found for the same thickness and band gap. When non-radiative recombination are included the maximum efficiency is found for a thinner intermediate band material. The efficiency is reduced to 19.7 % for X=1 and 29.9 % for X=1000. The maximum efficiency of the corresponding reference cell is obtained for the thinnes i-layer, equal to 21.4 % for X=1 and 32.5 % for X=1000.

The results show that for a width of the intermediate band material equal to 1.3 μm and using GaAs or $Al_{0.35}Ga_{0.65}As$ as the barriers layers, GaAs gives the highest

efficiency by using the value of E_H obtained from photoluminescence.

By comparing the results from the modeling with experimental data it is found that the model of the reference cell gives too high values of current and open-circuit voltage. The reason for this is expected to be the approximation of neglecting band gap narrowing in the heavily doped and layers and using a reflectivity equal to zero when an anti-reflective coating is present.

Chapter 9

Further work

This master thesis is based on an analytical approach. One task is to use numerical methods to model a reference cell and an intermediate band solar cell based on the equations presented in this thesis. By using numerical methods radiative recombination can be included in the i-layer in the p-i-n solar cell. The current-voltage characteristic under high-injection may be derived using numerical methods.

Another task is to continue to use the analytical approach and extend the models given in this thesis. The model of the reference cell can be further extended to include band gap narrowing in the heavily doped layers. $Al_xGa_{1-x}As$ solar cells with other aluminium concentrations than x=0.35 can be modeled to find the maximum efficiency for other values of the band gap E_G. To obtain a solar cell with the highest efficiency, the thickness and doping concentration of all the layers in the reference cell may be varied. An estimation of the series and shunt resistances in the solar cells may be done and included in the model.

The complete model of the intermediate band solar cell may be extended to model the intermediate band material placed in the depleted regions another way then treating it as an intrinsic material. A more realistic case of overlapping absorption coefficients may also be included in the model. How the values of the absorption coefficients affect the current-voltage characteristic may be studied.

Bibliography

[1] International Eenergy Outlook 2009. Energy Information Administration Office of Integrated Analysis and Forecasting U.S. Department of Energy, (Retrieved online on 2009-06-13). http://www.jointsolarpanel.nl/fileadmin/jointsolarpanel/user/documents/seminar2004/stanleyzc04.pdf.

[2] J. Twidell and T. Weir. *Renewable Eenergy Resources.* (Taylor and Francis, 2006).

[3] J. Nelson. *The Physics of Solar Cells.* (Imperial College Press, 2007).

[4] Greenpeace and European Photovoltaic Industry Association. *Solar Generation V-2008, Solar electricity for one billion people and two million jobs by 2020*, (2008).

[5] J. Nelson. *Quantum-Well Structures for Photovoltaic Energy Conversion.* (Thin Films, 21, 1995).

[6] M. A. Green. *Third Generation Photovoltaics.* (Springer, 2003).

[7] A. Luque and A. Martí. A Metallic Intermediate Band High Efficiency Solar Cell. *Prog. Photovolt: Res. Appl.* ***9***, (2001) 73.

[8] Photovoltaic cells (solar cells), how they work. SPECMAT (Retrieved online on 2008-12-12). http://www.specmat.com/Overview$\%$20of$\%$20Solar$\%$20Cells.htm.

[9] B. G. Streetman and S. K. Banerjee. *Solid state electronic devices.* (Pearson, 2006).

[10] J. L. Gray. *The Physics of the Solar Cell.* (John Wiley and Sons, Ltd, 2003).

[11] H. J. Hovel. *Semiconductors and Semimetals, vol. 11, Solar Cells.* (Academic press, 1975).

[12] W. Shockley and H. J. Qeisser. Detailed balance limit of efficiency of p-n junction solar cells. *J. Appl. Phys.* ***32***, (1961) 510.

[13] A. Martí, C. R. Stanley, and A. Luque. *Intermediate Band Solar Cells (IBSC) Using Nanotechnology, chapter 17 in Nanostructured Materials for Solar Energy Conversion.* (Elsevier B. V., 2006).

[14] A. Martí, E. Antolín, E. Cánovas, N. López, P.G. Linares, A. Luque, C.R. Stanley, and C.D. Farmer. Elements of the design and analysis of quantum-dot intermediate band solar cells. *Thin Solid Films* ***516***, (2008) 6716.

[15] P. C.Hemmer. *Kvantemekanikk.* (Tapir Akademisk Forlag, 2005).

[16] D. Bimberg, M. Grundmann, and N. N. Ledentsov. *Quantum dot heterostructures.* (John Wiley and Sons, Ltd, 1999).

[17] Ecse-6968 Quantum mechanics applied to semiconductor devices. Electrical, Computer, and Systems Engineering Department, Rensselaer Polytechnic Institute (Retrieved online on 2009-05-29). `http://www.ecse.rpi.edu/~schubert/Course-ECSE-6968Quantummechanics/Ch12Densityofstates.pdf`.

[18] B. R. Nag. *Physics of Quantum Well Devices.* (Kluwer academic publishers, 2000).

[19] Intermediate-band Solar Cells and the Quantum Dot Approach. Department of Electronics and Electrical Engineering, University of Glasgow, (Retrieved online on 2009-05-29). `http://www.jointsolarpanel.nl/fileadmin/jointsolarpanel/user/documents/seminar2004/stanleyzc04.pdf`.

[20] M. Y. Levy, C. Honsberg, A. Martí, and A. Luque. Quantum dot intermediate band solar cell material systems with negligible valence band offsets. *Presented at the 31st IEEE Photovoltaics Specialist Conference, Orlando Florida*, (January 3-7 2005).

[21] A. Martí, L. Cuadra, N. López, and A. Luque. Intermediate Band Solar Cells: Comparision with Shockley-Read-Hall Recombination. *Semiconductors **38***, (2004) 946.

[22] S. M. Hubbard, C. D. Cress, C. G. Bailey, 1 R. P. Raffaelle, 2 G. Bailey, and D. M. Wilt. Effect of strain compensation on quantum dot enhanced gaas solar cells. *Appl. Phys. Lett. **92***, (2008) 123512.

[23] R. Oshima, H. Komiyama, T. Hashimoto, H. Shigekawa, and Y. Okada. Fabrication of multi-layer self-assembled inas quantum dots for high-efficiency solar cells. *Conference Record of the 2006 IEEE 4th World Conference on Photovoltaic Energy Conversion*, (2006) 158.

[24] Z. H. Zhang, K. Y. Cheng, C. F. Xu, and K. C. Hsieh. Defect-free 100-layer strain-balanced inas quantum dot structure grown on inp substrate. *Appl. Phys. Lett. **89***, (2006) 063115.

[25] L. Cuadra, A. Martí, and A. Luque. Influence of the Overlap Between the Absorption Coefficients on the Efficiency of the Intermediate Band Solar Cell. *IEEE Trans. Electron Devices **51***, (2004) 1002.

[26] A. Luque and A. Martí. Increasing the Efficiency of Ideal Solar Cells by Photon Induced Ttransitions at Intermediate Levels. *Phys. Rev. Lett. **78***, (1997) 5014.

[27] X. M. Dai and Y. H. Tang. A simple general analytical solution for the quantum efficiency of front-surface-field solar cells. *Solar Eenergy Materials and Solar Cells **43***, (1996) 363.

[28] S. P. Tobin, S. M. Vernon, C. Bajgar, L. M. Geoffroy, C. J. Keavney, M. M. Sanfacon, and V. E. Haven. Device processing and analysis of high efficiency GaAs cells. *Solar Cells **24***, (1988) 103.

[29] P. D. Demoulin, M. S. Lundstrom, and R. J. Schartz. Back-surface field design for n^+p GaAs cells. *Solar Cells **20***, (1987) 229.

[30] J. R. Hauser and M. A. Littlejohn. Approximations for accumulation and inversion space-charge layers in semiconductors. *Solid-State Eelectronics **11***, (1968) 667.

[31] N. J. Ekins-Daukes. *An investigation into the efficiency of strained and strain-balanced quantum well solar cell, Phd thesis.* (Imperial College, 1999).

[32] S. R. Dhariwal, V. N. Ojha, and R. C. Sharma. Voltage saturation at the high-low junction and its effect on the I-V characteristics of a diode. *Solid-State Electronics **31***, (1988) 1383.

[33] J. R. Hauser. Boundary conditions at p-n junctions. *Solid-State Electronics **14***, (1971) 133.

[34] A. Martí, L. Cuadra, and A. Luque. Quasi-Drift Diffusion Model for the Quantum Dot Intermediate Band Solar Cell. *IEEE Trans. Electron Devices **49***, (2002) 1632.

[35] A. Martí, L. Cuadra, and A. Luque. Design constraints of the quantum-dot intermediate band solar cell. *Physica E **14***, (2002) 150.

[36] A. Luque, A. Martí, N. López, E. Antolín, E. Cánovas, C. Stanley, C. Farmer, and P. Díaz. Operation of the intermediate band solar cell under nonideal space charge region conditions and half filling of the intermediate band. *J. Appl. Phys. **99***, (2006) 094503-1.

[37] E. H. Lie. Material parameters of ingaasp and inalgaas systems for use in quantum well structures at low and room temperatures. *Physica E **5***, (2000) 215.

[38] S. Adachi. *Properties of Aluminium Gallium Arsenide.* (INSPEC, 1993).

[39] T. Markvart and L. Castañer. *Solar Cells: Materials, Manufacture and Operation.* Elsevier, (2005).

[40] M. R. Brozel and C. E. Stillman. *Properties of Gallium Arsenide.* (INSPEC, 1996).

[41] D. E. Aspnes. *Table of optical functions of intrinsic GaAs: Refractive index and absorption coefficient vs energy (0-155 eV) Properties of gallium arsenide.* (INSPEC, EMIS Datareviews Series No. 2, (990).

[42] M. Grundmann. *The Physics of Semiconductors.* (Springer, 2006).

[43] J. P. Connolly. *Modelling Multiple Quantum Well Solar Cells, MSc thesis.* (Imperial College, 1991).

[44] M. Paxman, J. Nelson, B. Braun, J. Connolly, and K.W.J. Barnham. Modeling the spectral response of the quantum well solar cell. *J. Appl. Phys. **74***, (1993) 614.

[45] J. S. Blakemore. Semiconducting and other major properties of gallim arsenide. *J. Appl. Phys.* ***53***, (1982) R123.

[46] O. Madelung, U. Rössler, and M. Schulz. *Landolt-Börnstein - Group III Condensed Matter Numerical Data and Functional Relationships in Science and Technology, Group IV Elements, IV-IV and III-V Compounds. Part b - Electronic, Transport, Optical and Other Properties.* (Springer, 2006).

[47] Reference solar spectral irradiance: Air mass 1.5. Renewabel Resource Data Center, National Renewable Energy Laboratory (Retrieved online on 2008-12-12). `http://rredc.nrel.gov/solar/spectra/am1.5/`.

[48] N. López, A. Martí, A. Luque, C. Stanley, C. Farmer, and P. Diaz. Experimental Analysis of the Operation of Quantum Dot Intermediate Band Solar Cells. *J. of Solar Energy Engineering* ***129***, (2007) 319.

[49] A. Luque, A. Martí, N. López, E. Antolín, E. Cánovas, C. Stanley, C. Farmer, L. J. Caballero, and L. Cuadra J. L. Balenzategui. Experimental analysis of the quasi-fermi level split in quantum dot intermediate-band solar cells. *Appl. Phys. Lett.* ***87***, (2005) 083505-1.

[50] A. Martí, E. Antolín, C. R. Stanley, C. D. Farmer, N. López, P. Díaz, E. Cánovas, P. G. Linares, and A. Luque. Production of Photocurrent due to Intermediate-to-Conduction-Band Transitions: A Demonstartion of a Key Operating Principle of the Intermediate-Band Solar Cell. *Phys. Rew. Lett.* ***97***, (2006) 247701-1.

[51] S. P. Bremner, M. Y. Levy, and C. B. Honsberg. Limiting efficiency of an intermediate band solar cell under a terrestrial spectrum. *Appl. Phys. Lett.* ***92***, (2008) 171110-1.

[52] A. Luque and S. Hegedus. *Handbook of Photovoltaic Science and Engineering.* (John Wiley & Sons Ltd,, 2003).

[53] M. E. Klausmeier-Brown, P. D. DeMoulin, H. L. Chuang, M. S. Lundstrom, M. R. Melloch, and S. P. Tobin. Influence of bandgap narrowing effects in p^+-GaAs on solar cell performance. *Conference Record of the Twentieth IEEE* ***1***, (1988) 503.

Appendix A

List of Symbols

Symbol	Description	Page
E_G	Band gap of semiconductor	3
n	Electron concentration	4
p	Hole concentration	4
n_i	Intrinsic carrier concentration	4
N_d	Donor concentration	4
N_a	Acceptor concentration	4
n_0	Equilibrium electron concentration	4
p_0	Equilibrium hole concentration	4
E_F	Fermi energy	4
E	Energy	5
$f(E)$	Fermi-Dirac distribution function	5
k_B	Boltzmann′s constant	5
T	Absolute temperature	5
E_i	Fermy energy in intrinsic material	5
μ	Chemical potential	5
F_n	Quasi-Fermi level electrons	5
F_p	Quasi-Fermi level holes	5
z	Coordinate	6
G	Total generation rate	6
U	Recombination rate	6
$R(E)$	Reflectivity	5
$\alpha(E)$	Absorption coefficient	6
$g(E,z)$	Generation rate per unit volume at a depth z	6
$F(E)$	Incident photon flux	6
U_{rad}	Excess radiative rec. rate	7
r_{sp}	Rate of spontaneous relaxation between two energy stats	7
n_r	Refractive index	7
h	Planck's constant	7
c	Speed of light	7
B_{rad}	Radiative rec. coefficient	7
Δn	Optically generated density of electrons	7
Δp	Optically generated density of holes	7
U_{rad_p}	Excess radiative rec. rate in p-type material	8

U_{rad_n} Excess radiative rec. rate in n-type material 8
$\tau_{n,rad}$ Minority electron radiative lifetime 8
$\tau_{p,rad}$ Minority hole radiative lifetime 8
U_{SRH} Excess Shockley Read Hall rec. rate 8
E_t Energy of trap 8
$\tau_{n,SRH}$ Lifetime for electron capture by a trap state 8
$\tau_{p,SRH}$ Lifetime for hole capture by a trap state 8
v_n Thermal velocity electron 8
v_p Thermal velocity hole 8
ω_n Capture cross section of trap for electrons 8
ω_p Capture cross section of trap for holes 8
N_t Density of traps per unit volume 8
U_{SRH_p} Excess non-radiative rec. rate in p-type material 8
U_{SRH_n} Excess non-radiative rec. rate in n-type material 8
N_s Density of traps per unit area 8
U_s Surface rec. flux 9
n_s Electron density at surface 9
p_s Hole density at surface 9
S_n Surface rec. velocity of electrons 9
S_p Surface rec. velocity of holes 9
U_{S_p} Surface rec. flux in p-type material 9
U_{S_n} Surface rec. flux in n-type material 9
U_{Aug} Excess Auger rec. rate 9
$\tau_{n,Aug}$ Electron lifetime for band-to-band Auger rec. in p-type material 9
$\tau_{n,Aug}$ Hole lifetime for band-to-band Auger rec. in n-type material 9
$J_n(\text{diff})$ Diffusive current density for electrons 10
$J_p(\text{diff})$ Diffusive current density for holes 10
D_n Electron diffusion coefficient 10
D_p Hole diffusion coefficient 10
q Electron charge 10
W Width of depletion region 10
$\mathscr{E}$ Electric field 11
$J_n(\text{drift})$ Drift current density for electrons 11
$J_p(\text{drift})$ Drift current density for holes 11
μ_n Mobility of electrons 11
μ_p Mobility of holes 11
V_0 Built-inn voltage p-n junction 11
z_p Width of p-layer 12
z_n Width of n-layer 12
w_p Width of depletion region into p-layer 12
w_n Width of depletion region into n-layer 12
U_n Excess rec. rate electrons 13
U_p Excess rec. rate holes 13
G_n Excess generation rate electrons 13
G_p Excess generation rate holes 13
L_n Diffusion length electrons 13

L_p	Diffusion length holes	13
τ_n	Electron lifetime	13
τ_p	Hole lifetime	13
J_n	Electron current density	13
J_p	Hole current density	13
J_{dark}	Dark-current density	14
J_{light}	Photocurrent density	14
QE	Quantum efficiency	15
QE_p	Quantum efficiency p-layer	15
QE_n	Quantum efficiency n-layer	15
J_{dep}	Net current denisty in depletion region	15
$J_{SRH,dep}$	Recombination current density in depletion region	15
$J_{gen,dep}$	Generation current density in depletion region	15
QE_{dep}	Quantum efficiency depletion region	16
J_0	Sum of dark-currents in p- and n-layer	16
A_0	Diode ideality factor	17
J_{sc}	Short-circuit current density	17
V_{oc}	Open circuit voltage	17
J_m	Current density giving maximum power density	17
V_m	Voltage giving maximum power denisty	17
P_m	Maximum power density	17
FF	Fill factor	17
η	Conversion efficiency	17
P_{in}	Incident power density	18
R_s	Series resistance	18
R_{sh}	Shunt resistance	18
A	Area of the solar cell	18
F_{BB}	Black-body spectrum	19
T_s	Temperature of the sun	19
T_c	Temperature of the solar cell	19
f_s	Geometrical factor for the sun	20
f_c	Geometrical factor for the solar cell	20
X	Concentration factor	21
E_H	Band gap between IB and VB	23
E_L	Band gap between CB and IB	23
E_I	Equilibrium Fermi-energy IB	23
E_v	Energy at top of VB	23
E_c	Energy at bottom of CB	23
α_{CI}	Absorption coefficient IB to CB transitions	28
α_{IV}	Absorption coefficient VB to IB transitions	28
α_{CV}	Absorption coefficient VB to CB transitions	28
F_i	Quasi-Fermi level for electrons in IB	29
μ_{CI}	Quasi-Fermi level split	29
μ_{IV}	Quasi-Fermi level split	29
μ_{CV}	Quasi-Fermi level split	29
N_i	Background doping i-layer	32

z_i	Width of i-layer	33
$\tau_{n,i,SRH}$	Non-radiative lifetime for electrons in i-layer	33
$\tau_{p,i,SRH}$	Non-radiative lifetime for holes in i-layer	33
z_w	Width of window layer	33
z_{p^+}	Width of p^+-layer	33
w_a	Width of depletion region between p^+- and p-layer	33
$J_{n,total}$	Total electron current density	33
J_{n,p^+}	Electron current density from p^+-layer	33
$J_{n,p}$	Electron current density from p-layer	33
$J_{n,dep}$	Electron current density from depeltion regino between p- and p^+-layer	33
N_a^+	Doping of p^+-layer	34
S_n^+	Front surface rec. velocity of p^+-layer	35
L_n^+	Diffusion length in p^+-layer	34
D_n^+	Diffusion coefficient in p^+-layer	34
$S_{n,pp^+,eff}$	Effective surface rec. velocity p-layer	34
V_{pp^+}	Built-in voltage p^+-p junction	34
S_n^+	Surface rec. velocity on top of p^+-layer	35
α_w	Absorption coefficient of window layer	33
$S_{n,eff,window}$	Effective surface rec. velocity p^+-layer by having a window layer	36
S_n^w	Front surface rec. velocity of the window layer	36
L_n^w	Diffusion length window layer	36
D_n^w	Diffusion coefficient in window layer	36
z_n^+	Width of n^+-layer	37
w_b	Width of depletion region between n^+- and n-layer	37
$J_{p,total}$	Total hole current density	37
J_{p,n^+}	Hole current density from n^+-layer	37
$J_{p,n}$	Hole current density from n-layer	37
$J_{p,dep}$	Hole current density from depletion region between n- and n^+-layer	37
$S_{p,nn^+,eff}$	Effective surface rec. velocity n-layer	37
V_{nn^+}	Built-in voltage n^+-n junction	37
S_p^+	Surface rec. velocity on top of n^+-layer	37
L_p^+	diffusion length in n^+-layer	37
D_p^+	Diffusion coefficient in n^+-layer	37
w_{in}	Width of depletion region between i-layer and n-layer	40
V_{ni}	Built-in potential i-n junction	40
V_n	Part of applied voltage over i-n junction	40
V_{pi}	Built-in potential p-i junction	40
V_p	Part of applied voltage over p-i junction	40
w_F	Width of flat band region	42
$w_{ip,min}$	Minimum width of depletion region between the p- and i-layer	42
$w_{in,min}$	Minimum width of depletion region between i- and n-layer	42
U_{SRH_i}	Non-radiative rec. rate in undepleted i-layer	42
U_{rad_i}	Radiative rec. rate in undepleted i-layer	42
$D_{n,i}$	Electron diffusion coefficient in i-layer	42
$D_{p,i}$	Hole diffusion coefficient in i-layer	42
$L_{n,i}$	Electron diffusion length in i-layer	42

$L_{p,i}$ Hole diffusion length in i-layer ... 42
G_{CV} Generation rate VB-CB ... 47
G_{IV} Generation rate VB-IB ... 47
G_{CI} Generation rate IB-CB ... 47
r_d Radius quantum dot ... 47
d Distance between quantum dots ... 47
$U_{rad,CI}$ Excess generation radiative rec. rate CB-IB ... 48
$U_{rad,IV}$ Excess generation radiative rec. rate IB-VB ... 48
$U_{rad,CV}$ Excess generation radiative rec. rate CB-VB ... 48
$B_{rad,CI}$ Radiative rec. coefficient for CB-IB transitions ... 48
$B_{rad,IV}$ Radiative rec. coefficient for IB-VB transitions ... 48
$B_{rad,CV}$ Radiative rec. coefficient for CB-VB transitions ... 48
N_{Dp} Density of empty states in the IB ... 48
N_{Dn} Density of occupied states in the IB ... 48
$D_{n,f}$ Diffusion coefficient for electrons in CB in IB material ... 49
$D_{p,f}$ Diffusion coefficient for holes in VB in IB material ... 49
$J_{p,IB}$ Hole current in VB in IB material ... 50
$J_{n,IB}$ Electron current in CB in IB material ... 50
μ_{ib} Mobility in IB ... 50
N_D Density of dots ... 49
J_{ib} Current denisty in IB ... 49
$\tau_{n,CV,SRH}$ Electron non-radiaitive lifetimes for CB-VB transitions in IB material ... 52
$\tau_{p,CV,SRH}$ Hole non-radiaitive lifetimes for CB-VB transitions in IB material ... 52
$U_{SRH,CI}$ Excess non-radiative rec. rate between CB and IB ... 52
$U_{SRH,IV}$ Excess non-radiative rec. rate between IB and VB ... 52
$\tau_{p,CI,SRH}$ Hole non-radiative lifetime CB-IB transitions ... 52
$\tau_{n,CI,SRH}$ Electron non-radiative lifetime CB-IB transitions ... 52
$\tau_{p,IV,SRH}$ Hole non-radiative lifetime IB-VB transitions ... 52
$\tau_{n,IV,SRH}$ Electron non-radiative lifetime IB-VB transitions ... 52
E_{GaAs} Band gap GaAs ... 55
$E_{Al_xGa_{1-x}As}$ Band gap $Al_xGa_{1-x}As$ ... 55
m_e^* Effective electron mass ... 57
m_{hh}^* Effective heavy hole mass ... 57
m_{lh}^* Effective light hole mass ... 57
m_0 Electron mass ... 57
ϵ_0 Permittivity of free space ... 57
γ_s Angle sun is placed ... 67
N_{Dp0} Density of empty states in IB at equilibrium ... 53
N_{Dn0} Density of filled states in IB at equilibrium ... 53

Appendix B

Source code from MATLAB

The modeling was done using MATLAB and in this section the source code is given.

B.1 Variables used for p-i-n reference cell with depleted i-layer

```
-------------------------------------------------------
Variables p-i-n solar cell, no flat band
-------------------------------------------------------
h_planck=6.62607e-34; %Plancks constant h in Js
h_dirac=1.05457e-34; %Diracs constant=h/2pi in Js
m_e=9.10938e-31; %Electron mass in kg
eV=1.60218e-19; %electronvolt to joule
k_Boltzman = 1.38065e-23; %Boltzman constant J/K
freediec = 8.85419e-12; %Free dielectric constant in F/m
e_charge=1.60218e-19; %Charge of an electron in C
c_light = 2.99792e+8; %velocity of light m/s
T=300; %temperature used in article for solar cells in K
E_rydberg=13.6057*eV; %Rydberg energy
T_sun=5780; %Temperature of sun i K


%To meter m
nm=1e-9; %nanometer to meter
cm=1e-2; %centimeter to meter
micm=1e-6; %micrometer to meter
mm=1e-3; % millimeter to meter
A=1e-10; % Aangstrom


numberofdevices=7;
window=[0 0 0 0 1 1 1]; %equal to 1 if we have a window layer,
    equal to 0 of we do not have a window layer

%Fraction of x in Al_xGa_(1-x)_As
x_window=[0.85 0.85 0.85 0.85 0.85 0.85 0.85];  %x in window layer
%x_window=[0.804 0.804];    %x in window layer
```

```
31 x_cell=[0 0 0 0 0 0 0];       %x in p, p-plus, n and n-plus layers
32 x_IB=[0 0 0 0 0 0 0];         %x in intermediate band layer
33
34
35 %Bandgap for GaAs
36 E_GaAs=(1.519-(5.405*(1e-4)*T^2/(T+204)))*eV; %from Lie!!
37
38 bandgap_GaAs=E_GaAs./eV
39
40 E_window=zeros(1,numberofdevices);              %Bandgap window layer
     (eV)
41 E_cell=zeros(1,numberofdevices);                %Bandgap in p, p-plus,
      n and n-plus layers (eV)
42
43 %Bandgap for Al_xGa_(1-x)As in the rest of the cell
44 for i=1:numberofdevices
45 E_window(i)=(1.911+(0.005.*x_window(i))+(0.245.*(x_window(i).^2)))
     *eV;   %Bandgap window layer for x>=0.45(eV) (Properties of
     AlGaAs)
46 E_cell(i)=(E_GaAs/eV+(1.247*x_cell(i)))*eV;        %Bandgap in p, p
     -plus, n and n-plus layers  for x<0.45(eV) (Properties of
     AlGaAs)
47 end
48
49
50
51 %Bandgaps in intermediate band
52 E_IV=[0 0 0 0 0 0 0]*eV; %Energy difference between the
     intermediate band and the valence band (eV)
53 E_CI=[0 0 0 0 0 0 0]*eV; %Energy difference between the conduction
      band and the intermediate band (eV)
54 E_CV=[E_cell(2) E_cell(2) E_cell(2) E_cell(2) E_cell(2) E_cell(2)
     E_cell(2)]; %Energy difference between the conduction band and
     the valence band (eV)
55
56
57 %Absorption coefficients and absorbance
58 alpha_CV=[1e7 1e7 1e7 1e7 1e7 1e7 1e7];        %Absorption
     coefficient optical transitions CB-VB  (/m)
59 alpha_CI=[0 0 0 0 0 0 0];      %Absorption coefficient optical
     transitions CB-IB  (/m)
60 alpha_IV=[0 0 0 0 0 0 0];      %Absorption coefficient optical
     transitions IB-VB  (/m)
61
62
63 %Effective masses for AlxGa1-xAs in intermediate band
64
65 m_e_IB=zeros(1,numberofdevices);          %Effective mass electrons
     in intermediate band (kg)
66 m_hh_IB=zeros(1,numberofdevices);         %Effective mass heavy
     holes in intermediate band (kg)
67 m_lh_IB=zeros(1,numberofdevices);         %Effective mass light
     holes in intermediate band (kg)
```

```
68
69 for i=1:numberofdevices
70     m_e_IB(i)=(0.0632+(0.0856*x_IB(i))+(0.0231*x_IB(i)^2))*m_e; %
         Effective mass electrons in intermediate band (kg), formula
          from LIE
71     m_hh_IB(i)=(0.50+(0.2*x_IB(i)))*m_e;                        %
         Effective mass heavy holes in intermediate band (kg),
         formula from LIE
72     m_lh_IB(i)=(0.088+(0.0372*x_IB(i))+(0.0163*x_IB(i)^2))*m_e; %
         Effective mass light holes in intermediate band (kg),
         formula from LIE
73 end
74
75 %Density of states and intrinsic carrier concentration
76 N_C_GaAs=4.7e23; %density of states in the conduction band at 300
      K in GaAs (m-3) from "Solar Cells Materials, Manufacture and
      Operation"
77 N_V_GaAs=7.0e24; %density of states in the valence band at 300 K
      in GaAs (m-3) from "Solar Cells Materials, Manufacture and
      Operation"
78
79 N_C_IB=[N_C_GaAs 0]; %density of states in conduction band in
      intermediate band material (m-3)
80 N_V_IB=[N_V_GaAs 0]; %density of states in valence band in
      intermediate band material (m-3)
81
82 ni_GaAs=1.79e12; %intrinsic carrier concentration at 300 K in GaAs
       (m-3) from "Solar Cells Materials, Manufacture and Operation"
83
84 ni_cell=[ni_GaAs ni_GaAs ni_GaAs ni_GaAs ni_GaAs ni_GaAs ni_GaAs];
       %intrinsic carrier concentration in p- and n-layer
85
86 ni_IB=[ni_GaAs ni_GaAs ni_GaAs ni_GaAs ni_GaAs ni_GaAs ni_GaAs]; %
      intrinsic carrier concentration in intermediate band
87
88
89 %Carrier lifetimes
90 tau_n_GaAs=7e-9; %s fra Nelson Quantum-Well Structures (egentlig
      sqrt(tau_n'tau_p)
91 tau_p_GaAs=7e-9;     % s fra Nelson Quantum-Well Structures
92
93 tau_n_IB=[tau_n_GaAs tau_n_GaAs tau_n_GaAs tau_n_GaAs tau_n_GaAs
      tau_n_GaAs tau_n_GaAs]; %electron lifetime in intermediate band
94 tau_p_IB=[tau_p_GaAs tau_p_GaAs tau_p_GaAs tau_p_GaAs tau_p_GaAs
      tau_p_GaAs tau_p_GaAs]; %hole lifetime in intermediate band
95
96
97 %Parameter for GaAs IKKE SJEKKET SIDEN IKKE INN I REFERENCE CELL
98 epsilon_GaAs=12.79.*(1+(T.*1e-4)).*freediec; %static dielectric
      constant for GaAs from Properties of GaAs
99
100 epsilon_p=[epsilon_GaAs epsilon_GaAs epsilon_GaAs epsilon_GaAs
      epsilon_GaAs epsilon_GaAs epsilon_GaAs]; %dielectric constant p
```

```
      and p-plus layer, here taken for GaAs
101 epsilon_n=[epsilon_GaAs epsilon_GaAs epsilon_GaAs epsilon_GaAs
     epsilon_GaAs epsilon_GaAs epsilon_GaAs]; %dielectric constant n
      and n-plus layer, here taken for GaAs
102
103
104 %Lengths in the devices
105 width_window=[0 0 0 0 5 5 5].*nm;    %with of window layer in m
106 %width_p_plus=[1000 100].*nm;    %with of p-plus layer in m
107 width_p_plus=[0 0 100 100 100 100 100].*nm;
108 %width_p=[200 200].*nm;          %with of p layer in m
109 width_p=[200 200 200 200 200 200 200].*nm;          %with of p
     layer in m
110 width_IB=[100 100 100 100 100 300 300].*nm;         %with of IB
     layer in m
111 width_n=[300 300 300 300 300 300 300].*nm;          %with of n
     layer in m
112 width_n_plus=[0 0 0 100 100 100 100].*nm;    %with of n-plus layer
      in m
113
114
115 %Doping of the devices
116 N_A_window=[2e18 2e18 2e19 2e19 2e19 2e18 2e19];      %doping
     concentration /cm3 in window layer (assumed p-type)
117 N_A_p_plus=[2e18 2e18 2e19 2e19 2e19 2e18 2e19];      %doping
     concentration /cm3 in p-plus layer
118 N_A_p=[2e18 2e18 2e18 2e18 2e18 2e18 2e19];           %doping
     concentration /cm3 in p layer
119 N_D_n=[2e17 2e17 2e17 2e17 2e17 2e17 2e17];           %doping
     concentration /cm3 in n layer
120 N_D_n_plus=[2e17 2e17 2e17 2e18 2e18 2e18 2e18];      %doping
     concentration /cm3 in n-plus layer
121
122
123 %Calculation of built-in voltage because in p-i-n structure (eq
     6.2 in
124 %Nelson)
125
126 V_bi=zeros(1,numberofdevices);
127
128 for i=1:numberofdevices
129     V_bi(i)=(k_Boltzman.*T./e_charge).*log((N_A_p(i)./cm.^3).*(
         N_D_n(i)./cm.^3)./(ni_cell(i).^2));
130 end
131
132 %Calculation of potential drop across the p_plus-p-junction,
     needed in
133 %determining the depletion width of the p_plus-p-junction
134 V_h_mi=0; %potential drop across the p-plus-p junction
135 V_h=zeros(1,numberofdevices);
136
137
138 for i=1:numberofdevices
```

```
139  V_h_mi=fsolve(@(V_h_mi) (e_charge.*V_h_mi./(k_Boltzman.*T))+log((
        N_A_p(i)./N_A_p_plus(i))+(0.5.*(e_charge.*V_h_mi./(k_Boltzman
        .*T))^2)),0,optimset('Display','off'));
140  V_h(i)=V_h_mi;
141  V_h_mi=0;
142 end
143
144 %Depletion width of the p_plus-p-junction, taken as the depletion
       width into the p-layer
145 dep_width_p_plus=zeros(1,numberofdevices);
146
147 for i=1:numberofdevices
148     dep_width_p_plus(i)=sqrt(2.*epsilon_p(i).*k_Boltzman.*T./(
           e_charge.^2.*(N_A_p(i)./cm.^3))).*atan((e_charge.*V_h(i)./(
           k_Boltzman.*T)).*sqrt(N_A_p_plus(i)./(N_A_p(i).*2)));
149 end
150
151 %Width of the undepleted p-layer
152 %The depletion width into the p_plus-layer is not taken into
       consideration
153 width_p_undepleted=zeros(1,numberofdevices);
154
155 for i=1:numberofdevices
156 width_p_undepleted(i)=width_p(i)-dep_width_p_plus(i);
157 end
158
159 %Calculation of potential drop across the n-n_plus-junction,
       needed in
160 %determining the depletion width of the n-n_plus-junction
161 V_h_mi_n_plus=0; %potential drop across the n-n_plus junction
162 V_h_n_plus=zeros(1,numberofdevices);
163
164
165 for i=1:numberofdevices
166  V_h_mi_n_plus=fsolve(@(V_h_mi_n_plus) (e_charge.*V_h_mi_n_plus./(
        k_Boltzman.*T))+log((N_D_n(i)./N_D_n_plus(i))+(0.5.*(e_charge
        .*V_h_mi_n_plus./(k_Boltzman.*T))^2)),0,optimset('Display','
        off'));
167  V_h_n_plus(i)=V_h_mi_n_plus;
168  V_h_mi_n_plus=0;
169 end
170
171 %Depletion width of the p_plus-p-junction, taken as the depletion
       width into the p-layer
172 dep_width_n_plus=zeros(1,numberofdevices);
173
174 for i=1:numberofdevices
175     dep_width_n_plus(i)=sqrt(2.*epsilon_n(i).*k_Boltzman.*T./(
           e_charge.^2.*(N_D_n(i)./cm.^3))).*atan((e_charge.*
           V_h_n_plus(i)./(k_Boltzman.*T)).*sqrt(N_D_n_plus(i)./(N_D_n
           (i).*2)));
176 end
177
```

```
178 %Width of the undepleted n-layer
179 %The depletion width into the n_plus-layer is not taken into
    consideration
180 width_n_undepleted=zeros(1,numberofdevices);
181
182 for i=1:numberofdevices
183 width_n_undepleted(i)=width_n(i)-dep_width_n_plus(i);
184 end
185
186
187
188 %Surface recombination
189 S_window=[1e4 1e4 1e4 1e4 1e4 1e4 1e4]; %surface recombination
    velocity top of window layer m/s
190 S_p_plus=[1e4 1e4 1e4 1e4 1e4 1e4 1e4]; %surface recombination
    velocity top of p_plus layer without window layer m/s
191 S_n_plus=[1e4 1e4 1e4 1e4 1e4 1e4 1e4];       %surface
    recombination velocity n-plus layer m/s (assumed rear surface
    is n-plus+substrate)
192
193
194 %Diffusion lengths and diffusion coeffecients in the devices
195 tau_n_p_layer=[3e-9 3e-9 3e-9 3e-9 3e-9 3e-9 0.5e-9]; %Landolt
    Bornstein for doping 2*10^18 (cm^-3)
196 tau_n_p_plus_layer=[0.5e-9 0.5e-9 0.5e-9 0.5e-9 0.5e-9 3e-9 0.5e
    -9]; %Landolt Bornstein for doping 2*10^19(cm^-3)
197 tau_p_n_layer=[32.5e-9 32.5e-9 32.5e-9 32.5e-9 32.5e-9 32.5e-9
    32.5e-9]; %GaAs book for doping 2*10^17 (cm^-3)
198 tau_p_n_plus_layer=[7e-9 7e-9 7e-9 7e-9 7e-9 7e-9 7e-9]; %GaAs
    book for doping 2*10^18 (cm^-3)
199
200
201 mu_n_p_layer=[0.125 0.125 0.125 0.125 0.125 0.125 0.1400]; %
    Landolt Bornstein for doping 2*10^18 (cm^-3)
202 mu_n_p_plus_layer=[0.1400 0.1400 0.1400 0.1400 0.1400 0.125
    0.1400]; %Landolt Bornstein for doping 2*10^19(cm^-3)
203 mu_p_n_layer=[0.0278 0.0278 0.0278 0.0278 0.0278 0.0278 0.0278]; %
    Landolt Bornstein for doping 2*10^17 (cm^-3)
204 mu_p_n_plus_layer=[0.0238 0.0238 0.0238 0.0238 0.0238 0.0238
    0.0238]; %Landolt Bornstein for doping 2*10^18 (cm^-3)
205
206
207 diffusioncoefficient_n_p=(k_Boltzman.*T./e_charge).*mu_n_p_layer;
208 diffusioncoefficient_n_p_plus=(k_Boltzman.*T./e_charge).*
    mu_n_p_plus_layer;
209
210 diffusioncoefficient_p_n=(k_Boltzman.*T./e_charge).*mu_p_n_layer;
211 diffusioncoefficient_p_n_plus=(k_Boltzman.*T./e_charge).*
    mu_p_n_plus_layer;
212
213
214 difflength_n_p=zeros(1,numberofdevices);
215 difflength_n_p_plus=zeros(1,numberofdevices);
```

```
216 difflength_p_n=zeros(1,numberofdevices);
217 difflength_p_n_plus=zeros(1,numberofdevices);
218
219 for i=1:numberofdevices
220 difflength_n_p(i)=sqrt(tau_n_p_layer(i).*diffusioncoefficient_n_p(
      i));
221 difflength_n_p_plus(i)=sqrt(tau_n_p_plus_layer(i).*
      diffusioncoefficient_n_p_plus(i));
222 difflength_p_n(i)=sqrt(tau_p_n_layer(i).*diffusioncoefficient_p_n(
      i));
223 difflength_p_n_plus(i)=sqrt(tau_p_n_plus_layer(i).*
      diffusioncoefficient_p_n_plus(i));
224 end
225
226 difflength_n_window=difflength_n_p; %does not matter since another
       window recombination velocity is used
227 diffusioncoefficient_n_window=diffusioncoefficient_n_p; %does not
      matter since another window recombination velocity is used
228
229
230 %Effective surface recombination velocities
231 S_eff_p=zeros(1,numberofdevices); %effective surface reombination
      velocity on edge of undepleted p-layer (placed on top of IB)
232 S_eff_n=zeros(1,numberofdevices); %effective surface recombination
       velocity on edge of n-layer (placed under IB)
233 S_eff_window=zeros(1,numberofdevices);  %effective surface
      recombination velocity between p_plus-layer and window layer
234 S_eff_p_plus_p=zeros(1,numberofdevices); %effective surface
      recombination velocity on edge of undepleted p_plus-layer,
      between p_plus-layer and depletion region
235 S_eff_n_plus_n=zeros(1,numberofdevices); %effective surface
      recombination velocity on edge of undepleted n-plus-layer,
      between n_plus-layer and depletion region
236
237 for i=1:numberofdevices
238     S_eff_n(i)=(diffusioncoefficient_p_n_plus(i)./
          difflength_p_n_plus(i)).*(N_D_n(i)./N_D_n_plus(i)).*((((
          S_n_plus(i).*difflength_p_n_plus(i)./
          diffusioncoefficient_p_n_plus(i)).*cosh(width_n_plus(i)./
          difflength_p_n_plus(i)))+sinh(width_n_plus(i)./
          difflength_p_n_plus(i)))./(((S_n_plus(i).*
          difflength_p_n_plus(i)./diffusioncoefficient_p_n_plus(i)).*
          sinh(width_n_plus(i)./difflength_p_n_plus(i)))+cosh(
          width_n_plus(i)./difflength_p_n_plus(i)))); %modification
          of eq 7.10 in Nelson
239     S_eff_p_plus_p(i)=(diffusioncoefficient_n_p(i)./difflength_n_p
          (i)).*(N_A_p_plus(i)./N_A_p(i)).*coth(width_p_undepleted(i)
          ./difflength_n_p(i)); %eq 14 in "A simple general
          analytical solution..."
240     S_eff_n_plus_n(i)=(diffusioncoefficient_p_n(i)./difflength_p_n
          (i)).*(N_D_n_plus(i)./N_D_n(i)).*coth(width_n_undepleted(i)
          ./difflength_p_n(i)); %eq 14 in "A simple general
          analytical solution..."
```

```
241
242
243     if window(i)==1
244     S_eff_window_test=(diffusioncoefficient_n_window(i)./
          difflength_n_window(i)).*exp((E_cell(i)-E_window(i))./(
          k_Boltzman.*T)).*((((S_window(i).*difflength_n_window(i)./
          diffusioncoefficient_n_window(i)).*cosh(width_window(i)./
          difflength_n_window(i)))+sinh(width_window(i)./
          difflength_n_window(i)))./(((S_window(i).*
          difflength_n_window(i)./diffusioncoefficient_n_window(i)).*
          sinh(width_window(i)./difflength_n_window(i)))+cosh(
          width_window(i)./difflength_n_window(i)))) %S_eff_window
          used for front surface velocity of the p_plus layer
245     S_eff_window(i)=1e2 %Takes value from Hovel
246     S_eff_p(i)=(diffusioncoefficient_n_p_plus(i)./
          difflength_n_p_plus(i)).*(N_A_p(i)./N_A_p_plus(i)).*(((
          S_eff_window(i).*difflength_n_p_plus(i)./
          diffusioncoefficient_n_p_plus(i)).*cosh(width_p_plus(i)./
          difflength_n_p_plus(i)))+sinh(width_p_plus(i)./
          difflength_n_p_plus(i)))./(((S_eff_window(i).*
          difflength_n_p_plus(i)./diffusioncoefficient_n_p_plus(i)).*
          sinh(width_p_plus(i)./difflength_n_p_plus(i)))+cosh(
          width_p_plus(i)./difflength_n_p_plus(i)))
247
248     else
249     S_eff_window(i)=S_p_plus(i); %S_eff_window used for front
          surface velocity of the p_plus layer
250     S_eff_p(i)=(diffusioncoefficient_n_p_plus(i)./
          difflength_n_p_plus(i)).*(N_A_p(i)./N_A_p_plus(i)).*((((
          S_p_plus(i).*difflength_n_p_plus(i)./
          diffusioncoefficient_n_p_plus(i)).*cosh(width_p_plus(i)./
          difflength_n_p_plus(i)))+sinh(width_p_plus(i)./
          difflength_n_p_plus(i)))./(((S_p_plus(i).*
          difflength_n_p_plus(i)./diffusioncoefficient_n_p_plus(i)).*
          sinh(width_p_plus(i)./difflength_n_p_plus(i)))+cosh(
          width_p_plus(i)./difflength_n_p_plus(i))));
251     end
252 end
253
254
255 %Area
256 area=[1.16e-5 1.16e-5 1.16e-5 1.16e-5 1.16e-5 1.16e-5 1.16e-5]; %
      area in m^2 TATT FRA ARTIKKEL MEN SJEKK!
257
258 %Resistance
259 R_sh=[50000000000 500000000000 50000000000 500000000000
      50000000000 50000000000 50000000000]; %shunt resistance in Ohm
260 R_s=[0 0 0 0 0 0 0]; %series resistance in  Ohm 500 gir mindre
      kortslutningsstrøm
261
262 quantumdot=[0 0 0 0 0 0 0]; %value equal to 1 if we have quantum
      dots, 0 if we do not have quantum dots
```

```
263 ARC=[0 1 1 1 1 1 1]; %value equal to 1 if we have anti-reflective
    coating, 0 in the opposite case
264
265 save 'var.mat'
```

Listing B.1: Variables

B.2 Photocurrent for p-i-n reference cell with depleted i-layer

```
1 %Determination of photocurrent for AlGaAs/GaAs solar cells
2 function generatedcurrent=Sollysstrom()
3 clear;
4
5 load 'var.mat' %Loading the file containing all constants,
    remember to first run the program Variables
6
7 %Reading the necessary excel files
8
9 step_endelig=0.001; %steplength used in interpolation
10
11 %USES SHIFT OF ENERGY AXIS
12 num4=xlsread('C:\Documents␣and␣Settings\Kirsti␣Kvanes\Mine␣
    dokumenter\MATLAB\Prosjekt\GaAs␣optiske␣parametre');%Optical
    parameters for GaAs using shift of energy axis
13 %Comment: alpha values were originally given as 10^-3 multiplied
    by the
14 %values in the excel file, this was pr cm, to get correct alpha
    values pr
15 %m, multiply with 10^2*10^3
16 photonenergy_GaAsny=num4(:,1); %photonenergies for GaAs used in
    the excel files
17 alpha_GaAsny=1e5.*num4(:,4); %alpha values for GaAs
18 R_GaAsny=num4(:,3); %Reflectivity values for GaAs
19 n_GaAsny=num4(:,2); %Refractive index for GaAs
20
21
22 w_p=0*nm; %For p-i-n solar cell, depletion region into p-layer
    equal to zero
23 w_n=0*nm; %For p-i-n solar cell, depletion region  into n-layer
    equal to zero
24
25 %Getting values for GaAs
26 %Bruker mindre steglengder frem til 1.5 eV for der har jeg flere
    verdier
27 %HUSK at når har man flere steglengder, en steglengde for energier
     mindre
28 %enn 1.5 eV, en annen for energier større enn 1.5 eV og en tredje
    brukt i
29 %interpolering
30 %må ta hensyn til at minste verdi i excel-fila er 1.36 eV, setter
31 %absorpsjonskoeffisienten lik 0 for mindre verdier
32 step_1_GaAs=0.01;%*eV; %Steplength 0.01 for energies less then 1.5
```

```
33 minimum_1_GaAs=0.32;%*eV; %minimum value in the excel files for
      solar spectrum is 0.3104
34 maximum_1_GaAs=1.5;%*eV; %maximum allowed value 1.5 for energies
      larger then 1.5 we need a greater steplength
35 energydifference_1=0.01;
36 E_1_GaAs=(minimum_1_GaAs:step_1_GaAs:maximum_1_GaAs); %energies
      with steplength 0.01
37 antall_1_GaAs=round(((maximum_1_GaAs-minimum_1_GaAs)/step_1_GaAs)
      +1); %antall E i intervallet miniumum1:maximum1 eV må ha
      heltall derfor round
38
39 step_2_GaAs=0.1; %Steplength 0.1 for energies greater then 1.5
40 minimum_2_GaAs=maximum_1_GaAs; %miniumvalue is maximum of the
      other interval
41 maximum_2_GaAs=4.4; %Maximum value in the excel files for solar
      spectrum is 4.45, maximum allowed value for the formulas used
      later is 5.6!!! Because we have not got values for the abs.
      koeff of Al_0.9Ga_0.1As for greater energies
42 energydifference_2=0.1;
43 E_2_GaAs=(minimum_2_GaAs:step_2_GaAs:maximum_2_GaAs); %energies
      with steplength 0.1
44 antall_2_GaAs=round(((maximum_2_GaAs-minimum_2_GaAs)/step_2_GaAs)
      +1); %antall E i intervallet miniumum2:maximum2 eV må ha
      heltall derfor round
45
46 alpha_GaAs_1=zeros(1,antall_1_GaAs); %alpha values for energies
      with steplength 0.01
47 alpha_GaAs_2=zeros(1,antall_2_GaAs); %alpha values for energies
      with steplength 0.1
48 R_GaAs_1=zeros(1,antall_1_GaAs); %reflectivity values for energies
       with steplength 0.01
49 R_GaAs_2=zeros(1,antall_2_GaAs); %reflectivity values for energies
       with steplength 0.1
50 n_GaAs_1=zeros(1,antall_1_GaAs); %refractive index
51 n_GaAs_2=zeros(1,antall_2_GaAs); %refractive index
52
53
54 k=1;
55
56  for i=1:antall_1_GaAs
57      if E_1_GaAs(i)<1.36
58           alpha_GaAs_1(i)=0; %for energies less than 1.36 eV the
                absorption coefficient is equal to zero
59           R_GaAs_1(i)=R_GaAsny(1);
60          n_GaAs_1(i)=n_GaAsny(1);
61      else
62          while ~(photonenergy_GaAsny(k)-(energydifference_1*0.5)<=
               E_1_GaAs(i)&& E_1_GaAs(i)<photonenergy_GaAsny(k)+(
               energydifference_1*0.5))
63               k=k+1;
64          end
65
66          alpha_GaAs_1(i)=alpha_GaAsny(k);
```

```
67          R_GaAs_1(i)=R_GaAsny(k);
68          n_GaAs_1(i)=n_GaAsny(k);
69       end
70   end
71
72   j=k;
73   for i=1:antall_2_GaAs
74      while ~(photonenergy_GaAsny(j)-(energydifference_2*0.5)<=
         E_2_GaAs(i)&& E_2_GaAs(i)<photonenergy_GaAsny(j)+(
         energydifference_2*0.5))
75          j=j+1;
76      end
77
78       alpha_GaAs_2(i)=alpha_GaAsny(j);
79       R_GaAs_2(i)=R_GaAsny(k);
80       n_GaAs_2(i)=n_GaAsny(k);
81   end
82
83  %Interpolation
84   pp_GaAs_1 = interp1(E_1_GaAs,alpha_GaAs_1,'cubic','pp'); %
       interpolates alpha values
85   pp_GaAs_1_R = interp1(E_1_GaAs,R_GaAs_1,'cubic','pp'); %
       interpolates reflectivity values
86   pp_GaAs_1_n=interp1(E_1_GaAs,n_GaAs_1,'cubic','pp'); %
       interpolates refractive index values
87
88   zi_GaAs_1 = minimum_1_GaAs:step_endelig:maximum_1_GaAs;
89
90   yi_GaAs_1 = ppval(pp_GaAs_1,zi_GaAs_1); %interpolates alpha
       values
91   yi_GaAs_1_R = ppval(pp_GaAs_1_R,zi_GaAs_1); %interpolates
       reflectivity values
92   yi_GaAs_1_n = ppval(pp_GaAs_1_n,zi_GaAs_1); %interpolates
       refractive index values
93
94   antall_endelig_1_GaAs=round(((maximum_1_GaAs-minimum_1_GaAs)/
       step_endelig)+1); %number of values for alpha for energies
       less then 1.5
95
96   pp_GaAs_2 = interp1(E_2_GaAs,alpha_GaAs_2,'cubic','pp'); %
       interpolates alpha values
97   pp_GaAs_2_R = interp1(E_2_GaAs,R_GaAs_2,'cubic','pp'); %
       interpolates reflectivity values
98   pp_GaAs_2_n = interp1(E_2_GaAs,n_GaAs_2,'cubic','pp'); %
       interpolates refractive index values
99
100  zi_GaAs_2 = minimum_2_GaAs:step_endelig:maximum_2_GaAs;
101
102  yi_GaAs_2 = ppval(pp_GaAs_2,zi_GaAs_2); %interpolates alpha
       values
103  yi_GaAs_2_R = ppval(pp_GaAs_2_R,zi_GaAs_2); %interpolates
       reflectivity values
```

```
104 yi_GaAs_2_n = ppval(pp_GaAs_2_n,zi_GaAs_2); %interpolates
        refractive index values
105
106 antall_endelig_2_GaAs=round(((maximum_2_GaAs-minimum_2_GaAs)/
        step_endelig)+1); %number of values for alpha for energies
        greater then 1.5
107
108 antall_endelig=antall_endelig_1_GaAs+antall_endelig_2_GaAs-1; %
        number of values in the final tables for alpha, (minus 1
        because the value for E=1.5 eV should not be counted to times)
109
110 zi_endelig=zeros(1,antall_endelig); %final energies,
111 alpha_GaAs_endelig=zeros(1,antall_endelig); %interpolated
        alphavalues, the values will be used later
112 R_GaAs_endelig=zeros(numberofdevices,antall_endelig); %
        interpolated reflectivity values
113 n_GaAs_endelig=zeros(1,antall_endelig); %interpolated refractive
        index values
114
115 for i=1:antall_endelig_1_GaAs
116     zi_endelig(i)=zi_GaAs_1(i);
117     for a=1:numberofdevices
118        if ARC(a)==0 %no anti-reflective coating
119        R_GaAs_endelig(a,i)=yi_GaAs_1_R(i);
120        else
121         R_GaAs_endelig(a,i)=0;
122        end
123     end
124     n_GaAs_endelig(i)=yi_GaAs_1_n(i);
125     alpha_GaAs_endelig(i)=yi_GaAs_1(i);
126 end
127
128 for i=antall_endelig_1_GaAs+1:antall_endelig;
129     zi_endelig(i)=zi_GaAs_2(i+1-antall_endelig_1_GaAs); %the
           value for E=1.5 eV should not be counted to times,
           therefore i+1
130      for a=1:numberofdevices
131        if ARC(a)==0 %no anti-reflective coating
132        R_GaAs_endelig(a,i)=yi_GaAs_2_R(i+1-antall_endelig_1_GaAs)
            ;
133        else
134         R_GaAs_endelig(a,i)=0;
135        end
136      end
137      n_GaAs_endelig(i)=yi_GaAs_2_n(i+1-antall_endelig_1_GaAs);
138      alpha_GaAs_endelig(i)=yi_GaAs_2(i+1-antall_endelig_1_GaAs);
139 end
140
141
142 %Values for absorption coefficient for Al_0.804Ga_0.196As
143 numwindow_0804=xlsread('C:\Documents␣and␣Settings\Kirsti␣Kvanes\
       Mine␣dokumenter\MATLAB\Master\AlGaAs␣0804␣optiske␣parametre');
```

```
144 %Comment: alpha values were originally given as 10^-3 multiplied
    by the
145 %values in the excel file, this was pr cm, to get correct alpha
    values pr
146 %m, multiply with 10^2*10^3
147 photonenergy_window=numwindow_0804(:,1); %photonenergies for Al_0
    .804Ga_0.196As used in the excel files
148 alpha_window_0804=1e5.*numwindow_0804(:,2); %alpha values for Al_0
    .804Ga_0.196As
149
150
151 %Values for absorption coefficient for Al_0.900Ga_0.100As
152 numwindow_0900=xlsread('C:\Documents␣and␣Settings\Kirsti␣Kvanes\
    Mine␣dokumenter\MATLAB\Master\AlGaAs␣0900␣optiske␣parametre');
153 %Comment: alpha values were originally given as 10^-3 multiplied
    by the
154 %values in the excel file, this was pr cm, to get correct alpha
    values pr
155 %m, multiply with 10^2*10^3
156 alpha_window_0900=1e5.*numwindow_0900(:,2); %alpha values for Al_0
    .900Ga_0.100As
157
158
159 %Getting values for Al_0.804Ga0.196As
160  %The absorption coefficient is set to zero for energies less than
      1.5 eV
161  %Uses the excel file for energies greater than 1.5 eV which has
     an energy
162  %step equal to 0.1 eV. This is different than the values for GaAs
      where
163  %two different energy steps are used
164
165 step_window=0.1; %Steplength 0.1 in the excel file
166 minimum_window=minimum_1_GaAs;%*eV; %minimum value in the excel
    files for solar spectrum is 0.3104, minium value in the excel
    file for absorption coeff is 1.36!!!
167 maximum_window=maximum_2_GaAs;%*eV; %maximum allowed value 1.5 for
     energies larger then 1.5 we need a greater steplength
168 E_window_table=(minimum_window:step_window:maximum_window);
169 antall_window=floor((maximum_window-minimum_window)./step_window
    +1); %number of E in the excel file
170
171 alpha_AlGaAs_window_temp_0804=zeros(1,antall_window);
172
173 windownumber_0804=1;
174
175  for i=1:antall_window
176      if E_window_table(i)<1.5
177          alpha_AlGaAs_window_temp_0804(i)=0; %for energies less
              than 1.5 eV the absorption coefficient is equal to
              zero
178      else
```

```
179         while ~(photonenergy_window(windownumber_0804)-(
               step_window*0.5)<=E_window_table(i)&& E_window_table(i)
               <photonenergy_window(windownumber_0804)+(step_window
               *0.5))
180             windownumber_0804=windownumber_0804+1;
181         end
182 
183         alpha_AlGaAs_window_temp_0804(i)=alpha_window_0804(
               windownumber_0804);
184     end
185 end
186 
187 %Interpolation
188 pp_window_0804 = interp1(E_window_table,
       alpha_AlGaAs_window_temp_0804,'cubic','pp'); %interpolates
       alpha values
189 yi_window_0804 = ppval(pp_window_0804,zi_endelig); %interpolates
       alpha values
190 alpha_AlGaAs_window_0804_final=zeros(antall_endelig); %
       interpolated alphavalues, the values will be used later
191 for i=1:antall_endelig
192     alpha_AlGaAs_window_0804_final(i)=yi_window_0804(i);
193 end
194 
195 %Getting values for Al_0.900Ga0.100As
196 %The absorption coefficient is set to zero for energies less than
        1.5 eV
197 %Uses the excel file for energies greater than 1.5 eV which has
       an energy
198 %step equal to 0.1 eV. This is different than the values for GaAs
        where
199 %two different energy steps are used
200 
201 alpha_AlGaAs_window_temp_0900=zeros(1,antall_window);
202 
203 windownumber_0900=1;
204 
205 for i=1:antall_window
206     if E_window_table(i)<1.5
207         alpha_AlGaAs_window_temp_0900(i)=0; %for energies less
               than 1.5 eV the absorption coefficient is equal to
               zero
208     else
209         while ~(photonenergy_window(windownumber_0900)-(
               step_window*0.5)<=E_window_table(i)&& E_window_table(i)
               <photonenergy_window(windownumber_0900)+(step_window
               *0.5))
210             windownumber_0900=windownumber_0900+1;
211         end
212         alpha_AlGaAs_window_temp_0900(i)=alpha_window_0900(
               windownumber_0900);
213     end
214 end
```

```
215
216 %Interpolation
217  pp_window_0900 = interp1(E_window_table,
        alpha_AlGaAs_window_temp_0900,'cubic','pp'); %interpolates
        alpha values
218  yi_window_0900 = ppval(pp_window_0900,zi_endelig); %interpolates
        alpha values
219
220  alpha_AlGaAs_window_0900_final=zeros(antall_endelig); %
        interpolated alphavalues, the values will be used later
221  for i=1:antall_endelig
222      alpha_AlGaAs_window_0900_final(i)=yi_window_0900(i);
223  end
224 % figure(13)
225 % semilogy(zi_endelig,alpha_AlGaAs_window_0900_final);
226 % hold on
227 % %axis([1.2 3.7 0 1.0e9])
228 % semilogy(zi_endelig,alpha_AlGaAs_window_0804_final);
229 % %axis([1.2 3.7 0 1.0e9])
230
231
232
233  %Getting values for AlGaAs in window layer uses energy shift and
        average
234  %value of x=0.804 and x=0.90 from "Properties of AlGaAs book"
235
236  alpha_AlGaAs_window_0804_shifted=zeros(numberofdevices,
        antall_endelig);
237  alpha_AlGaAs_window_0900_shifted=zeros(numberofdevices,
        antall_endelig);
238  alpha_AlGaAs_window=zeros(numberofdevices,antall_endelig);
239
240   for a=1:numberofdevices
241         for i=1:antall_endelig
242           if (i-round(((0.005.*x_window(a))+(0.245.*x_window(a)
                 .^2)-((0.005.*0.804)+(0.245.*0.804.^2)))./
                 step_endelig)) <=0 &&(i-round(((0.005.*x_window(a))
                 +(0.245.*x_window(a).^2)-((0.005.*0.900)
                 +(0.245.*0.900.^2)))./step_endelig))>antall_endelig
243           alpha_AlGaAs_window_0804_shifted(a,i)=0;
244           alpha_AlGaAs_window_0900_shifted(a,i)=
                 alpha_AlGaAs_window_0900_final(antall_endelig);
245           elseif (i-round(((0.005.*x_window(a))+(0.245.*x_window(a
                 ).^2)-((0.005.*0.804)+(0.245.*0.804.^2)))./
                 step_endelig)) <=0
246              alpha_AlGaAs_window_0804_shifted(a,i)=0;
247              alpha_AlGaAs_window_0900_shifted(a,i)=
                    alpha_AlGaAs_window_0900_final(i-round(((0.005.*
                    x_window(a))+(0.245.*x_window(a).^2)
                    -((0.005.*0.900)+(0.245.*0.900.^2)))./step_endelig
                    ));
248           elseif (i-round(((0.005.*x_window(a))+(0.245.*x_window(a
                 ).^2)-((0.005.*0.900)+(0.245.*0.900.^2)))./
```

```
                step_endelig))>antall_endelig
249             alpha_AlGaAs_window_0900_shifted(a,i)=
                    alpha_AlGaAs_window_0900_final(antall_endelig);
250             alpha_AlGaAs_window_0804_shifted(a,i)=
                    alpha_AlGaAs_window_0804_final(i-round(((0.005.*
                    x_window(a))+(0.245.*x_window(a).^2)
                    -((0.005.*0.804)+(0.245.*0.804.^2)))./step_endelig
                    ));
251          else
252         alpha_AlGaAs_window_0804_shifted(a,i)=
                alpha_AlGaAs_window_0804_final(i-round(((0.005.*
                x_window(a))+(0.245.*x_window(a).^2)-((0.005.*0.804)
                +(0.245.*0.804.^2)))./step_endelig));
253         alpha_AlGaAs_window_0900_shifted(a,i)=
                alpha_AlGaAs_window_0900_final(i-round(((0.005.*
                x_window(a))+(0.245.*x_window(a).^2)-((0.005.*0.900)
                +(0.245.*0.900.^2)))./step_endelig));
254         end
255       alpha_AlGaAs_window(a,i)=0.5.*(
              alpha_AlGaAs_window_0804_shifted(a,i)+
              alpha_AlGaAs_window_0900_shifted(a,i));
256        end
257  end
258
259
260 %
261 %  figure(12)
262 % semilogy(zi_endelig,alpha_AlGaAs_window_0804_shifted(1,:));
263 % hold on
264 % axis([minimum_1_GaAs maximum_2_GaAs 0 1.0e9])
265 % semilogy(zi_endelig,alpha_AlGaAs_window_0900_shifted(1,:));
266 % axis([minimum_1_GaAs maximum_2_GaAs 0 1.0e9])
267 % semilogy(zi_endelig,alpha_AlGaAs_window(1,:));
268 % axis([minimum_1_GaAs maximum_2_GaAs 0 1.0e9])
269 % hold off
270
271
272
273 %Tables for the calculations
274 Q_p=zeros(numberofdevices,antall_endelig); %Quantum efficiency for
        holes in n-layer
275 Q_p_plus=zeros(numberofdevices,antall_endelig); %Quantum
      efficiency for holes in n-plus-layer
276 Q_p_dep=zeros(numberofdevices,antall_endelig); %Quantum efficiency
        for holes in depletion layer between n and n-plus
277 Q_n=zeros(numberofdevices,antall_endelig); %Quantum efficiency for
        electrons in p-layer
278 Q_n_plus=zeros(numberofdevices,antall_endelig); %Quantum
      efficiency for electrons in p-plus-layer
279 Q_n_dep=zeros(numberofdevices,antall_endelig); %Quantum efficiency
        for electrons in depletion-layer between p and p-plus
280 Q_CI=zeros(numberofdevices,antall_endelig); %Quantum efficiency in
        IB giving CI transitions, contribution to J_CI
```

```
281 Q_IV=zeros(numberofdevices,antall_endelig); %Quantum efficiency in
      IB giving IV transitions, contribution to J_IV
282 Q_CV=zeros(numberofdevices,antall_endelig); %Quantum efficiency in
      IB giving CV transitions,contriution to J_CV
283 Q_intrinsic_reference=zeros(numberofdevices,antall_endelig); %
     Quantum efficiency in intrinsic layer for reference cells
284
285 current_CV_intervall_1=zeros(1,numberofdevices);
286 current_CV_intervall_2=zeros(1,numberofdevices);
287 current_CV_intervall_3=zeros(1,numberofdevices);
288 current_CV=zeros(1,numberofdevices);
289 current_CI_intervall_1=zeros(1,numberofdevices);
290 current_CI_intervall_2=zeros(1,numberofdevices);
291 current_CI_intervall_3=zeros(1,numberofdevices);
292 current_CI=zeros(1,numberofdevices);
293 current_IV_intervall_1=zeros(1,numberofdevices);
294 current_IV_intervall_2=zeros(1,numberofdevices);
295 current_IV_intervall_3=zeros(1,numberofdevices);
296 current_IV=zeros(1,numberofdevices);
297 current_reference=zeros(1,numberofdevices); %generated current in
     reference cell
298
299 alpha_IB=zeros(numberofdevices,antall_endelig); %
     Absorptioncoefficient in intermediate band material
300 alpha_GaAs_enkel=zeros(numberofdevices,antall_endelig);
301
302
303 l_n=zeros(1,numberofdevices); %Definition
304 l_p=zeros(1,numberofdevices); %Definition
305 l_n_plus=zeros(1,numberofdevices); %Definition
306 l_p_plus=zeros(1,numberofdevices); %Definition
307 delta_p=width_p_undepleted; %Widht of undepleted p-layer
308 delta_n=width_n; %Foreløpig tar man ikke hensyn til intrinsikt lag
     . ER TABELL
309
310 for i=1:numberofdevices
311     l_n(i)=((S_eff_p(i).*difflength_n_p(i))./
        diffusioncoefficient_n_p(i));
312     l_n_plus(i)=((S_eff_window(i).*difflength_n_p_plus(i))./
        diffusioncoefficient_n_p_plus(i)); %S_eff_window is front
        surface recombination velocity of the p_plus layer with or
        without window layer
313     l_p(i)=((S_eff_n(i).*difflength_p_n(i))./
        diffusioncoefficient_p_n(i));
314     l_p_plus(i)=((S_n_plus(i).*difflength_p_n_plus(i))./
        diffusioncoefficient_p_n_plus(i)); %S_n-plus is surface
        recombination velocity of the n_plus layer
315
316 end
317
318 J_0_diode_1=zeros(1,numberofdevices);
319 J_0_diode_1_p_layer=zeros(1,numberofdevices);
320 J_0_diode_1_n_layer=zeros(1,numberofdevices);
```

```
321 J_0_diode_2_SCR=zeros(1,numberofdevices);
322
323
324 for a=1:numberofdevices
325     J_0_diode_1_p_layer(a)=e_charge.*(ni_GaAs.^2./(N_A_p(a)./cm
        .^3)).*(diffusioncoefficient_n_p(a)./difflength_n_p(a)).*((
        l_n(a)*cosh(width_p_undepleted(a)./difflength_n_p(a)))+(
        sinh(width_p_undepleted(a)./difflength_n_p(a))))./((l_n(a)
        .*sinh(width_p_undepleted(a)./difflength_n_p(a)))+cosh(
        width_p_undepleted(a)./difflength_n_p(a)));
326     J_0_diode_1_n_layer(a)=e_charge.*(ni_GaAs.^2./(N_D_n(a)./cm
        .^3)).*(diffusioncoefficient_p_n(a)./difflength_p_n(a)).*((
        l_p(a)*cosh(width_n_undepleted(a)./difflength_p_n(a)))+(
        sinh(width_n_undepleted(a)./difflength_p_n(a))))./((l_p(a)
        .*sinh(width_n_undepleted(a)./difflength_p_n(a)))+cosh(
        width_n_undepleted(a)./difflength_p_n(a)));
327     J_0_diode_1(a)=J_0_diode_1_p_layer(a)+J_0_diode_1_n_layer(a)
328     J_0_diode_2_SCR(a)=e_charge.*ni_IB(a).*width_IB(a)./(sqrt(
        tau_n_IB(a).*tau_p_IB(a))).*pi %maximum recombination
        current, using equation (54) in Hovel with GaAs in
        intrinsic region
329 end
330
331
332
333 teller1=0;
334 teller2=0;
335 teller3=0;
336
337
338 %OVERLAPP!!
339 for a=1:numberofdevices
340     for i=1:antall_endelig
341
342         if (zi_endelig(i)*eV)<E_CI(a)
343                 alpha_IB(a,i)=0;
344                 alpha_GaAs_enkel(a,i)=0;
345                 Q_CI(a,i)=0;
346                 Q_IV(a,i)=0;
347                 Q_CV(a,i)=0;
348
349                 Q_n_dep(a,i)=(1-R_GaAs_endelig(a,i)).*exp(-((
                    alpha_GaAs_endelig(i).*width_p_plus(a))+(
                    alpha_AlGaAs_window(a,i).*width_window(a))))
                    .*(1-exp(-alpha_GaAs_endelig(i).*
                    dep_width_p_plus(a)))./cosh(width_p_undepleted(
                    a)./difflength_n_p(a));
350
351                 Q_n_plus(a,i)=(1-R_GaAs_endelig(a,i)).*(
                    alpha_GaAs_endelig(i).*difflength_n_p_plus(a)
                    ./(((alpha_GaAs_endelig(i).*difflength_n_p_plus
                    (a)).^2)-1)).*exp(-(alpha_AlGaAs_window(a,i).*
                    width_window(a))).*((l_n_plus(a)+(
```

```
        alpha_GaAs_endelig(i).*difflength_n_p_plus(a))
        -(exp(-alpha_GaAs_endelig(i).*width_p_plus(a))
        .*((l_n_plus(a)*cosh(width_p_plus(a)./
        difflength_n_p_plus(a)))+(sinh(width_p_plus(a)
        ./difflength_n_p_plus(a)))))./((l_n_plus(a).*
        sinh(width_p_plus(a)./difflength_n_p_plus(a)))+
        cosh(width_p_plus(a)./difflength_n_p_plus(a)))
        -(alpha_GaAs_endelig(i).*difflength_n_p_plus(a)
        .*exp(-(alpha_GaAs_endelig(i).*width_p_plus(a))
        ))).*(1./(1+(N_A_p_plus(a).*S_eff_p(a)./(N_A_p(
        a).*S_eff_plus_p(a))))))./cosh(
        width_p_undepleted(a)./difflength_n_p(a));
352
353     Q_n(a,i)=(1-R_GaAs_endelig(a,i)).*(
        alpha_GaAs_endelig(i).*difflength_n_p(a)./(((
        alpha_GaAs_endelig(i).*difflength_n_p(a)).^2)
        -1)).*exp(-((alpha_AlGaAs_window(a,i).*
        width_window(a))+(alpha_GaAs_endelig(i).*(
        width_p_plus(a)+dep_width_p_plus(a))))).*((l_n(
        a)+(alpha_GaAs_endelig(i).*difflength_n_p(a))-(
        exp(-alpha_GaAs_endelig(i).*width_p_undepleted(
        a)).*((l_n(a)*cosh(width_p_undepleted(a)./
        difflength_n_p(a)))+(sinh(width_p_undepleted(a)
        ./difflength_n_p(a))))))./((l_n(a).*sinh(
        width_p_undepleted(a)./difflength_n_p(a)))+cosh
        (width_p_undepleted(a)./difflength_n_p(a)))-(
        alpha_GaAs_endelig(i).*difflength_n_p(a).*exp
        (-(alpha_GaAs_endelig(i).*width_p_undepleted(a)
        ))));
354
355     %Uses equation (6.62) in Nelson this is for the p
        emiter
356     %Contributions from p-plus layer and depletion
        layer
357     %between p-plus and p-layer are included
358
359     Q_p(a,i)=(1-R_GaAs_endelig(a,i)).*
        alpha_GaAs_endelig(i).*difflength_p_n(a)./((
        alpha_GaAs_endelig(i).*difflength_p_n(a)).^2-1)
        .*exp(-((alpha_GaAs_endelig(i).*(width_p_plus(a
        )+width_p(a)+w_n+width_IB(a)))+(
        alpha_AlGaAs_window(a,i).*width_window(a))))
        .*((alpha_GaAs_endelig(i).*difflength_p_n(a))
        -(((l_p(a).*(cosh(width_n_undepleted(a)./
        difflength_p_n(a))-exp(-alpha_GaAs_endelig(i).*
        width_n_undepleted(a))))+sinh(
        width_n_undepleted(a)./difflength_p_n(a))+(
        alpha_GaAs_endelig(i).*difflength_p_n(a).*exp(-
        alpha_GaAs_endelig(i).*width_n_undepleted(a))))
        ./((l_p(a).*sinh(width_n_undepleted(a)./
        difflength_p_n(a)))+cosh(width_n_undepleted(a)
        ./difflength_p_n(a))));
360
```

```
361                 Q_p_dep(a,i)=(1-R_GaAs_endelig(a,i)).*exp(-((
                        alpha_GaAs_endelig(i).*(width_p_plus(a)+width_p
                        (a)+width_IB(a)+width_n_undepleted(a)))+(
                        alpha_AlGaAs_window(a,i).*width_window(a))))
                        .*(1-exp(-alpha_GaAs_endelig(i).*
                        dep_width_n_plus(a)))./cosh(width_n_undepleted(
                        a)./difflength_p_n(a));
362
363                 Q_p_plus(a,i)=(1-R_GaAs_endelig(a,i)).*
                        alpha_GaAs_endelig(i).*difflength_p_n_plus(a)
                        ./((alpha_GaAs_endelig(i).*difflength_p_n_plus(
                        a)).^2-1).*exp(-((alpha_GaAs_endelig(i).*(
                        width_p_plus(a)+width_p(a)+width_IB(a)+width_n(
                        a)))+(alpha_AlGaAs_window(a,i).*width_window(a)
                        ))).*((alpha_GaAs_endelig(i).*
                        difflength_p_n_plus(a))-(((l_p_plus(a).*(cosh(
                        width_n_plus(a)./difflength_p_n_plus(a))-exp(-
                        alpha_GaAs_endelig(i).*width_n_plus(a))))+sinh(
                        width_n_plus(a)./difflength_p_n_plus(a))+(
                        alpha_GaAs_endelig(i).*difflength_p_n_plus(a).*
                        exp(-alpha_GaAs_endelig(i).*width_n_plus(a))))
                        ./((l_p_plus(a).*sinh(width_n_plus(a)./
                        difflength_p_n_plus(a))+cosh(width_n_plus(a)./
                        difflength_p_n_plus(a))))).*(1./(1+(N_D_n_plus(
                        a).*S_eff_n(a)./(N_D_n(a).*S_eff_n_plus_n(a))))
                        )./cosh(width_n_undepleted(a)./difflength_p_n(a
                        ));
364
365                 %Uses equation (6.63) in Nelson this is for the n
                        base
366                 %Contributions from n-plus layer and depletion
                        layer
367                 %between n-plus and n-layer are included
368
369                 Q_intrinsic_reference(a,i)=(1-R_GaAs_endelig(a,i))
                        .*exp(-((alpha_GaAs_endelig(i).*(width_p_plus(a
                        )+width_p(a)))+(alpha_AlGaAs_window(a).*
                        width_window(a)))).*(1-exp(-alpha_GaAs_endelig(
                        i).*(width_IB(a)+w_n+w_p)));
370                 %Quantum efficiency in intrinsic layer if no
                        quantum dots
371                 %are placed
372
373         elseif (zi_endelig(i)*eV)>=E_CI(a)&&(zi_endelig(i)*eV)<
                E_IV(a)
374                 alpha_IB(a,i)=alpha_CI(a);
375                 alpha_GaAs_enkel(a,i)=0;
376                 %Q_CI(a,i)=(1-R_GaAs_endelig(i)).*exp(-
                        alpha_GaAs_enkel(a,i)*width_p(a)).*(1-exp(-(
                        alpha_GaAs_enkel(a,i).*w_p)-(alpha_GaAs_enkel(a
                        ,i).*w_n)-(alpha_IB(a,i).*W_IB(a)))).*alpha_CI
                        ./alpha_IB(a,i);
```

```
377             Q_CI(a,i)=exp(-((alpha_GaAs_enkel(a,i)*(width_p(a)
                    +width_p_plus(a)))+(alpha_AlGaAs_window(a,i).*
                    width_window(a)))).*(1-exp(-(alpha_GaAs_enkel(a
                    ,i).*w_p)-(alpha_GaAs_enkel(a,i).*w_n)-(
                    alpha_IB(a,i).*width_IB(a)))).*alpha_CI(a)./
                    alpha_IB(a,i);
378             %Tar ikke hensyn til refleksjon fra overflaten
379             Q_IV(a,i)=0;
380             Q_CV(a,i)=0;
381
382             Q_n_dep(a,i)=(1-R_GaAs_endelig(a,i)).*exp(-((
                    alpha_GaAs_endelig(i).*width_p_plus(a))+(
                    alpha_AlGaAs_window(a,i).*width_window(a))))
                    .*(1-exp(-alpha_GaAs_endelig(i).*
                    dep_width_p_plus(a)))./cosh(width_p_undepleted(
                    a)./difflength_n_p(a));
383
384             Q_n_plus(a,i)=(1-R_GaAs_endelig(a,i)).*(
                    alpha_GaAs_endelig(i).*difflength_n_p_plus(a)
                    ./(((alpha_GaAs_endelig(i).*difflength_n_p_plus
                    (a)).^2)-1)).*exp(-(alpha_AlGaAs_window(a,i).*
                    width_window(a))).*((l_n_plus(a)+(
                    alpha_GaAs_endelig(i).*difflength_n_p_plus(a))
                    -(exp(-alpha_GaAs_endelig(i).*width_p_plus(a))
                    .*((l_n_plus(a)*cosh(width_p_plus(a)./
                    difflength_n_p_plus(a)))+(sinh(width_p_plus(a)
                    ./difflength_n_p_plus(a))))))./((l_n_plus(a).*
                    sinh(width_p_plus(a)./difflength_n_p_plus(a)))+
                    cosh(width_p_plus(a)./difflength_n_p_plus(a)))
                    -(alpha_GaAs_endelig(i).*difflength_n_p_plus(a)
                    .*exp(-(alpha_GaAs_endelig(i).*width_p_plus(a))
                    ))).*(1./(1+(N_A_p_plus(a).* S_eff_p(a)./(N_A_p
                    (a).*S_eff_p_plus_p(a))))))./cosh(
                    width_p_undepleted(a)./difflength_n_p(a));
385
386             Q_n(a,i)=(1-R_GaAs_endelig(a,i)).*(
                    alpha_GaAs_endelig(i).*difflength_n_p(a)./(((
                    alpha_GaAs_endelig(i).*difflength_n_p(a)).^2)
                    -1)).*exp(-((alpha_AlGaAs_window(a,i).*
                    width_window(a))+(alpha_GaAs_endelig(i).*(
                    width_p_plus(a)+dep_width_p_plus(a))))).*((l_n(
                    a)+(alpha_GaAs_endelig(i).*difflength_n_p(a))-(
                    exp(-alpha_GaAs_endelig(i).*width_p_undepleted(
                    a)).*((l_n(a)*cosh(width_p_undepleted(a)./
                    difflength_n_p(a)))+(sinh(width_p_undepleted(a)
                    ./difflength_n_p(a))))))./((l_n(a).*sinh(
                    width_p_undepleted(a)./difflength_n_p(a))+cosh
                    (width_p_undepleted(a)./difflength_n_p(a)))-(
                    alpha_GaAs_endelig(i).*difflength_n_p(a).*exp
                    (-(alpha_GaAs_endelig(i).*width_p_undepleted(a)
                    ))));
387
```

```
388                 %Uses equation (6.62) in Nelson this is for the p
                        emiter
389                 %Contributions from p-plus layer and depletion
                        layer
390                 %between p-plus and p-layer are included
391
392                 Q_p(a,i)=(1-R_GaAs_endelig(a,i)).*
                        alpha_GaAs_endelig(i).*difflength_p_n(a)./((
                        alpha_GaAs_endelig(i).*difflength_p_n(a)).^2-1)
                        .*exp(-((alpha_GaAs_endelig(i).*(width_p_plus(a
                        )+width_p(a)+w_n+width_IB(a)))+(
                        alpha_AlGaAs_window(a,i).*width_window(a))))
                        .*((alpha_GaAs_endelig(i).*difflength_p_n(a))
                        -(((l_p(a).*(cosh(width_n_undepleted(a)./
                        difflength_p_n(a))-exp(-alpha_GaAs_endelig(i).*
                        width_n_undepleted(a))))+sinh(
                        width_n_undepleted(a)./difflength_p_n(a))+(
                        alpha_GaAs_endelig(i).*difflength_p_n(a).*exp(-
                        alpha_GaAs_endelig(i).*width_n_undepleted(a))))
                        ./((l_p(a).*sinh(width_n_undepleted(a)./
                        difflength_p_n(a))+cosh(width_n_undepleted(a)
                        ./difflength_p_n(a)))));
393
394                 Q_p_dep(a,i)=(1-R_GaAs_endelig(a,i)).*exp(-((
                        alpha_GaAs_endelig(i).*(width_p_plus(a)+width_p
                        (a)+w_n+width_IB(a)+width_n_undepleted(a)))+(
                        alpha_AlGaAs_window(a,i).*width_window(a))))
                        .*(1-exp(-alpha_GaAs_endelig(i).*
                        dep_width_n_plus(a)))./cosh(width_n_undepleted(
                        a)./difflength_p_n(a));
395
396                 Q_p_plus(a,i)=(1-R_GaAs_endelig(a,i)).*
                        alpha_GaAs_endelig(i).*difflength_p_n_plus(a)
                        ./((alpha_GaAs_endelig(i).*difflength_p_n_plus(
                        a)).^2-1).*exp(-((alpha_GaAs_endelig(i).*(
                        width_p_plus(a)+width_p(a)+w_n+width_IB(a)+
                        width_n(a)))+(alpha_AlGaAs_window(a,i).*
                        width_window(a)))).*((alpha_GaAs_endelig(i).*
                        difflength_p_n_plus(a))-(((l_p_plus(a).*(cosh(
                        width_n_plus(a)./difflength_p_n_plus(a))-exp(-
                        alpha_GaAs_endelig(i).*width_n_plus(a))))+sinh(
                        width_n_plus(a)./difflength_p_n_plus(a))+(
                        alpha_GaAs_endelig(i).*difflength_p_n_plus(a).*
                        exp(-alpha_GaAs_endelig(i).*width_n_plus(a))))
                        ./((l_p_plus(a).*sinh(width_n_plus(a)./
                        difflength_p_n_plus(a))+cosh(width_n_plus(a)./
                        difflength_p_n_plus(a))))).*(1./(1+(N_D_n_plus(
                        a).*S_eff_n(a)./(N_D_n(a).*S_eff_n_plus_n(a))))
                        )./cosh(width_n_undepleted(a)./difflength_p_n(a
                        ));
397
398                 %Uses equation (6.63) in Nelson this is for the n
                        base
```

```
399                 %Contributions from n-plus layer and depletion
                        layer
400                 %between n-plus and n-layer are included
401
402                 Q_intrinsic_reference(a,i)=(1-R_GaAs_endelig(a,i))
                        .*exp(-((alpha_GaAs_endelig(i).*(width_p_plus(a
                        )+width_p(a)))+(alpha_AlGaAs_window(a).*
                        width_window(a)))).*(1-exp(-alpha_GaAs_endelig(
                        i).*(width_IB(a)+w_n+w_p)));
403                 %Quantum efficiency in intrinsic layer if no
                        quantum dots
404                 %are placed
405
406                 current_CI_intervall_1(a)=(current_CI_intervall_1(
                        a))+(current_fit.*Q_CI(a,i));
407                 current_IV_intervall_1(a)=(current_IV_intervall_1(
                        a))+(current_fit.*Q_IV(a,i));
408                 current_CV_intervall_1(a)=(current_CV_intervall_1(
                        a))+(current_fit.*(Q_CV(a,i)+Q_n(a,i)+Q_p(a,i))
                        );
409                 teller1=teller1+1;
410
411         elseif (zi_endelig(i)*eV)>=E_IV(a)&&(zi_endelig(i)*eV)<
                E_CV(a)
412                 alpha_IB(a,i)=alpha_IV(a)+alpha_CI(a);
413                 alpha_GaAs_enkel(a,i)=0;
414                 %Q_CI(a,i)=(1-R_GaAs_endelig(i)).*exp(-
                        alpha_GaAs_enkel(a,i)*width_p(a)).*(1-exp(-(
                        alpha_GaAs_enkel(a,i).*w_p)-(alpha_GaAs_enkel(a
                        ,i).*w_n)-(alpha_IB(a,i).*W_IB(a)))).*alpha_CI
                        ./alpha_IB(a,i);
415                 Q_CI(a,i)=exp(-((alpha_GaAs_enkel(a,i)*(width_p(a)
                        +width_p_plus(a)))+(alpha_AlGaAs_window(a,i).*
                        width_window(a)))).*(1-exp(-(alpha_GaAs_enkel(a
                        ,i).*w_p)-(alpha_GaAs_enkel(a,i).*w_n)-(
                        alpha_IB(a,i).*width_IB(a)))).*alpha_CI(a)./
                        alpha_IB(a,i);
416                 %Tar ikke hensyn til refleksjon fra overfalten
417                 %Q_IV(a,i)=(1-R_GaAs_endelig(i)).*exp(-
                        alpha_GaAs_enkel(a,i)*width_p(a)).*(1-exp(-(
                        alpha_GaAs_enkel(a,i).*w_p)-(alpha_GaAs_enkel(a
                        ,i).*w_n)-(alpha_IB(a,i).*W_IB(a)))).*alpha_IV
                        ./alpha_IB(a,i);
418                 Q_IV(a,i)=exp(-((alpha_GaAs_enkel(a,i)*(width_p(a)
                        +width_p_plus(a)))+(alpha_AlGaAs_window(a,i).*
                        width_window(a)))).*(1-exp(-(alpha_GaAs_enkel(a
                        ,i).*w_p)-(alpha_GaAs_enkel(a,i).*w_n)-(
                        alpha_IB(a,i).*width_IB(a)))).*alpha_IV(a)./
                        alpha_IB(a,i);
419                 %Tar ikke hensyn til refleksjon fra overflaten
420                 Q_CV(a,i)=0;
421
```

```
422                 Q_n_dep(a,i)=(1-R_GaAs_endelig(a,i)).*exp(-((
                        alpha_GaAs_endelig(i).*width_p_plus(a))+(
                        alpha_AlGaAs_window(a,i).*width_window(a))))
                        .*(1-exp(-alpha_GaAs_endelig(i).*
                        dep_width_p_plus(a)))./cosh(width_p_undepleted(
                        a)./difflength_n_p(a));
423
424                 Q_n_plus(a,i)=(1-R_GaAs_endelig(a,i)).*(
                        alpha_GaAs_endelig(i).*difflength_n_p_plus(a)
                        ./(((alpha_GaAs_endelig(i).*difflength_n_p_plus
                        (a)).^2)-1)).*exp(-(alpha_AlGaAs_window(a,i).*
                        width_window(a))).*((l_n_plus(a)+(
                        alpha_GaAs_endelig(i).*difflength_n_p_plus(a))
                        -(exp(-alpha_GaAs_endelig(i).*width_p_plus(a))
                        .*((l_n_plus(a)*cosh(width_p_plus(a)./
                        difflength_n_p_plus(a)))+(sinh(width_p_plus(a)
                        ./difflength_n_p_plus(a))))))./((l_n_plus(a).*
                        sinh(width_p_plus(a)./difflength_n_p_plus(a)))+
                        cosh(width_p_plus(a)./difflength_n_p_plus(a)))
                        -(alpha_GaAs_endelig(i).*difflength_n_p_plus(a)
                        .*exp(-(alpha_GaAs_endelig(i).*width_p_plus(a))
                        ))).*(1./(1+(N_A_p_plus(a).* S_eff_p(a)./(N_A_p
                        (a).*S_eff_p_plus_p(a))))))./cosh(
                        width_p_undepleted(a)./difflength_n_p(a));
425
426                 Q_n(a,i)=(1-R_GaAs_endelig(a,i)).*(
                        alpha_GaAs_endelig(i).*difflength_n_p(a)./(((
                        alpha_GaAs_endelig(i).*difflength_n_p(a)).^2)
                        -1)).*exp(-((alpha_AlGaAs_window(a,i).*
                        width_window(a))+(alpha_GaAs_endelig(i).*(
                        width_p_plus(a)+dep_width_p_plus(a))))).*((l_n(
                        a)+(alpha_GaAs_endelig(i).*difflength_n_p(a))-(
                        exp(-alpha_GaAs_endelig(i).*width_p_undepleted(
                        a)).*((l_n(a)*cosh(width_p_undepleted(a)./
                        difflength_n_p(a)))+(sinh(width_p_undepleted(a)
                        ./difflength_n_p(a))))))./((l_n(a).*sinh(
                        width_p_undepleted(a)./difflength_n_p(a)))+cosh
                        (width_p_undepleted(a)./difflength_n_p(a)))-(
                        alpha_GaAs_endelig(i).*difflength_n_p(a).*exp
                        (-(alpha_GaAs_endelig(i).*width_p_undepleted(a)
                        ))));
427
428                 %Uses equation (6.62) in Nelson this is for the p
                        emiter
429                 %Contributions from p-plus layer and depletion
                        layer
430                 %between p-plus and p-layer are included
431                 Q_p(a,i)=(1-R_GaAs_endelig(a,i)).*
                        alpha_GaAs_endelig(i).*difflength_p_n(a)./((
                        alpha_GaAs_endelig(i).*difflength_p_n(a)).^2-1)
                        .*exp(-((alpha_GaAs_endelig(i).*(width_p_plus(a
                        )+width_p(a)+w_n+width_IB(a)))+(
                        alpha_AlGaAs_window(a,i).*width_window(a))))
```

```
        .*((alpha_GaAs_endelig(i).*difflength_p_n(a))
        -(((l_p(a).*(cosh(width_n_undepleted(a)./
        difflength_p_n(a))-exp(-alpha_GaAs_endelig(i).*
        width_n_undepleted(a))))+sinh(
        width_n_undepleted(a)./difflength_p_n(a))+(
        alpha_GaAs_endelig(i).*difflength_p_n(a).*exp(-
        alpha_GaAs_endelig(i).*width_n_undepleted(a))))
        ./((l_p(a).*sinh(width_n_undepleted(a)./
        difflength_p_n(a))+cosh(width_n_undepleted(a)
        ./difflength_p_n(a)))));
432
433     Q_p_dep(a,i)=(1-R_GaAs_endelig(a,i)).*exp(-((
        alpha_GaAs_endelig(i).*(width_p_plus(a)+width_p
        (a)+w_n+width_IB(a)+width_n_undepleted(a)))+(
        alpha_AlGaAs_window(a,i).*width_window(a))))
        .*(1-exp(-alpha_GaAs_endelig(i).*
        dep_width_n_plus(a)))./cosh(width_n_undepleted(
        a)./difflength_p_n(a));
434
435     Q_p_plus(a,i)=(1-R_GaAs_endelig(a,i)).*
        alpha_GaAs_endelig(i).*difflength_p_n_plus(a)
        ./((alpha_GaAs_endelig(i).*difflength_p_n_plus(
        a)).^2-1).*exp(-((alpha_GaAs_endelig(i).*(
        width_p_plus(a)+width_p(a)+w_n+width_IB(a)+
        width_n(a)))+(alpha_AlGaAs_window(a,i).*
        width_window(a)))).*((alpha_GaAs_endelig(i).*
        difflength_p_n_plus(a))-(((l_p_plus(a).*(cosh(
        width_n_plus(a)./difflength_p_n_plus(a))-exp(-
        alpha_GaAs_endelig(i).*width_n_plus(a))))+sinh(
        width_n_plus(a)./difflength_p_n_plus(a))+(
        alpha_GaAs_endelig(i).*difflength_p_n_plus(a).*
        exp(-alpha_GaAs_endelig(i).*width_n_plus(a))))
        ./((l_p_plus(a).*sinh(width_n_plus(a)./
        difflength_p_n_plus(a))+cosh(width_n_plus(a)./
        difflength_p_n_plus(a))))).*(1./(1+(N_D_n_plus(
        a).*S_eff_n(a)./(N_D_n(a).*S_eff_n_plus_n(a))))
        )./cosh(width_n_undepleted(a)./difflength_p_n(a
        ));
436
437     %Uses equation (6.63) in Nelson this is for the n
        base
438     %Contributions from n-plus layer and depletion
        layer
439     %between n-plus and n-layer are included
440
441     Q_intrinsic_reference(a,i)=(1-R_GaAs_endelig(a,i))
        .*exp(-((alpha_GaAs_endelig(i).*(width_p_plus(a
        )+width_p(a)))+(alpha_AlGaAs_window(a).*
        width_window(a)))).*(1-exp(-alpha_GaAs_endelig(
        i).*(width_IB(a)+w_n+w_p)));
442     %Quantum efficiency in intrinsic layer if no
        quantum dots
443     %are placed
```

```
444
445                 current_CI_intervall_2(a)=(current_CI_intervall_2(
                       a))+(current_fit.*Q_CI(a,i));
446                 current_IV_intervall_2(a)=(current_IV_intervall_2(
                       a))+(current_fit.*Q_IV(a,i));
447                 current_CV_intervall_2(a)=(current_CV_intervall_2(
                       a))+(current_fit.*(Q_CV(a,i)+Q_n(a,i)+Q_p(a,i))
                       );
448                 teller2=teller2+1;
449         else
450                 alpha_IB(a,i)=alpha_CV(a)+alpha_IV(a)+alpha_CI(a);
451                 alpha_GaAs_enkel(a,i)=alpha_CV(a);
452                 %Q_CI(a,i)=(1-R_GaAs_endelig(i)).*exp(-
                       alpha_GaAs_enkel(a,i)*width_p(a)).*(1-exp(-(
                       alpha_GaAs_enkel(a,i).*w_p)-(alpha_GaAs_enkel(a
                       ,i).*w_n)-(alpha_IB(a,i).*W_IB(a)))).*alpha_CI
                       ./alpha_IB(a,i);
453                 Q_CI(a,i)=exp(-((alpha_GaAs_enkel(a,i)*(width_p(a)
                       +width_p_plus(a)))+(alpha_AlGaAs_window(a,i).*
                       width_window(a)))).*(1-exp(-(alpha_GaAs_enkel(a
                       ,i).*w_p)-(alpha_GaAs_enkel(a,i).*w_n)-(
                       alpha_IB(a,i).*width_IB(a)))).*alpha_CI(a)./
                       alpha_IB(a,i);
454                 %Tar ikke hensyn til refleksjon fra overflaten
455                 %Q_IV(a,i)=(1-R_GaAs_endelig(i)).*exp(-
                       alpha_GaAs_enkel(a,i)*width_p(a)).*(1-exp(-(
                       alpha_GaAs_enkel(a,i).*w_p)-(alpha_GaAs_enkel(a
                       ,i).*w_n)-(alpha_IB(a,i).*W_IB(a)))).*alpha_IV
                       ./alpha_IB(a,i);
456                 Q_IV(a,i)=exp(-((alpha_GaAs_enkel(a,i)*(width_p(a)
                       +width_p_plus(a)))+(alpha_AlGaAs_window(a,i).*
                       width_window(a)))).*(1-exp(-(alpha_GaAs_enkel(a
                       ,i).*w_p)-(alpha_GaAs_enkel(a,i).*w_n)-(
                       alpha_IB(a,i).*width_IB(a)))).*alpha_IV(a)./
                       alpha_IB(a,i);
457                 %Tar ikke hensyn til refleksjon fra overflaten
458                 %Q_CV(a,i)=(1-R_GaAs_endelig(i)).*exp(-
                       alpha_GaAs_enkel(a,i)*width_p(a)).*(1-exp(-(
                       alpha_GaAs_enkel(a,i).*w_p)-(alpha_GaAs_enkel(a
                       ,i).*w_n)-(alpha_IB(a,i).*W_IB(a)))).*alpha_CV
                       ./alpha_IB(a,i);
459                 Q_CV(a,i)=exp(-((alpha_GaAs_enkel(a,i)*(width_p(a)
                       +width_p_plus(a)))+(alpha_AlGaAs_window(a,i).*
                       width_window(a)))).*(1-exp(-(alpha_GaAs_enkel(a
                       ,i).*w_p)-(alpha_GaAs_enkel(a,i).*w_n)-(
                       alpha_IB(a,i).*width_IB(a)))).*alpha_CV(a)./
                       alpha_IB(a,i);
460                 %Tar ikke hensyn til refleksjon fra overflaten
461
462                 Q_n_dep(a,i)=(1-R_GaAs_endelig(a,i)).*exp(-((
                       alpha_GaAs_endelig(i).*width_p_plus(a))+(
                       alpha_AlGaAs_window(a,i).*width_window(a))))
                       .*(1-exp(-alpha_GaAs_endelig(i).*
```

```
            dep_width_p_plus(a)))./cosh(width_p_undepleted(
            a)./difflength_n_p(a));
463
464         Q_n_plus(a,i)=(1-R_GaAs_endelig(a,i)).*(
            alpha_GaAs_endelig(i).*difflength_n_p_plus(a)
            ./(((alpha_GaAs_endelig(i).*difflength_n_p_plus
            (a)).^2)-1)).*exp(-(alpha_AlGaAs_window(a,i).*
            width_window(a))).*((l_n_plus(a)+(
            alpha_GaAs_endelig(i).*difflength_n_p_plus(a))
            -(exp(-alpha_GaAs_endelig(i).*width_p_plus(a))
            .*((l_n_plus(a)*cosh(width_p_plus(a)./
            difflength_n_p_plus(a)))+(sinh(width_p_plus(a)
            ./difflength_n_p_plus(a))))))./((l_n_plus(a).*
            sinh(width_p_plus(a)./difflength_n_p_plus(a)))+
            cosh(width_p_plus(a)./difflength_n_p_plus(a)))
            -(alpha_GaAs_endelig(i).*difflength_n_p_plus(a)
            .*exp(-(alpha_GaAs_endelig(i).*width_p_plus(a))
            ))).*(1./(1+(N_A_p_plus(a).* S_eff_p(a)./(N_A_p
            (a).*S_eff_p_plus_p(a)))))./cosh(
            width_p_undepleted(a)./difflength_n_p(a));
465
466         Q_n(a,i)=(1-R_GaAs_endelig(a,i)).*(
            alpha_GaAs_endelig(i).*difflength_n_p(a)./(((
            alpha_GaAs_endelig(i).*difflength_n_p(a)).^2)
            -1)).*exp(-((alpha_AlGaAs_window(a,i).*
            width_window(a))+(alpha_GaAs_endelig(i).*(
            width_p_plus(a)+dep_width_p_plus(a))))).*((l_n(
            a)+(alpha_GaAs_endelig(i).*difflength_n_p(a))-(
            exp(-alpha_GaAs_endelig(i).*width_p_undepleted(
            a)).*((l_n(a)*cosh(width_p_undepleted(a)./
            difflength_n_p(a)))+(sinh(width_p_undepleted(a)
            ./difflength_n_p(a))))))./((l_n(a).*sinh(
            width_p_undepleted(a)./difflength_n_p(a)))+cosh
            (width_p_undepleted(a)./difflength_n_p(a)))-(
            alpha_GaAs_endelig(i).*difflength_n_p(a).*exp
            (-(alpha_GaAs_endelig(i).*width_p_undepleted(a)
            ))));
467
468         %Uses equation (6.62) in Nelson this is for the p
            emiter
469         %Contributions from p-plus layer and depletion
            layer
470         %between p-plus and p-layer are included
471
472         Q_p(a,i)=(1-R_GaAs_endelig(a,i)).*
            alpha_GaAs_endelig(i).*difflength_p_n(a)./((
            alpha_GaAs_endelig(i).*difflength_p_n(a)).^2-1)
            .*exp(-((alpha_GaAs_endelig(i).*(width_p_plus(a
            )+width_p(a)+w_n+width_IB(a)))+(
            alpha_AlGaAs_window(a,i).*width_window(a))))
            .*((alpha_GaAs_endelig(i).*difflength_p_n(a))
            -(((l_p(a).*(cosh(width_n_undepleted(a)./
            difflength_p_n(a))-exp(-alpha_GaAs_endelig(i).*
```

```
        width_n_undepleted(a))))+sinh(
        width_n_undepleted(a)./difflength_p_n(a))+(
        alpha_GaAs_endelig(i).*difflength_p_n(a).*exp(-
        alpha_GaAs_endelig(i).*width_n_undepleted(a))))
        ./((l_p(a).*sinh(width_n_undepleted(a)./
        difflength_p_n(a))+cosh(width_n_undepleted(a)
        ./difflength_p_n(a)))));
473
474     Q_p_dep(a,i)=(1-R_GaAs_endelig(a,i)).*exp(-((
        alpha_GaAs_endelig(i).*(width_p_plus(a)+width_p
        (a)+w_n+width_IB(a)+width_n_undepleted(a)))+(
        alpha_AlGaAs_window(a,i).*width_window(a))))
        .*(1-exp(-alpha_GaAs_endelig(i).*
        dep_width_n_plus(a)))./cosh(width_n_undepleted(
        a)./difflength_p_n(a));
475
476     Q_p_plus(a,i)=(1-R_GaAs_endelig(a,i)).*
        alpha_GaAs_endelig(i).*difflength_p_n_plus(a)
        ./((alpha_GaAs_endelig(i).*difflength_p_n_plus(
        a)).^2-1).*exp(-((alpha_GaAs_endelig(i).*(
        width_p_plus(a)+width_p(a)+w_n+width_IB(a)+
        width_n(a)))+(alpha_AlGaAs_window(a,i).*
        width_window(a)))).*((alpha_GaAs_endelig(i).*
        difflength_p_n_plus(a))-(((l_p_plus(a).*(cosh(
        width_n_plus(a)./difflength_p_n_plus(a))-exp(-
        alpha_GaAs_endelig(i).*width_n_plus(a))))+sinh(
        width_n_plus(a)./difflength_p_n_plus(a))+(
        alpha_GaAs_endelig(i).*difflength_p_n_plus(a).*
        exp(-alpha_GaAs_endelig(i).*width_n_plus(a))))
        ./((l_p_plus(a).*sinh(width_n_plus(a)./
        difflength_p_n_plus(a))+cosh(width_n_plus(a)./
        difflength_p_n_plus(a))))).*(1./(1+(N_D_n_plus(
        a).*S_eff_n(a)./(N_D_n(a).*S_eff_n_plus_n(a))))
        )./cosh(width_n_undepleted(a)./difflength_p_n(a
        ));
477
478     %Uses equation (6.63) in Nelson this is for the n
        base
479     %Contributions from n-plus layer and depletion
        layer
480     %between n-plus and n-layer are included
481
482     Q_intrinsic_reference(a,i)=(1-R_GaAs_endelig(a,i))
        .*exp(-((alpha_GaAs_endelig(i).*(width_p_plus(a
        )+width_p(a)))+(alpha_AlGaAs_window(a).*
        width_window(a)))).*(1-exp(-alpha_GaAs_endelig(
        i).*(width_IB(a)+w_n+w_p)));
483     %Quantum efficiency in intrinsic layer if no
        quantum dots
484     %are placed
485
486     current_CI_intervall_3(a)=(current_CI_intervall_3(
        a))+(current_fit.*Q_CI(a,i));
```

```
487                    current_IV_intervall_3(a)=(current_IV_intervall_3(
                          a))+(current_fit.*Q_IV(a,i));
488                    current_CV_intervall_3(a)=(current_CV_intervall_3(
                          a))+(current_fit.*(Q_CV(a,i)+Q_n(a,i)+Q_p(a,i))
                          );
489                    teller3=teller3+1;
490            end
491
492        end
493
494 end
495
496 % for a=1:numberofdevices
497 % current_CI(a)=(current_CI_intervall_1(a)./teller1)+(
      current_CI_intervall_2(a)./teller2)+(current_CI_intervall_3(a)
      ./teller3);
498 %
499 % current_IV(a)=(current_IV_intervall_1(a)./teller1)+(
      current_IV_intervall_2(a)./teller2)+(current_IV_intervall_3(a)
      ./teller3);
500 %
501 % current_CV(a)=(current_CV_intervall_1(a)./teller1)+(
      current_CV_intervall_2(a)./teller2)+(current_CV_intervall_3(a)
      ./teller3);
502 %
503 % end
504
505
506
507   wavelength=1e+9.*(h_planck*c_light)./(zi_endelig.*eV); %
         Wavelength in nm
508
509 %Reading the necessary excel files
510
511 num = xlsread('C:\Documents␣and␣Settings\Kirsti␣Kvanes\Mine␣
      dokumenter\MATLAB\Prosjekt\Sp'); %Solar spectrum. Column 1 is
      wavelengths, column 2 is AM 1.5 given in W/(nm*m2), column 3 is
       incoming radiation in an energy intervall
512 %Column 4 is photonenergies, column 5 is photonflux in an
      energyinterval
513 wavelengthAM=num(:,1); %Wavelengths from excel
514 flux=num(:,5); %Incoming energy flux from excel
515
516 startexcel=1;
517
518 for a=1:numberofdevices
519 for i=antall_endelig:-1:1
520     if wavelengthAM(startexcel)<400
521         if abs((wavelengthAM(startexcel)-wavelength(i)))<0.25
522
523         else
524             current_CI(a)=(current_CI(a))+flux(startexcel).*
                   e_charge.*Q_CI(a,i); %Light generated CI current for
```

```
             energies betwwen the energy difference between C-
            band and I-band and the energy differnece between
            the I-band and the V-band
525         current_IV(a)=(current_IV(a))+flux(startexcel).*
            e_charge.*Q_IV(a,i); %Light generated IV current for
             energies between the energy difference between I-
            band and V-band and the energy difference between
            the C-band and V-band
526         current_CV(a)=(current_CV(a))+flux(startexcel).*
            e_charge.*(Q_CV(a,i)+Q_n(a,i)+Q_p(a,i)+Q_n_dep(a,i)+
            Q_n_plus(a,i)); %Light generated CV current for
            energies higher than the energy difference between
            the C-band and the V-band
527         current_reference(a)=(current_reference(a))+flux(
            startexcel).*e_charge.*(Q_intrinsic_reference(a,i)+
            Q_n(a,i)+Q_p(a,i)+Q_p_plus(a,i)+Q_p_dep(a,i)+Q_n_dep
            (a,i)+Q_n_plus(a,i)); %Light generated current in
            reference cell
528         startexcel=startexcel+1;
529       end
530
531   elseif wavelengthAM(startexcel)>=400&&wavelengthAM(startexcel)
         <1700
532       if abs((wavelengthAM(startexcel)-wavelength(i)))<0.5
533
534       else
535         current_CI(a)=(current_CI(a))+flux(startexcel).*
            e_charge.*Q_CI(a,i); %Light generated CI current for
             energies betwwen the energy difference between C-
            band and I-band and the energy differnece between
            the I-band and the V-band
536         current_IV(a)=(current_IV(a))+flux(startexcel).*
            e_charge.*Q_IV(a,i); %Light generated IV current for
             energies between the energy difference between I-
            band and V-band and the energy difference between
            the C-band and V-band
537         current_CV(a)=(current_CV(a))+flux(startexcel).*
            e_charge.*(Q_CV(a,i)+Q_n(a,i)+Q_p(a,i)+Q_n_dep(a,i)+
            Q_n_plus(a,i)); %Light generated CV current for
            energies higher than the energy difference between
            the C-band and the V-band
538         current_reference(a)=(current_reference(a))+flux(
            startexcel).*e_charge.*(Q_intrinsic_reference(a,i)+
            Q_n(a,i)+Q_p(a,i)+Q_p_plus(a,i)+Q_p_dep(a,i)+Q_n_dep
            (a,i)+Q_n_plus(a,i)); %Light generated current in
            reference cell
539         startexcel=startexcel+1;
540       end
541
542   elseif wavelengthAM(startexcel)>=1700
543       if abs((wavelengthAM(startexcel)-wavelength(i)))<2.5
544
545       else
```

```
546             current_CI(a)=(current_CI(a))+flux(startexcel).*
                    e_charge.*Q_CI(a,i); %Light generated CI current for
                     energies betwwen the energy difference between C-
                    band and I-band and the energy differnece between
                    the I-band and the V-band
547             current_IV(a)=(current_IV(a))+flux(startexcel).*
                    e_charge.*Q_IV(a,i); %Light generated IV current for
                     energies between the energy difference between I-
                    band and V-band and the energy difference between
                    the C-band and V-band
548             current_CV(a)=(current_CV(a))+flux(startexcel).*
                    e_charge.*(Q_CV(a,i)+Q_n(a,i)+Q_p(a,i)+Q_n_dep(a,i)+
                    Q_n_plus(a,i)); %Light generated CV current for
                    energies higher than the energy difference between
                    the C-band and the V-band
549             current_reference(a)=(current_reference(a))+flux(
                    startexcel).*e_charge.*(Q_intrinsic_reference(a,i)+
                    Q_n(a,i)+Q_p(a,i)+Q_p_plus(a,i)+Q_p_dep(a,i)+Q_n_dep
                    (a,i)+Q_n_plus(a,i)); %Light generated current in
                    reference cell
550             startexcel=startexcel+1;
551         end
552     end
553
554  end
555
556 startexcel=1;
557 end
558
559 figure(20)
560 plot(wavelength,(Q_n(1,:)+Q_n_plus(1,:)+Q_n_dep(1,:)+
        Q_intrinsic_reference(1,:)+Q_p(1,:)+Q_p_plus(1,:)+Q_p_dep(1,:))
        ,'k-','LineWidth',1.3)
561 axis([400 1000 0 1])
562 hold on
563 plot(wavelength,Q_n(1,:),'b:','LineWidth',1.3)
564 plot(wavelength,Q_intrinsic_reference(1,:),'r-.','LineWidth',1.3)
565 plot(wavelength,Q_p(1,:),'g--','LineWidth',1.3)
566 legend('total', 'p-layer', 'i-layer', 'n-layer')
567 legend BOXOFF
568 xlabel('Wavelength␣(nm)')
569 ylabel('Quantum␣efficiency')
570 hold off
571 exportfig(20, 'QE-p-i-n.eps', 'Color','rgb')
572 system('epstopdf␣QE-p-i-n.eps')
573
574 figure(21)
575 plot(wavelength,(Q_n(2,:)+Q_n_plus(2,:)+Q_n_dep(2,:)+
        Q_intrinsic_reference(2,:)+Q_p(2,:)+Q_p_plus(1,:)+Q_p_dep(1,:))
        ,'k-','LineWidth',1.3)
576 axis([400 1000 0 1])
577 hold on
578 plot(wavelength,Q_n(2,:),'b:','LineWidth',1.3)
```

```
579 plot(wavelength,Q_intrinsic_reference(2,:),'r-.','LineWidth',1.3)
580 plot(wavelength,Q_p(2,:),'g--')
581 legend('total', 'p-layer', 'i-layer', 'n-layer')
582 xlabel('Wavelength␣(nm)')
583 ylabel('Quantum␣efficiency')
584 legend BOXOFF
585 hold off
586 exportfig(21, 'QE-p-i-n-ARC.eps', 'Color','rgb')
587 system('epstopdf␣QE-p-i-n-ARC.eps')
588
589 figure(22)
590 plot(wavelength,(Q_n(3,:)+Q_n_plus(3,:)+Q_n_dep(3,:)+
    Q_intrinsic_reference(3,:)+Q_p(3,:)+Q_p_plus(3,:)+Q_p_dep(3,:))
    ,'k-','LineWidth',1.3)
591 axis([400 1000 0 1])
592 hold on
593 plot(wavelength,Q_n_plus(3,:),'y-.','LineWidth',1.3)
594 plot(wavelength,Q_n(3,:),'b:','LineWidth',1.3)
595 plot(wavelength,Q_intrinsic_reference(3,:),'r-.','LineWidth',1.3)
596 plot(wavelength,Q_p(3,:),'g--','LineWidth',1.3)
597 plot(wavelength,Q_n_dep(3,:),'c--','LineWidth',1.3)
598 legend('total','p^+-layer','p-layer', 'i-layer', 'n-layer', 'p-p
    ^+-dep-layer')
599 legend BOXOFF
600 xlabel('Wavelength␣(nm)')
601 ylabel('Quantum␣efficiency')
602 hold off
603 exportfig(22, 'QE-pplus-p-i-n.eps', 'Color','rgb')
604 system('epstopdf␣QE-pplus-p-i-n.eps')
605
606
607
608 figure(23)
609 plot(wavelength,(Q_n(4,:)+Q_n_plus(4,:)+Q_n_dep(4,:)+
    Q_intrinsic_reference(4,:)+Q_p(4,:)+Q_p_plus(4,:)+Q_p_dep(4,:))
    ,'k-','LineWidth',1.3)
610 axis([400 1000 0 1])
611 hold on
612 plot(wavelength,Q_n(4,:)+Q_n_plus(4,:)+Q_n_dep(4,:),'b:','
    LineWidth',1.3)
613 plot(wavelength,Q_p(4,:),'y--','LineWidth',1.3)
614 plot(wavelength,Q_intrinsic_reference(4,:),'r-.','LineWidth',1.3)
615 plot(wavelength,Q_p_plus(4,:),'g:','LineWidth',1.3)
616 plot(wavelength,Q_p_dep(4,:),'c--','LineWidth',1.3)
617 legend('total', 'total␣p/p^+-layer', 'n-layer', 'i-layer','n^+-
    layer','n-n^+-dep-layer','total','Location','West')
618 legend BOXOFF
619 xlabel('Wavelength␣(nm)')
620 ylabel('Quantum␣efficiency')
621 hold off
622 exportfig(23, 'QE-pplus-p-i-n-nplus.eps', 'Color','rgb')
623 system('epstopdf␣QE-pplus-p-i-n-nplus.eps')
624
```

```
625
626
627 figure(24)
628 plot(wavelength,(Q_n(5,:)+Q_n_plus(5,:)+Q_n_dep(5,:)+
    Q_intrinsic_reference(5,:)+Q_p(5,:)+Q_p_plus(5,:)+Q_p_dep(5,:))
    ,'k-','LineWidth',1.3)
629 axis([400 1000 0 1])
630 hold on
631 plot(wavelength,Q_n(5,:)+Q_n_plus(5,:)+Q_n_dep(5,:),'b:','
    LineWidth',1.3)
632 plot(wavelength,Q_p(5,:)+Q_p_plus(5,:)+Q_p_dep(5,:),'g--','
    LineWidth',1.3)
633 plot(wavelength,Q_intrinsic_reference(5,:),'r-.','LineWidth',1.3)
634 legend('total', 'total␣p/p^+-layer', 'total␣n/n^+-layer','i-layer'
    )
635 legend BOXOFF
636 xlabel('Wavelength␣(nm)')
637 ylabel('Quantum␣efficiency')
638 hold off
639 exportfig(23, 'QE-window-pplus-p-i-n-nplus.eps', 'Color','rgb')
640 system('epstopdf␣QE-window-pplus-p-i-n-nplus.eps')
641
642
643 figure(30)
644 plot(wavelength,Q_n_plus(5,:),'r:','LineWidth',1.3)
645 axis([400 1000 0 1])
646 hold on
647 plot(wavelength,Q_n_plus(4,:),'r-','LineWidth',1.3)
648 plot(wavelength,Q_n(5,:),'b:')
649 plot(wavelength,Q_n(4,:),'b-','LineWidth',1.3)
650 hold off
651 legend('p^+-layer␣when␣window␣layer␣present','p^+-layer␣when␣no␣
    window␣layer␣present','p-layer␣when␣window␣layer␣present','p-
    layer␣when␣no␣window␣layer␣present')
652 legend BOXOFF
653 exportfig(30, 'QE-onlyp.eps', 'Color','rgb')
654 system('epstopdf␣QE-onlyp.eps')
655
656
657 %
658 % figure(25)
659 % plot(wavelength,Q_n(6,:)+Q_n_plus(6,:)+Q_n_dep(6,:),'b:')
660 % axis([400 1000 0 1])
661 % hold on
662 % plot(wavelength,Q_intrinsic_reference(6,:),'r-.')
663 % plot(wavelength,Q_p(6,:)+Q_p_plus(6,:)+Q_p_dep(6,:),'y--')
664 % plot(wavelength,(Q_n(6,:)+Q_n_plus(6,:)+Q_n_dep(6,:)+
    Q_intrinsic_reference(6,:)+Q_p(6,:)),'k-')
665 % legend('p+p^++p-p^+-dep-layer', 'intrinsic-layer', 'n+n^++n-n^+-
    dep-layer','total')
666 % xlabel('Wavelength (nm)')
667 % ylabel('Quantum efficiency')
668
```

```
669 figure(26)
670 plot(wavelength,(Q_n(5,:)+Q_n_plus(5,:)+Q_n_dep(5,:)+
        Q_intrinsic_reference(5,:)+Q_p(5,:)+Q_p_plus(5,:)+Q_p_dep(5,:))
        ,'k-','LineWidth',1.3)
671 axis([400 1000 0 1])
672 hold on
673 plot(wavelength,(Q_n(4,:)+Q_n_plus(4,:)+Q_n_dep(4,:)+
        Q_intrinsic_reference(4,:)+Q_p(4,:)+Q_p_plus(4,:)+Q_p_dep(4,:))
        ,'g:','LineWidth',1.3)
674 plot(wavelength,(Q_n(3,:)+Q_n_plus(3,:)+Q_n_dep(3,:)+
        Q_intrinsic_reference(3,:)+Q_p(3,:)+Q_p_plus(3,:)+Q_p_dep(3,:))
        ,'b--','LineWidth',1.3)
675 plot(wavelength,(Q_n(2,:)+Q_n_plus(2,:)+Q_n_dep(2,:)+
        Q_intrinsic_reference(2,:)+Q_p(2,:)+Q_p_plus(2,:)+Q_p_dep(2,:))
        ,'r:','LineWidth',1.3)
676 plot(wavelength,(Q_n(1,:)+Q_n_plus(1,:)+Q_n_dep(1,:)+
        Q_intrinsic_reference(1,:)+Q_p(1,:)+Q_p_plus(1,:)+Q_p_dep(1,:))
        ,'c-.','LineWidth',1.3)
677 legend('window-p^+-p-i-n-n^+ with ARC','p^+-p-i-n-n^+ with ARC','p
        ^+-p-i-n with ARC','p-i-n with ARC','p-i-n without ARC','
        Location','SouthWest')
678 legend BOXOFF
679 xlabel('Wavelength (nm)')
680 ylabel('Quantum efficiency')
681 hold off
682 exportfig(26, 'QE-all.eps', 'Color','rgb')
683 system('epstopdf QE-all.eps')
684
685
686 % exportfig(20, 'QE-p-i-n.eps', 'Color','rgb')
687 % system('epstopdf QE-p-i-n.eps')
688 % exportfig(21, 'QE-p-i-n-ARC.eps', 'Color','rgb')
689 % system('epstopdf QE-p-i-n-ARC.eps')
690 % exportfig(22, 'QE-pplus-p-i-n.eps', 'Color','rgb')
691 % system('epstopdf QE-pplus-p-i-n.eps')
692 % exportfig(23, 'QE-pplus-p-i-n-nplus.eps', 'Color','rgb')
693 % system('epstopdf QE-pplus-p-i-n-nplus.eps')
694 % exportfig(24, 'QE-window-pplus-p-i-n-nplus.eps', 'Color','rgb')
695 % system('epstopdf QE-window-pplus-p-i-n-nplus.eps')
696 %exportfig(25, 'QE-window-pplus-p-i-n-nplus-2e19doping.eps', '
        Color','rgb')
697 %system('epstopdf QE-window-pplus-p-i-n-nplus-2e19doping.eps')
698
699
700
701 figure(29)
702 plot(wavelength,(Q_n(5,:)+Q_n_plus(5,:)+Q_n_dep(5,:)+
        Q_intrinsic_reference(5,:)+Q_p(1,:)+Q_p_plus(5,:)+Q_p_dep(5,:))
        ,'c-','LineWidth',1.3)
703 axis([400 1000 0 1])
704 hold on
705 plot(wavelength,(Q_n(6,:)+Q_n_plus(6,:)+Q_n_dep(6,:)+
        Q_intrinsic_reference(6,:)+Q_p(6,:)+Q_p_plus(6,:)+Q_p_dep(6,:))
```

```
    ,'r:','LineWidth',1.3)
706 plot(wavelength,(Q_n(7,:)+Q_n_plus(7,:)+Q_n_dep(7,:)+
    Q_intrinsic_reference(7,:)+Q_p(7,:)+Q_p_plus(7,:)+Q_p_dep(7,:))
    ,'b--','LineWidth',1.3)
707 legend('window-p^+-p-i-n-n^+␣with␣ARC','window-p-i-n-n^+␣with␣ARC'
    ,'window-p^+-i-n-n^+␣with␣ARC','Location','SouthWest')
708 legend BOXOFF
709 xlabel('Wavelength␣(nm)')
710 ylabel('Quantum␣efficiency')
711 hold off
712
713 exportfig(29, 'QE-varywindow.eps', 'Color','rgb')
714 system('epstopdf␣QE-varywindow.eps')
715
716
717
718
719
720
721
722
723
724
725
726
727
728
729
730
731 % figure(30)
732 %
733 % semilogy(wavelength,(Q_n(6,:)+Q_n_plus(6,:)+Q_n_dep(6,:)+
    Q_intrinsic_reference(6,:)+Q_p(6,:)+Q_p_plus(6,:)+Q_p_dep(6,:))
    ,'k-')
734 % axis([400 1000 1e-4 1])
735 % hold on
736 % xlabel('Wavelength (nm)')
737 % ylabel('Quantum efficiency')
738
739
740
741
742
743
744 % figure(10);
745 %
746 % plot(wavelength,Q_n(1,:),'m');
747 % %axis([750 1000 0 0.3])
748 % hold on
749 % plot(wavelength,Q_p(1,:),'k');
750 % %axis([750 1200 1e-3 1e0])
751 % plot(wavelength,Q_intrinsic_reference(1,:),'c');
752 % %axis([750 1200 1e-3 1e0])
```

```
753 % plot(wavelength,(Q_n(1,:)+Q_p(1,:)+Q_intrinsic_reference(1,:)),'
    y');
754 % hold off
755 % xlabel('Wavelength (nm)')
756 % ylabel('Quantum efficiency')
757 % legend('N', 'P', 'intrinsic', 'Total' )
758 % title('Quantum efficiency curves of IB solar cell')
759
760
761
762 % figure(7)
763 % semilogy(zi_endelig,alpha_GaAs_endelig);
764 % hold on
765 % axis([1.2 3.7 0 1.0e9])
766 % semilogy(zi_endelig,alpha_AlGaAs_window(1,:));
767 % axis([1.2 3.7 0 1.0e9])
768
769
770 referencecell=current_reference;
771
772 currentvalues=[current_CI current_IV current_CV current_reference
    J_0_diode_1 J_0_diode_2_SCR];
773
774 generatedcurrent=currentvalues;
775 maximum_QE_3_dep_n=max(Q_n_dep(3,:))
776 maximum_QE_4_p_plus=max(Q_p_plus(4,:))
777 maximum_QE_1=max(Q_n(1,:)+Q_n_plus(1,:)+Q_n_dep(1,:)+
    Q_intrinsic_reference(1,:)+Q_p(1,:)+Q_p_plus(1,:)+Q_p_dep(1,:))
778 maximum_QE_2=max(Q_n(2,:)+Q_n_plus(2,:)+Q_n_dep(2,:)+
    Q_intrinsic_reference(2,:)+Q_p(2,:)+Q_p_plus(2,:)+Q_p_dep(2,:))
779
780 maximum_QE_5=max(Q_n(5,:)+Q_n_plus(5,:)+Q_n_dep(5,:)+
    Q_intrinsic_reference(5,:)+Q_p(5,:)+Q_p_plus(5,:)+Q_p_dep(5,:))
781
782 return
```

Listing B.2: Photocurrent for p-i-n reference cell with depleted i-layer

B.3 Current-voltage characteristic p-i-n reference cell with depleted i-layer

```
1 ------------------------------------------------
2 Current-voltage characteristic p-i-n solar cell,
3 no flat band
4 ------------------------------------------------
5 %Paramters taken from the program Variables
6 clear;
7 load 'var.mat' %Loading the file containing all constants,
    remember to first run the program Variables
8
9 %Photogenerated current
10 J_L_reference=zeros(1,numberofdevices);
11
```

```
12 currentvalues=Sollysstrom(); %Use of AM 1.5 spectrum
13
14 for i=1:numberofdevices
15 J_L_reference(i)=currentvalues(i+(numberofdevices.*3)); %
      photocurrent from the reference cells
16 end
17
18 %Recombination current
19 J_0_CV_diode_1=zeros(1,numberofdevices);
20 J_0_CV_diode_2=zeros(1,numberofdevices);
21
22 for i=1:numberofdevices
23 J_0_CV_diode_1(i)=currentvalues(i+(numberofdevices.*4));
24 J_0_CV_diode_2(i)=currentvalues(i+(numberofdevices.*5));
25 end
26
27
28 %Voltages
29 minimum=0.0;
30 maximum=1.05;
31 step=0.001;
32 antall=round((maximum-minimum)/step+1);
33
34 Voltage=zeros(numberofdevices,antall); %voltage over cell Voltage=
      V_VC-J*R_s*area
35
36 V_VC=minimum:step:maximum; %e_charge*V_VC difference between the
      CB and VB quasi-Fermi levels
37
38 J_CV=zeros(numberofdevices,antall);
39 J=zeros(numberofdevices,antall);
40
41 for i=1:antall
42     for a=1:numberofdevices
43 J_CV(a,i)=J_0_CV_diode_1(a).*(exp((e_charge.*V_VC(i))./(k_Boltzman
      .*T))-1)+(J_0_CV_diode_2(a).*sinh(e_charge.*V_VC(i)./(2.*
      k_Boltzman.*T))./(e_charge.*(V_bi(a)-V_VC(i))./(k_Boltzman.*T))
      ); %recombination current
44 J(a,i)=J_L_reference(a)-J_CV(a,i)-(V_VC(i)./(R_sh(a).*area(a))); %
      current-voltage characteristic from equivalent circuit
45 Voltage(a,i)=V_VC(i)-(J(a,i).*R_s(a).*area(a));
46     end
47 end
48
49
50 V_OC_mi=0; %open-circuit voltage
51 V_OC=zeros(1,numberofdevices);
52
53
54 for a=1:numberofdevices
55     V_OC_mi=fsolve(@(V_OC_mi) (J_L_reference(a)-(J_0_CV_diode_1(a)
          .*(exp((e_charge.*V_OC_mi)./(k_Boltzman.*T))-1))-(
          J_0_CV_diode_2(a).*sinh(e_charge.*V_OC_mi./(2.*k_Boltzman.*T
```

```
        )) ./(e_charge.*(V_bi(a)-V_OC_mi)./(k_Boltzman.*T)))-(V_OC_mi
        ./(R_sh(a).*area(a)))),0,optimset('Display','off'));
56    V_OC(a)=V_OC_mi;
57    V_OC_mi=0;
58 end
59
60
61 J_sc=zeros(1,numberofdevices); %short-circuit current
62 %Simple version J_sc (that is no series resistance)
63 for a=1:numberofdevices
64      J_sc(a)=J_L_reference(a)-J_0_CV_diode_1(a).*(exp((e_charge
            .*0)./(k_Boltzman.*T))-1)-(J_0_CV_diode_2(a).*sinh(
            e_charge.*0./(2.*k_Boltzman.*T))./(e_charge.*(V_bi(a)-0)
            ./(k_Boltzman.*T))); %recombination current
65 end
66
67 V_OC
68 J_sc
69
70
71 %Efficiency of cells
72 efficiency=zeros(numberofdevices,antall);
73 P_in=1e+3; %Power incident for AM 1.5
74 for a=1:numberofdevices
75     for i=1:antall
76         if J(a,i)>0
77             efficiency(a,i) = abs(Voltage(a,i)*J(a,i)*100)/P_in;
78         else
79             efficiency(a,i)=0;
80         end
81     end
82 end
83
84 efficiencymax=zeros(1,numberofdevices);
85 for a=1:numberofdevices
86 efficiencymax(a)=max(efficiency(a,:));
87 end
88
89 efficiencymax
90
91 figure(10)
92 plot(Voltage(5,:), J(5,:),'r-.','LineWidth',1.3);
93 hold on
94 axis([minimum maximum 0 270])
95 plot(Voltage(4,:), J(4,:),'b:','LineWidth',1.3);
96 plot(Voltage(3,:), J(3,:),'c--','LineWidth',1.3);
97 plot(Voltage(2,:), J(2,:),'g-.','LineWidth',1.3);
98 plot(Voltage(1,:), J(1,:),'k-','LineWidth',1.3);
99 %plot(Voltage(6,:), J(6,:),'k:','LineWidth',1.3);
100 xlabel('Voltage␣(V)')
101 ylabel('Current␣density␣(A/m^2)')
102 legend('window-p^+-p-i-n-n^+␣with␣ARC','p^+-p-i-n-n^+␣with␣ARC','p
      ^+-p-i-n␣with␣ARC','p-i-n␣with␣ARC','p-i-n␣without␣ARC','
```

```
    Location','SouthWest')
103 legend BOXOFF
104 hold off
105
106 exportfig(10, 'IValllayers', 'Color','rgb')
107 system('epstopdf␣IValllayers.eps')
108
109 voltage_12=V_VC(801)
110
111 figure(11)
112 plot(Voltage(1,:), J(1,:),'r-.','LineWidth',1.3);
113 hold on
114 axis([minimum maximum 0 290])
115 plot(Voltage(2,:), J(2,:),'b:','LineWidth',1.3);
116 plot(Voltage(3,:), J(3,:),'c--','LineWidth',1.3);
117 plot(Voltage(4,:), J(4,:),'g-.','LineWidth',1.3);
118 plot(Voltage(5,:), J(5,:),'k-','LineWidth',1.3);
119 %plot(Voltage(6,:), J(6,:),'k:','LineWidth',1.3);
120 xlabel('Voltage␣(V)')
121 ylabel('Current␣density␣(A/m^2)')
122 legend('p-i-n␣without␣ARC','p-i-n␣with␣ARC','p^+-p-i-n␣with␣ARC','
    p^+-p-i-n-n^+␣with␣ARC','window-p^+-p-i-n-n^+␣with␣ARC','
    Location','SouthWest')
123 legend BOXOFF
124 hold off
125
126
127
128 figure(13)
129 plot(Voltage(6,:), J(6,:),'b:','LineWidth',1.3);
130 axis([minimum maximum 0 290])
131 hold on
132 plot(Voltage(7,:), J(7,:),'c-','LineWidth',1.3);
133 plot(Voltage(5,:), J(5,:),'r-.','LineWidth',1.3);
134 xlabel('Voltage␣(V)')
135 ylabel('Current␣density␣(A/m^2)')
136 legend('window-p-i-n-n^+␣with␣ARC','window-p^+-i-n-n^+␣with␣ARC','
    window-p^+-p-i-n-n^+␣with␣ARC','Location','SouthWest')
137 legend BOXOFF
138 hold off
139
140 exportfig(13, 'IVvarywindow', 'Color','rgb')
141 system('epstopdf␣IVvarywindow.eps')
142
143
144
145
146
147
148 dark_1=J_CV(1,801)
149 dark_2=J_CV(2,801)
150 dark_3=J_CV(3,801)
151 dark_4=J_CV(4,801)
```

```
152 dark_5=J_CV(5,801)
153 dark_6=J_CV(6,801)
```

Listing B.3: Photocurrent

B.4 Current-voltage characteristic p-i-n reference cell with undepleted i-layer

```
1 ------------------------------------------------
2 Current-voltage characteristic p-i-n solar cell
3 with flat band
4 ------------------------------------------------
5 function IVcurve=IVflatband(minimumvoltage, maximumvoltage,
    stepvoltage,widthintrinsic)
6
7
8 %Constants used in the different programs
9 h_planck=6.62607e-34; %Plancks constant h in Js
10 h_dirac=1.05457e-34; %Diracs constant=h/2pi in Js
11 m_e=9.10938e-31; %Electron mass in kg
12 eV=1.60218e-19; %electronvolt to joule
13 k_Boltzman = 1.38065e-23; %Boltzman constant J/K
14 freediec = 8.85419e-12; %Free dielectric constant in F/m
15 e_charge=1.60218e-19; %Charge of an electron in C
16 c_light = 2.99792e+8; %velocity of light m/s
17 T=300; %temperature used in article for solar cells in K
18
19 %To meter m
20 nm=1e-9; %nanometer to meter
21 cm=1e-2; %centimeter to meter
22
23 %DATA USED IN THE MODEL
24 numberofdevices=4;
25
26 window=[1 1 1 1]; %equal to 1 if we have a window layer, equal to
    0 of we do not have a window layer
27 ARC=[1 1 1 1]; %1 if anti-reflective coating, 0 if not
28
29 %Fraction of x in Al_xGa_(1-x)_As
30 x_window=[0.85 0.85 0.85 0.85];  %x in window layer
31 x_cell=[0 0 0.35 0.35];       %x in p, p-plus, n and n-plus layers
32
33 %Bandgap for GaAs
34 E_GaAs=(1.519-(5.405*(1e-4)*T^2/(T+204)))*eV; %from Lie!!
35
36 E_window=zeros(1,numberofdevices);          %Bandgap window layer
    (eV)
37 E_cell=zeros(1,numberofdevices);            %Bandgap in p, p-plus,
     n and n-plus layers (eV)
38
39 %Bandgap for Al_xGa_(1-x)As in the rest of the cell
40 for i=1:numberofdevices
```

```
41 E_window(i)=(1.911+(0.005.*x_window(i))+(0.245.*(x_window(i).^2)))
     *eV;   %Bandgap window layer for x>=0.45(eV) (Properties of
     AlGaAs)
42 E_cell(i)=(E_GaAs/eV+(1.247*x_cell(i)))*eV;       %Bandgap in p, p
     -plus, n and n-plus layers  for x<0.45(eV) (Properties of
     AlGaAs)
43 end
44
45
46 concentration=[1 1 1 1]; %light concentration
47
48 %Energysteps used to find the maximum efficiency
49
50
51 energystep=0.0;
52
53
54 GaAs_min=1.22.*(1.519-(5.405*(1e-4)*T^2/(T+204)))
     ./((1.519-(5.405*(1e-4)*2^2/(2+204)))); %Energy measured in
     Tronheim at 2K
55
56 %energymin=0.9; %minimum value of E_H
57
58 %energymax=1.2; %maximum value of E_H
59 %energymax=energymin; %maximum value of E_H
60
61
62 %energyvalues=round((energymax-energymin)./energystep)+1; %number
     of energies
63 energyvalues=1;
64
65 %E_H=(energymin:energystep:energymax).*eV; %bandgap
     intermediateband-valenceband
66 %E_H=energymin.*eV;
67 E_H=[1.12 1.12 1.12 1.12].*eV;
68
69 E_L=zeros(numberofdevices,energyvalues); %bandgap conductionband-
     intermediateband
70 E_G=zeros(numberofdevices,energyvalues); %bandgap conductionband-
     valenceband
71
72 for i=1:energyvalues
73     for a=1:numberofdevices
74 %E_G(a,i)=E_cell(a);    %bandgap conductionband-valenceband
75 E_G(a,i)=1.38.*eV;    %bandgap conductionband-valenceband
76 E_L(a,i)=E_G(a,i)-E_H(a); %bandgap conductionband-intermediate
     band
77     end
78 end
79
80
81 mu_e=[0.8 0.8 0.8 0.8 0.8 0.8 0.8 0.8];       %GaAs mobility
     electrons in m^2/(Vs)from Semiconducting and other properties
```

```
    of GaAs
82 mu_h=[0.04 0.04 0.04 0.04 0.04 0.04 0.04 0.04];      %GaAs
    mobility holes in m^2/(Vs) from semiconducting and other
    properties of GaAs
83
84 %mu_e=[ 0.185 0.185];        %Al0.35Ga0.65As mobility electrons in
    m^2/(Vs)from Landolt Bornstein
85 %mu_h=[0.0110 0.0110];        %Al0.35Ga0.65As mobility holes in m
    ^2/(Vs) from Properties of AlGaAs
86
87
88 diffusionconstant_e=zeros(1,numberofdevices); %diffusion constant
    electrons in CB in IB material
89 diffusionconstant_h=zeros(1,numberofdevices); %diffusion constant
    holes in VB in IB material
90
91 for i=1:numberofdevices
92 diffusionconstant_e(i)=(k_Boltzman.*T.*mu_e(i))./e_charge;
93 diffusionconstant_h(i)=(k_Boltzman.*T.*mu_h(i))./e_charge;
94 end
95 m_e_AlGaAs=zeros(1,numberofdevices);
96 m_hh_AlGaAs=zeros(1,numberofdevices);
97 m_lh_AlGaAs=zeros(1,numberofdevices);
98 N_C_AlGaAs=zeros(1,numberofdevices);
99 N_V_AlGaAs=zeros(1,numberofdevices);
100 ni_AlGaAs=zeros(1,numberofdevices);
101
102 for i=3:numberofdevices
103
104 m_e_AlGaAs(i)=(0.0632+(0.0856.*x_cell(i))+(0.0231.*x_cell(i).^2))
    .*m_e;
105 m_hh_AlGaAs(i)=(0.50+(0.2.*x_cell(i))).*m_e;
106 m_lh_AlGaAs(i)=(0.088+(0.0372.*x_cell(i))+(0.0163.*x_cell(i).^2))
    .*m_e;
107
108 N_C_AlGaAs(i)=2.*((2.*pi.*m_e_AlGaAs(i).*k_Boltzman.*T./(h_planck
    .^2)).^(1.5));
109 N_V_AlGaAs(i)=2.*((2.*pi.*((m_hh_AlGaAs(i)^(1.5)+m_lh_AlGaAs(i)
    .^(1.5)).^(2./3)).*k_Boltzman.*T./(h_planck.^2)).^(1.5));
110 ni_AlGaAs(i)=sqrt(N_C_AlGaAs(i).*N_V_AlGaAs(i)).*exp(-E_cell(i)
    ./(2.*k_Boltzman.*T));
111
112 end
113
114
115 N_C=[4.7e23 4.7e23 N_C_AlGaAs(3) N_C_AlGaAs(4];      %GaAs
    densities of states conduction band in /m^3 from "Solar Cells
    Materials, Manufacture and Operation"
116 N_V=[7e24 7e24 N_V_AlGaAs(3) N_V_AlGaAs(4;      %GaAs densities
    of states valence band in /m^3 from "Solar Cells Materials,
    Manufacture and Operation"
117
118
```

```
119 ni_GaAs=1.79e12; %intrinsic carrier concentration at 300 K in GaAs
     (m-3) from "Solar Cells Materials, Manufacture and Operation"
120
121 %ni_cell=[ni_GaAs ni_GaAs ni_GaAs ni_GaAs]; %intrinsic carrier
    concentration in p- and n-layer
122 ni_cell=[ni_GaAs ni_GaAs ni_AlGaAs(3) ni_AlGaAs(4)]; %when AlGaAs
    instead of GaAs
123
124 %ni_intrinsic=[ni_GaAs ni_GaAs ni_GaAs ni_GaAs]; %intrinsic
    carrier concentration in the intrinsic layers
125 ni_intrinsic=[ni_GaAs ni_GaAs ni_AlGaAs(3) ni_AlGaAs(4)]; %when
    AlGaAs instead of GaAs
126
127 n_0=ni_intrinsic;
128 p_0=ni_intrinsic;
129
130
131 %Non-radiative recombination lifetimes Taken from "Intermediate
    Band Solar
132 %Cells Using Nanotechnology"
133 tau_SRH_CI=[1e15 1e15 1e15 1e15];   %non-radiative lifetime
    conduction band to intermediate band (in s), set equal to great
     value if only radiative recombination
134
135 tau_SRH_IV=[1e15 1e15 1e15 1e15];   %non-radiative lifetime
    intermediate band to valence band (in s), set equal to great
    value if only radiative recombination
136
137
138 %Carrier lifetimes
139 tau_n_GaAs=7e-9; %(s) fra Nelson Quantum-Well Structures
140 tau_p_GaAs=7e-9;     % (s) fra Nelson Quantum-Well Structures
141
142 %Carrier lifetimes for AlGaAs
143 %tau_n_GaAs=18e-9; %(s) fra Properties of AlGaAs
144 %tau_p_GaAs=18e-9;     % (s) fra Properties of AlGaAs
145
146
147 %Dielectric constants
148 epsilon_GaAs=12.79.*(1+(T.*1e-4)).*freediec; %static dielectric
    constant for GaAs from "Properties of GaAs"
149
150 epsilon_AlGaAs=zeros(1,numberofdevices);
151
152 for i=3:numberofdevices
153
154 epsilon_AlGaAs(i)=(13.1-(2.2.*x_cell(i))).*freediec;
155 end
156
157 %epsilon_p=[epsilon_GaAs epsilon_GaAs epsilon_GaAs epsilon_GaAs];
    %dielectric constant p and p-plus layer, here taken for GaAs
158 %epsilon_n=[epsilon_GaAs epsilon_GaAs epsilon_GaAs epsilon_GaAs];
    %dielectric constant n and n-plus layer, here taken for GaAs
```

```
159 epsilon_p=[epsilon_GaAs epsilon_GaAs epsilon_AlGaAs(3)
        epsilon_AlGaAs(4)]; %if AlGaAs
160 epsilon_n=[epsilon_GaAs epsilon_GaAs epsilon_AlGaAs(3)
        epsilon_AlGaAs(4)]; %if AlGaAs
161
162 %Lengths in the devices
163 width_window=[5 5 5 5].*nm;     %width of window layer in m
164 width_p_plus=[100 100 100 100].*nm; %width of p-plus layer in m
165 width_p=[200 200 200 200].*nm;          %with of p layer in m
166 %width_IB=[200 200 200 200].*nm; %width of intermediate band layer
         in m
167 width_n=[300 300 300 300].*nm;          %with of n layer in m
168 width_n_plus=[100 100 100 100].*nm;     %with of n-plus layer in m
169
170 %Doping of the devices
171 N_I=1e14; %backrground doping in GaAs, assumed p-type, in /cm3
172 N_A_window=[2e19 2e19 2e19 2e19];       %doping concentration in
        window layer (assumed p-type), in /cm3
173 N_A_p_plus=[2e19 2e19 2e19 2e19];       %doping concentration in p-
        plus layer, in /cm3
174 N_A_p=[2e18 2e18 2e18 2e18];            %doping concentration in p
        layer, in /cm3
175 N_D_n=[2e17 2e17 2e17 2e17];            %doping concentration in n
        layer, in /cm3
176 N_D_n_plus=[2e18 2e18 2e18 2e18];       %doping concentration in n-
        plus layer, in /cm3
177
178
179 %Calculation of built-in voltage in p-i-n structure
180
181 V_bi=zeros(1,numberofdevices);
182 V_bi_p_i=zeros(1,numberofdevices); %built-in voltage p-intrinisic
        layer
183 V_bi_n_i=zeros(1,numberofdevices); %built-in voltage n-intrinsic
        layer
184 V_max=[0.85 1.2 0.85 1.2]; %maximum applied voltage may be changed
        ..
185 %V_max=[0.85 0.85 0.85 0.85];
186
187
188
189 for i=1:numberofdevices
190     V_bi(i)=(k_Boltzman.*T./e_charge).*log((N_A_p(i)./cm.^3).*(
           N_D_n(i)./cm.^3)./(ni_cell(i).^2)); % (eq 6.2 in Nelson)
191     V_bi_n_i(i)=(k_Boltzman.*T./e_charge).*log((N_D_n(i)./cm.^3)
           .*(N_I./cm.^3)./(ni_cell(i).^2));
192 end
193
194
195 V_bi_p_i_mi=0; %Temporary built-in voltage p-intrinsic layer
196
197 for i=1:numberofdevices
198  %V_bi_p_i_mi=fsolve(@(V_bi_p_i_mi)
```

```
199  %(e_charge.*V_bi_p_i_mi./(k_Boltzman.*T))+log((N_I./N_A_p(i))
       +(0.5.*(e_charge.*V_bi_p_i_mi./(k_Boltzman.*T))^2)),0,optimset
       ('Display','off'))
200  %V_bi_p_i(i)=V_bi_p_i_mi
201  V_bi_p_i(i)=(k_Boltzman.*T./e_charge).*log(N_A_p(i)./(N_I));
202  V_bi_p_i_mi=0;
203 end
204
205
206 B_factor_max=zeros(numberofdevices); %factor important in
      determining the voltage over the p-i and i-n junction
207 equationvoltage_max=zeros(numberofdevices); %equation needed in
      finding the voltage over the p-i and i-n junction
208 V_p_max=zeros(numberofdevices); %part of the maximum applied
      voltage over the p-i junction
209 V_n_max=zeros(numberofdevices);  %part of the maximum applied
      voltage over the n-i junction
210
211 for a=1:numberofdevices
212 B_factor_max(a)=((N_I./cm^3)/ni_intrinsic(a)).^2.*exp(-e_charge.*
      V_max(a)./(k_Boltzman.*T));
213 equationvoltage_max(a)=0.5.*(-B_factor_max(a)+sqrt(B_factor_max(a)
      .^2+(4.*(B_factor_max(a)+exp(-2.*e_charge.*V_bi_p_i(a)./(
      k_Boltzman.*T))))));
214 V_p_max(a)=-log(equationvoltage_max(a)).*k_Boltzman.*T./e_charge;
215 V_n_max(a)=V_max(a)-V_p_max(a);
216 end
217
218 %Depletion width
219 dep_width_p_i_max=zeros(1,numberofdevices); %maximum width of
      depletion region between p and intrinsic layer, taken as width
      into intrinsic layer
220 dep_width_p_i_min=zeros(1,numberofdevices);  %minimum width of
      depletion region between p and intrinsic layer, taken as width
      into intrinsic layer
221 for i=1:numberofdevices
222     dep_width_p_i_max(i)=sqrt(2.*epsilon_p(i).*k_Boltzman.*T./(
          e_charge.^2.*(N_I./cm.^3))).*atan((e_charge.*V_bi_p_i(i)./(
          k_Boltzman.*T)).*sqrt(N_A_p(i)./(N_I.*2)));
223     dep_width_p_i_min(i)=sqrt(2.*epsilon_p(i).*k_Boltzman.*T./(
          e_charge.^2.*(N_I./cm.^3))).*atan((e_charge.*(V_bi_p_i(i)-
          V_p_max(i))./(k_Boltzman.*T)).*sqrt(N_A_p(i)./(N_I.*2)));
224
225 end
226
227 dep_width_n_i_max=zeros(1,numberofdevices); %maximum width of
      depletion region between n and intrinsic layer (this is in
      equilibrium)
228 dep_width_n_i_min=zeros(1,numberofdevices); %minimum width of
      depletion region between n and intrinsic layer (this is for
      maximum applied voltage)
229
230 for i=1:numberofdevices
```

```
231  dep_width_n_i_max(i)=sqrt((V_bi_n_i(i)).*2.*epsilon_n(i).*(N_D_n(
        i)./cm.^3)./(e_charge.*(((N_D_n(i)./cm.^3).*(N_I./cm.^3))+((
        N_I./cm.^3).^2))));%equilibrium, appplied voltage V=0
232  dep_width_n_i_min(i)=sqrt((V_bi_n_i(i)-V_n_max(a)).*2.*epsilon_n(
        i).*(N_D_n(i)./cm.^3)./(e_charge.*(((N_D_n(i)./cm.^3).*(N_I./
        cm.^3))+((N_I./cm.^3).^2)))); %built-in voltage minus maximum
        applied voltage, must be found after open-circuit voltage is
        found
233 end
234
235 %Calculation of built-in voltage of the p_plus-p-junction, needed
       in
236 %determining the depletion width of the p_plus-p-junction
237 V_h_mi=0; %built-in voltage of the p-plus-p junction
238 V_h=zeros(1,numberofdevices);
239
240
241
242 for i=1:numberofdevices
243   V_h(i)=(k_Boltzman.*T./e_charge).*log(N_A_p_plus(i)./(N_A_p(i)))
        ;
244  V_h_mi=0;
245 end
246
247 %Depletion width of the p_plus-p-junction, taken as the depletion
       width into the p-layer
248 dep_width_p_plus=zeros(1,numberofdevices);
249
250 for i=1:numberofdevices
251     dep_width_p_plus(i)=sqrt(2.*epsilon_p(i).*k_Boltzman.*T./(
           e_charge.^2.*(N_A_p(i)./cm.^3))).*atan((e_charge.*V_h(i)./(
           k_Boltzman.*T)).*sqrt(N_A_p_plus(i)./(N_A_p(i).*2)));
252 end
253
254 %Width of the undepleted p-layer
255 %The depletion width into the p_plus-layer is not taken into
       consideration
256 width_p_undepleted=zeros(1,numberofdevices);
257
258 for i=1:numberofdevices
259 width_p_undepleted(i)=width_p(i)-dep_width_p_plus(i);
260 end
261
262 %Calculation of built-in voltage of the n-n_plus-junction, needed
       in
263 %determining the depletion width of the n-n_plus-junction
264 V_h_mi_n_plus=0; %built-in voltage of the n-n_plus junction
265 V_h_n_plus=zeros(1,numberofdevices);
266
267
268 for i=1:numberofdevices
269  V_h_n_plus(i)=(k_Boltzman.*T./e_charge).*log(N_D_n_plus(i)./(
        N_D_n(i)));
```

```
270  V_h_mi_n_plus=0;
271 end
272
273 %Depletion width of the n_plus-n-junction, taken as the depletion
       width into the n-layer
274 dep_width_n_plus=zeros(1,numberofdevices);
275
276 for i=1:numberofdevices
277     dep_width_n_plus(i)=sqrt(2.*epsilon_n(i).*k_Boltzman.*T./(
           e_charge.^2.*(N_D_n(i)./cm.^3))).*atan((e_charge.*
           V_h_n_plus(i)./(k_Boltzman.*T)).*sqrt(N_D_n_plus(i)./(N_D_n
           (i).*2)));
278 end
279
280 %Width of the undepleted n-layer
281 %The depletion width into the n_plus-layer is not taken into
       consideration
282 width_n_undepleted=zeros(1,numberofdevices);
283
284 for i=1:numberofdevices
285 width_n_undepleted(i)=width_n(i)-dep_width_n_plus(i);
286 end
287
288 %Surface recombination
289 S_window=[1e4 1e4 1e4 1e4]; %surface recombination velocity top of
        window layer (m/s)
290 S_p_plus=[1e4 1e4 1e4 1e4]; %surface recombination velocity top of
        p_plus layer without window layer (m/s)
291 S_n_plus=[1e4 1e4 1e4 1e4];        %surface recombination velocity
        n-plus layer (m/s) (assumed rear surface is n-plus+substrate)
292
293 %Lifetimes
294  tau_n_p_layer=[3e-9 3e-9 3e-9 3e-9]; %GaAs book for doping
        2*10^18 (cm^-3) in (s)
295  tau_n_p_plus_layer=[0.5e-9 0.5e-9 0.5e-9 0.5e-9]; %GaAs book for
        doping 2*10^19(cm^-3) in (s)
296  tau_p_n_layer=[32.5e-9 32.5e-9 32.5e-9 32.5e-9]; %GaAs book for
        doping 2*10^17 (cm^-3) in (s)
297  tau_p_n_plus_layer=[7e-9 7e-9 7e-9 7e-9]; %GaAs book for doping
        2*10^18 (cm^-3) in (s)
298 %
299 %tau_n_p_layer=[ 2.3e-9 2.3e-9]; %AlGaAs Properties of AlGaAs book
         in (s)
300 %tau_n_p_plus_layer=[0.5e-9 0.5e-9]; %Taken same as GaAs  in (s)
301 %tau_p_n_layer=[3.1e-9 3.1e-9]; %AlGaAs Properties of AlGaAs book
        in (s)
302 %tau_p_n_plus_layer=[0.7e-9 0.7e-9]; %AlGaAs Properties of AlGaAs
       book  in (s)
303
304
305
306
307 %Mobilities
```

```
308
309  mu_n_p_layer=[0.125 0.125 0.125 0.125]; %GaAs book for doping
       2*10^18 (cm^-3) in (m^2/(Vs))
310  mu_n_p_plus_layer=[0.1400 0.1400 0.1400 0.1400]; %GaAs book for
       doping 2*10^19(cm^-3) in (m^2/(Vs))
311  mu_p_n_layer=[0.0278 0.0278 0.0278 0.0278]; %GaAs book for doping
        2*10^17 (cm^-3) in (m^2/(Vs))
312 mu_p_n_plus_layer=[0.0238 0.0238 0.0238 0.0238]; %GaAs book for
      doping 2*10^18 (cm^-3) in (m^2/(Vs))
313
314 %mu_n_p_layer=[0.100 0.100]; %GaAs book for doping 2*10^18 (cm^-3)
       in (m^2/(Vs))
315 %mu_n_p_plus_layer=[ 0.0830 0.0830]; %GaAs book for doping
      2*10^19(cm^-3) in (m^2/(Vs))
316 %mu_p_n_layer=[0.0100 0.0100]; %GaAs book for doping 2*10^17 (cm
      ^-3) in (m^2/(Vs))
317 %mu_p_n_plus_layer=[0.0065 0.0065]; %GaAs book for doping 2*10^18
      (cm^-3) in (m^2/(Vs))
318
319
320 %Diffusion lengths and diffusion coeffecients in the devices
321 diffusioncoefficient_n_p=(k_Boltzman.*T./e_charge).*mu_n_p_layer;
      %diffusion coefficient electrons in p-layer
322 diffusioncoefficient_n_p_plus=(k_Boltzman.*T./e_charge).*
      mu_n_p_plus_layer; %diffusion coefficient electrons in p_plus-
      layer
323
324 diffusioncoefficient_p_n=(k_Boltzman.*T./e_charge).*mu_p_n_layer;
      %diffusion coefficient holes in n-layer
325 diffusioncoefficient_p_n_plus=(k_Boltzman.*T./e_charge).*
      mu_p_n_plus_layer; %diffusion coefficient holes in n_plus-layer
326
327 difflength_n_p=zeros(1,numberofdevices); %diffusion length
      electrons in p-layer
328 difflength_n_p_plus=zeros(1,numberofdevices); %diffusion length
      electrons in p_plus-layer
329 difflength_p_n=zeros(1,numberofdevices); %diffusion length holes
      in n-layer
330 difflength_p_n_plus=zeros(1,numberofdevices); %diffusion length
      holes in n_plus-layer
331
332 for i=1:numberofdevices
333 difflength_n_p(i)=sqrt(tau_n_p_layer(i).*diffusioncoefficient_n_p(
      i));
334 difflength_n_p_plus(i)=sqrt(tau_n_p_plus_layer(i).*
      diffusioncoefficient_n_p_plus(i));
335 difflength_p_n(i)=sqrt(tau_p_n_layer(i).*diffusioncoefficient_p_n(
      i));
336 difflength_p_n_plus(i)=sqrt(tau_p_n_plus_layer(i).*
      diffusioncoefficient_p_n_plus(i));
337 end
338
```

```
339 difflength_n_window=difflength_n_p; %does not matter since another
     window recombination velocity is used
340 diffusioncoefficient_n_window=diffusioncoefficient_n_p; %does not
    matter since another window recombination velocity is used
341
342
343 %Effective surface recombination velocities
344 S_eff_p=zeros(1,numberofdevices); %effective surface reombination
    velocity close to p_plus-layer, on edge of undepleted p-layer (
    placed on top of intrinsic layer) (m/s)
345 S_eff_n=zeros(1,numberofdevices); %effective surface recombination
     velocity on edge of undepleted n-layer (placed under intrinsic
     layer) (m/s)
346 S_eff_window=zeros(1,numberofdevices);  %effective surface
    recombination velocity between p_plus-layer and window layer (m
    /s)
347 S_eff_p_plus_p=zeros(1,numberofdevices); %effective surface
    recombination velocity on edge of undepleted p_plus-layer (m/s)
    ,between p_plus-layer and depletion region
348 S_eff_n_plus_n=zeros(1,numberofdevices); %effective surface
    recombination velocity on edge of undepleted n-plus-layer (m/s)
    ,between n_plus-layer and depletion region
349
350
351
352 for i=1:numberofdevices
353     S_eff_n(i)=(diffusioncoefficient_p_n_plus(i)./
        difflength_p_n_plus(i)).*(N_D_n(i)./N_D_n_plus(i)).*((((
        S_n_plus(i).*difflength_p_n_plus(i)./
        diffusioncoefficient_p_n_plus(i)).*cosh(width_n_plus(i)./
        difflength_p_n_plus(i)))+sinh(width_n_plus(i)./
        difflength_p_n_plus(i)))./(((S_n_plus(i).*
        difflength_p_n_plus(i)./diffusioncoefficient_p_n_plus(i)).*
        sinh(width_n_plus(i)./difflength_p_n_plus(i)))+cosh(
        width_n_plus(i)./difflength_p_n_plus(i)))); %modification
        of eq 7.10 in Nelson
354     S_eff_p_plus_p(i)=(diffusioncoefficient_n_p(i)./difflength_n_p
        (i)).*(N_A_p_plus(i)./N_A_p(i)).*coth(width_p_undepleted(i)
        ./difflength_n_p(i)); %eq 14 in "A simple general
        analytical solution..."
355     S_eff_n_plus_n(i)=(diffusioncoefficient_p_n(i)./difflength_p_n
        (i)).*(N_D_n_plus(i)./N_D_n(i)).*coth(width_n_undepleted(i)
        ./difflength_p_n(i)); %eq 14 in "A simple general
        analytical solution..."
356
357
358     if window(i)==1
359     S_eff_window_test=(diffusioncoefficient_n_window(i)./
        difflength_n_window(i)).*exp((E_cell(i)-E_window(i))./(
        k_Boltzman.*T)).*((((S_window(i).*difflength_n_window(i)./
        diffusioncoefficient_n_window(i)).*cosh(width_window(i)./
        difflength_n_window(i)))+sinh(width_window(i)./
        difflength_n_window(i)))./(((S_window(i).*
```

```
        difflength_n_window(i)./diffusioncoefficient_n_window(i)).*
        sinh(width_window(i)./difflength_n_window(i)))+cosh(
        width_window(i)./difflength_n_window(i)))); %S_eff_window
        used for front surface velocity of the p_plus layer
360     S_eff_window(i)=1e2; %Takes value from Hovel since
        S_eff_window_test too small, see report
361     S_eff_p(i)=(diffusioncoefficient_n_p_plus(i)./
        difflength_n_p_plus(i)).*(N_A_p(i)./N_A_p_plus(i)).*(((
        S_eff_window(i).*difflength_n_p_plus(i)./
        diffusioncoefficient_n_p_plus(i)).*cosh(width_p_plus(i)./
        difflength_n_p_plus(i)))+sinh(width_p_plus(i)./
        difflength_n_p_plus(i)))./(((S_eff_window(i).*
        difflength_n_p_plus(i)./diffusioncoefficient_n_p_plus(i)).*
        sinh(width_p_plus(i)./difflength_n_p_plus(i)))+cosh(
        width_p_plus(i)./difflength_n_p_plus(i)));
362
363     else
364     S_eff_window(i)=S_p_plus(i); %S_eff_window used for front
        surface velocity of the p_plus layer
365     S_eff_p(i)=(diffusioncoefficient_n_p_plus(i)./
        difflength_n_p_plus(i)).*(N_A_p(i)./N_A_p_plus(i)).*((((
        S_p_plus(i).*difflength_n_p_plus(i)./
        diffusioncoefficient_n_p_plus(i)).*cosh(width_p_plus(i)./
        difflength_n_p_plus(i)))+sinh(width_p_plus(i)./
        difflength_n_p_plus(i)))./(((S_p_plus(i).*
        difflength_n_p_plus(i)./diffusioncoefficient_n_p_plus(i)).*
        sinh(width_p_plus(i)./difflength_n_p_plus(i)))+cosh(
        width_p_plus(i)./difflength_n_p_plus(i))));
366     end
367
368
369 end
370
371
372
373 width_intrinsic=widthintrinsic
374
375 %Reading the necessary excel files
376
377 step_endelig=0.001; %steplength used in interpolation
378
379 %USES SHIFT OF ENERGY AXIS
380 num4=xlsread('C:\Documents␣and␣Settings\Kirsti␣Kvanes\Mine␣
    dokumenter\MATLAB\Prosjekt\GaAs␣optiske␣parametre');%Optical
    parameters for GaAs using shift of energy axis
381 %Comment: alpha values were originally given as 10^-3 multiplied
    by the
382 %values in the excel file, this was pr cm, to get correct alpha
    values pr
383 %m, multiply with 10^2*10^3
384 photonenergy_GaAsny=num4(:,1); %photonenergies for GaAs used in
    the excel files
385 alpha_GaAsny=1e5.*num4(:,4); %absorption coefficient GaAs
```

```
386 R_GaAsny=num4(:,3); %Reflectivity values for GaAs
387 n_GaAsny=num4(:,2); %Refractive index for GaAs
388
389
390 w_p=0*nm; %For p-i-n solar cell, depletion region into p-layer
      equal to zero
391 w_n=0*nm; %For p-i-n solar cell, depletion region  into n-layer
      equal to zero
392
393 %Getting values for GaAs
394 %Bruker mindre steglengder frem til 1.5 eV for der har jeg flere
      verdier
395 %HUSK at man har flere steglengder, en steglengde for energier
      mindre
396 %enn 1.5 eV, en annen for energier større enn 1.5 eV og en tredje
      brukt i
397 %interpolering
398 %må ta hensyn til at minste verdi i excel-fila er 1.36 eV, setter
399 %absorpsjonskoeffisienten lik 0 for mindre verdier
400 step_1_GaAs=0.01;%*eV; %Steplength 0.01 for energies less then 1.5
401 minimum_1_GaAs=0.32;%*eV; %minimum value in the excel files for
      solar spectrum is 0.3104
402 maximum_1_GaAs=1.5;%*eV; %maximum allowed value 1.5 for energies
      larger then 1.5 we need a greater steplength
403 energydifference_1=0.01;
404 E_1_GaAs=(minimum_1_GaAs:step_1_GaAs:maximum_1_GaAs); %energies
      with steplength 0.01
405 antall_1_GaAs=round(((maximum_1_GaAs-minimum_1_GaAs)/step_1_GaAs)
      +1); %antall E i intervallet miniumum1:maximum1 eV må ha
      heltall derfor round
406
407 step_2_GaAs=0.1; %Steplength 0.1 for energies greater then 1.5
408 minimum_2_GaAs=maximum_1_GaAs; %miniumvalue is maximum of the
      other interval
409 maximum_2_GaAs=4.4; %Maximum value in the excel files for solar
      spectrum is 4.45, maximum allowed value for the formulas used
      later is 5.6!!! Because we have not got values for the abs.
      koeff of Al_0.9Ga_0.1As for greater energies
410 energydifference_2=0.1;
411 E_2_GaAs=(minimum_2_GaAs:step_2_GaAs:maximum_2_GaAs); %energies
      with steplength 0.1
412 antall_2_GaAs=round(((maximum_2_GaAs-minimum_2_GaAs)/step_2_GaAs)
      +1); %antall E i intervallet miniumum2:maximum2 eV må ha
      heltall derfor round
413
414 alpha_GaAs_1=zeros(1,antall_1_GaAs); %absorption coefficient for
      energies with steplength 0.01
415 alpha_GaAs_2=zeros(1,antall_2_GaAs); %absorption coefficient for
      energies with steplength 0.1
416 R_GaAs_1=zeros(1,antall_1_GaAs); %reflectivity values for energies
       with steplength 0.01
417 R_GaAs_2=zeros(1,antall_2_GaAs); %reflectivity values for energies
       with steplength 0.1
```

```
418 n_GaAs_1=zeros(1,antall_1_GaAs); %refractive index
419 n_GaAs_2=zeros(1,antall_2_GaAs); %refractive index
420
421
422 k=1;
423
424  for i=1:antall_1_GaAs
425      if E_1_GaAs(i)<1.36
426          alpha_GaAs_1(i)=0; %for energies less than 1.36 eV the
                absorption coefficient is equal to zero
427          R_GaAs_1(i)=R_GaAsny(1);
428         n_GaAs_1(i)=n_GaAsny(1);
429      else
430         while ~(photonenergy_GaAsny(k)-(energydifference_1*0.5)<=
               E_1_GaAs(i)&& E_1_GaAs(i)<photonenergy_GaAsny(k)+(
               energydifference_1*0.5))
431             k=k+1;
432         end
433
434         alpha_GaAs_1(i)=alpha_GaAsny(k);
435         R_GaAs_1(i)=R_GaAsny(k);
436         n_GaAs_1(i)=n_GaAsny(k);
437      end
438  end
439
440  j=k;
441  for i=1:antall_2_GaAs
442     while ~(photonenergy_GaAsny(j)-(energydifference_2*0.5)<=
           E_2_GaAs(i)&& E_2_GaAs(i)<photonenergy_GaAsny(j)+(
           energydifference_2*0.5))
443         j=j+1;
444     end
445
446      alpha_GaAs_2(i)=alpha_GaAsny(j);
447      R_GaAs_2(i)=R_GaAsny(k);
448      n_GaAs_2(i)=n_GaAsny(k);
449  end
450
451 %Interpolation
452  pp_GaAs_1 = interp1(E_1_GaAs,alpha_GaAs_1,'cubic','pp'); %
        interpolates absorption coefficient
453  pp_GaAs_1_R = interp1(E_1_GaAs,R_GaAs_1,'cubic','pp'); %
        interpolates reflectivity values
454  pp_GaAs_1_n=interp1(E_1_GaAs,n_GaAs_1,'cubic','pp'); %
        interpolates refractive index values
455
456  zi_GaAs_1 = minimum_1_GaAs:step_endelig:maximum_1_GaAs;
457
458  yi_GaAs_1 = ppval(pp_GaAs_1,zi_GaAs_1); %interpolates absorption
        coefficient
459  yi_GaAs_1_R = ppval(pp_GaAs_1_R,zi_GaAs_1); %interpolates
        reflectivity values
```

```
460 yi_GaAs_1_n = ppval(pp_GaAs_1_n,zi_GaAs_1); %interpolates
       refractive index values
461
462 antall_endelig_1_GaAs=round(((maximum_1_GaAs-minimum_1_GaAs)/
       step_endelig)+1); %number of values for alpha for energies
       less then 1.5
463
464 pp_GaAs_2 = interp1(E_2_GaAs,alpha_GaAs_2,'cubic','pp'); %
       interpolates absorption coefficient
465 pp_GaAs_2_R = interp1(E_2_GaAs,R_GaAs_2,'cubic','pp'); %
       interpolates reflectivity values
466 pp_GaAs_2_n = interp1(E_2_GaAs,n_GaAs_2,'cubic','pp'); %
       interpolates refractive index values
467
468 zi_GaAs_2 = minimum_2_GaAs:step_endelig:maximum_2_GaAs;
469
470 yi_GaAs_2 = ppval(pp_GaAs_2,zi_GaAs_2); %interpolates absorption
       coefficient
471 yi_GaAs_2_R = ppval(pp_GaAs_2_R,zi_GaAs_2); %interpolates
       reflectivity values
472 yi_GaAs_2_n = ppval(pp_GaAs_2_n,zi_GaAs_2); %interpolates
       refractive index values
473
474 antall_endelig_2_GaAs=round(((maximum_2_GaAs-minimum_2_GaAs)/
       step_endelig)+1); %number of values for absorption
       coefficients for energies greater then 1.5
475
476 antall_endelig=antall_endelig_1_GaAs+antall_endelig_2_GaAs-1; %
       number of values in the final tables for alpha, (minus 1
       because the value for E=1.5 eV should not be counted to times)
477
478 zi_endelig=zeros(1,antall_endelig); %final energies,
479 alpha_GaAs_endelig=zeros(1,antall_endelig); %interpolated
       absorption coefficient, the values will be used later
480 R_GaAs_endelig=zeros(numberofdevices,antall_endelig); %
       interpolated reflectivity values
481 n_GaAs_endelig=zeros(1,antall_endelig); %interpolated refractive
       index values
482
483 for i=1:antall_endelig_1_GaAs
484     zi_endelig(i)=zi_GaAs_1(i);
485     for a=1:numberofdevices
486         if ARC(a)==0 %no anti-reflective coating
487         R_GaAs_endelig(a,i)=yi_GaAs_1_R(i);
488         else
489          R_GaAs_endelig(a,i)=0;
490         end
491     end
492     n_GaAs_endelig(i)=yi_GaAs_1_n(i);
493     alpha_GaAs_endelig(i)=yi_GaAs_1(i);
494 end
495
496 for i=antall_endelig_1_GaAs+1:antall_endelig;
```

```
497        zi_endelig(i)=zi_GaAs_2(i+1-antall_endelig_1_GaAs); %the
              value for E=1.5 eV should not be counted to times,
              therefore i+1
498         for a=1:numberofdevices
499           if ARC(a)==0 %no anti-reflective coating
500           R_GaAs_endelig(a,i)=yi_GaAs_2_R(i+1-antall_endelig_1_GaAs)
                 ;
501           else
502            R_GaAs_endelig(a,i)=0;
503           end
504         end
505         n_GaAs_endelig(i)=yi_GaAs_2_n(i+1-antall_endelig_1_GaAs);
506         alpha_GaAs_endelig(i)=yi_GaAs_2(i+1-antall_endelig_1_GaAs);
507   end
508
509
510     %Getting values for AlGaAs uses energy shift from paxmann and
            connolly
511
512   E_AlGaAs=zeros(numberofdevices,antall_endelig);
513
514   alpha_AlGaAs=zeros(numberofdevices,antall_endelig);
515
516
517   alpha_AlGaAs_sameenergy=zeros(numberofdevices,antall_endelig);
518
519   for h=1:numberofdevices
520      for i=1:antall_endelig
521      alpha_AlGaAs(h,i)=alpha_GaAs_endelig(i);
522      E_AlGaAs(h,i)=zi_endelig(i)+(1.247*x_cell(h))-(0.62*x_cell(h)*
            sqrt(zi_endelig(i)-(E_GaAs./eV))*(1/(exp(-10*(zi_endelig(i)
            -(E_GaAs./eV)))+1)));
523      end
524   end
525   E_AlGaAs(2,antall_endelig)
526
527    f=[1,1,1,1,1,1,1,1,1,1];
528    for h=1:numberofdevices
529      for i=1:antall_endelig
530          if x_cell(h)==0
531          else
532              if imag(E_AlGaAs(h,f(h)))~=0
533              alpha_AlGaAs_sameenergy(h,i)=0;
534              f(h)=f(h)+1;
535              else
536
537                  if (zi_endelig(i)<E_AlGaAs(h,f(h))&&imag(E_AlGaAs(
                        h,f(h)-1))~=0)
538                  alpha_AlGaAs_sameenergy(h,i)=0;
539                  else
540
541                      while ~ (E_AlGaAs(h,f(h))<=zi_endelig(i) &&
                            zi_endelig(i)<E_AlGaAs(h,f(h)+1))
```

```
542                             f(h)=f(h)+1;
543                         end
544                     alpha_AlGaAs_sameenergy(h,i)=alpha_AlGaAs(h,f(h));
545                     end
546                 end
547             end
548         end
549     end
550
551
552 %Values for absorption coefficient for Al_0.804Ga_0.196As
553 numwindow_0804=xlsread('C:\Documents␣and␣Settings\Kirsti␣Kvanes\
        Mine␣dokumenter\MATLAB\Master\AlGaAs␣0804␣optiske␣parametre');
554 %Comment: absorption coefficients were originally given as 10^-3
        multiplied by the
555 %values in the excel file, this was pr cm, to get correct
        absorption coefficients pr
556 %m, multiply with 10^2*10^3
557 photonenergy_window=numwindow_0804(:,1); %photonenergies for Al_0
        .804Ga_0.196As used in the excel files
558 alpha_window_0804=1e5.*numwindow_0804(:,2); %absorption
        coefficient for Al_0.804Ga_0.196As
559
560
561 %Values for absorption coefficient for Al_0.900Ga_0.100As
562 numwindow_0900=xlsread('C:\Documents␣and␣Settings\Kirsti␣Kvanes\
        Mine␣dokumenter\MATLAB\Master\AlGaAs␣0900␣optiske␣parametre');
563 %Comment: absorption coefficients were originally given as 10^-3
        multiplied by the
564 %values in the excel file, this was pr cm, to get correct
        absorption coefficients pr
565 %m, multiply with 10^2*10^3
566 alpha_window_0900=1e5.*numwindow_0900(:,2); %absorption
        coefficient for Al_0.900Ga_0.100As
567
568
569 %Getting values for Al_0.804Ga0.196As
570  %The absorption coefficient is set to zero for energies less than
          1.5 eV
571  %Uses the excel file for energies greater than 1.5 eV which has
         an energy
572  %step equal to 0.1 eV. This is different than the values for GaAs
          where
573  %two different energy steps are used
574
575 step_window=0.1; %Steplength 0.1 in the excel file
576 minimum_window=minimum_1_GaAs;%*eV; %minimum value in the excel
        files for solar spectrum is 0.3104, minium value in the excel
        file for absorption coeff is 1.36!!!
577 maximum_window=maximum_2_GaAs;%*eV; %Maximum value in the excel
        files for solar spectrum is 4.45, maximum allowed value for the
         formulas used later is 5.6!!! Because we have not got values
        for the abs.koeff of Al_0.9Ga_0.1As for greater energies
```

```
578 E_window_table=(minimum_window:step_window:maximum_window);
579 antall_window=floor((maximum_window-minimum_window)./step_window
        +1); %number of E in the excel file
580
581 alpha_AlGaAs_window_temp_0804=zeros(1,antall_window);
582
583 windownumber_0804=1;
584
585  for i=1:antall_window
586       if E_window_table(i)<1.5
587            alpha_AlGaAs_window_temp_0804(i)=0; %for energies less
                 than 1.5 eV the absorption coefficient is equal to
                 zero
588       else
589          while ~(photonenergy_window(windownumber_0804)-(
             step_window*0.5)<=E_window_table(i)&& E_window_table(i)
             <photonenergy_window(windownumber_0804)+(step_window
             *0.5))
590               windownumber_0804=windownumber_0804+1;
591          end
592
593          alpha_AlGaAs_window_temp_0804(i)=alpha_window_0804(
             windownumber_0804);
594       end
595  end
596
597 %Interpolation
598  pp_window_0804 = interp1(E_window_table,
        alpha_AlGaAs_window_temp_0804,'cubic','pp'); %interpolates
        absorption coefficients
599  yi_window_0804 = ppval(pp_window_0804,zi_endelig); %interpolates
        absorption coefficients
600  alpha_AlGaAs_window_0804_final=zeros(antall_endelig); %
        interpolated absorption coefficients, the values will be used
        later
601  for i=1:antall_endelig
602       alpha_AlGaAs_window_0804_final(i)=yi_window_0804(i);
603  end
604
605 %Getting values for Al_0.900Ga0.100As
606  %The absorption coefficient is set to zero for energies less than
         1.5 eV
607  %Uses the excel file for energies greater than 1.5 eV which has
        an energy
608  %step equal to 0.1 eV. This is different than the values for GaAs
         where
609  %two different energy steps are used
610
611 alpha_AlGaAs_window_temp_0900=zeros(1,antall_window);
612
613 windownumber_0900=1;
614
615  for i=1:antall_window
```

```
616       if E_window_table(i)<1.5
617           alpha_AlGaAs_window_temp_0900(i)=0; %for energies less
                 than 1.5 eV the absorption coefficient is equal to
                 zero
618       else
619          while ~(photonenergy_window(windownumber_0900)-(
                step_window*0.5)<=E_window_table(i)&& E_window_table(i)
                <photonenergy_window(windownumber_0900)+(step_window
                *0.5))
620              windownumber_0900=windownumber_0900+1;
621          end
622          alpha_AlGaAs_window_temp_0900(i)=alpha_window_0900(
                windownumber_0900);
623       end
624   end
625
626  %Interpolation
627   pp_window_0900 = interp1(E_window_table,
         alpha_AlGaAs_window_temp_0900,'cubic','pp'); %interpolates
         absorption coefficients
628   yi_window_0900 = ppval(pp_window_0900,zi_endelig); %interpolates
         absorption coefficients
629
630   alpha_AlGaAs_window_0900_final=zeros(antall_endelig); %
         interpolated absorption coefficients, the values will be used
         later
631   for i=1:antall_endelig
632       alpha_AlGaAs_window_0900_final(i)=yi_window_0900(i);
633   end
634
635
636   %Getting values for absorption coefficient in window layer made
         of Al_0.85Ga_0.15As uses energy shift and average
637   %value of x=0.804 and x=0.90 from "Properties of AlGaAs book"
638
639   alpha_AlGaAs_window_0804_shifted=zeros(numberofdevices,
         antall_endelig);
640   alpha_AlGaAs_window_0900_shifted=zeros(numberofdevices,
         antall_endelig);
641   alpha_AlGaAs_window=zeros(numberofdevices,antall_endelig);
642
643   for a=1:numberofdevices
644          for i=1:antall_endelig
645            if (i-round(((0.005.*x_window(a))+(0.245.*x_window(a)
                 .^2)-((0.005.*0.804)+(0.245.*0.804.^2)))./
                 step_endelig)) <=0 &&(i-round(((0.005.*x_window(a))
                 +(0.245.*x_window(a).^2)-((0.005.*0.900)
                 +(0.245.*0.900.^2)))./step_endelig))>antall_endelig
646            alpha_AlGaAs_window_0804_shifted(a,i)=0;
647            alpha_AlGaAs_window_0900_shifted(a,i)=
                 alpha_AlGaAs_window_0900_final(antall_endelig);
648            elseif (i-round(((0.005.*x_window(a))+(0.245.*x_window(a
                 ).^2)-((0.005.*0.804)+(0.245.*0.804.^2)))./
```

```
                step_endelig)) <=0
649             alpha_AlGaAs_window_0804_shifted(a,i)=0;
650             alpha_AlGaAs_window_0900_shifted(a,i)=
                    alpha_AlGaAs_window_0900_final(i-round(((0.005.*
                    x_window(a))+(0.245.*x_window(a).^2)
                    -((0.005.*0.900)+(0.245.*0.900.^2)))./step_endelig
                    ));
651         elseif (i-round(((0.005.*x_window(a))+(0.245.*x_window(a
                ).^2)-((0.005.*0.900)+(0.245.*0.900.^2)))./
                step_endelig))>antall_endelig
652             alpha_AlGaAs_window_0900_shifted(a,i)=
                    alpha_AlGaAs_window_0900_final(antall_endelig);
653             alpha_AlGaAs_window_0804_shifted(a,i)=
                    alpha_AlGaAs_window_0804_final(i-round(((0.005.*
                    x_window(a))+(0.245.*x_window(a).^2)
                    -((0.005.*0.804)+(0.245.*0.804.^2)))./step_endelig
                    ));
654         else
655           alpha_AlGaAs_window_0804_shifted(a,i)=
                alpha_AlGaAs_window_0804_final(i-round(((0.005.*
                x_window(a))+(0.245.*x_window(a).^2)-((0.005.*0.804)
                +(0.245.*0.804.^2)))./step_endelig));
656           alpha_AlGaAs_window_0900_shifted(a,i)=
                alpha_AlGaAs_window_0900_final(i-round(((0.005.*
                x_window(a))+(0.245.*x_window(a).^2)-((0.005.*0.900)
                +(0.245.*0.900.^2)))./step_endelig));
657           end
658         alpha_AlGaAs_window(a,i)=0.5.*(
              alpha_AlGaAs_window_0804_shifted(a,i)+
              alpha_AlGaAs_window_0900_shifted(a,i));
659         end
660  end
661
662
663 %MODEL
664 L_e=zeros(1,numberofdevices); %electron diffusion length in
        intermediate band material
665 L_h=zeros(1,numberofdevices); %hole diffusion length in
        intermediate band material
666
667 for i=1:numberofdevices
668 L_e(i)=sqrt(diffusionconstant_e(i).*(tau_n_GaAs+tau_p_GaAs));
669 L_h(i)=sqrt(diffusionconstant_h(i).*(tau_n_GaAs+tau_p_GaAs));
670 end
671
672 l_n=zeros(1,numberofdevices); %Definition
673 l_p=zeros(1,numberofdevices); %Definition
674 l_n_plus=zeros(1,numberofdevices); %Definition
675 l_p_plus=zeros(1,numberofdevices); %Definition
676
677 for i=1:numberofdevices
678     l_n(i)=((S_eff_p(i).*difflength_n_p(i))./
            diffusioncoefficient_n_p(i));
```

```
679      l_n_plus(i)=((S_eff_window(i).*difflength_n_p_plus(i))./
            diffusioncoefficient_n_p_plus(i)); %S_eff_window is front
            surface recombination velocity of the p_plus layer with or
            without window layer
680      l_p(i)=((S_eff_n(i).*difflength_p_n(i))./
            diffusioncoefficient_p_n(i));
681      l_p_plus(i)=((S_n_plus(i).*difflength_p_n_plus(i))./
            diffusioncoefficient_p_n_plus(i)); %S_n-plus is surface
            recombination velocity of the n_plus layer
682
683  end
684
685
686  alpha_CI_new=zeros(numberofdevices,antall_endelig); %absorption
        coefficient IB-CB transitions in (/m)
687  alpha_IV_new=zeros(numberofdevices,antall_endelig); %absorption
        coefficient VB-IB transitions in (/m)
688  alpha_CV_new=zeros(numberofdevices,antall_endelig); %absorption
        coefficient VB-CB transitions in (/m)
689
690  for a=1:numberofdevices
691      for i=1:antall_endelig
692          if (zi_endelig(i)<(E_L(a)/eV))
693              alpha_CI_new(a,i)=0;
694              alpha_IV_new(a,i)=0;
695              alpha_CV_new(a,i)=0;
696
697          elseif ((E_L(a)/eV)<=zi_endelig(i)&&zi_endelig(i)<E_H(a)/
                eV)
698              alpha_CI_new(a,i)=0;
699               alpha_IV_new(a,i)=0;
700              alpha_CV_new(a,i)=0;
701
702          elseif ((E_H(a)/eV)<=zi_endelig(i)&&zi_endelig(i)<E_G(a)/
                eV)
703              alpha_CI_new(a,i)=0;
704               alpha_IV_new(a,i)=0;
705              alpha_CV_new(a,i)=0;
706          else
707                  alpha_CI_new(a,i)=0;
708               alpha_IV_new(a,i)=0;
709                  if x_cell(a)==0
710                  alpha_CV_new(a,i)=alpha_GaAs_endelig(i); %use
                        tabulated values for the absorption coefficient
                         of GaAs
711                  else
712                  alpha_CV_new(a,i)=alpha_AlGaAs_sameenergy(a,i);
713                  %alpha_CV_new(1,i)=alpha_CV_temp(1);
714                  %alpha_CV_new(2,i)=alpha_GaAs_endelig(i);
715                  end
716          end
717      end
718  end
```

```
719
720 %Voltages
721 minimumv=minimumvoltage;
722 maximumv=maximumvoltage;
723 stepv=stepvoltage;
724 antall=round((maximumv-minimumv)/stepv+1);
725
726 %Voltage=zeros(antall); %voltage over cell Voltage=V_VC-J*R_s*area
727 V_VC=minimumv:stepv:maximumv; %e_charge*V_VC difference between
      the CB and VB quasi-Fermi levels
728 Voltage=V_VC;
729
730 Q_electron=zeros(numberofdevices,antall_endelig,antall); %Quantum
      efficiency for electrons in IB material
731 Q_hole=zeros(numberofdevices,antall_endelig,antall);     %Quantum
      efficiency for holes in IB material
732 Q_p_plus_special=zeros(numberofdevices,antall_endelig,antall); %
      Quantum efficiency for holes in n-plus-layer
733 Q_p_dep_special=zeros(numberofdevices,antall_endelig,antall); %
      Quantum efficiency for holes in depletion layer between n and n
      -plus
734 Q_p_special=zeros(numberofdevices,antall_endelig,antall); %Quantum
       efficiency for holes in n-layer
735 Q_dep_i_p_special=zeros(numberofdevices,antall_endelig,antall); %
      Quantum efficiency for electrons in depletion region between p
      layer and IB material
736 Q_dep_i_n_special=zeros(numberofdevices,antall_endelig,antall); %
      Quantum efficiency for holes in depletion region between IB
      material and n layer
737 Q_n_special=zeros(numberofdevices,antall_endelig,antall); %Quantum
       efficiency for electrons in p-layer
738 Q_n_dep_special=zeros(numberofdevices,antall_endelig,antall); %
      Quantum efficiency for electrons in depletion-layer between p
      and p-plus
739 Q_n_plus_special=zeros(numberofdevices,antall_endelig,antall); %
      Quantum efficiency for electrons in p-plus-layer
740
741 dep_width_n_i=zeros(numberofdevices,antall); %depletion width
      between i and n layer
742 dep_width_p_i=zeros(numberofdevices,antall); %depletion width
      between i and p layer
743
744 width_FB_IB=zeros(numberofdevices,antall); %width of IB in flat
      band
745
746
747 B_factor=zeros(numberofdevices,antall); %factor important in
      determining the voltage over the p-i and i-n junction
748 equationvoltage=zeros(numberofdevices,antall); %equation needed in
       finding the voltage over the p-i and i-n junction
749 V_p=zeros(numberofdevices,antall); %part of the applied voltage
      over the p-i junction
```

```
750 V_n=zeros(numberofdevices,antall);  %part of the applied voltage
        over the n-i junction
751
752 for a=1:numberofdevices
753     for i=1:antall
754 B_factor(a,i)=((N_I./cm^3)/ni_intrinsic(a)).^2.*exp(-e_charge.*
        V_VC(i)./(k_Boltzman.*T));
755 equationvoltage(a,i)=0.5.*(-B_factor(a,i)+sqrt(B_factor(a,i)
        .^2+(4.*(B_factor(a,i)+exp(-2.*e_charge.*V_bi_p_i(a)./(
        k_Boltzman.*T))))));
756
757 V_p(a,i)=-log(equationvoltage(a,i)).*k_Boltzman.*T./e_charge;
758 V_n(a,i)=V_VC(i)-V_p(a,i);
759     end
760 end
761
762     figure(200)
763 plot(V_VC,V_p(1,:))
764
765 figure(201)
766 plot(V_VC,V_n(1,:))
767
768
769 for a=1:numberofdevices
770     for i=1:antall
771         dep_width_n_i(a,i)=sqrt((V_bi_n_i(a)-(V_n(a,i))).*2.*
                epsilon_n(a).*(N_D_n(a)./cm.^3)./(e_charge.*(((N_D_n(a)
                ./cm.^3).*(N_I./cm.^3))+((N_I./cm.^3).^2))));
772         dep_width_p_i(a,i)=sqrt(2.*epsilon_p(a).*k_Boltzman.*T./(
                e_charge.^2.*(N_I./cm.^3))).*atan((e_charge.*(V_bi_p_i(
                a)-V_p(a,i))./(k_Boltzman.*T)).*sqrt(N_A_p(a)./(N_I.*2)
                ));
773
774         if (width_intrinsic(a)-dep_width_p_i(a,i)-dep_width_n_i(a,
                i))>0
775              width_FB_IB(a,i)=width_intrinsic(a)-dep_width_p_i(a,i)
                     -dep_width_n_i(a,i);
776
777        else
778            width_FB_IB(a,i)=0;
779             dep_width_n_i(a,i)=width_intrinsic(a);
780
781        end
782     end
783 end
784
785
786 for i=1:antall_endelig
787     for a=1:numberofdevices
788         for b=1:antall
789  Q_electron(a,i,b)=-(1-R_GaAs_endelig(a,i)).*(exp(-
        alpha_AlGaAs_window(a,i).*width_window(a)).*exp(-alpha_CV_new(
        a,i).*(width_p_plus(a)+width_p(a)+dep_width_p_i(a,b))).*(
```

```
     alpha_CI_new(a,i).*L_e(a)./((alpha_CI_new(a,i).*L_e(a)).^2-1))
     .*((((exp(-alpha_CI_new(a,i).*width_FB_IB(a,b)).*(sinh(
     width_FB_IB(a,b)./L_e(a))))-((alpha_CI_new(a,i).*L_e(a)))))./(
     cosh(width_FB_IB(a,b)./L_e(a))))+alpha_CI_new(a,i).*L_e(a).*
     exp(-alpha_CI_new(a,i).*width_FB_IB(a,b))))-(1-R_GaAs_endelig(
     a,i)).*(exp(-alpha_AlGaAs_window(a,i).*width_window(a)).*exp(-
     alpha_CV_new(a,i).*(width_p_plus(a)+width_p(a)+dep_width_p_i(a
     ,b))).*(alpha_CV_new(a,i).*L_e(a)./((alpha_CV_new(a,i).*L_e(a)
     ).^2-1)).*((((exp(-alpha_CV_new(a,i).*width_FB_IB(a,b)).*(sinh
     (width_FB_IB(a,b)./L_e(a))))-((alpha_CV_new(a,i).*L_e(a))))./(
     cosh(width_FB_IB(a,b)./L_e(a))))+alpha_CV_new(a,i).*L_e(a).*
     exp(-alpha_CV_new(a,i).*width_FB_IB(a,b))));
790  Q_hole(a,i,b)=-(1-R_GaAs_endelig(a,i)).*(exp(-alpha_AlGaAs_window
     (a,i).*width_window(a)).*exp(-alpha_CV_new(a,i).*(width_p_plus
     (a)+width_p(a)+dep_width_p_i(a,b))).*(alpha_IV_new(a,i).*L_h(a
     )./((alpha_IV_new(a,i).*L_h(a)).^2-1)).*(((((sinh(width_FB_IB(
     a,b)./L_h(a))))-(exp(-alpha_IV_new(a,i).*width_FB_IB(a,b))
     .*(-(alpha_IV_new(a,i).*L_h(a))))))./(cosh(width_FB_IB(a,b)./
     L_h(a))))-alpha_IV_new(a,i).*L_h(a)))-(1-R_GaAs_endelig(a,i))
     .*(exp(-alpha_AlGaAs_window(a,i).*width_window(a)).*exp(-
     alpha_CV_new(a,i).*(width_p_plus(a)+width_p(a)+dep_width_p_i(a
     ,b))).*(alpha_CV_new(a,i).*L_h(a)./((alpha_CV_new(a,i).*L_h(a)
     ).^2-1)).*(((((sinh(width_FB_IB(a,b)./L_h(a))))-(exp(-
     alpha_CV_new(a,i).*width_FB_IB(a,b)).*(-(alpha_CV_new(a,i).*
     L_h(a))))))./(cosh(width_FB_IB(a,b)./L_h(a))))-alpha_CV_new(a,i
     ).*L_h(a)));
791
792  Q_n_dep_special(a,i,b)=(1-R_GaAs_endelig(a,i)).*exp(-((
     alpha_CV_new(a,i).*width_p_plus(a))+(alpha_AlGaAs_window(a,i)
     .*width_window(a)))).*(1-exp(-alpha_CV_new(a,i).*
     dep_width_p_plus(a)))./cosh(width_p_undepleted(a)./
     difflength_n_p(a));
793  Q_n_plus_special(a,i,b)=(1-R_GaAs_endelig(a,i)).*(alpha_CV_new(a,
     i).*difflength_n_p_plus(a)./(((alpha_CV_new(a,i).*
     difflength_n_p_plus(a)).^2)-1)).*exp(-(alpha_AlGaAs_window(a,i
     ).*width_window(a))).*((l_n_plus(a)+(alpha_CV_new(a,i).*
     difflength_n_p_plus(a))-(exp(-alpha_CV_new(a,i).*width_p_plus(
     a)).*((l_n_plus(a)*cosh(width_p_plus(a)./difflength_n_p_plus(a
     )))+(sinh(width_p_plus(a)./difflength_n_p_plus(a))))))./((
     l_n_plus(a).*sinh(width_p_plus(a)./difflength_n_p_plus(a)))+
     cosh(width_p_plus(a)./difflength_n_p_plus(a)))-(alpha_CV_new(a
     ,i).*difflength_n_p_plus(a).*exp(-(alpha_CV_new(a,i).*
     width_p_plus(a))))).*((1./(1+(N_A_p_plus(a).*S_eff_p(a)./(
     N_A_p(a).*S_eff_p_plus_p(a)))))./cosh(width_p_undepleted(a)./
     difflength_n_p(a));
794  Q_n_special(a,i,b)=(1-R_GaAs_endelig(a,i)).*((alpha_CV_new(a,i).*
     difflength_n_p(a)./(((alpha_CV_new(a,i).*difflength_n_p(a))
     .^2)-1)).*exp(-((alpha_AlGaAs_window(a,i).*width_window(a))+(
     alpha_CV_new(a,i).*(width_p_plus(a)+dep_width_p_plus(a)))))
     .*((l_n(a)+(alpha_CV_new(a,i).*difflength_n_p(a))-(exp(-
     alpha_CV_new(a,i).*width_p_undepleted(a)).*((l_n(a)*cosh(
     width_p_undepleted(a)./difflength_n_p(a)))+(sinh(
     width_p_undepleted(a)./difflength_n_p(a))))))./((l_n(a).*sinh(
```

```
    width_p_undepleted(a)./difflength_n_p(a)))+cosh(
    width_p_undepleted(a)./difflength_n_p(a)))-(alpha_CV_new(a,i)
    .*difflength_n_p(a).*exp(-(alpha_CV_new(a,i).*
    width_p_undepleted(a))))));
795
796 Q_p_special(a,i,b)=(1-R_GaAs_endelig(a,i)).*(alpha_CV_new(a,i).*
    difflength_p_n(a)./((alpha_CV_new(a,i).*difflength_p_n(a))
    .^2-1).*exp(-((alpha_CV_new(a,i).*(width_p_plus(a)+width_p(a)+
    width_intrinsic(a)))+(alpha_AlGaAs_window(a,i).*width_window(a
    )))).*((alpha_CV_new(a,i).*difflength_p_n(a))-(((l_p(a).*(cosh
    (width_n_undepleted(a)./difflength_p_n(a))-exp(-alpha_CV_new(a
    ,i).*width_n_undepleted(a))))+sinh(width_n_undepleted(a)./
    difflength_p_n(a))+(alpha_CV_new(a,i).*difflength_p_n(a).*exp
    (-alpha_CV_new(a,i).*width_n_undepleted(a)))./((l_p(a).*sinh(
    width_n_undepleted(a)./difflength_p_n(a))+cosh(
    width_n_undepleted(a)./difflength_p_n(a))))));
797 Q_p_dep_special(a,i,b)=(1-R_GaAs_endelig(a,i)).*exp(-((
    alpha_CV_new(a,i).*(width_p_plus(a)+width_p(a)+width_intrinsic
    (a)+width_n_undepleted(a)))+(alpha_AlGaAs_window(a,i).*
    width_window(a)))).*(1-exp(-alpha_CV_new(a,i).*
    dep_width_n_plus(a)))./cosh(width_n_undepleted(a)./
    difflength_p_n(a));
798 Q_p_plus_special(a,i,b)=(1-R_GaAs_endelig(a,i)).*alpha_CV_new(a,i
    ).*difflength_p_n_plus(a)./((alpha_CV_new(a,i).*
    difflength_p_n_plus(a)).^2-1).*exp(-((alpha_CV_new(a,i).*(
    width_p_plus(a)+width_p(a)+width_intrinsic(a)+width_n(a)))+(
    alpha_AlGaAs_window(a,i).*width_window(a)))).*((alpha_CV_new(a
    ,i).*difflength_p_n_plus(a))-(((l_p_plus(a).*(cosh(
    width_n_plus(a)./difflength_p_n_plus(a))-exp(-alpha_CV_new(a,i
    ).*width_n_plus(a))))+sinh(width_n_plus(a)./
    difflength_p_n_plus(a))+(alpha_CV_new(a,i).*
    difflength_p_n_plus(a).*exp(-alpha_CV_new(a,i).*width_n_plus(a
    )))./((l_p_plus(a).*sinh(width_n_plus(a)./difflength_p_n_plus
    (a))+cosh(width_n_plus(a)./difflength_p_n_plus(a)))))
    .*(1./(1+(N_D_n_plus(a).*S_eff_n(a)./(N_D_n(a).*S_eff_n_plus_n
    (a))))))./cosh(width_n_undepleted(a)./difflength_p_n(a));
799
800 if   width_FB_IB(a,b)~=0
801 Q_dep_i_p_special(a,i,b)=(1-R_GaAs_endelig(a,i)).*exp(-((
    alpha_AlGaAs_window(a,i).*width_window(a))+(alpha_CV_new(a,i)
    .*(width_p_plus(a)+width_p(a))))).*(1-exp(-alpha_CV_new(a,i).*
    dep_width_p_i(a,b)));
802 Q_dep_i_n_special(a,i,b)=(1-R_GaAs_endelig(a,i)).*exp(-
    alpha_AlGaAs_window(a,i).*width_window(a)).*exp(-alpha_CV_new(
    a,i).*(width_p_plus(a)+width_p(a)+dep_width_p_i(a,b)+
    width_FB_IB(a,b))).*(1-exp(-alpha_CV_new(a,i).*dep_width_n_i(a
    ,b)));
803 end
804
805 if width_FB_IB(a,b)==0
806 Q_dep_i_p_special(a,i,b)=(1-R_GaAs_endelig(a,i)).*exp(-((
    alpha_AlGaAs_window(a,i).*width_window(a))+(alpha_CV_new(a,i)
    .*(width_p_plus(a)+width_p(a))))).*(1-exp(-alpha_CV_new(a,i).*
```

```
        width_intrinsic(a)));
807  Q_dep_i_n_special(a,i,b)=0;
808   end
809
810          end
811      end
812 end
813
814
815
816
817 %Strøm her tatt som negativ
818 photo_electron_current_IB=zeros(numberofdevices,antall); %
       photogenerated electron current at end of flat band (beginning
       of n-layer)
819 photo_hole_current_IB=zeros(numberofdevices,antall);      %
       photogenerated hole current at beginning of flat band (end of p
       -layer)
820 photo_electron_current=zeros(numberofdevices,antall);     %
       photogenerated electron current into p-layer
821 photo_hole_current=zeros(numberofdevices,antall);         %
       photogenerated hole current into n-layer
822 photo_current_0=zeros(numberofdevices,antall);            %total
       photogenerated current at beginning of flat band
823 photo_current_W=zeros(numberofdevices,antall);            %total
       photogenerated current at end of flat band
824
825 wavelength=1e+9.*(h_planck*c_light)./(zi_endelig.*eV); %Wavelength
        in (nm)
826
827 %Reading the necessary excel files
828
829 num = xlsread('C:\Documents␣and␣Settings\Kirsti␣Kvanes\Mine␣
       dokumenter\MATLAB\Prosjekt\Sp'); %Solar spectrum. Column 1 is
       wavelengths, column 2 is AM 1.5 given in W/(nm*m2), column 3 is
        incoming radiation in an energy intervall
830 %Column 4 is photonenergies, column 5 is photonflux in an
       energyinterval
831 wavelengthAM=num(:,1); %Wavelengths from excel
832 flux=num(:,5); %Incoming energy flux from excel
833
834 startexcel=1;
835
836 for a=1:numberofdevices
837     for b=1:antall
838         for i=antall_endelig:-1:1
839
840     if wavelengthAM(startexcel)<400
841         if abs((wavelengthAM(startexcel)-wavelength(i)))<0.25
842
843         else
844             photo_electron_current_IB(a,b)=(
                   photo_electron_current_IB(a,b))+(-1).*concentration(
```

```
                a).*flux(startexcel).*e_charge.*(1./cosh(width_FB_IB
                (a,b)./L_e(a))).*(Q_electron(a,i,b)+Q_n_special(a,i,
                b)+Q_n_plus_special(a,i,b)+Q_n_dep_special(a,i,b)+
                Q_dep_i_p_special(a,i,b)); %Photogenerated electron
                current at end of flat band
845             photo_hole_current_IB(a,b)=(photo_hole_current_IB(a,b))
                +(-1).*concentration(a).*flux(startexcel).*e_charge
                .*(1./cosh(width_FB_IB(a,b)./L_h(a))).*(Q_hole(a,i,b
                )+Q_p_special(a,i,b)+Q_p_plus_special(a,i,b)+
                Q_p_dep_special(a,i,b)+Q_dep_i_n_special(a,i,b)); %
                Photogenerated hole current at beginning of flat
                band
846             photo_electron_current(a,b)=photo_electron_current(a,b)
                +(-1).*concentration(a).*flux(startexcel).*e_charge
                .*(Q_n_special(a,i,b)+Q_n_plus_special(a,i,b)+
                Q_n_dep_special(a,i,b)+Q_dep_i_p_special(a,i,b));
847             photo_hole_current(a,b)=photo_hole_current(a,b)+(-1).*
                concentration(a).*flux(startexcel).*e_charge.*(
                Q_p_special(a,i,b)+Q_p_plus_special(a,i,b)+
                Q_p_dep_special(a,i,b)+Q_dep_i_n_special(a,i,b));
848              startexcel=startexcel+1;
849         end
850
851     elseif wavelengthAM(startexcel)>=400&&wavelengthAM(startexcel)
            <1700
852         if abs((wavelengthAM(startexcel)-wavelength(i)))<0.5
853
854         else
855             photo_electron_current_IB(a,b)=(
                photo_electron_current_IB(a,b))+(-1).*concentration(
                a).*flux(startexcel).*e_charge.*(1./cosh(width_FB_IB
                (a,b)./L_e(a))).*(Q_electron(a,i,b)+Q_n_special(a,i,
                b)+Q_n_plus_special(a,i,b)+Q_n_dep_special(a,i,b)+
                Q_dep_i_p_special(a,i,b)); %Photogenerated electron
                current at end of flat band
856             photo_hole_current_IB(a,b)=(photo_hole_current_IB(a,b))
                +(-1).*concentration(a).*flux(startexcel).*e_charge
                .*(1./cosh(width_FB_IB(a,b)./L_h(a))).*(Q_hole(a,i,b
                )+Q_p_special(a,i,b)+Q_p_plus_special(a,i,b)+
                Q_p_dep_special(a,i,b)+Q_dep_i_n_special(a,i,b)); %
                Photogenerated hole current at beginning of flat
                band
857             photo_electron_current(a,b)=photo_electron_current(a,b)
                +(-1).*concentration(a).*flux(startexcel).*e_charge
                .*(Q_n_special(a,i,b)+Q_n_plus_special(a,i,b)+
                Q_n_dep_special(a,i,b)+Q_dep_i_p_special(a,i,b));
858             photo_hole_current(a,b)=photo_hole_current(a,b)+(-1).*
                concentration(a).*flux(startexcel).*e_charge.*(
                Q_p_special(a,i,b)+Q_p_plus_special(a,i,b)+
                Q_p_dep_special(a,i,b)+Q_dep_i_n_special(a,i,b));
859
860              startexcel=startexcel+1;
861         end
```

```
862
863     elseif wavelengthAM(startexcel)>=1700
864         if abs((wavelengthAM(startexcel)-wavelength(i)))<2.5
865
866         else
867            photo_electron_current_IB(a,b)=(
               photo_electron_current_IB(a,b))+(-1).*concentration(
               a).*flux(startexcel).*e_charge.*(1./cosh(width_FB_IB
               (a,b)./L_e(a))).*(Q_electron(a,i,b)+Q_n_special(a,i,
               b)+Q_n_plus_special(a,i,b)+Q_n_dep_special(a,i,b)+
               Q_dep_i_p_special(a,i,b)); %Photogenerated electron
               current at end of flat band
868            photo_hole_current_IB(a,b)=(photo_hole_current_IB(a,b))
               +(-1).*concentration(a).*flux(startexcel).*e_charge
               .*(1./cosh(width_FB_IB(a,b)./L_h(a))).*(Q_hole(a,i,b
               )+Q_p_special(a,i,b)+Q_p_plus_special(a,i,b)+
               Q_p_dep_special(a,i,b)+Q_dep_i_n_special(a,i,b)); %
               Photogenerated hole current at beginning of flat
               band
869            photo_electron_current(a,b)=photo_electron_current(a,b)
               +(-1).*concentration(a).*flux(startexcel).*e_charge
               .*(Q_n_special(a,i,b)+Q_n_plus_special(a,i,b)+
               Q_n_dep_special(a,i,b)+Q_dep_i_p_special(a,i,b));
870            photo_hole_current(a,b)=photo_hole_current(a,b)+(-1).*
               concentration(a).*flux(startexcel).*e_charge.*(
               Q_p_special(a,i,b)+Q_p_plus_special(a,i,b)+
               Q_p_dep_special(a,i,b)+Q_dep_i_n_special(a,i,b));
871
872
873             startexcel=startexcel+1;
874         end
875
876     end
877         end
878         startexcel=1;
879         photo_current_0(a,b)=photo_electron_current(a,b)+
            photo_hole_current_IB(a,b);
880         photo_current_W(a,b)=photo_hole_current(a,b)+
            photo_electron_current_IB(a,b);
881
882     end
883
884 end
885
886
887 J_0_diode_1=zeros(1,numberofdevices);
888 J_0_diode_1_p_layer=zeros(1,numberofdevices);
889 J_0_diode_1_n_layer=zeros(1,numberofdevices);
890 J_0_diode_2_SCR=zeros(1,numberofdevices);
891
892
893 for a=1:numberofdevices
```

```
894     J_0_diode_1_p_layer(a)=e_charge.*(ni_GaAs.^2./(N_A_p(a)./cm
            .^3)).*(diffusioncoefficient_n_p(a)./difflength_n_p(a)).*((
            l_n(a)*cosh(width_p_undepleted(a)./difflength_n_p(a))+(
            sinh(width_p_undepleted(a)./difflength_n_p(a)))./((l_n(a)
            .*sinh(width_p_undepleted(a)./difflength_n_p(a))+cosh(
            width_p_undepleted(a)./difflength_n_p(a)));
895     J_0_diode_1_n_layer(a)=e_charge.*(ni_GaAs.^2./(N_D_n(a)./cm
            .^3)).*(diffusioncoefficient_p_n(a)./difflength_p_n(a)).*((
            l_p(a)*cosh(width_n_undepleted(a)./difflength_p_n(a))+(
            sinh(width_n_undepleted(a)./difflength_p_n(a)))./((l_p(a)
            .*sinh(width_n_undepleted(a)./difflength_p_n(a))+cosh(
            width_n_undepleted(a)./difflength_p_n(a)));
896     J_0_diode_1(a)=J_0_diode_1_p_layer(a)+J_0_diode_1_n_layer(a);
897     J_0_diode_2_SCR(a)=e_charge.*ni_intrinsic(a).*width_intrinsic(
            a)./(sqrt(tau_n_GaAs.*tau_p_GaAs)).*pi; %maximum
            recombination current, using equation (54) in Hovel with
            GaAs in intrinsic region
898 end
899
900
901
902 V_VI=zeros(numberofdevices,antall); %e_charge*V_VI difference
        between the IB and VB quasi-Fermi levels
903
904 V_IC=zeros(numberofdevices,antall); %e_charge*V_IC difference
        between the CV and IB quasi-Fermi levels
905
906 V_VI_mi=0;
907
908
909
910 %Need to find the value of the voltages, uses that
911 %V_VC=V_IC+V_VI %and that the currents from both of the terminals
        have to
912 %be equal
913 for a=1:numberofdevices
914     for i=1:antall
915
916    if   width_FB_IB(a,i)~=0
917      V_VI_mi=fsolve(@(V_VI_mi) photo_current_0(a,i)+(
             J_0_diode_1_p_layer(a).*(exp(e_charge.*V_VC(i)./(
             k_Boltzman.*T))-1))+((ni_cell(a).* dep_width_p_i(a,i)./
             sqrt(tau_p_GaAs.*tau_n_GaAs)).*pi.*sinh(e_charge.*V_p(a,i)
             ./(2.*k_Boltzman.*T))./((V_bi_p_i(a)-(V_p(a,i)))./(
             k_Boltzman.*T)))+(((1./cosh(width_FB_IB(a,i)./L_h(a))).*
             J_0_diode_1_n_layer(a)).*(exp(e_charge.*V_VC(i)./(
             k_Boltzman.*T))-1))+((1./cosh(width_FB_IB(a,i)./L_h(a)))
             .*((ni_cell(a).*dep_width_n_i(a,i)./sqrt(tau_p_GaAs.*
             tau_n_GaAs)).*pi.*sinh(e_charge.*V_n(a,i)./(2.*k_Boltzman
             .*T))./((V_bi_n_i(a)-(V_n(a,i)))./(k_Boltzman.*T))))+((
             e_charge.*diffusionconstant_h(a).*p_0(a).*(exp(e_charge.*
             V_VI_mi./(k_Boltzman.*T))-1)./L_h(a)).*(sinh(width_FB_IB(a
             ,i)./L_h(a)))./(cosh(width_FB_IB(a,i)./L_h(a))))-(
```

```
        photo_current_W(a,i)+(J_0_diode_1_n_layer(a).*(exp(
        e_charge.*V_VC(i)./(k_Boltzman.*T))-1))+((ni_cell(a).*
        dep_width_n_i(a,i)./sqrt(tau_p_GaAs.*tau_n_GaAs)).*pi.*
        sinh(e_charge.*V_n(a,i)./(2.*k_Boltzman.*T))./((V_bi_n_i(a
        )-(V_n(a,i)))./(k_Boltzman.*T)))+(((1./cosh(width_FB_IB(a,
        i)./L_e(a))).*J_0_diode_1_p_layer(a)).*(exp(e_charge.*V_VC
        (i)./(k_Boltzman.*T))-1))+((1./cosh(width_FB_IB(a,i)./L_e(
        a))).*((ni_cell(a).*dep_width_p_i(a,i)./sqrt(tau_p_GaAs.*
        tau_n_GaAs)).*pi.*sinh(e_charge.*V_p(a,i)./(2.*k_Boltzman
        .*T))./((V_bi_p_i(a)-(V_p(a,i)))./(k_Boltzman.*T))))+((
        e_charge.*diffusionconstant_e(a).*n_0(a).*(exp(e_charge.*(
        V_VC(i)-V_VI_mi)./(k_Boltzman.*T))-1)./L_e(a)).*(sinh(
        width_FB_IB(a,i)./L_e(a)))./(cosh(width_FB_IB(a,i)./L_e(a)
        )))),0,optimset('Display','off'));
918     end
919
920     if width_FB_IB(a,i)==0
921         V_VI_mi=0;
922     end
923
924      V_VI(a,i)=V_VI_mi;
925      end
926 end
927
928 for i=1:antall
929     for a=1:numberofdevices
930     V_IC(a,i)=V_VC(i)-V_VI(a,i);
931     end
932 end
933
934 total_current_0=zeros(numberofdevices,antall);
935 total_current_W=zeros(numberofdevices,antall);
936 J=zeros(numberofdevices,antall);
937 J_CV=zeros(numberofdevices,antall);
938 V_OC=zeros(1,numberofdevices); %open-circuit voltage
939 J_SC=zeros(1,numberofdevices); %short-circuit current
940
941
942
943 for a=1:numberofdevices
944     for i=1:antall
945  if   width_FB_IB(a,i)~=0
946
947      total_current_0(a,i)=(1/concentration(a)).*(photo_current_0(a
        ,i)+(J_0_diode_1_p_layer(a).*(exp(e_charge.*V_VC(i)./(
        k_Boltzman.*T))-1))+((ni_cell(a).* dep_width_p_i(a,i)./
        sqrt(tau_p_GaAs.*tau_n_GaAs)).*pi.*sinh(e_charge.*V_p(a,i)
        ./(2.*k_Boltzman.*T))./((V_bi_p_i(a)-(V_p(a,i)))./(
        k_Boltzman.*T)))+(((1./cosh(width_FB_IB(a,i)./L_h(a))).*
        J_0_diode_1_n_layer(a)).*(exp(e_charge.*V_VC(i)./(
        k_Boltzman.*T))-1))+((1./cosh(width_FB_IB(a,i)./L_h(a)))
        .*((ni_cell(a).*dep_width_n_i(a,i)./sqrt(tau_p_GaAs.*
        tau_n_GaAs)).*pi.*sinh(e_charge.*V_n(a,i)./(2.*k_Boltzman
```

```
            .*T))./((V_bi_n_i(a)-(V_n(a,i)))./(k_Boltzman.*T))))+((
            e_charge.*diffusionconstant_h(a).*p_0(a).*(exp(e_charge.*
            V_VI(a,i)./(k_Boltzman.*T))-1)./L_h(a)).*(sinh(width_FB_IB
            (a,i)./L_h(a)))./(cosh(width_FB_IB(a,i)./L_h(a)))));
948       total_current_W(a,i)=(1/concentration(a)).*(photo_current_W(a
            ,i)+(J_0_diode_1_n_layer(a).*(exp(e_charge.*V_VC(i)./(
            k_Boltzman.*T))-1))+((ni_cell(a).* dep_width_n_i(a,i)./
            sqrt(tau_p_GaAs.*tau_n_GaAs)).*pi.*sinh(e_charge.*V_n(a,i)
            ./(2.*k_Boltzman.*T))./((V_bi_n_i(a)-(V_n(a,i)))./(
            k_Boltzman.*T)))+(((1./cosh(width_FB_IB(a,i)./L_e(a))).*
            J_0_diode_1_p_layer(a)).*(exp(e_charge.*V_VC(i)./(
            k_Boltzman.*T))-1))+((1./cosh(width_FB_IB(a,i)./L_e(a)))
            .*((ni_cell(a).*dep_width_p_i(a,i)./sqrt(tau_p_GaAs.*
            tau_n_GaAs)).*pi.*sinh(e_charge.*V_p(a,i)./(2.*k_Boltzman
            .*T))./((V_bi_p_i(a)-(V_p(a,i)))./(k_Boltzman.*T))))+((
            e_charge.*diffusionconstant_e(a).*n_0(a).*(exp(e_charge.*(
            V_VC(i)-V_VI(a,i))./(k_Boltzman.*T))-1)./L_e(a)).*(sinh(
            width_FB_IB(a,i)./L_e(a)))./(cosh(width_FB_IB(a,i)./L_e(a)
            ))));
949
950      J(a,i)=-total_current_W(a,i);
951
952   end
953   if width_FB_IB(a,i)==0
954
955      J_CV(a,i)=J_0_diode_1(a).*(exp((e_charge.*V_VC(i))./(
           k_Boltzman.*T))-1)+(J_0_diode_2_SCR(a).*sinh(e_charge.*V_VC
           (i)./(2.*k_Boltzman.*T))./(e_charge.*(V_bi(a)-V_VC(i))./(
           k_Boltzman.*T))); %recombination current
956      J(a,i)=(1/concentration(a)).*(-photo_current_W(a,i)-J_CV(a,i))
           ; %current-voltage characteristic from equivalent circuit
957
958   end
959               if(abs(J(a,i))<=50)
960                   V_OC(a)=V_VC(i) %open-circuit voltage
961               end
962
963      end
964  end
965
966
967
968   for i=1:numberofdevices
969       J_SC(i)=J(i,1)
970   end
971
972  %Efficiency of cells
973  efficiency=zeros(numberofdevices,antall);
974  P_in=1e+3; %Power incident for AM 1.5
975
976  for a=1:numberofdevices
977      for i=1:antall
978          if J(a,i)>0
```

```
979                efficiency(a,i) = abs(V_VC(i)*J(a,i)*100)/P_in;
980            else
981                efficiency(a,i)=0;
982            end
983        end
984    end
985
986
987    efficiencymax=zeros(1,numberofdevices);
988    for i=1:numberofdevices
989    efficiencymax(i)=max(efficiency(i,:))
990    end
991    IVcurve=J;
```

Listing B.4: Photocurrent

B.5 Variables simple model of intermediate band solar cell

```
1  ---------------------------------------
2  Variables simple model of IB solar cell
3  ---------------------------------------
4  %Constants used in the different programs
5  h_planck=6.62607e-34; %Plancks constant h in Js
6  h_dirac=1.05457e-34; %Diracs constant=h/2pi in Js
7  m_e=9.10938e-31; %Electron mass in kg
8  eV=1.60218e-19; %electronvolt to joule
9  k_Boltzman = 1.38065e-23; %Boltzman constant J/K
10 freediec = 8.85419e-12; %Free dielectric constant in F/m
11 e_charge=1.60218e-19; %Charge of an electron in C
12 c_light = 2.99792e+8; %velocity of light m/s
13 T=300; %temperature used in article for solar cells in K
14 E_rydberg=13.6057*eV; %Rydberg energy
15 T_sun=6000; %Temperature of sun i K
16
17
18 %To meter m
19 nm=1e-9; %nanometer to meter
20 cm=1e-2; %centimeter to meter
21 micm=1e-6; %micrometer to meter
22 mm=1e-3; % millimeter to meter
23
24 %DATA USED IN THE MODEL
25 numberofdevices=1;
26
27 concentration=[1 1000 1000 1000 1 1000 1 1000]; %light
       concentration
28 width_IB=[0.65e-6 1.3e-6 1.3e-6 5.2e-6 5.2e-6]; %width of
       intermediate band
29
30 %Bandgap for GaAs
31 E_GaAs=(1.519-(5.405*(1e-4)*T^2/(T+204)))*eV; %from Lie!!
32
33 %Energysteps used to find the maximum efficiency
```

```
34 energystep=0.01;
35
36 energymin=1.39; %minimum value of E_H
37
38 energymax=1.39; %maximum value of E_H
39
40 energyvalues=round((energymax-energymin)./energystep)+1; %number
     of energies
41 %energyvalues=1;
42
43 E_H=(energymin:energystep:energymax).*eV; %bandgap
     intermediateband-valenceband
44 E_L=zeros(1,energyvalues); %bandgap conductionband-
     intermediateband
45 E_G=zeros(1,energyvalues); %bandgap conductionband-valenceband
46
47 %E_H=1.10.*eV;
48
49 for i=1:energyvalues
50 E_G(i)=E_GaAs;    %bandgap conductionband-valenceband
51 %E_G(i)=1.67.*eV;
52 E_L(i)=E_G(i)-E_H(i); %bandgap conductionband-intermediate band
53 %E_L=0.57.*eV;
54
55 end
56
57
58 alpha_CI_temp=[4e6 4e6 4e6 4e6 4e6 4e6 4e6 4e6]; %absorption
     coefficient intermediate band to conduction band transitions in
      /m
59 alpha_IV_temp=[4e6 4e6 4e6 4e6 4e6 4e6 4e6 4e6]; %absorption
     coefficient valence band to intermediate band transitions in /m
60 alpha_CV_temp=[4e6 4e6 4e6 4e6 4e6 4e6 4e6 4e6]; %absorption
     coefficient valence band to conduction band transitions in /m
61
62 mu_e=[0.8 0.2 0.8 0.8 0.8 0.8 0.8];       %mobility electrons in m
     ^2/(Vs)from Semiconducting and other properties of GaAs
63 mu_h=[0.04 0.2 0.04 0.04 0.04 0.04 0.04];       %mobility holes in
      m^2/(Vs) from semiconducting and other properties of GaAs
64
65 diffusionconstant_e=zeros(1,numberofdevices);
66 diffusionconstant_h=zeros(1,numberofdevices);
67
68 for i=1:numberofdevices
69 diffusionconstant_e(i)=(k_Boltzman.*T.*mu_e(i))./e_charge;    %
     diffusionconstant electrons
70 diffusionconstant_h(i)=(k_Boltzman.*T.*mu_h(i))./e_charge;    %
     diffusionconstant holes
71 end
72
73 %Non-radiative recombination lifetimes Taken from "Intermediate
     Band Solar
74 %Cells Using Nanotechnology"
```

```
75
76 tau_SRH_CI=[0.5e-12];   %non-radiative lifetime conduction band to
      intermediate band (in s), set equal to great value if only
     radiative recombination
77
78 tau_SRH_IV=[40e-12];   %non-radiative lifetime intermediate band
     to valence band (in s), set equal to great value if only
     radiative recombination
79
80 N_C=[4.7e23 5e24 4.7e23 4.7e23 4.7e23 4.7e23 4.7e23];       %
     densities of states conduction band in /m^3 from "Solar Cells
     Materials, Manufacture and Operation"
81 N_V=[7e24 5e24 7e24 7e24 7e24 7e24 7e24];       %densities of
     states valence band in /m^3 from "Solar Cells Materials,
     Manufacture and Operation"
82
83 n_0=zeros(energyvalues,numberofdevices);
84 p_0=zeros(energyvalues,numberofdevices);
85
86 for i=1:numberofdevices
87     for c=1:energyvalues
88 n_0(i,c)=N_C(i).*exp(-E_L(c)./(k_Boltzman.*T));     %equilibrium
     electron concentration in the conduction band
89 p_0(i,c)=N_V(i).*exp(-E_H(c)./(k_Boltzman.*T));     %equilibrium
     hole concentration in the valence band
90     end
91 end
92 ARC=[1 1 1 1 1 1 1 1]; %1 if anti-reflective coating, 0 if not
93 %Fraction of x in Al_xGa_(1-x)_As
94 x_window=[0.85 0.85 0.85 0.85 0.85 0.85 0.85 0.85];  %x in window
     layer
95
96 save 'simple.mat'
```

Listing B.5: Photocurrent

B.6 Radiative recombination coefficient in intermediate band solar cell

```
1 -----------------------------------------
2 Radiative recombination coefficient
3 -----------------------------------------
4 function integralcalculation=radiative_rec_coeff(alpha_a, y)
5
6 load 'simple.mat' %Loading the file containing all constants,
     remember to first run the program Variables
7 %Har regnet ut det bestemte integralet av E^2e^{-E/kT)
8
9
10 integralcalculation=-(8.*pi./(h_planck.^3.*c_light.^2)).*alpha_a.*
     k_Boltzman.*T.*((2.*k_Boltzman.^2*T.^2)+(2.*y.*k_Boltzman.*T)+y
```

```
.^2).*exp(-y/(k_Boltzman.*T));
```

Listing B.6: Photocurrent

B.7 Current-voltage characteristic simple model of intermediate band solar cell

```
1  -------------------------------------------------
2  Current voltage characteristic p-i-n solar cell,
3  no flat band
4  -------------------------------------------------
5  clear; %Clear all variables
6
7  load 'simple.mat' %Loading the file containing all constants,
      remember to first run the program Simplevariables
8
9  %Reading the necessary excel files
10
11 step_endelig=0.001; %steplength used in interpolation
12
13 %USES SHIFT OF ENERGY AXIS
14 num4=xlsread('C:\Documents␣and␣Settings\Kirsti␣Kvanes\Mine␣
      dokumenter\MATLAB\Prosjekt\GaAs␣optiske␣parametre');%Optical
      parameters for GaAs using shift of energy axis
15 %Comment: alpha values were originally given as 10^-3 multiplied
      by the
16 %values in the excel file, this was pr cm, to get correct alpha
      values pr
17 %m, multiply with 10^2*10^3
18 photonenergy_GaAsny=num4(:,1); %photonenergies for GaAs used in
      the excel files
19 alpha_GaAsny=1e5.*num4(:,4); %alpha values for GaAs
20 R_GaAsny=num4(:,3); %Reflectivity values for GaAs
21 n_GaAsny=num4(:,2); %Refractive index for GaAs
22
23
24 w_p=0*nm; %For p-i-n solar cell, depletion region into p-layer
      equal to zero
25 w_n=0*nm; %For p-i-n solar cell, depletion region  into n-layer
      equal to zero
26
27 %Getting values for GaAs
28 %Bruker mindre steglengder frem til 1.5 eV for der har jeg flere
      verdier
29 %HUSK at når har man flere steglengder, en steglengde for energier
       mindre
30 %enn 1.5 eV, en annen for energier større enn 1.5 eV og en tredje
      brukt i
31 %interpolering
32 %må ta hensyn til at minste verdi i excel-fila er 1.36 eV, setter
33 %absorpsjonskoeffisienten lik 0 for mindre verdier
34 step_1_GaAs=0.01;%*eV; %Steplength 0.01 for energies less then 1.5
```

```
35 minimum_1_GaAs=0.32;%*eV; %minimum value in the excel files for
      solar spectrum is 0.3104
36 maximum_1_GaAs=1.5;%*eV; %maximum allowed value 1.5 for energies
      larger then 1.5 we need a greater steplength
37 energydifference_1=0.01;
38 E_1_GaAs=(minimum_1_GaAs:step_1_GaAs:maximum_1_GaAs); %energies
      with steplength 0.01
39 antall_1_GaAs=round(((maximum_1_GaAs-minimum_1_GaAs)/step_1_GaAs)
      +1); %antall E i intervallet miniumum1:maximum1 eV må ha
      heltall derfor round
40
41 step_2_GaAs=0.1; %Steplength 0.1 for energies greater then 1.5
42 minimum_2_GaAs=maximum_1_GaAs; %miniumvalue is maximum of the
      other interval
43 maximum_2_GaAs=4.4; %Maximum value in the excel files for solar
      spectrum is 4.45, maximum allowed value for the formulas used
      later is 5.6!!!Because we have not got values for the abs.koeff
       of Al_0.9Ga_0.1As for greater energies
44 energydifference_2=0.1;
45 E_2_GaAs=(minimum_2_GaAs:step_2_GaAs:maximum_2_GaAs); %energies
      with steplength 0.1
46 antall_2_GaAs=round(((maximum_2_GaAs-minimum_2_GaAs)/step_2_GaAs)
      +1); %antall E i intervallet miniumum2:maximum2 eV må ha
      heltall derfor round
47
48 alpha_GaAs_1=zeros(1,antall_1_GaAs); %alpha values for energies
      with steplength 0.01
49 alpha_GaAs_2=zeros(1,antall_2_GaAs); %alpha values for energies
      with steplength 0.1
50 R_GaAs_1=zeros(1,antall_1_GaAs); %reflectivity values for energies
       with steplength 0.01
51 R_GaAs_2=zeros(1,antall_2_GaAs); %reflectivity values for energies
       with steplength 0.1
52 n_GaAs_1=zeros(1,antall_1_GaAs); %refractive index
53 n_GaAs_2=zeros(1,antall_2_GaAs); %refractive index
54
55
56 k=1;
57
58  for i=1:antall_1_GaAs
59      if E_1_GaAs(i)<1.36
60            alpha_GaAs_1(i)=0; %for energies less than 1.36 eV the
                  absorption coefficient is equal to zero
61            R_GaAs_1(i)=R_GaAsny(1);
62           n_GaAs_1(i)=n_GaAsny(1);
63      else
64           while ~(photonenergy_GaAsny(k)-(energydifference_1*0.5)<=
                 E_1_GaAs(i)&& E_1_GaAs(i)<photonenergy_GaAsny(k)+(
                 energydifference_1*0.5))
65               k=k+1;
66           end
67
68           alpha_GaAs_1(i)=alpha_GaAsny(k);
```

```
69          R_GaAs_1(i)=R_GaAsny(k);
70          n_GaAs_1(i)=n_GaAsny(k);
71       end
72   end
73
74   j=k;
75   for i=1:antall_2_GaAs
76      while ~(photonenergy_GaAsny(j)-(energydifference_2*0.5)<=
          E_2_GaAs(i)&& E_2_GaAs(i)<photonenergy_GaAsny(j)+(
          energydifference_2*0.5))
77          j=j+1;
78      end
79
80       alpha_GaAs_2(i)=alpha_GaAsny(j);
81       R_GaAs_2(i)=R_GaAsny(k);
82       n_GaAs_2(i)=n_GaAsny(k);
83   end
84
85  %Interpolation
86   pp_GaAs_1 = interp1(E_1_GaAs,alpha_GaAs_1,'cubic','pp'); %
        interpolates alpha values
87   pp_GaAs_1_R = interp1(E_1_GaAs,R_GaAs_1,'cubic','pp'); %
        interpolates reflectivity values
88   pp_GaAs_1_n=interp1(E_1_GaAs,n_GaAs_1,'cubic','pp'); %
        interpolates refractive index values
89
90   zi_GaAs_1 = minimum_1_GaAs:step_endelig:maximum_1_GaAs;
91
92   yi_GaAs_1 = ppval(pp_GaAs_1,zi_GaAs_1); %interpolates alpha
        values
93   yi_GaAs_1_R = ppval(pp_GaAs_1_R,zi_GaAs_1); %interpolates
        reflectivity values
94   yi_GaAs_1_n = ppval(pp_GaAs_1_n,zi_GaAs_1); %interpolates
        refractive index values
95
96   antall_endelig_1_GaAs=round(((maximum_1_GaAs-minimum_1_GaAs)/
        step_endelig)+1); %number of values for alpha for energies
        less then 1.5
97
98   pp_GaAs_2 = interp1(E_2_GaAs,alpha_GaAs_2,'cubic','pp'); %
        interpolates alpha values
99   pp_GaAs_2_R = interp1(E_2_GaAs,R_GaAs_2,'cubic','pp'); %
        interpolates reflectivity values
100  pp_GaAs_2_n = interp1(E_2_GaAs,n_GaAs_2,'cubic','pp'); %
        interpolates refractive index values
101
102  zi_GaAs_2 = minimum_2_GaAs:step_endelig:maximum_2_GaAs;
103
104  yi_GaAs_2 = ppval(pp_GaAs_2,zi_GaAs_2); %interpolates alpha
        values
105  yi_GaAs_2_R = ppval(pp_GaAs_2_R,zi_GaAs_2); %interpolates
        reflectivity values
```

```
106 yi_GaAs_2_n = ppval(pp_GaAs_2_n,zi_GaAs_2); %interpolates
       refractive index values
107
108 antall_endelig_2_GaAs=round(((maximum_2_GaAs-minimum_2_GaAs)/
       step_endelig)+1); %number of values for alpha for energies
       greater then 1.5
109
110 antall_endelig=antall_endelig_1_GaAs+antall_endelig_2_GaAs-1; %
       number of values in the final tables for alpha, (minus 1
       because the value for E=1.5 eV should not be counted to times)
111
112 zi_endelig=zeros(1,antall_endelig); %final energies,
113 alpha_GaAs_endelig=zeros(1,antall_endelig); %interpolated
       alphavalues, the values will be used later
114 R_GaAs_endelig=zeros(numberofdevices,antall_endelig); %
       interpolated reflectivity values
115 n_GaAs_endelig=zeros(1,antall_endelig); %interpolated refractive
       index values
116
117 for i=1:antall_endelig_1_GaAs
118     zi_endelig(i)=zi_GaAs_1(i);
119     for a=1:numberofdevices
120        if ARC(a)==0 %no anti-reflective coating
121        R_GaAs_endelig(a,i)=yi_GaAs_1_R(i);
122        else
123         R_GaAs_endelig(a,i)=0;
124        end
125     end
126     n_GaAs_endelig(i)=yi_GaAs_1_n(i);
127     alpha_GaAs_endelig(i)=yi_GaAs_1(i);
128 end
129
130 for i=antall_endelig_1_GaAs+1:antall_endelig;
131     zi_endelig(i)=zi_GaAs_2(i+1-antall_endelig_1_GaAs); %the
          value for E=1.5 eV should not be counted to times,
          therefore i+1
132      for a=1:numberofdevices
133        if ARC(a)==0 %no anti-reflective coating
134        R_GaAs_endelig(a,i)=yi_GaAs_2_R(i+1-antall_endelig_1_GaAs)
            ;
135        else
136         R_GaAs_endelig(a,i)=0;
137        end
138      end
139      n_GaAs_endelig(i)=yi_GaAs_2_n(i+1-antall_endelig_1_GaAs);
140      alpha_GaAs_endelig(i)=yi_GaAs_2(i+1-antall_endelig_1_GaAs);
141 end
142
143
144 %Values for absorption coefficient for Al_0.804Ga_0.196As
145 numwindow_0804=xlsread('C:\Documents and Settings\Kirsti Kvanes\
      Mine dokumenter\MATLAB\Master\AlGaAs 0804 optiske parametre');
```

```
146 %Comment: alpha values were originally given as 10^-3 multiplied
      by the
147 %values in the excel file, this was pr cm, to get correct alpha
      values pr
148 %m, multiply with 10^2*10^3
149 photonenergy_window=numwindow_0804(:,1); %photonenergies for Al_0
      .804Ga_0.196As used in the excel files
150 alpha_window_0804=1e5.*numwindow_0804(:,2); %alpha values for Al_0
      .804Ga_0.196As
151
152
153 %Values for absorption coefficient for Al_0.900Ga_0.100As
154 numwindow_0900=xlsread('C:\Documents␣and␣Settings\Kirsti␣Kvanes\
      Mine␣dokumenter\MATLAB\Master\AlGaAs␣0900␣optiske␣parametre');
155 %Comment: alpha values were originally given as 10^-3 multiplied
      by the
156 %values in the excel file, this was pr cm, to get correct alpha
      values pr
157 %m, multiply with 10^2*10^3
158 alpha_window_0900=1e5.*numwindow_0900(:,2); %alpha values for Al_0
      .900Ga_0.100As
159
160
161 %Getting values for Al_0.804Ga0.196As
162  %The absorption coefficient is set to zero for energies less than
        1.5 eV
163  %Uses the excel file for energies greater than 1.5 eV which has
       an energy
164  %step equal to 0.1 eV. This is different than the values for GaAs
        where
165  %two different energy steps are used
166
167 step_window=0.1; %Steplength 0.1 in the excel file
168 minimum_window=minimum_1_GaAs;%*eV; %minimum value in the excel
      files for solar spectrum is 0.3104, minium value in the excel
      file for absorption coeff is 1.36!!!
169 maximum_window=maximum_2_GaAs;%*eV; %maximum allowed value 1.5 for
       energies larger then 1.5 we need a greater steplength
170 E_window_table=(minimum_window:step_window:maximum_window);
171 antall_window=floor((maximum_window-minimum_window)./step_window
      +1); %number of E in the excel file
172
173 alpha_AlGaAs_window_temp_0804=zeros(1,antall_window);
174
175 windownumber_0804=1;
176
177  for i=1:antall_window
178      if E_window_table(i)<1.5
179          alpha_AlGaAs_window_temp_0804(i)=0; %for energies less
                than 1.5 eV the absorption coefficient is equal to
                zero
180      else
```

```
181         while ~(photonenergy_window(windownumber_0804)-(
               step_window*0.5)<=E_window_table(i)&& E_window_table(i)
               <photonenergy_window(windownumber_0804)+(step_window
               *0.5))
182                 windownumber_0804=windownumber_0804+1;
183         end
184 
185         alpha_AlGaAs_window_temp_0804(i)=alpha_window_0804(
               windownumber_0804);
186     end
187 end
188 
189 %Interpolation
190 pp_window_0804 = interp1(E_window_table,
       alpha_AlGaAs_window_temp_0804,'cubic','pp'); %interpolates
       alpha values
191 yi_window_0804 = ppval(pp_window_0804,zi_endelig); %interpolates
       alpha values
192 alpha_AlGaAs_window_0804_final=zeros(antall_endelig); %
       interpolated alphavalues, the values will be used later
193 for i=1:antall_endelig
194     alpha_AlGaAs_window_0804_final(i)=yi_window_0804(i);
195 end
196 
197 %Getting values for Al_0.900Ga0.100As
198 %The absorption coefficient is set to zero for energies less than
        1.5 eV
199 %Uses the excel file for energies greater than 1.5 eV which has
       an energy
200 %step equal to 0.1 eV. This is different than the values for GaAs
        where
201 %two different energy steps are used
202 
203 alpha_AlGaAs_window_temp_0900=zeros(1,antall_window);
204 
205 windownumber_0900=1;
206 
207 for i=1:antall_window
208     if E_window_table(i)<1.5
209          alpha_AlGaAs_window_temp_0900(i)=0; %for energies less
                than 1.5 eV the absorption coefficient is equal to
                zero
210     else
211         while ~(photonenergy_window(windownumber_0900)-(
               step_window*0.5)<=E_window_table(i)&& E_window_table(i)
               <photonenergy_window(windownumber_0900)+(step_window
               *0.5))
212                 windownumber_0900=windownumber_0900+1;
213         end
214         alpha_AlGaAs_window_temp_0900(i)=alpha_window_0900(
               windownumber_0900);
215     end
216 end
```

```
217
218 %Interpolation
219  pp_window_0900 = interp1(E_window_table,
        alpha_AlGaAs_window_temp_0900,'cubic','pp'); %interpolates
        alpha values
220  yi_window_0900 = ppval(pp_window_0900,zi_endelig); %interpolates
        alpha values
221
222  alpha_AlGaAs_window_0900_final=zeros(antall_endelig); %
        interpolated alphavalues, the values will be used later
223  for i=1:antall_endelig
224       alpha_AlGaAs_window_0900_final(i)=yi_window_0900(i);
225  end
226
227
228  %Getting values for AlGaAs in window layer uses energy shift and
        average
229  %value of x=0.804 and x=0.90 from "Properties of AlGaAs book"
230
231  alpha_AlGaAs_window_0804_shifted=zeros(numberofdevices,
        antall_endelig);
232  alpha_AlGaAs_window_0900_shifted=zeros(numberofdevices,
        antall_endelig);
233  alpha_AlGaAs_window=zeros(numberofdevices,antall_endelig);
234
235  for a=1:numberofdevices
236          for i=1:antall_endelig
237            if (i-round(((0.005.*x_window(a))+(0.245.*x_window(a)
                .^2)-((0.005.*0.804)+(0.245.*0.804.^2)))./
                step_endelig)) <=0 &&(i-round(((0.005.*x_window(a))
                +(0.245.*x_window(a).^2)-((0.005.*0.900)
                +(0.245.*0.900.^2)))./step_endelig))>antall_endelig
238            alpha_AlGaAs_window_0804_shifted(a,i)=0;
239            alpha_AlGaAs_window_0900_shifted(a,i)=
                alpha_AlGaAs_window_0900_final(antall_endelig);
240            elseif (i-round(((0.005.*x_window(a))+(0.245.*x_window(a
                ).^2)-((0.005.*0.804)+(0.245.*0.804.^2)))./
                step_endelig)) <=0
241               alpha_AlGaAs_window_0804_shifted(a,i)=0;
242               alpha_AlGaAs_window_0900_shifted(a,i)=
                   alpha_AlGaAs_window_0900_final(i-round(((0.005.*
                   x_window(a))+(0.245.*x_window(a).^2)
                   -((0.005.*0.900)+(0.245.*0.900.^2)))./step_endelig
                   ));
243            elseif (i-round(((0.005.*x_window(a))+(0.245.*x_window(a
                ).^2)-((0.005.*0.900)+(0.245.*0.900.^2)))./
                step_endelig))>antall_endelig
244               alpha_AlGaAs_window_0900_shifted(a,i)=
                   alpha_AlGaAs_window_0900_final(antall_endelig);
245               alpha_AlGaAs_window_0804_shifted(a,i)=
                   alpha_AlGaAs_window_0804_final(i-round(((0.005.*
                   x_window(a))+(0.245.*x_window(a).^2)
                   -((0.005.*0.804)+(0.245.*0.804.^2)))./step_endelig
```

```
                  ));
246             else
247            alpha_AlGaAs_window_0804_shifted(a,i)=
               alpha_AlGaAs_window_0804_final(i-round(((0.005.*
               x_window(a))+(0.245.*x_window(a).^2)-((0.005.*0.804)
               +(0.245.*0.804.^2)))./step_endelig));
248            alpha_AlGaAs_window_0900_shifted(a,i)=
               alpha_AlGaAs_window_0900_final(i-round(((0.005.*
               x_window(a))+(0.245.*x_window(a).^2)-((0.005.*0.900)
               +(0.245.*0.900.^2)))./step_endelig));
249            end
250          alpha_AlGaAs_window(a,i)=0.5.*(
              alpha_AlGaAs_window_0804_shifted(a,i)+
              alpha_AlGaAs_window_0900_shifted(a,i));
251           end
252  end
253
254
255
256
257
258 %MODEL
259 radiative_rec_e=zeros(numberofdevices,energyvalues);
260 radiative_rec_h=zeros(numberofdevices,energyvalues);
261 L_e=zeros(numberofdevices,energyvalues); %definition
262 L_h=zeros(numberofdevices,energyvalues); %definition
263
264 for i=1:numberofdevices
265     for c=1:energyvalues
266 radiative_rec_e(i,c)=(1./n_0(i,c)).*(radiative_rec_coeff(
    alpha_CI_temp(i),E_H(c))-radiative_rec_coeff(alpha_CI_temp(i),
    E_L(c)));    %uses the function radiative_rec_coeff which
    calculates the value of the integral (8pi/h^3c^2)int(alphaE^2
    exp(-E/kT)dE)
267 radiative_rec_h(i,c)=(1./p_0(i,c)).*(radiative_rec_coeff(
    alpha_IV_temp(i),E_G(c))-radiative_rec_coeff(alpha_IV_temp(i),
    E_H(c)));    %uses the function radiative_rec_coeff which
    calculates the value of the integral (8pi/h^3c^2)int(alphaE^2
    exp(-E/kT)dE)
268 L_e(i,c)=sqrt(diffusionconstant_e(i)./(radiative_rec_e(i,c)+(1./
    tau_SRH_CI(i))))
269 L_h(i,c)=sqrt(diffusionconstant_h(i)./(radiative_rec_h(i,c)+(1./
    tau_SRH_IV(i))))
270
271
272
273     end
274 end
275
276
277
278 alpha_CI_new=zeros(numberofdevices,antall_endelig,energyvalues);
279 alpha_IV_new=zeros(numberofdevices,antall_endelig,energyvalues);
```

```
280 alpha_CV_new=zeros(numberofdevices,antall_endelig,energyvalues);
281
282 for c=1:energyvalues
283     for i=1:antall_endelig
284         for a=1:numberofdevices
285             if (zi_endelig(i)<(E_L(c)/eV))
286             alpha_CI_new(a,i,c)=0;
287             alpha_IV_new(a,i,c)=0;
288             alpha_CV_new(a,i,c)=0;
289
290             elseif ((E_L(c)/eV)<=zi_endelig(i)&&zi_endelig(i)<E_H(
                   c)/eV)
291             alpha_CI_new(a,i,c)=alpha_CI_temp(a);
292              alpha_IV_new(a,i,c)=0;
293             alpha_CV_new(a,i,c)=0;
294
295             elseif ((E_H(c)/eV)<=zi_endelig(i)&&zi_endelig(i)<E_G(
                   c)/eV)
296             alpha_CI_new(a,i,c)=0;
297              alpha_IV_new(a,i,c)=alpha_IV_temp(a);
298             alpha_CV_new(a,i,c)=0;
299             else
300                 alpha_CI_new(a,i,c)=0;
301              alpha_IV_new(a,i,c)=0;
302
303              if a==3
304             alpha_CV_new(a,i,c)=alpha_GaAs_endelig(i); %use
                   tabulated values for the absorption coefficient of
                   GaAs
305              else
306             alpha_CV_new(a,i,c)=alpha_CV_temp(a);
307              end
308            %alpha_CV_new(1,i)=alpha_CV_temp(1);
309             %alpha_CV_new(2,i)=alpha_GaAs_endelig(i);
310
311             end
312
313         end
314     end
315  end
316
317 Q_electron=zeros(numberofdevices,antall_endelig,energyvalues);
318 Q_hole=zeros(numberofdevices,antall_endelig,energyvalues);
319 for i=1:antall_endelig
320     for a=1:numberofdevices
321         for c=1:energyvalues
322  Q_electron(a,i,c)=-(((alpha_CI_new(a,i,c).*L_e(a,c)./((
       alpha_CI_new(a,i,c).*L_e(a,c)).^2-1)).*(((exp(-alpha_CI_new(a,
       i,c).*width_IB(a)).*sinh(width_IB(a)./L_e(a,c))-(alpha_CI_new(
       a,i,c).*L_e(a,c))./cosh(width_IB(a)./L_e(a,c))+(alpha_CI_new
       (a,i,c).*L_e(a,c).*exp(-alpha_CI_new(a,i,c).*width_IB(a)))))
       +((alpha_CV_new(a,i,c).*L_e(a,c)./((alpha_CV_new(a,i,c).*L_e(a
       ,c)).^2-1)).*(((exp(-alpha_CV_new(a,i,c).*width_IB(a)).*sinh(
```

```
    width_IB(a)./L_e(a,c))-(alpha_CV_new(a,i,c).*L_e(a,c))./cosh(
    width_IB(a)./L_e(a,c)))+(alpha_CV_new(a,i,c).*L_e(a,c).*exp(-
    alpha_CV_new(a,i,c).*width_IB(a))))));
323  Q_hole(a,i,c)=-(((alpha_IV_new(a,i,c).*L_h(a,c)./((alpha_IV_new(a
    ,i,c).*L_h(a,c)).^2-1)).*((((alpha_IV_new(a,i,c).*L_h(a,c).*
    exp(-alpha_IV_new(a,i,c).*width_IB(a)))+sinh(width_IB(a)./L_h(
    a,c)))./cosh(width_IB(a)./L_h(a,c)))-(alpha_IV_new(a,i,c).*L_h
    (a,c))))+((alpha_CV_new(a,i,c).*L_h(a,c)./((alpha_CV_new(a,i,c
    ).*L_h(a,c)).^2-1)).*((((alpha_CV_new(a,i,c).*L_h(a,c).*exp(-
    alpha_CV_new(a,i,c).*width_IB(a)))+sinh(width_IB(a)./L_h(a,c))
    )./cosh(width_IB(a)./L_h(a,c)))-(alpha_CV_new(a,i,c).*L_h(a,c)
    ))));
324          end
325       end
326 end
327
328
329
330
331
332 wavelength=1e+9.*(h_planck*c_light)./(zi_endelig.*eV); %Wavelength
     in nm
333
334 %Reading the necessary excel files
335
336 num = xlsread('C:\Documents␣and␣Settings\Kirsti␣Kvanes\Mine␣
    dokumenter\MATLAB\Prosjekt\Sp'); %Solar spectrum. Column 1 is
    wavelengths, column 2 is AM 1.5 given in W/(nm*m2), column 3 is
     incoming radiation in an energy intervall
337 %Column 4 is photonenergies, column 5 is photonflux in an
    energyinterval
338 wavelengthAM=num(:,1); %Wavelengths from excel
339 flux=num(:,5); %Incoming energy flux from excel
340 photonenergyexcel=num(:,4);
341
342 startexcel=1;
343
344 photo_electron_current=zeros(numberofdevices,energyvalues); %
    photogenerated electron current at beginning of IB material (
    end of p-layer)
345 photo_hole_current=zeros(numberofdevices,energyvalues);     %
    photogenerated hole current at end of IB material (beginning of
     n-layer)
346
347
348
349
350 for a=1:numberofdevices
351     for c=1:energyvalues
352 for i=antall_endelig:-1:1
353     if wavelengthAM(startexcel)<400
354         if abs((wavelengthAM(startexcel)-wavelength(i)))<0.25
355
```

```
356         else
357             photo_electron_current(a,c)=(photo_electron_current(a,c
                ))+concentration(a).*flux(startexcel).*e_charge.*
                Q_electron(a,i,c); %Light generated electron current
                 at beginning of IB material
358             photo_hole_current(a,c)=(photo_hole_current(a,c))+
                concentration(a).*flux(startexcel).*e_charge.*Q_hole
                (a,i,c); %Light generated hole current at end of IB
                material
359             startexcel=startexcel+1;
360         end
361
362     elseif wavelengthAM(startexcel)>=400&&wavelengthAM(startexcel)
            <1700
363         if abs((wavelengthAM(startexcel)-wavelength(i)))<0.5
364
365         else
366             photo_electron_current(a,c)=(photo_electron_current(a,c
                ))+concentration(a).*flux(startexcel).*e_charge.*
                Q_electron(a,i,c); %Light generated electron current
                 at beginning of IB material
367             photo_hole_current(a,c)=(photo_hole_current(a,c))+
                concentration(a).*flux(startexcel).*e_charge.*Q_hole
                (a,i,c); %Light generated hole current at end of IB
                material
368             startexcel=startexcel+1;
369         end
370
371     elseif wavelengthAM(startexcel)>=1700
372         if abs((wavelengthAM(startexcel)-wavelength(i)))<2.5
373
374         else
375             photo_electron_current(a,c)=(photo_electron_current(a,c
                ))+concentration(a).*flux(startexcel).*e_charge.*
                Q_electron(a,i,c); %Light generated electron current
                 at beginning of IB material
376             photo_hole_current(a,c)=(photo_hole_current(a,c))+
                concentration(a).*flux(startexcel).*e_charge.*Q_hole
                (a,i,c); %Light generated hole current at end of IB
                material
377             startexcel=startexcel+1;
378
379              startexcel=startexcel+1;
380         end
381     end
382
383  end
384
385 startexcel=1;
386     end
387 end
388
389
```

```
390
391
392
393 %photo_electron_current(1)
394 %photo_hole_current(1)
395
396
397 %Voltages
398 minimum=0.0;
399 maximum=1.5;
400 step=0.001;
401 antall=round((maximum-minimum)/step+1);
402
403 %simplecurrent=blackcurrent(minimum,maximum,step);
404
405
406
407 %Voltage=zeros(antall); %voltage over cell Voltage=V_VC-J*R_s*area
408 V_VC=minimum:step:maximum; %e_charge*V_VC difference between the
        CB and VB quasi-Fermi levels
409 Voltage=V_VC;
410
411 V_VI=zeros(numberofdevices,antall,energyvalues); %e_charge*V_VI
        difference between the IB and VB quasi-Fermi levels
412
413 V_IC=zeros(numberofdevices,antall,energyvalues); %e_charge*V_IC
        difference between the CV and IB quasi-Fermi levels
414
415 V_IC_mi=0;
416
417
418 %Need to find the value of the voltages, uses that
419 %V_VC=V_IC+V_VI %and that the currents from both of the terminals
        have to
420 %be equal
421 for a=1:numberofdevices
422     for c=1:energyvalues
423         for i=1:antall
424     V_IC_mi=fsolve(@(V_IC_mi) -((e_charge.*diffusionconstant_h(a)
            .*p_0(a,c).*(exp(e_charge.*(V_VC(i)-V_IC_mi)./(k_Boltzman.*
            T))-1)./L_h(a,c)).*sinh(width_IB(a)./L_h(a,c))./cosh(
            width_IB(a)./L_h(a,c)))+photo_hole_current(a,c)-(-((
            e_charge.*diffusionconstant_e(a).*n_0(a,c).*(exp(e_charge
            .*(V_IC_mi)./(k_Boltzman.*T))-1)./L_e(a,c)).*sinh(width_IB(
            a)./L_e(a,c))./cosh(width_IB(a)./L_e(a,c))))-
            photo_electron_current(a,c),0,optimset('Display','off'));
425     V_IC(a,i,c)=V_IC_mi;
426         end
427
428     end
429 end
430
431 for a=1:numberofdevices
```

```
432     for c=1:energyvalues
433         for i=1:antall
434             V_VI(a,i,c)=V_VC(i)-V_IC(a,i,c);
435         end
436     end
437 end
438
439
440
441 total_current_1=zeros(numberofdevices,antall,energyvalues);
442 total_current_2=zeros(numberofdevices,antall,energyvalues);
443 J=zeros(numberofdevices,antall,energyvalues);
444 V_OC=zeros(numberofdevices,energyvalues); %open-cirucit voltage
445 J_sc=zeros(numberofdevices,energyvalues); %photo-current
446 J_dark08V=zeros(numberofdevices,energyvalues); %dark-current for V
      =0.8V
447 J_sc_2=zeros(numberofdevices,energyvalues);
448 for a=1:numberofdevices
449     for c=1:energyvalues
450         for i=1:antall
451 total_current_1(a,i,c)=(1/concentration(a)).*(-((e_charge.*
      diffusionconstant_h(a).*p_0(a,c).*(exp(e_charge.*V_VI(a,i,c)./(
      k_Boltzman.*T))-1)./L_h(a,c)).*sinh(width_IB(a)./L_h(a,c))./
      cosh(width_IB(a)./L_h(a,c)))+photo_hole_current(a,c));
452 total_current_2(a,i,c)=(1/concentration(a)).*(-(((e_charge).*
      diffusionconstant_e(a).*n_0(a,c).*(exp(e_charge.*V_IC(a,i,c)./(
      k_Boltzman.*T))-1)./L_e(a,c)).*sinh(width_IB(a)./L_e(a,c))./
      cosh(width_IB(a)./L_e(a,c)))+photo_electron_current(a,c));
453 J(a,i,c)=total_current_2(a,i,c);
454             if(abs(total_current_2(a,i,c))<=10)
455                 V_OC(a,c)=V_VC(i); %open-circuit voltage
456             end
457         end
458
459 J_sc(a,c)=(1/concentration(a)).*(-(((e_charge).*
      diffusionconstant_e(a).*n_0(a,c).*(exp(e_charge.*V_IC(a,1,c)./(
      k_Boltzman.*T))-1)./L_e(a,c)).*sinh(width_IB(a)./L_e(a,c))./
      cosh(width_IB(a)./L_e(a,c)))+photo_electron_current(a,c));
460 J_sc_2(a,c)=(1/concentration(a)).*(-((e_charge.*
      diffusionconstant_h(a).*p_0(a,c).*(exp(e_charge.*V_VI(a,1,c)./(
      k_Boltzman.*T))-1)./L_h(a,c)).*sinh(width_IB(a)./L_h(a,c))./
      cosh(width_IB(a)./L_h(a,c)))+photo_hole_current(a,c));
461 %J_dark08V(a,c)=(1/concentration(a)).*(-(((e_charge).*
      diffusionconstant_e(a).*n_0(a,c).*(exp(e_charge.*V_IC(a,801,c)
      ./(k_Boltzman.*T))-1)./L_e(a,c)).*sinh(width_IB(a)./L_e(a,c))./
      cosh(width_IB(a)./L_e(a,c))));
462     end
463 end
464
465
466 %Efficiency of cells
467 efficiency=zeros(numberofdevices,antall,energyvalues);
468 P_in=1e+3; %Power incident for AM 1.5
```

```
469 for a=1:numberofdevices
470     for c=1:energyvalues
471         for i=1:antall
472             if J(a,i,c)>0
473             efficiency(a,i,c) = abs(V_VC(i)*J(a,i,c)*100)/P_in;
474             else
475             efficiency(a,i,c)=0;
476             end
477
478         end
479     end
480 end
481
482
483 efficiencymax=zeros(numberofdevices,energyvalues);
484 for i=1:numberofdevices
485     for c=1:energyvalues
486 efficiencymax(i,c)=max(efficiency(i,:,c));
487     end
488 end
489
490
491 %
492 % figure(2)
493 % plot(E_H./eV,efficiencymax(1,:),'b-','LineWidth',1.3);
494 % axis([energymin energymax 30 50])
495 % hold on
496 % %plot(E_H./eV,efficiencymax(2,:),'r-','LineWidth',1.3);
497 % xlabel('E_H (eV)')
498 % ylabel('\eta (%)')
499 % %legend('w_{IB}=0.65 \mum','w_{IB}=1.30 \mum','w_{IB}=2.60 \mum
    ', 'w_{IB}=5.20 \mum','Location','SouthEast');
500 % %text(0.905,19,'X=1000, non-radiative rec.','HorizontalAlignment
    ','left')
501 % legend BOXOFF
502 % hold off
503 % exportfig(2, 'IBvarybandgapefficiency', 'Color','rgb')
504 %  system('epstopdf IBvarybandgapefficiency.eps')
505 %
506
507 energy_max=zeros(1,numberofdevices);
508 finalmaximumefficiency=zeros(numberofdevices);
509 loc=zeros(1,numberofdevices);
510
511 for i=1:numberofdevices
512     [finalmaximumefficiency(i),loc(i)]=max(efficiencymax(i,:))
513     energy_max(i)=E_H(loc(i))./eV
514 end
515
516 figure(1)
517 plot(V_VC,J(1,:,loc(1)),'b-','LineWidth',1.3);
518 axis([minimum maximum 0 420])
519 hold on
```

```
520 xlabel('Voltage␣(V)')
521 ylabel('Current␣density␣divided␣by␣concentration␣(A/m^2)')
522 legend('Reference␣cell,␣non-radiative␣rec.','Change␣of␣absorption␣
    coefficient','Change␣of␣mobility␣and␣density␣of␣states','
    Location','SouthWest');
523 %text(0.01,475,'X=1000, non-radiative rec.','HorizontalAlignment
    ','left')
524 legend BOXOFF
525 hold off
526   exportfig(1, 'tekst', 'Color','rgb')
527   system('epstopdf␣tekst.eps')
528 %
529 V_OC(1,loc(1))
530 J_sc(1,loc(1))
```

Listing B.7: `currentvoltage`

B.8 Variables complete model of intermediate band solar cell

```
1 ----------------------------------------
2 Variables complete model of IB solar cell
3 ----------------------------------------
4 %Constants used in the different programs
5 h_planck=6.62607e-34; %Plancks constant h in Js
6 h_dirac=1.05457e-34; %Diracs constant=h/2pi in Js
7 m_e=9.10938e-31; %Electron mass in kg
8 eV=1.60218e-19; %electronvolt to joule
9 k_Boltzman = 1.38065e-23; %Boltzman constant J/K
10 freediec = 8.85419e-12; %Free dielectric constant in F/m
11 e_charge=1.60218e-19; %Charge of an electron in C
12 c_light = 2.99792e+8; %velocity of light m/s
13 T=300; %temperature used in article for solar cells in K
14 E_rydberg=13.6057*eV; %Rydberg energy
15 T_sun=6000; %Temperature of sun i K
16
17
18 %To meter m
19 nm=1e-9; %nanometer to meter
20 cm=1e-2; %centimeter to meter
21 micm=1e-6; %micrometer to meter
22 mm=1e-3; % millimeter to meter
23
24 %DATA USED IN THE MODEL
25 numberofdevices=2;
26
27
28 window=[1 1 1 1]; %equal to 1 if we have a window layer, equal to
    0 of we do not have a window layer
29 ARC=[1 1 1 1]; %1 if anti-reflective coating, 0 if not
30
31
32 %Fraction of x in Al_xGa_(1-x)_As
```

```
33 x_window=[0.85 0.85 0.85 0.85];  %x in window layer
34 x_cell=[0 0 0.35 0.35];       %x in p, p-plus, n and n-plus layers
35 x_IB=[0 0 0.35 0.35];         %x in intermediate band layer
36
37
38 %Bandgap for GaAs
39 E_GaAs=(1.519-(5.405*(1e-4)*T^2/(T+204)))*eV; %from Lie!!
40
41 E_window=zeros(1,numberofdevices);          %Bandgap window layer
     (eV)
42 E_cell=zeros(1,numberofdevices);            %Bandgap in p, p-plus,
     n and n-plus layers (eV)
43
44 %Bandgap for Al_xGa_(1-x)As in the rest of the cell
45 for i=1:numberofdevices
46 E_window(i)=(1.911+(0.005.*x_window(i))+(0.245.*(x_window(i).^2)))
     *eV;   %Bandgap window layer for x>=0.45(eV) (Properties of
     AlGaAs)
47 E_cell(i)=(E_GaAs/eV+(1.247*x_cell(i)))*eV;       %Bandgap in p, p
     -plus, n and n-plus layers  for x<0.45(eV) (Properties of
     AlGaAs)
48 end
49
50 R_s=[0 0];
51 area=[1.71e-6 1.71e-6];
52 concentration=[1 1 1 1000]; %light concentration
53 %concentration=[1 1 1 1]; %light concentration
54
55 alpha_CI_temp=[4e6 4e6 4e6 4e6]; %absorption coefficient
     intermediate band to conduction band transitions in /m
56 alpha_IV_temp=[4e6 4e6 4e6 4e6]; %absorption coefficient valence
     band to intermediate band transitions in /m
57 alpha_CV_temp=[4e6 4e6 4e6 4e6]; %absorption coefficient valence
     band to conduction band transitions in /m
58
59
60 %Energysteps used to find the maximum efficiency
61
62
63 energystep=0.0;
64
65
66 GaAs_min=1.22.*(1.519-(5.405*(1e-4)*T^2/(T+204)))
     ./((1.519-(5.405*(1e-4)*2^2/(2+204)))); %Energy measured in
     Tronheim at 2K
67
68 %energymin=0.9; %minimum value of E_H
69
70 %energymax=1.2; %maximum value of E_H
71 %energymax=energymin; %maximum value of E_H
72
73
```

```
74 %energyvalues=round((energymax-energymin)./energystep)+1; %number
     of energies
75 energyvalues=1;
76
77 %E_H=(energymin:energystep:energymax).*eV; %bandgap
     intermediateband-valenceband
78 %E_H=energymin.*eV;
79 %E_H=[GaAs_min GaAs_min 1.12 1.12].*eV;
80 E_H=[1.12 1.12].*eV;
81 E_L=zeros(numberofdevices,energyvalues); %bandgap conductionband-
     intermediateband
82 E_G=zeros(numberofdevices,energyvalues); %bandgap conductionband-
     valenceband
83 %
84 % for i=1:energyvalues
85 %     for a=1:numberofdevices
86 % E_G(a,i)=E_cell(a)    %bandgap conductionband-valenceband
87 % E_L(a,i)=E_G(a,i)-E_H(a) %bandgap conductionband-intermediate
     band
88 %     end
89 % end
90
91 for i=1:energyvalues
92     for a=1:numberofdevices
93 E_G(a,i)=1.38.*eV   %bandgap conductionband-valenceband
94 E_L(a,i)=E_G(a,i)-E_H(a) %bandgap conductionband-intermediate band
95     end
96 end
97
98 mu_e=[0.8 0.8 0.8 0.8 0.8 0.8 0.8 0.8];       %GaAs mobility
     electrons in m^2/(Vs)from Semiconducting and other properties
     of GaAs
99 mu_h=[0.04 0.04 0.04 0.04 0.04 0.04 0.04 0.04];       %GaAs
     mobility holes in m^2/(Vs) from semiconducting and other
     properties of GaAs
100
101 %mu_e=[ 0.185 0.185];        %Al0.35Ga0.65As mobility electrons in
     m^2/(Vs)from Landolt Bornstein
102 %mu_h=[ 0.0110 0.0110];        %Al0.35Ga0.65As mobility holes in m
     ^2/(Vs) from Properties of AlGaAs
103
104
105 diffusionconstant_e=zeros(1,numberofdevices); %diffusion constant
     electrons in CB in IB material
106 diffusionconstant_h=zeros(1,numberofdevices); %diffusion constant
     holes in VB in IB material
107
108 for i=1:numberofdevices
109 diffusionconstant_e(i)=(k_Boltzman.*T.*mu_e(i))./e_charge;
110 diffusionconstant_h(i)=(k_Boltzman.*T.*mu_h(i))./e_charge;
111 end
112 m_e_AlGaAs=zeros(1,numberofdevices);
113 m_hh_AlGaAs=zeros(1,numberofdevices);
```

```
114 m_lh_AlGaAs=zeros(1,numberofdevices);
115 N_C_AlGaAs=zeros(1,numberofdevices);
116 N_V_AlGaAs=zeros(1,numberofdevices);
117 ni_AlGaAs=zeros(1,numberofdevices);
118
119 for i=3:numberofdevices
120
121 m_e_AlGaAs(i)=(0.0632+(0.0856.*x_cell(i))+(0.0231.*x_cell(i).^2))
      .*m_e;
122 m_hh_AlGaAs(i)=(0.50+(0.2.*x_cell(i))).*m_e;
123 m_lh_AlGaAs(i)=(0.088+(0.0372.*x_cell(i))+(0.0163.*x_cell(i).^2))
      .*m_e;
124
125 N_C_AlGaAs(i)=2.*((2.*pi.*m_e_AlGaAs(i).*k_Boltzman.*T./(h_planck
      .^2)).^(1.5));
126 N_V_AlGaAs(i)=2.*((2.*pi.*((m_hh_AlGaAs(i)^(1.5)+m_lh_AlGaAs(i)
      .^(1.5)).^(2./3)).*k_Boltzman.*T./(h_planck.^2)).^(1.5));
127 ni_AlGaAs(i)=sqrt(N_C_AlGaAs(i).*N_V_AlGaAs(i)).*exp(-E_cell(i)
      ./(2.*k_Boltzman.*T));
128
129 end
130
131
132
133
134
135 N_C=[4.7e23 4.7e23 4.7e23 4.7e23 4.7e23 4.7e23 4.7e23 4.7e23];
          %GaAs densities of states conduction band in /m^3 from "
      Solar Cells Materials, Manufacture and Operation"
136 N_V=[7e24 7e24 7e24 7e24 7e24 7e24 7e24 7e24];       %GaAs
      densities of states valence band in /m^3 from "Solar Cells
      Materials, Manufacture and Operation"
137
138 %N_C=[4.7e23 4.7e23 N_C_AlGaAs(3) N_C_AlGaAs(4)];
139 %N_V=[7e24 7e24 N_V_AlGaAs(3) N_V_AlGaAs(4)];
140
141 n_0=zeros(energyvalues,numberofdevices);
142 p_0=zeros(energyvalues,numberofdevices);
143
144 for i=1:numberofdevices
145     for c=1:energyvalues
146 n_0(i,c)=N_C(i).*exp(-E_L(c)./(k_Boltzman.*T));     %equilibrium
      electron concentration in the conduction band
147 p_0(i,c)=N_V(i).*exp(-E_H(c)./(k_Boltzman.*T));     %equilibrium
      hole concentration in the valence band
148     end
149 end
150
151 ni_GaAs=1.79e12; %intrinsic carrier concentration at 300 K in GaAs
       (m-3) from "Solar Cells Materials, Manufacture and Operation"
152
153 ni_cell=[ni_GaAs ni_GaAs ni_GaAs ni_GaAs]; %intrinsic carrier
      concentration in p- and n-layer
```

```
154 %ni_cell=[ni_GaAs ni_GaAs ni_AlGaAs(3) ni_AlGaAs(4)]; %when AlGaAs
     instead of GaAs
155
156 ni_intrinsic=[ni_GaAs ni_GaAs ni_GaAs ni_GaAs]; %intrinsic carrier
     concentration in the intrinsic layers
157 %ni_intrinsic=[ni_GaAs ni_GaAs ni_AlGaAs(3) ni_AlGaAs(4)] %when
    AlGaAs instead of GaAs
158
159
160 %Non-radiative recombination lifetimes Taken from "Intermediate
    Band Solar
161 %Cells Using Nanotechnology"
162 tau_SRH_CI=[1e15 0.5e-12 1e15 1e15];   %non-radiative lifetime
    conduction band to intermediate band (in s), set equal to great
     value if only radiative recombination
163
164 tau_SRH_IV=[1e15 40e-12 1e15 1e15];   %non-radiative lifetime
    intermediate band to valence band (in s), set equal to great
    value if only radiative recombination
165
166
167
168 %Carrier lifetimes
169 tau_n_GaAs=7e-9; %(s) fra Nelson Quantum-Well Structures
170 tau_p_GaAs=7e-9;     % (s) fra Nelson Quantum-Well Structures
171
172 %Carrier lifetimes for AlGaAs
173 %tau_n_GaAs=18e-9; %(s) fra Properties of AlGaAs
174 %tau_p_GaAs=18e-9;     % (s) fra Properties of AlGaAs
175
176
177
178 %Dielectric constants
179 epsilon_GaAs=12.79.*(1+(T.*1e-4)).*freediec; %static dielectric
    constant for GaAs from "Properties of GaAs"
180
181 epsilon_AlGaAs=zeros(1,numberofdevices);
182
183 for i=3:numberofdevices
184
185 epsilon_AlGaAs(i)=(13.1-(2.2.*x_cell(i))).*freediec;
186 end
187
188 epsilon_p=[epsilon_GaAs epsilon_GaAs epsilon_GaAs epsilon_GaAs]; %
    dielectric constant p and p-plus layer, here taken for GaAs
189 epsilon_n=[epsilon_GaAs epsilon_GaAs epsilon_GaAs epsilon_GaAs]; %
    dielectric constant n and n-plus layer, here taken for GaAs
190 %epsilon_p=[epsilon_GaAs epsilon_GaAs epsilon_AlGaAs(3)
    epsilon_AlGaAs(4)]; %if AlGaAs
191 %epsilon_n=[epsilon_GaAs epsilon_GaAs epsilon_AlGaAs(3)
    epsilon_AlGaAs(4)]; %if AlGaAs
192
193
```

```
194 %Lengths in the devices
195 width_window=[5 5 5 5].*nm;     %width of window layer in m
196 width_p_plus=[100 100 100 100].*nm; %width of p-plus layer in m
197 width_p=[200 200 200 200].*nm;          %with of p layer in m
198 width_IB=[100 100 1300 1300].*nm; %width of intermediate band
       layer in m
199 width_n=[300 300 300 300].*nm;          %with of n layer in m
200 width_n_plus=[100 100 100 100].*nm;     %with of n-plus layer in m
201
202 %Doping of the devices
203 N_I=1e14; %backrground doping in GaAs, assumed p-type, in /cm3
204 N_A_window=[2e19 2e19 2e19 2e19];       %doping concentration in
       window layer (assumed p-type), in /cm3
205 N_A_p_plus=[2e19 2e19 2e19 2e19];       %doping concentration in p-
       plus layer, in /cm3
206 N_A_p=[2e18 2e18 2e18 2e18];            %doping concentration in p
       layer, in /cm3
207 N_D_n=[2e17 2e17 2e17 2e17];            %doping concentration in n
       layer, in /cm3
208 N_D_n_plus=[2e18 2e18 2e18 2e18];       %doping concentration in n-
       plus layer, in /cm3
209
210
211 %Calculation of built-in voltage in p-i-n structure
212
213 V_bi=zeros(1,numberofdevices);
214 V_bi_p_i=zeros(1,numberofdevices); %built-in voltage p-intrinisic
       layer
215 V_bi_n_i=zeros(1,numberofdevices); %built-in voltage n-intrinsic
       layer
216 V_max=[0.9 1.25 0.9 1.25]; %maximum applied voltage may be changed
       ..
217 %V_max=[0.85 0.85 0.85 0.85];
218
219
220
221 for i=1:numberofdevices
222     V_bi(i)=(k_Boltzman.*T./e_charge).*log((N_A_p(i)./cm.^3).*(
           N_D_n(i)./cm.^3)./(ni_cell(i).^2)); % (eq 6.2 in Nelson)
223     V_bi_n_i(i)=(k_Boltzman.*T./e_charge).*log((N_D_n(i)./cm.^3)
           .*(N_I./cm.^3)./(ni_cell(i).^2));
224 end
225
226
227 V_bi_p_i_mi=0; %Temporary built-in voltage p-intrinsic layer
228
229 for i=1:numberofdevices
230  %V_bi_p_i_mi=fsolve(@(V_bi_p_i_mi)
231  %(e_charge.*V_bi_p_i_mi./(k_Boltzman.*T))+log((N_I./N_A_p(i))
        +(0.5.*(e_charge.*V_bi_p_i_mi./(k_Boltzman.*T))^2)),0,optimset
        ('Display','off'))
232  %V_bi_p_i(i)=V_bi_p_i_mi
233  V_bi_p_i(i)=(k_Boltzman.*T./e_charge).*log(N_A_p(i)./(N_I));
```

```
234  V_bi_p_i_mi=0;
235 end
236
237
238 B_factor_max=zeros(numberofdevices); %factor important in
      determining the voltage over the p-i and i-n junction
239 equationvoltage_max=zeros(numberofdevices); %equation needed in
      finding the voltage over the p-i and i-n junction
240 V_p_max=zeros(numberofdevices); %part of the maximum applied
      voltage over the p-i junction
241 V_n_max=zeros(numberofdevices);  %part of the maximum applied
      voltage over the n-i junction
242
243 for a=1:numberofdevices
244 B_factor_max(a)=((N_I./cm^3)/ni_intrinsic(a)).^2.*exp(-e_charge.*
      V_max(a)./(k_Boltzman.*T));
245 equationvoltage_max(a)=0.5.*(-B_factor_max(a)+sqrt(B_factor_max(a)
      .^2+(4.*(B_factor_max(a)+exp(-2.*e_charge.*V_bi_p_i(a)./(
      k_Boltzman.*T))))));
246 V_p_max(a)=-log(equationvoltage_max(a)).*k_Boltzman.*T./e_charge;
247 V_n_max(a)=V_max(a)-V_p_max(a);
248 end
249
250 %Depletion width
251 dep_width_p_i_max=zeros(1,numberofdevices); %maximum width of
      depletion region between p and intrinsic layer, taken as width
      into intrinsic layer
252 dep_width_p_i_min=zeros(1,numberofdevices);  %minimum width of
      depletion region between p and intrinsic layer, taken as width
      into intrinsic layer
253 for i=1:numberofdevices
254     dep_width_p_i_max(i)=sqrt(2.*epsilon_p(i).*k_Boltzman.*T./(
          e_charge.^2.*(N_I./cm.^3))).*atan((e_charge.*V_bi_p_i(i)./(
          k_Boltzman.*T)).*sqrt(N_A_p(i)./(N_I.*2)));
255     dep_width_p_i_min(i)=sqrt(2.*epsilon_p(i).*k_Boltzman.*T./(
          e_charge.^2.*(N_I./cm.^3))).*atan((e_charge.*(V_bi_p_i(i)-
          V_p_max(i))./(k_Boltzman.*T)).*sqrt(N_A_p(i)./(N_I.*2)));
256
257 end
258
259 dep_width_n_i_max=zeros(1,numberofdevices); %maximum width of
      depletion region between n and intrinsic layer (this is in
      equilibrium)
260 dep_width_n_i_min=zeros(1,numberofdevices); %minimum width of
      depletion region between n and intrinsic layer (this is for
      maximum applied voltage)
261
262 for i=1:numberofdevices
263  dep_width_n_i_max(i)=sqrt((V_bi_n_i(i)).*2.*epsilon_n(i).*(N_D_n(
       i)./cm.^3)./(e_charge.*(((N_D_n(i)./cm.^3).*(N_I./cm.^3))+((
       N_I./cm.^3).^2))));%equilibrium, appplied voltage V=0
264  dep_width_n_i_min(i)=sqrt((V_bi_n_i(i)-V_n_max(i)).*2.*epsilon_n(
       i).*(N_D_n(i)./cm.^3)./(e_charge.*(((N_D_n(i)./cm.^3).*(N_I./
```

```
    cm.^3))+((N_I./cm.^3).^2)))); %built-in voltage minus maximum
    applied voltage, must be found after open-circuit voltage is
    found
265 end
266
267 % width_intrinsic=[4.246 3.179  4.246 3.179].*1e-6; %width of
    intrinsic layer plus intermediate band material
268  %for i=1:numberofdevices
269  width_intrinsic=width_IB;
270 %width_intrinsic(i)=dep_width_p_i_min(i)+dep_width_n_i_min(i)+
    width_IB(i)
271    % width_intrinsic(i)=width_IB(i)
272   %  width_intrinsic(i)=4e-6;
273  %end
274
275 %Calculation of built-in voltage of the p_plus-p-junction, needed
    in
276 %determining the depletion width of the p_plus-p-junction
277 V_h_mi=0; %built-in voltage of the p-plus-p junction
278 V_h=zeros(1,numberofdevices);
279
280
281
282 for i=1:numberofdevices
283  %V_h_mi=fsolve(@(V_h_mi) (e_charge.*V_h_mi./(k_Boltzman.*T))+log
    ((N_A_p(i)./N_A_p_plus(i))+(0.5.*(e_charge.*V_h_mi./(
    k_Boltzman.*T))^2)),0,optimset('Display','off'));
284  %V_h(i)=V_h_mi;
285   V_h(i)=(k_Boltzman.*T./e_charge).*log(N_A_p_plus(i)./(N_A_p(i)))
    ;
286  V_h_mi=0;
287 end
288
289 %Depletion width of the p_plus-p-junction, taken as the depletion
    width into the p-layer
290 dep_width_p_plus=zeros(1,numberofdevices);
291
292 for i=1:numberofdevices
293     dep_width_p_plus(i)=sqrt(2.*epsilon_p(i).*k_Boltzman.*T./(
        e_charge.^2.*(N_A_p(i)./cm.^3))).*atan((e_charge.*V_h(i)./(
        k_Boltzman.*T)).*sqrt(N_A_p_plus(i)./(N_A_p(i).*2)));
294 end
295
296 %Width of the undepleted p-layer
297 %The depletion width into the p_plus-layer is not taken into
    consideration
298 width_p_undepleted=zeros(1,numberofdevices);
299
300 for i=1:numberofdevices
301 width_p_undepleted(i)=width_p(i)-dep_width_p_plus(i);
302 end
303
```

```
304 %Calculation of built-in voltage of the n-n_plus-junction, needed
    in
305 %determining the depletion width of the n-n_plus-junction
306 V_h_mi_n_plus=0; %built-in voltage of the n-n_plus junction
307 V_h_n_plus=zeros(1,numberofdevices);
308
309
310 for i=1:numberofdevices
311  %V_h_mi_n_plus=fsolve(@(V_h_mi_n_plus) (e_charge.*V_h_mi_n_plus
     ./(k_Boltzman.*T))+log((N_D_n(i)./N_D_n_plus(i))+(0.5.*(
     e_charge.*V_h_mi_n_plus./(k_Boltzman.*T))^2)),0,optimset('
     Display','off'));
312  %V_h_n_plus(i)=V_h_mi_n_plus;
313  V_h_n_plus(i)=(k_Boltzman.*T./e_charge).*log(N_D_n_plus(i)./(
     N_D_n(i)));
314  V_h_mi_n_plus=0;
315 end
316
317 %Depletion width of the n_plus-n-junction, taken as the depletion
    width into the n-layer
318 dep_width_n_plus=zeros(1,numberofdevices);
319
320 for i=1:numberofdevices
321     dep_width_n_plus(i)=sqrt(2.*epsilon_n(i).*k_Boltzman.*T./(
        e_charge.^2.*(N_D_n(i)./cm.^3))).*atan((e_charge.*
        V_h_n_plus(i)./(k_Boltzman.*T)).*sqrt(N_D_n_plus(i)./(N_D_n
        (i).*2)));
322 end
323
324 %Width of the undepleted n-layer
325 %The depletion width into the n_plus-layer is not taken into
    consideration
326 width_n_undepleted=zeros(1,numberofdevices);
327
328 for i=1:numberofdevices
329 width_n_undepleted(i)=width_n(i)-dep_width_n_plus(i);
330 end
331
332 %Surface recombination
333 S_window=[1e4 1e4 1e4 1e4]; %surface recombination velocity top of
     window layer (m/s)
334 S_p_plus=[1e4 1e4 1e4 1e4]; %surface recombination velocity top of
     p_plus layer without window layer (m/s)
335 S_n_plus=[1e4 1e4 1e4 1e4];        %surface recombination velocity
     n-plus layer (m/s) (assumed rear surface is n-plus+substrate)
336
337 %Lifetimes
338 % tau_n_p_layer=[3e-9 3e-9 3e-9 3e-9]; %GaAs book for doping
    2*10^18 (cm^-3) in (s)
339 % tau_n_p_plus_layer=[0.5e-9 0.5e-9 0.5e-9 0.5e-9]; %GaAs book for
     doping 2*10^19(cm^-3) in (s)
340 % tau_p_n_layer=[32.5e-9 32.5e-9 32.5e-9 32.5e-9]; %GaAs book for
    doping 2*10^17 (cm^-3) in (s)
```

```
341 % tau_p_n_plus_layer=[7e-9 7e-9 7e-9 7e-9]; %GaAs book for doping
        2*10^18 (cm^-3) in (s)
342 %
343 tau_n_p_layer=[3e-9 3e-9 2.3e-9 2.3e-9]; %AlGaAs Properties of
        AlGaAs book  in (s)
344 tau_n_p_plus_layer=[0.5e-9 0.5e-9 0.4e-9 0.4e-9]; %Taken same as
        GaAs  in (s)
345 tau_p_n_layer=[32.5e-9 32.5e-9 3.1e-9 3.1e-9]; %AlGaAs Properties
        of AlGaAs book  in (s)
346 tau_p_n_plus_layer=[7e-9 7e-9 0.7e-9 0.7e-9]; %AlGaAs Properties
        of AlGaAs book  in (s)
347
348
349
350
351 %Mobilities
352
353 % mu_n_p_layer=[0.125 0.125 0.125 0.125]; %GaAs book for doping
        2*10^18 (cm^-3) in (m^2/(Vs))
354 % mu_n_p_plus_layer=[0.1400 0.1400 0.1400 0.1400]; %GaAs book for
        doping 2*10^19(cm^-3) in (m^2/(Vs))
355 % mu_p_n_layer=[0.0278 0.0278 0.0278 0.0278]; %GaAs book for
        doping 2*10^17 (cm^-3) in (m^2/(Vs))
356 % mu_p_n_plus_layer=[0.0238 0.0238 0.0238 0.0238]; %GaAs book for
        doping 2*10^18 (cm^-3) in (m^2/(Vs))
357
358
359
360
361 mu_n_p_layer=[0.125 0.125 0.100 0.100]; %GaAs book for doping
        2*10^18 (cm^-3) in (m^2/(Vs))
362 mu_n_p_plus_layer=[0.1400 0.1400 0.0830 0.0830]; %GaAs book for
        doping 2*10^19(cm^-3) in (m^2/(Vs))
363 mu_p_n_layer=[0.0278 0.0278 0.0100 0.0100]; %GaAs book for doping
        2*10^17 (cm^-3) in (m^2/(Vs))
364 mu_p_n_plus_layer=[0.0238 0.0238 0.0065 0.0065]; %GaAs book for
        doping 2*10^18 (cm^-3) in (m^2/(Vs))
365
366
367 %Diffusion lengths and diffusion coeffecients in the devices
368 diffusioncoefficient_n_p=(k_Boltzman.*T./e_charge).*mu_n_p_layer;
        %diffusion coefficient electrons in p-layer
369 diffusioncoefficient_n_p_plus=(k_Boltzman.*T./e_charge).*
        mu_n_p_plus_layer; %diffusion coefficient electrons in p_plus-
        layer
370
371 diffusioncoefficient_p_n=(k_Boltzman.*T./e_charge).*mu_p_n_layer;
        %diffusion coefficient holes in n-layer
372 diffusioncoefficient_p_n_plus=(k_Boltzman.*T./e_charge).*
        mu_p_n_plus_layer; %diffusion coefficient holes in n_plus-layer
373
374 difflength_n_p=zeros(1,numberofdevices); %diffusion length
        electrons in p-layer
```

```
375 difflength_n_p_plus=zeros(1,numberofdevices); %diffusion length
      electrons in p_plus-layer
376 difflength_p_n=zeros(1,numberofdevices); %diffusion length holes
      in n-layer
377 difflength_p_n_plus=zeros(1,numberofdevices); %diffusion length
      holes in n_plus-layer
378
379 for i=1:numberofdevices
380 difflength_n_p(i)=sqrt(tau_n_p_layer(i).*diffusioncoefficient_n_p(
      i));
381 difflength_n_p_plus(i)=sqrt(tau_n_p_plus_layer(i).*
      diffusioncoefficient_n_p_plus(i));
382 difflength_p_n(i)=sqrt(tau_p_n_layer(i).*diffusioncoefficient_p_n(
      i));
383 difflength_p_n_plus(i)=sqrt(tau_p_n_plus_layer(i).*
      diffusioncoefficient_p_n_plus(i));
384 end
385
386 difflength_n_window=difflength_n_p; %does not matter since another
       window recombination velocity is used
387 diffusioncoefficient_n_window=diffusioncoefficient_n_p; %does not
      matter since another window recombination velocity is used
388
389
390 %Effective surface recombination velocities
391 S_eff_p=zeros(1,numberofdevices); %effective surface reombination
      velocity close to p_plus-layer, on edge of undepleted p-layer (
      placed on top of intrinsic layer) (m/s)
392 S_eff_n=zeros(1,numberofdevices); %effective surface recombination
       velocity on edge of undepleted n-layer (placed under intrinsic
       layer) (m/s)
393 S_eff_window=zeros(1,numberofdevices);  %effective surface
      recombination velocity between p_plus-layer and window layer (m
      /s)
394 S_eff_p_plus_p=zeros(1,numberofdevices); %effective surface
      recombination velocity on edge of undepleted p_plus-layer (m/s)
      ,between p_plus-layer and depletion region
395 S_eff_n_plus_n=zeros(1,numberofdevices); %effective surface
      recombination velocity on edge of undepleted n-plus-layer (m/s)
      ,between n_plus-layer and depletion region
396
397
398
399 for i=1:numberofdevices
400     S_eff_n(i)=(diffusioncoefficient_p_n_plus(i)./
          difflength_p_n_plus(i)).*(N_D_n(i)./N_D_n_plus(i)).*((((
          S_n_plus(i).*difflength_p_n_plus(i)./
          diffusioncoefficient_p_n_plus(i)).*cosh(width_n_plus(i)./
          difflength_p_n_plus(i)))+sinh(width_n_plus(i)./
          difflength_p_n_plus(i)))./(((S_n_plus(i).*
          difflength_p_n_plus(i)./diffusioncoefficient_p_n_plus(i)).*
          sinh(width_n_plus(i)./difflength_p_n_plus(i)))+cosh(
          width_n_plus(i)./difflength_p_n_plus(i)))); %modification
```

```
    of eq 7.10 in Nelson
401     S_eff_p_plus_p(i)=(diffusioncoefficient_n_p(i)./difflength_n_p
        (i)).*(N_A_p_plus(i)./N_A_p(i)).*coth(width_p_undepleted(i)
        ./difflength_n_p(i)); %eq 14 in "A simple general
        analytical solution..."
402     S_eff_n_plus_n(i)=(diffusioncoefficient_p_n(i)./difflength_p_n
        (i)).*(N_D_n_plus(i)./N_D_n(i)).*coth(width_n_undepleted(i)
        ./difflength_p_n(i)); %eq 14 in "A simple general
        analytical solution..."
403
404
405     if window(i)==1
406     S_eff_window_test=(diffusioncoefficient_n_window(i)./
        difflength_n_window(i)).*exp((E_cell(i)-E_window(i))./(
        k_Boltzman.*T)).*((((S_window(i).*difflength_n_window(i)./
        diffusioncoefficient_n_window(i)).*cosh(width_window(i)./
        difflength_n_window(i)))+sinh(width_window(i)./
        difflength_n_window(i)))./(((S_window(i).*
        difflength_n_window(i)./diffusioncoefficient_n_window(i)).*
        sinh(width_window(i)./difflength_n_window(i)))+cosh(
        width_window(i)./difflength_n_window(i)))); %S_eff_window
        used for front surface velocity of the p_plus layer
407     S_eff_window(i)=1e2; %Takes value from Hovel since
        S_eff_window_test too small, see report
408     S_eff_p(i)=(diffusioncoefficient_n_p_plus(i)./
        difflength_n_p_plus(i)).*(N_A_p(i)./N_A_p_plus(i)).*(((
        S_eff_window(i).*difflength_n_p_plus(i)./
        diffusioncoefficient_n_p_plus(i)).*cosh(width_p_plus(i)./
        difflength_n_p_plus(i)))+sinh(width_p_plus(i)./
        difflength_n_p_plus(i)))./(((S_eff_window(i).*
        difflength_n_p_plus(i)./diffusioncoefficient_n_p_plus(i)).*
        sinh(width_p_plus(i)./difflength_n_p_plus(i)))+cosh(
        width_p_plus(i)./difflength_n_p_plus(i)));
409
410     else
411     S_eff_window(i)=S_p_plus(i); %S_eff_window used for front
        surface velocity of the p_plus layer
412     S_eff_p(i)=(diffusioncoefficient_n_p_plus(i)./
        difflength_n_p_plus(i)).*(N_A_p(i)./N_A_p_plus(i)).*((((
        S_p_plus(i).*difflength_n_p_plus(i)./
        diffusioncoefficient_n_p_plus(i)).*cosh(width_p_plus(i)./
        difflength_n_p_plus(i)))+sinh(width_p_plus(i)./
        difflength_n_p_plus(i)))./(((S_p_plus(i).*
        difflength_n_p_plus(i)./diffusioncoefficient_n_p_plus(i)).*
        sinh(width_p_plus(i)./difflength_n_p_plus(i)))+cosh(
        width_p_plus(i)./difflength_n_p_plus(i))));
413     end
414
415
416 end
417
418
419
```

```
420
421 save 'simple.mat'
```

Listing B.8: variablescomplete

B.9 Current-voltage characteristic complete model of intermediate band solar cell

```
1  --------------------------------
2  Current-voltage characteristic
3  complete model IB solar cell
4  --------------------------------
5
6  clear; %Clear all variables
7
8  load 'simple.mat' %Loading the file containing all constants,
      remember to first run the program Simplevariables
9
10 %Reading the necessary excel files
11
12 step_endelig=0.001; %steplength used in interpolation
13
14 %USES SHIFT OF ENERGY AXIS
15 num4=xlsread('C:\Documents␣and␣Settings\Kirsti␣Kvanes\Mine␣
      dokumenter\MATLAB\Prosjekt\GaAs␣optiske␣parametre');%Optical
      parameters for GaAs using shift of energy axis
16 %Comment: alpha values were originally given as 10^-3 multiplied
      by the
17 %values in the excel file, this was pr cm, to get correct alpha
      values pr
18 %m, multiply with 10^2*10^3
19 photonenergy_GaAsny=num4(:,1); %photonenergies for GaAs used in
      the excel files
20 alpha_GaAsny=1e5.*num4(:,4); %absorption coefficient GaAs
21 R_GaAsny=num4(:,3); %Reflectivity values for GaAs
22 n_GaAsny=num4(:,2); %Refractive index for GaAs
23
24
25 w_p=0*nm; %For p-i-n solar cell, depletion region into p-layer
      equal to zero
26 w_n=0*nm; %For p-i-n solar cell, depletion region  into n-layer
      equal to zero
27
28 %Getting values for GaAs
29 %Bruker mindre steglengder frem til 1.5 eV for der har jeg flere
      verdier
30 %HUSK at man har flere steglengder, en steglengde for energier
      mindre
31 %enn 1.5 eV, en annen for energier større enn 1.5 eV og en tredje
      brukt i
32 %interpolering
33 %må ta hensyn til at minste verdi i excel-fila er 1.36 eV, setter
34 %absorpsjonskoeffisienten lik 0 for mindre verdier
```

```
35 step_1_GaAs=0.01;%*eV; %Steplength 0.01 for energies less then 1.5
36 minimum_1_GaAs=0.32;%*eV; %minimum value in the excel files for
     solar spectrum is 0.3104
37 maximum_1_GaAs=1.5;%*eV; %maximum allowed value 1.5 for energies
     larger then 1.5 we need a greater steplength
38 energydifference_1=0.01;
39 E_1_GaAs=(minimum_1_GaAs:step_1_GaAs:maximum_1_GaAs); %energies
     with steplength 0.01
40 antall_1_GaAs=round(((maximum_1_GaAs-minimum_1_GaAs)/step_1_GaAs)
     +1); %antall E i intervallet miniumum1:maximum1 eV må ha
     heltall derfor round
41
42 step_2_GaAs=0.1; %Steplength 0.1 for energies greater then 1.5
43 minimum_2_GaAs=maximum_1_GaAs; %miniumvalue is maximum of the
     other interval
44 maximum_2_GaAs=4.43; %Maximum value in the excel files for solar
     spectrum is 4.43, maximum allowed value for the formulas used
     later is 5.6!!! Because we have not got values for the abs.
     koeff of Al_0.9Ga_0.1As for greater energies
45 energydifference_2=0.1;
46 E_2_GaAs=(minimum_2_GaAs:step_2_GaAs:maximum_2_GaAs); %energies
     with steplength 0.1
47 antall_2_GaAs=round(((maximum_2_GaAs-minimum_2_GaAs)/step_2_GaAs)
     +1); %antall E i intervallet miniumum2:maximum2 eV må ha
     heltall derfor round
48
49 alpha_GaAs_1=zeros(1,antall_1_GaAs); %absorption coefficient for
     energies with steplength 0.01
50 alpha_GaAs_2=zeros(1,antall_2_GaAs); %absorption coefficient for
     energies with steplength 0.1
51 R_GaAs_1=zeros(1,antall_1_GaAs); %reflectivity values for energies
      with steplength 0.01
52 R_GaAs_2=zeros(1,antall_2_GaAs); %reflectivity values for energies
      with steplength 0.1
53 n_GaAs_1=zeros(1,antall_1_GaAs); %refractive index
54 n_GaAs_2=zeros(1,antall_2_GaAs); %refractive index
55
56
57 k=1;
58
59  for i=1:antall_1_GaAs
60      if E_1_GaAs(i)<1.36
61          alpha_GaAs_1(i)=0; %for energies less than 1.36 eV the
              absorption coefficient is equal to zero
62          R_GaAs_1(i)=R_GaAsny(1);
63         n_GaAs_1(i)=n_GaAsny(1);
64      else
65         while ~(photonenergy_GaAsny(k)-(energydifference_1*0.5)<=
             E_1_GaAs(i)&& E_1_GaAs(i)<photonenergy_GaAsny(k)+(
             energydifference_1*0.5))
66              k=k+1;
67         end
68
```

```
69          alpha_GaAs_1(i)=alpha_GaAsny(k);
70          R_GaAs_1(i)=R_GaAsny(k);
71          n_GaAs_1(i)=n_GaAsny(k);
72       end
73   end
74
75   j=k;
76   for i=1:antall_2_GaAs
77      while ~(photonenergy_GaAsny(j)-(energydifference_2*0.5)<=
            E_2_GaAs(i)&& E_2_GaAs(i)<photonenergy_GaAsny(j)+(
            energydifference_2*0.5))
78          j=j+1;
79      end
80
81       alpha_GaAs_2(i)=alpha_GaAsny(j);
82       R_GaAs_2(i)=R_GaAsny(k);
83       n_GaAs_2(i)=n_GaAsny(k);
84   end
85
86  %Interpolation
87   pp_GaAs_1 = interp1(E_1_GaAs,alpha_GaAs_1,'cubic','pp'); %
        interpolates absorption coefficient
88   pp_GaAs_1_R = interp1(E_1_GaAs,R_GaAs_1,'cubic','pp'); %
        interpolates reflectivity values
89   pp_GaAs_1_n=interp1(E_1_GaAs,n_GaAs_1,'cubic','pp'); %
        interpolates refractive index values
90
91   zi_GaAs_1 = minimum_1_GaAs:step_endelig:maximum_1_GaAs;
92
93   yi_GaAs_1 = ppval(pp_GaAs_1,zi_GaAs_1); %interpolates absorption
        coefficient
94   yi_GaAs_1_R = ppval(pp_GaAs_1_R,zi_GaAs_1); %interpolates
        reflectivity values
95   yi_GaAs_1_n = ppval(pp_GaAs_1_n,zi_GaAs_1); %interpolates
        refractive index values
96
97   antall_endelig_1_GaAs=round(((maximum_1_GaAs-minimum_1_GaAs)/
        step_endelig)+1); %number of values for alpha for energies
        less then 1.5
98
99   pp_GaAs_2 = interp1(E_2_GaAs,alpha_GaAs_2,'cubic','pp'); %
        interpolates absorption coefficient
100  pp_GaAs_2_R = interp1(E_2_GaAs,R_GaAs_2,'cubic','pp'); %
        interpolates reflectivity values
101  pp_GaAs_2_n = interp1(E_2_GaAs,n_GaAs_2,'cubic','pp'); %
        interpolates refractive index values
102
103  zi_GaAs_2 = minimum_2_GaAs:step_endelig:maximum_2_GaAs;
104
105  yi_GaAs_2 = ppval(pp_GaAs_2,zi_GaAs_2); %interpolates absorption
        coefficient
106  yi_GaAs_2_R = ppval(pp_GaAs_2_R,zi_GaAs_2); %interpolates
        reflectivity values
```

```
107 yi_GaAs_2_n = ppval(pp_GaAs_2_n,zi_GaAs_2); %interpolates
        refractive index values
108
109 antall_endelig_2_GaAs=round(((maximum_2_GaAs-minimum_2_GaAs)/
        step_endelig)+1); %number of values for absorption
        coefficients for energies greater then 1.5
110
111 antall_endelig=antall_endelig_1_GaAs+antall_endelig_2_GaAs-1; %
        number of values in the final tables for alpha, (minus 1
        because the value for E=1.5 eV should not be counted to times)
112
113 zi_endelig=zeros(1,antall_endelig); %final energies,
114 alpha_GaAs_endelig=zeros(1,antall_endelig); %interpolated
        absorption coefficient, the values will be used later
115 R_GaAs_endelig=zeros(numberofdevices,antall_endelig); %
        interpolated reflectivity values
116 n_GaAs_endelig=zeros(1,antall_endelig); %interpolated refractive
        index values
117
118 for i=1:antall_endelig_1_GaAs
119     zi_endelig(i)=zi_GaAs_1(i);
120     for a=1:numberofdevices
121        if ARC(a)==0 %no anti-reflective coating
122        R_GaAs_endelig(a,i)=yi_GaAs_1_R(i);
123        else
124         R_GaAs_endelig(a,i)=0;
125        end
126     end
127     n_GaAs_endelig(i)=yi_GaAs_1_n(i);
128     alpha_GaAs_endelig(i)=yi_GaAs_1(i);
129 end
130
131 for i=antall_endelig_1_GaAs+1:antall_endelig;
132     zi_endelig(i)=zi_GaAs_2(i+1-antall_endelig_1_GaAs); %the
           value for E=1.5 eV should not be counted to times,
           therefore i+1
133      for a=1:numberofdevices
134        if ARC(a)==0 %no anti-reflective coating
135        R_GaAs_endelig(a,i)=yi_GaAs_2_R(i+1-antall_endelig_1_GaAs)
               ;
136        else
137         R_GaAs_endelig(a,i)=0;
138        end
139      end
140      n_GaAs_endelig(i)=yi_GaAs_2_n(i+1-antall_endelig_1_GaAs);
141      alpha_GaAs_endelig(i)=yi_GaAs_2(i+1-antall_endelig_1_GaAs);
142 end
143
144  %Getting values for AlGaAs uses energy shift from paxmann and
       connolly
145
146 E_AlGaAs=zeros(numberofdevices,antall_endelig);
147
```

```
148 alpha_AlGaAs=zeros(numberofdevices,antall_endelig);
149
150
151 alpha_AlGaAs_sameenergy=zeros(numberofdevices,antall_endelig);
152
153 for h=1:numberofdevices
154    for i=1:antall_endelig
155    alpha_AlGaAs(h,i)=alpha_GaAs_endelig(i);
156    E_AlGaAs(h,i)=zi_endelig(i)+(1.247*x_cell(h))-(0.62*x_cell(h)*
         sqrt(zi_endelig(i)-(E_GaAs./eV))*(1/(exp(-10*(zi_endelig(i)
         -(E_GaAs./eV)))+1)));
157    end
158 end
159 E_AlGaAs(2,antall_endelig)
160
161  f=[1 1 1 1 1 1 1 1 1];
162  teller=[1 1 1 1 1 1 1 1 1 1 1];
163  for h=1:numberofdevices
164    for i=1:antall_endelig
165        if x_cell(h)==0
166        else
167            if imag(E_AlGaAs(h,f(h)))~=0
168                teller(h)=teller(h)+1;
169            alpha_AlGaAs_sameenergy(h,i)=0;
170            f(h)=f(h)+1;
171            else
172
173                if (zi_endelig(i)<E_AlGaAs(h,f(h))&&imag(E_AlGaAs(
                   h,f(h)-1))~=0)
174                alpha_AlGaAs_sameenergy(h,i)=0;
175                teller(h)=teller(h)+1;
176                else
177
178                    while ~ (E_AlGaAs(h,f(h))<=zi_endelig(i) &&
                       zi_endelig(i)<E_AlGaAs(h,f(h)+1))
179                     f(h)=f(h)+1;
180                    end
181                alpha_AlGaAs_sameenergy(h,i)=alpha_AlGaAs(h,f(h));
182                end
183            end
184        end
185    end
186  end
187 teller
188 ikkeutnyttet=round((E_GaAs./eV-minimum_1_GaAs)./step_endelig)+1
189
190 for a=1:numberofdevices
191        if x_cell(a)==0
192        else
193    for i=teller(a)-ikkeutnyttet:teller(a) %Takes the values from
         GaAs for energies less than the bandgap of AlGaAs
194    alpha_AlGaAs_sameenergy(a,i)=alpha_AlGaAs(a,i+1-(teller(a)-
         ikkeutnyttet));
```

```
195      end
196          end
197  end
198
199
200 %Values for absorption coefficient for Al_0.804Ga_0.196As
201 numwindow_0804=xlsread('C:\Documents and Settings\Kirsti Kvanes\
       Mine dokumenter\MATLAB\Master\AlGaAs 0804 optiske parametre');
202 %Comment: absorption coefficients were originally given as 10^-3
       multiplied by the
203 %values in the excel file, this was pr cm, to get correct
       absorption coefficients pr
204 %m, multiply with 10^2*10^3
205 photonenergy_window=numwindow_0804(:,1); %photonenergies for Al_0
       .804Ga_0.196As used in the excel files
206 alpha_window_0804=1e5.*numwindow_0804(:,2); %absorption
       coefficient for Al_0.804Ga_0.196As
207
208
209 %Values for absorption coefficient for Al_0.900Ga_0.100As
210 numwindow_0900=xlsread('C:\Documents and Settings\Kirsti Kvanes\
       Mine dokumenter\MATLAB\Master\AlGaAs 0900 optiske parametre');
211 %Comment: absorption coefficients were originally given as 10^-3
       multiplied by the
212 %values in the excel file, this was pr cm, to get correct
       absorption coefficients pr
213 %m, multiply with 10^2*10^3
214 alpha_window_0900=1e5.*numwindow_0900(:,2); %absorption
       coefficient for Al_0.900Ga_0.100As
215
216
217 %Getting values for Al_0.804Ga0.196As
218  %The absorption coefficient is set to zero for energies less than
         1.5 eV
219  %Uses the excel file for energies greater than 1.5 eV which has
        an energy
220  %step equal to 0.1 eV. This is different than the values for GaAs
         where
221  %two different energy steps are used
222
223 step_window=0.1; %Steplength 0.1 in the excel file
224 minimum_window=minimum_1_GaAs;%*eV; %minimum value in the excel
       files for solar spectrum is 0.3104, minium value in the excel
       file for absorption coeff is 1.36!!!
225 maximum_window=maximum_2_GaAs;%*eV; %Maximum value in the excel
       files for solar spectrum is 4.45, maximum allowed value for the
        formulas used later is 5.6!!! Because we have not got values
       for the abs.koeff of Al_0.9Ga_0.1As for greater energies
226 E_window_table=(minimum_window:step_window:maximum_window);
227 antall_window=floor((maximum_window-minimum_window)./step_window
       +1); %number of E in the excel file
228
229 alpha_AlGaAs_window_temp_0804=zeros(1,antall_window);
```

```
230
231 windownumber_0804=1;
232
233  for i=1:antall_window
234      if E_window_table(i)<1.5
235           alpha_AlGaAs_window_temp_0804(i)=0; %for energies less
              than 1.5 eV the absorption coefficient is equal to
              zero
236      else
237         while ~(photonenergy_window(windownumber_0804)-(
             step_window*0.5)<=E_window_table(i)&& E_window_table(i)
             <photonenergy_window(windownumber_0804)+(step_window
             *0.5))
238              windownumber_0804=windownumber_0804+1;
239         end
240
241         alpha_AlGaAs_window_temp_0804(i)=alpha_window_0804(
             windownumber_0804);
242      end
243  end
244
245 %Interpolation
246  pp_window_0804 = interp1(E_window_table,
        alpha_AlGaAs_window_temp_0804,'cubic','pp'); %interpolates
        absorption coefficients
247  yi_window_0804 = ppval(pp_window_0804,zi_endelig); %interpolates
        absorption coefficients
248  alpha_AlGaAs_window_0804_final=zeros(antall_endelig); %
        interpolated absorption coefficients, the values will be used
        later
249  for i=1:antall_endelig
250      alpha_AlGaAs_window_0804_final(i)=yi_window_0804(i);
251  end
252
253 %Getting values for Al_0.900Ga0.100As
254  %The absorption coefficient is set to zero for energies less than
         1.5 eV
255  %Uses the excel file for energies greater than 1.5 eV which has
        an energy
256  %step equal to 0.1 eV. This is different than the values for GaAs
         where
257  %two different energy steps are used
258
259 alpha_AlGaAs_window_temp_0900=zeros(1,antall_window);
260
261 windownumber_0900=1;
262
263  for i=1:antall_window
264      if E_window_table(i)<1.5
265           alpha_AlGaAs_window_temp_0900(i)=0; %for energies less
              than 1.5 eV the absorption coefficient is equal to
              zero
266      else
```

```
267         while ~(photonenergy_window(windownumber_0900)-(
               step_window*0.5)<=E_window_table(i)&& E_window_table(i)
               <photonenergy_window(windownumber_0900)+(step_window
               *0.5))
268             windownumber_0900=windownumber_0900+1;
269         end
270         alpha_AlGaAs_window_temp_0900(i)=alpha_window_0900(
               windownumber_0900);
271     end
272 end
273
274 %Interpolation
275 pp_window_0900 = interp1(E_window_table,
       alpha_AlGaAs_window_temp_0900,'cubic','pp'); %interpolates
       absorption coefficients
276 yi_window_0900 = ppval(pp_window_0900,zi_endelig); %interpolates
       absorption coefficients
277
278 alpha_AlGaAs_window_0900_final=zeros(antall_endelig); %
       interpolated absorption coefficients, the values will be used
       later
279 for i=1:antall_endelig
280      alpha_AlGaAs_window_0900_final(i)=yi_window_0900(i);
281 end
282
283
284 %Getting values for absorption coefficient in window layer made
       of Al_0.85Ga_0.15As uses energy shift and average
285 %value of x=0.804 and x=0.90 from "Properties of AlGaAs book"
286
287 alpha_AlGaAs_window_0804_shifted=zeros(numberofdevices,
       antall_endelig);
288 alpha_AlGaAs_window_0900_shifted=zeros(numberofdevices,
       antall_endelig);
289 alpha_AlGaAs_window=zeros(numberofdevices,antall_endelig);
290
291 for a=1:numberofdevices
292         for i=1:antall_endelig
293           if (i-round(((0.005.*x_window(a))+(0.245.*x_window(a)
                 .^2)-((0.005.*0.804)+(0.245.*0.804.^2)))./
                 step_endelig)) <=0 &&(i-round(((0.005.*x_window(a))
                 +(0.245.*x_window(a).^2)-((0.005.*0.900)
                 +(0.245.*0.900.^2)))./step_endelig))>antall_endelig
294           alpha_AlGaAs_window_0804_shifted(a,i)=0;
295           alpha_AlGaAs_window_0900_shifted(a,i)=
                 alpha_AlGaAs_window_0900_final(antall_endelig);
296           elseif (i-round(((0.005.*x_window(a))+(0.245.*x_window(a
                 ).^2)-((0.005.*0.804)+(0.245.*0.804.^2)))./
                 step_endelig)) <=0
297              alpha_AlGaAs_window_0804_shifted(a,i)=0;
298              alpha_AlGaAs_window_0900_shifted(a,i)=
                    alpha_AlGaAs_window_0900_final(i-round(((0.005.*
                    x_window(a))+(0.245.*x_window(a).^2)
```

```
                    -((0.005.*0.900)+(0.245.*0.900.^2)))./step_endelig
                    ));
299             elseif (i-round(((0.005.*x_window(a))+(0.245.*x_window(a
                ).^2)-((0.005.*0.900)+(0.245.*0.900.^2)))./
                step_endelig))>antall_endelig
300                 alpha_AlGaAs_window_0900_shifted(a,i)=
                    alpha_AlGaAs_window_0900_final(antall_endelig);
301                 alpha_AlGaAs_window_0804_shifted(a,i)=
                    alpha_AlGaAs_window_0804_final(i-round(((0.005.*
                    x_window(a))+(0.245.*x_window(a).^2)
                    -((0.005.*0.804)+(0.245.*0.804.^2)))./step_endelig
                    ));
302             else
303             alpha_AlGaAs_window_0804_shifted(a,i)=
                alpha_AlGaAs_window_0804_final(i-round(((0.005.*
                x_window(a))+(0.245.*x_window(a).^2)-((0.005.*0.804)
                +(0.245.*0.804.^2)))./step_endelig));
304             alpha_AlGaAs_window_0900_shifted(a,i)=
                alpha_AlGaAs_window_0900_final(i-round(((0.005.*
                x_window(a))+(0.245.*x_window(a).^2)-((0.005.*0.900)
                +(0.245.*0.900.^2)))./step_endelig));
305             end
306         alpha_AlGaAs_window(a,i)=0.5.*(
            alpha_AlGaAs_window_0804_shifted(a,i)+
            alpha_AlGaAs_window_0900_shifted(a,i));
307         end
308  end
309
310
311
312 %MODEL
313 radiative_rec_e=zeros(numberofdevices,energyvalues);
314 radiative_rec_h=zeros(numberofdevices,energyvalues);
315 L_e=zeros(numberofdevices,energyvalues); %definition
316 L_h=zeros(numberofdevices,energyvalues); %definition
317
318 for i=1:numberofdevices
319     for c=1:energyvalues
320 radiative_rec_e(i,c)=(1./n_0(i,c)).*(radiative_rec_coeff(
    alpha_CI_temp(i),E_H(c))-radiative_rec_coeff(alpha_CI_temp(i),
    E_L(c)));    %uses the function radiative_rec_coeff which
    calculates the value of the integral (8pi/h^3c^2)int(alphaE^2
    exp(-E/kT)dE)
321 radiative_rec_h(i,c)=(1./p_0(i,c)).*(radiative_rec_coeff(
    alpha_IV_temp(i),E_G(c))-radiative_rec_coeff(alpha_IV_temp(i),
    E_H(c)));  %uses the function radiative_rec_coeff which
    calculates the value of the integral (8pi/h^3c^2)int(alphaE^2
    exp(-E/kT)dE)
322 L_e(i,c)=sqrt(diffusionconstant_e(i)./(radiative_rec_e(i,c)+(1./
    tau_SRH_CI(i))));
323 L_h(i,c)=sqrt(diffusionconstant_h(i)./(radiative_rec_h(i,c)+(1./
    tau_SRH_IV(i))));
324     end
```

```
325 end
326 
327 l_n=zeros(1,numberofdevices); %Definition
328 l_p=zeros(1,numberofdevices); %Definition
329 l_n_plus=zeros(1,numberofdevices); %Definition
330 l_p_plus=zeros(1,numberofdevices); %Definition
331 
332 for i=1:numberofdevices
333     l_n(i)=((S_eff_p(i).*difflength_n_p(i))./
        diffusioncoefficient_n_p(i));
334     l_n_plus(i)=((S_eff_window(i).*difflength_n_p_plus(i))./
        diffusioncoefficient_n_p_plus(i)); %S_eff_window is front
        surface recombination velocity of the p_plus layer with or
        without window layer
335     l_p(i)=((S_eff_n(i).*difflength_p_n(i))./
        diffusioncoefficient_p_n(i));
336     l_p_plus(i)=((S_n_plus(i).*difflength_p_n_plus(i))./
        diffusioncoefficient_p_n_plus(i)); %S_n-plus is surface
        recombination velocity of the n_plus layer
337 
338 end
339 
340 
341 alpha_CI_new=zeros(numberofdevices,antall_endelig,energyvalues);
342 alpha_IV_new=zeros(numberofdevices,antall_endelig,energyvalues);
343 alpha_CV_new=zeros(numberofdevices,antall_endelig,energyvalues);
344 
345 for c=1:energyvalues
346     for i=1:antall_endelig
347         for a=1:numberofdevices
348             if (zi_endelig(i)<(E_L(c)/eV))
349             alpha_CI_new(a,i,c)=0;
350             alpha_IV_new(a,i,c)=0;
351             alpha_CV_new(a,i,c)=0;
352 
353             elseif ((E_L(c)/eV)<=zi_endelig(i)&&zi_endelig(i)<E_H(
                c)/eV)
354             alpha_CI_new(a,i,c)=alpha_CI_temp(a);
355              alpha_IV_new(a,i,c)=0;
356             alpha_CV_new(a,i,c)=0;
357 
358             elseif ((E_H(c)/eV)<=zi_endelig(i)&&zi_endelig(i)<E_G(
                c)/eV)
359             alpha_CI_new(a,i,c)=0;
360              alpha_IV_new(a,i,c)=alpha_IV_temp(a);
361             alpha_CV_new(a,i,c)=0;
362             else
363                 alpha_CI_new(a,i,c)=0;
364                 alpha_IV_new(a,i,c)=0;
365 
366                 if x_cell(a)==0
367                 alpha_CV_new(a,i,c)=alpha_GaAs_endelig(i); %use
                    tabulated values for the absorption coefficient
```

```
                    of GaAs
368                 else
369                 alpha_CV_new(a,i,c)=alpha_AlGaAs_sameenergy(a,i);
370                 %alpha_CV_new(1,i)=alpha_CV_temp(1);
371                 %alpha_CV_new(2,i)=alpha_GaAs_endelig(i);
372                 end
373             end
374
375         end
376     end
377 end
378
379
380
381 %Voltages
382 minimum=0;
383 maximum=1.1;
384 step=0.01;
385 %step=0.1;
386
387 antall=round((maximum-minimum)/step+1);
388
389 %Voltage=zeros(antall); %voltage over cell Voltage=V_VC-J*R_s*area
390 V_VC=minimum:step:maximum; %e_charge*V_VC difference between the
       CB and VB quasi-Fermi levels
391 %Voltage=V_VC;
392 Voltage=zeros(numberofdevices,antall);
393
394 B_factor=zeros(numberofdevices,antall); %factor important in
       determining the voltage over the p-i and i-n junction
395 equationvoltage=zeros(numberofdevices,antall); %equation needed in
        finding the voltage over the p-i and i-n junction
396 V_p=zeros(numberofdevices,antall); %part of the applied voltage
       over the p-i junction
397 V_n=zeros(numberofdevices,antall);  %part of the applied voltage
       over the n-i junction
398
399 for a=1:numberofdevices
400     for i=1:antall
401 B_factor(a,i)=((N_I./cm^3)/ni_intrinsic(a)).^2.*exp(-e_charge.*
       V_VC(i)./(k_Boltzman.*T));
402 equationvoltage(a,i)=0.5.*(-B_factor(a,i)+sqrt(B_factor(a,i)
       .^2+(4.*(B_factor(a,i)+exp(-2.*e_charge.*V_bi_p_i(a)./(
       k_Boltzman.*T))))));
403
404 V_p(a,i)=-log(equationvoltage(a,i)).*k_Boltzman.*T./e_charge;
405 V_n(a,i)=V_VC(i)-V_p(a,i);
406     end
407 end
408
409
410
```

```
411 Q_electron=zeros(numberofdevices,antall_endelig,antall,
        energyvalues); %Quantum efficiency for electrons in IB material
412 Q_hole=zeros(numberofdevices,antall_endelig,antall,energyvalues);
         %Quantum efficiency for holes in IB material
413 Q_p_plus_special=zeros(numberofdevices,antall_endelig,antall,
        energyvalues); %Quantum efficiency for holes in n-plus-layer
414 Q_p_dep_special=zeros(numberofdevices,antall_endelig,antall,
        energyvalues); %Quantum efficiency for holes in depletion layer
         between n and n-plus
415 Q_p_special=zeros(numberofdevices,antall_endelig,antall,
        energyvalues); %Quantum efficiency for holes in n-layer
416 Q_dep_i_p_special=zeros(numberofdevices,antall_endelig,antall,
        energyvalues); %Quantum efficiency for electrons in depletion
        region between p layer and IB material
417 Q_dep_i_n_special=zeros(numberofdevices,antall_endelig,antall,
        energyvalues); %Quantum efficiency for holes in depletion
        region between IB material and n layer
418 Q_n_special=zeros(numberofdevices,antall_endelig,antall,
        energyvalues); %Quantum efficiency for electrons in p-layer
419 Q_n_dep_special=zeros(numberofdevices,antall_endelig,antall,
        energyvalues); %Quantum efficiency for electrons in depletion-
        layer between p and p-plus
420 Q_n_plus_special=zeros(numberofdevices,antall_endelig,antall,
        energyvalues); %Quantum efficiency for electrons in p-plus-
        layer
421
422 dep_width_n_i=zeros(numberofdevices,antall); %depletion width
        between i and n layer
423 dep_width_p_i=zeros(numberofdevices,antall); %depletion width
        between i and p layer
424
425 width_FB_IB=zeros(numberofdevices,antall); %width of IB in flat
        band
426
427 for a=1:numberofdevices
428     for i=1:antall
429         dep_width_n_i(a,i)=sqrt((V_bi_n_i(a)-(V_n(a,i))).*2.*
                epsilon_n(a).*(N_D_n(a)./cm.^3)./(e_charge.*(((N_D_n(a)
                ./cm.^3).*(N_I./cm.^3))+((N_I./cm.^3).^2))));
430         dep_width_p_i(a,i)=sqrt(2.*epsilon_p(a).*k_Boltzman.*T./(
                e_charge.^2.*(N_I./cm.^3))).*atan((e_charge.*(V_bi_p_i(
                a)-V_p(a,i))./(k_Boltzman.*T)).*sqrt(N_A_p(a)./(N_I.*2)
                ));
431
432         if (width_intrinsic(a)-dep_width_p_i(a,i)-dep_width_n_i(a,
                i))>0
433              width_FB_IB(a,i)=width_intrinsic(a)-dep_width_p_i(a,i)
                    -dep_width_n_i(a,i);
434
435        else
436            width_FB_IB(a,i)=0;
437             dep_width_n_i(a,i)=width_intrinsic(a);
438
```

```
439         end
440     end
441 end
442
443
444 for i=1:antall_endelig
445     for a=1:numberofdevices
446         for c=1:energyvalues
447             for b=1:antall
448  Q_electron(a,i,b,c)=-(1-R_GaAs_endelig(a,i)).*(exp(-
     alpha_AlGaAs_window(a,i).*width_window(a)).*exp(-alpha_CV_new(
     a,i,c).*(width_p_plus(a)+width_p(a)+dep_width_p_i(a,b))).*(
     alpha_CI_new(a,i,c).*L_e(a,c)./((alpha_CI_new(a,i,c).*L_e(a,c)
     ).^2-1)).*((((exp(-alpha_CI_new(a,i,c).*width_FB_IB(a,b)).*(
     sinh(width_FB_IB(a,b)./L_e(a,c))))-((alpha_CI_new(a,i,c).*L_e(
     a,c))))./(cosh(width_FB_IB(a,b)./L_e(a,c))))+alpha_CI_new(a,i,
     c).*L_e(a,c).*exp(-alpha_CI_new(a,i,c).*width_FB_IB(a,b))))
     -(1-R_GaAs_endelig(a,i)).*(exp(-alpha_AlGaAs_window(a,i).*
     width_window(a)).*exp(-alpha_CV_new(a,i,c).*(width_p_plus(a)+
     width_p(a)+dep_width_p_i(a,b))).*(alpha_CV_new(a,i,c).*L_e(a,c
     )./((alpha_CV_new(a,i,c).*L_e(a,c)).^2-1)).*((((exp(-
     alpha_CV_new(a,i,c).*width_FB_IB(a,b)).*(sinh(width_FB_IB(a,b)
     ./L_e(a,c))))-((alpha_CV_new(a,i,c).*L_e(a,c))))./(cosh(
     width_FB_IB(a,b)./L_e(a,c))))+alpha_CV_new(a,i,c).*L_e(a,c).*
     exp(-alpha_CV_new(a,i,c).*width_FB_IB(a,b))));
449  Q_hole(a,i,b,c)=-(1-R_GaAs_endelig(a,i)).*(exp(-
     alpha_AlGaAs_window(a,i).*width_window(a)).*exp(-alpha_CV_new(
     a,i,c).*(width_p_plus(a)+width_p(a)+dep_width_p_i(a,b))).*(
     alpha_IV_new(a,i,c).*L_h(a,c)./((alpha_IV_new(a,i,c).*L_h(a,c)
     ).^2-1)).*(((((sinh(width_FB_IB(a,b)./L_h(a,c))))-(exp(-
     alpha_IV_new(a,i,c).*width_FB_IB(a,b)).*(-(alpha_IV_new(a,i,c)
     .*L_h(a,c))))))./(cosh(width_FB_IB(a,b)./L_h(a,c))))-
     alpha_IV_new(a,i,c).*L_h(a,c))-(1-R_GaAs_endelig(a,i)).*(exp
     (-alpha_AlGaAs_window(a,i).*width_window(a)).*exp(-
     alpha_CV_new(a,i,c).*(width_p_plus(a)+width_p(a)+dep_width_p_i
     (a,b))).*(alpha_CV_new(a,i,c).*L_h(a,c)./((alpha_CV_new(a,i,c)
     .*L_h(a,c)).^2-1)).*(((((sinh(width_FB_IB(a,b)./L_h(a,c))))-(
     exp(-alpha_CV_new(a,i,c).*width_FB_IB(a,b)).*(-(alpha_CV_new(a
     ,i,c).*L_h(a,c))))))./(cosh(width_FB_IB(a,b)./L_h(a,c))))-
     alpha_CV_new(a,i,c).*L_h(a,c));
450
451  Q_n_dep_special(a,i,b,c)=(1-R_GaAs_endelig(a,i)).*exp(-((
     alpha_CV_new(a,i,c).*width_p_plus(a))+(alpha_AlGaAs_window(a,i
     ).*width_window(a)))).*(1-exp(-alpha_CV_new(a,i,c).*
     dep_width_p_plus(a)))./cosh(width_p_undepleted(a)./
     difflength_n_p(a));
452  Q_n_plus_special(a,i,b,c)=(1-R_GaAs_endelig(a,i)).*(alpha_CV_new(
     a,i,c).*difflength_n_p_plus(a)./(((alpha_CV_new(a,i,c).*
     difflength_n_p_plus(a)).^2)-1)).*exp(-(alpha_AlGaAs_window(a,i
     ).*width_window(a))).*((l_n_plus(a)+(alpha_CV_new(a,i,c).*
     difflength_n_p_plus(a))-(exp(-alpha_CV_new(a,i,c).*
     width_p_plus(a)).*((l_n_plus(a)*cosh(width_p_plus(a)./
     difflength_n_p_plus(a)))+(sinh(width_p_plus(a)./
```

```
    difflength_n_p_plus(a)))))./((l_n_plus(a).*sinh(width_p_plus(
    a)./difflength_n_p_plus(a)))+cosh(width_p_plus(a)./
    difflength_n_p_plus(a)))-(alpha_CV_new(a,i,c).*
    difflength_n_p_plus(a).*exp(-(alpha_CV_new(a,i,c).*
    width_p_plus(a))))).*((1./(1+(N_A_p_plus(a).*S_eff_p(a)./(
    N_A_p(a).*S_eff_p_plus_p(a)))))./cosh(width_p_undepleted(a)./
    difflength_n_p(a)));
453 Q_n_special(a,i,b,c)=(1-R_GaAs_endelig(a,i)).*((alpha_CV_new(a,i,
    c).*difflength_n_p(a)./(((alpha_CV_new(a,i,c).*difflength_n_p(
    a)).^2)-1)).*exp(-((alpha_AlGaAs_window(a,i).*width_window(a))
    +(alpha_CV_new(a,i,c).*(width_p_plus(a)+dep_width_p_plus(a))))
    ).*((l_n(a)+(alpha_CV_new(a,i,c).*difflength_n_p(a))-(exp(-
    alpha_CV_new(a,i,c).*width_p_undepleted(a)).*((l_n(a)*cosh(
    width_p_undepleted(a)./difflength_n_p(a)))+(sinh(
    width_p_undepleted(a)./difflength_n_p(a))))))./((l_n(a).*sinh(
    width_p_undepleted(a)./difflength_n_p(a)))+cosh(
    width_p_undepleted(a)./difflength_n_p(a)))-(alpha_CV_new(a,i,c
    ).*difflength_n_p(a).*exp(-(alpha_CV_new(a,i,c).*
    width_p_undepleted(a))))));
454
455 Q_p_special(a,i,b,c)=(1-R_GaAs_endelig(a,i)).*(alpha_CV_new(a,i,c
    ).*difflength_p_n(a)./((alpha_CV_new(a,i,c).*difflength_p_n(a)
    ).^2-1).*exp(-((alpha_CV_new(a,i,c).*(width_p_plus(a)+width_p(
    a)+width_intrinsic(a)))+(alpha_AlGaAs_window(a,i).*
    width_window(a)))).*((alpha_CV_new(a,i,c).*difflength_p_n(a))
    -(((l_p(a).*(cosh(width_n_undepleted(a)./difflength_p_n(a))-
    exp(-alpha_CV_new(a,i,c).*width_n_undepleted(a))))+sinh(
    width_n_undepleted(a)./difflength_p_n(a))+(alpha_CV_new(a,i,c)
    .*difflength_p_n(a).*exp(-alpha_CV_new(a,i,c).*
    width_n_undepleted(a))))./((l_p(a).*sinh(width_n_undepleted(a)
    ./difflength_p_n(a)))+cosh(width_n_undepleted(a)./
    difflength_p_n(a))))));
456 Q_p_dep_special(a,i,b,c)=(1-R_GaAs_endelig(a,i)).*exp(-((
    alpha_CV_new(a,i,c).*(width_p_plus(a)+width_p(a)+
    width_intrinsic(a)+width_n_undepleted(a)))+(
    alpha_AlGaAs_window(a,i).*width_window(a)))).*(1-exp(-
    alpha_CV_new(a,i,c).*dep_width_n_plus(a)))./cosh(
    width_n_undepleted(a)./difflength_p_n(a));
457 Q_p_plus_special(a,i,b,c)=(1-R_GaAs_endelig(a,i)).*alpha_CV_new(a
    ,i,c).*difflength_p_n_plus(a)./((alpha_CV_new(a,i,c).*
    difflength_p_n_plus(a)).^2-1).*exp(-((alpha_CV_new(a,i,c).*(
    width_p_plus(a)+width_p(a)+width_intrinsic(a)+width_n(a)))+(
    alpha_AlGaAs_window(a,i).*width_window(a)))).*((alpha_CV_new(a
    ,i,c).*difflength_p_n_plus(a))-(((l_p_plus(a).*(cosh(
    width_n_plus(a)./difflength_p_n_plus(a))-exp(-alpha_CV_new(a,i
    ,c).*width_n_plus(a))))+sinh(width_n_plus(a)./
    difflength_p_n_plus(a))+(alpha_CV_new(a,i,c).*
    difflength_p_n_plus(a).*exp(-alpha_CV_new(a,i,c).*width_n_plus
    (a))))./((l_p_plus(a).*sinh(width_n_plus(a)./
    difflength_p_n_plus(a)))+cosh(width_n_plus(a)./
    difflength_p_n_plus(a))))).*(1./(1+(N_D_n_plus(a).*S_eff_n(a)
    ./(N_D_n(a).*S_eff_n_plus_n(a)))))./cosh(width_n_undepleted(a)
    ./difflength_p_n(a));
```

```
458
459  if    width_FB_IB(a,b)~=0
460  Q_dep_i_p_special(a,i,b,c)=(1-R_GaAs_endelig(a,i)).*exp(-((
        alpha_AlGaAs_window(a,i).*width_window(a))+(alpha_CV_new(a,i,c
        ).*(width_p_plus(a)+width_p(a))))).*(1-exp(-alpha_CV_new(a,i,c
        ).*dep_width_p_i(a,b)));
461  Q_dep_i_n_special(a,i,b,c)=(1-R_GaAs_endelig(a,i)).*exp(-
        alpha_AlGaAs_window(a,i).*width_window(a)).*exp(-alpha_CV_new(
        a,i,c).*(width_p_plus(a)+width_p(a)+dep_width_p_i(a,b)+
        width_FB_IB(a,b))).*(1-exp(-alpha_CV_new(a,i,c).*dep_width_n_i
        (a,b)));
462  end
463
464  if width_FB_IB(a,b)==0
465  Q_dep_i_p_special(a,i,b,c)=(1-R_GaAs_endelig(a,i)).*exp(-((
        alpha_AlGaAs_window(a,i).*width_window(a))+(alpha_CV_new(a,i,c
        ).*(width_p_plus(a)+width_p(a))))).*(1-exp(-alpha_CV_new(a,i,c
        ).*width_intrinsic(a)));
466  Q_dep_i_n_special(a,i,b,c)=0;
467  end
468              end
469          end
470      end
471 end
472
473
474
475 %Strøm her tatt som negativ
476 photo_electron_current_IB=zeros(numberofdevices,antall,
       energyvalues); %photogenerated electron current at end of flat
       band (beginning of n-layer)
477 photo_hole_current_IB=zeros(numberofdevices,antall,energyvalues);
           %photogenerated hole current at beginning of flat band (end
        of p-layer)
478 photo_electron_current=zeros(numberofdevices,antall,energyvalues);
           %photogenerated electron current into p-layer
479 photo_hole_current=zeros(numberofdevices,antall,energyvalues);
              %photogenerated hole current into n-layer
480 photo_current_0=zeros(numberofdevices,antall,energyvalues);
                 %total photogenerated current at beginning of flat
       band
481 photo_current_W=zeros(numberofdevices,antall,energyvalues);
                 %total photogenerated current at end of flat band
482
483 wavelength=1e+9.*(h_planck*c_light)./(zi_endelig.*eV); %Wavelength
        in (nm)
484
485 %Reading the necessary excel files
486
487 num = xlsread('C:\Documents and Settings\Kirsti Kvanes\Mine 
       dokumenter\MATLAB\Prosjekt\Sp'); %Solar spectrum. Column 1 is
       wavelengths, column 2 is AM 1.5 given in W/(nm*m2), column 3 is
        incoming radiation in an energy intervall
```

```
488 %Column 4 is photonenergies, column 5 is photonflux in an
    energyinterval
489 wavelengthAM=num(:,1); %Wavelengths from excel
490 flux=num(:,5); %Incoming energy flux from excel
491
492 startexcel=1;
493
494 for a=1:numberofdevices
495     for c=1:energyvalues
496         for b=1:antall
497              for i=antall_endelig:-1:1
498
499     if wavelengthAM(startexcel)<400
500         if abs((wavelengthAM(startexcel)-wavelength(i)))<0.25
501
502         else
503            photo_electron_current_IB(a,b,c)=(
               photo_electron_current_IB(a,b,c))+(-1).*
               concentration(a).*flux(startexcel).*e_charge.*(1./
               cosh(width_FB_IB(a,b)./L_e(a,c))).*(Q_electron(a,i,b
               ,c)+Q_n_special(a,i,b,c)+Q_n_plus_special(a,i,b,c)+
               Q_n_dep_special(a,i,b,c)+Q_dep_i_p_special(a,i,b,c))
               ; %Photogenerated electron current at end of flat
               band
504            photo_hole_current_IB(a,b,c)=(photo_hole_current_IB(a,b
               ,c))+(-1).*concentration(a).*flux(startexcel).*
               e_charge.*(1./cosh(width_FB_IB(a,b)./L_h(a,c))).*(
               Q_hole(a,i,b,c)+Q_p_special(a,i,b,c)+
               Q_p_plus_special(a,i,b,c)+Q_p_dep_special(a,i,b,c)+
               Q_dep_i_n_special(a,i,b,c)); %Photogenerated hole
               current at beginning of flat band
505            photo_electron_current(a,b,c)=photo_electron_current(a,
               b,c)+(-1).*concentration(a).*flux(startexcel).*
               e_charge.*(Q_n_special(a,i,b,c)+Q_n_plus_special(a,i
               ,b,c)+Q_n_dep_special(a,i,b,c)+Q_dep_i_p_special(a,i
               ,b,c));
506            photo_hole_current(a,b,c)=photo_hole_current(a,b,c)
               +(-1).*concentration(a).*flux(startexcel).*e_charge
               .*(Q_p_special(a,i,b,c)+Q_p_plus_special(a,i,b,c)+
               Q_p_dep_special(a,i,b,c)+Q_dep_i_n_special(a,i,b,c))
               ;
507             startexcel=startexcel+1;
508         end
509
510     elseif wavelengthAM(startexcel)>=400&&wavelengthAM(startexcel)
        <1700
511         if abs((wavelengthAM(startexcel)-wavelength(i)))<0.5
512
513         else
514            photo_electron_current_IB(a,b,c)=(
               photo_electron_current_IB(a,b,c))+(-1).*
               concentration(a).*flux(startexcel).*e_charge.*(1./
               cosh(width_FB_IB(a,b)./L_e(a,c))).*(Q_electron(a,i,b
```

```
                ,c)+Q_n_special(a,i,b,c)+Q_n_plus_special(a,i,b,c)+
                Q_n_dep_special(a,i,b,c)+Q_dep_i_p_special(a,i,b,c))
                ; %Photogenerated electron current at end of flat
                band
515             photo_hole_current_IB(a,b,c)=(photo_hole_current_IB(a,b
                ,c))+(-1).*concentration(a).*flux(startexcel).*
                e_charge.*(1./cosh(width_FB_IB(a,b)./L_h(a,c))).*(
                Q_hole(a,i,b,c)+Q_p_special(a,i,b,c)+
                Q_p_plus_special(a,i,b,c)+Q_p_dep_special(a,i,b,c)+
                Q_dep_i_n_special(a,i,b,c)); %Photogenerated hole
                current at beginning of flat band
516             photo_electron_current(a,b,c)=photo_electron_current(a,
                b,c)+(-1).*concentration(a).*flux(startexcel).*
                e_charge.*(Q_n_special(a,i,b,c)+Q_n_plus_special(a,i
                ,b,c)+Q_n_dep_special(a,i,b,c)+Q_dep_i_p_special(a,i
                ,b,c));
517             photo_hole_current(a,b,c)=photo_hole_current(a,b,c)
                +(-1).*concentration(a).*flux(startexcel).*e_charge
                .*(Q_p_special(a,i,b,c)+Q_p_plus_special(a,i,b,c)+
                Q_p_dep_special(a,i,b,c)+Q_dep_i_n_special(a,i,b,c))
                ;
518
519              startexcel=startexcel+1;
520         end
521
522     elseif wavelengthAM(startexcel)>=1700
523         if abs((wavelengthAM(startexcel)-wavelength(i)))<2.5
524
525         else
526             photo_electron_current_IB(a,b,c)=(
                photo_electron_current_IB(a,b,c))+(-1).*
                concentration(a).*flux(startexcel).*e_charge.*(1./
                cosh(width_FB_IB(a,b)./L_e(a,c))).*(Q_electron(a,i,b
                ,c)+Q_n_special(a,i,b,c)+Q_n_plus_special(a,i,b,c)+
                Q_n_dep_special(a,i,b,c)+Q_dep_i_p_special(a,i,b,c))
                ; %Photogenerated electron current at end of flat
                band
527             photo_hole_current_IB(a,b,c)=(photo_hole_current_IB(a,b
                ,c))+(-1).*concentration(a).*flux(startexcel).*
                e_charge.*(1./cosh(width_FB_IB(a,b)./L_h(a,c))).*(
                Q_hole(a,i,b,c)+Q_p_special(a,i,b,c)+
                Q_p_plus_special(a,i,b,c)+Q_p_dep_special(a,i,b,c)+
                Q_dep_i_n_special(a,i,b,c)); %Photogenerated hole
                current at beginning of flat band
528             photo_electron_current(a,b,c)=photo_electron_current(a,
                b,c)+(-1).*concentration(a).*flux(startexcel).*
                e_charge.*(Q_n_special(a,i,b,c)+Q_n_plus_special(a,i
                ,b,c)+Q_n_dep_special(a,i,b,c)+Q_dep_i_p_special(a,i
                ,b,c));
529             photo_hole_current(a,b,c)=photo_hole_current(a,b,c)
                +(-1).*concentration(a).*flux(startexcel).*e_charge
                .*(Q_p_special(a,i,b,c)+Q_p_plus_special(a,i,b,c)+
                Q_p_dep_special(a,i,b,c)+Q_dep_i_n_special(a,i,b,c))
```

```
                ;
530
531
532             startexcel=startexcel+1;
533         end
534
535     end
536             end
537         startexcel=1;
538         photo_current_0(a,b,c)=photo_electron_current(a,b,c)+
                photo_hole_current_IB(a,b,c);
539         photo_current_W(a,b,c)=photo_hole_current(a,b,c)+
                photo_electron_current_IB(a,b,c);
540         end
541     end
542 end
543
544
545 J_0_diode_1=zeros(1,numberofdevices);
546 J_0_diode_1_p_layer=zeros(1,numberofdevices);
547 J_0_diode_1_n_layer=zeros(1,numberofdevices);
548 J_0_diode_2_SCR=zeros(1,numberofdevices);
549
550
551 for a=1:numberofdevices
552     J_0_diode_1_p_layer(a)=e_charge.*(ni_GaAs.^2./(N_A_p(a)./cm
            .^3)).*(diffusioncoefficient_n_p(a)./difflength_n_p(a)).*((
            l_n(a)*cosh(width_p_undepleted(a)./difflength_n_p(a)))+(
            sinh(width_p_undepleted(a)./difflength_n_p(a))))./((l_n(a)
            .*sinh(width_p_undepleted(a)./difflength_n_p(a)))+cosh(
            width_p_undepleted(a)./difflength_n_p(a)));
553     J_0_diode_1_n_layer(a)=e_charge.*(ni_GaAs.^2./(N_D_n(a)./cm
            .^3)).*(diffusioncoefficient_p_n(a)./difflength_p_n(a)).*((
            l_p(a)*cosh(width_n_undepleted(a)./difflength_p_n(a)))+(
            sinh(width_n_undepleted(a)./difflength_p_n(a))))./((l_p(a)
            .*sinh(width_n_undepleted(a)./difflength_p_n(a)))+cosh(
            width_n_undepleted(a)./difflength_p_n(a)));
554     J_0_diode_1(a)=J_0_diode_1_p_layer(a)+J_0_diode_1_n_layer(a);
555     J_0_diode_2_SCR(a)=e_charge.*ni_intrinsic(a).*width_intrinsic(
            a)./(sqrt(tau_n_GaAs.*tau_p_GaAs)).*pi; %maximum
            recombination current, using equation (54) in Hovel with
            GaAs in intrinsic region
556 end
557
558
559
560 V_VI=zeros(numberofdevices,antall,energyvalues); %e_charge*V_VI
        difference between the IB and VB quasi-Fermi levels
561
562 V_IC=zeros(numberofdevices,antall,energyvalues); %e_charge*V_IC
        difference between the CV and IB quasi-Fermi levels
563
564 V_VI_mi=0;
```

```
565
566
567
568 %Need to find the value of the voltages, uses that
569 %V_VC=V_IC+V_VI %and that the currents from both of the terminals
        have to
570 %be equal
571 for a=1:numberofdevices
572     for c=1:energyvalues
573         for i=1:antall
574
575    if   width_FB_IB(a,i)~=0
576      V_VI_mi=fsolve(@(V_VI_mi) photo_current_0(a,i,c)+(
            J_0_diode_1_p_layer(a).*(exp(e_charge.*V_VC(i)./(
            k_Boltzman.*T))-1))+((ni_cell(a).* dep_width_p_i(a,i)./
            sqrt(tau_p_GaAs.*tau_n_GaAs)).*pi.*sinh(e_charge.*V_p(a,i)
            ./(2.*k_Boltzman.*T))./((V_bi_p_i(a)-(V_p(a,i)))./(
            k_Boltzman.*T)))+(((1./cosh(width_FB_IB(a,i)./L_h(a,c))).*
            J_0_diode_1_n_layer(a)).*(exp(e_charge.*V_VC(i)./(
            k_Boltzman.*T))-1))+((1./cosh(width_FB_IB(a,i)./L_h(a,c)))
            .*((ni_cell(a).*dep_width_n_i(a,i)./sqrt(tau_p_GaAs.*
            tau_n_GaAs)).*pi.*sinh(e_charge.*V_n(a,i)./(2.*k_Boltzman
            .*T))./((V_bi_n_i(a)-(V_n(a,i)))./(k_Boltzman.*T))))+((
            e_charge.*diffusionconstant_h(a).*p_0(a).*(exp(e_charge.*
            V_VI_mi./(k_Boltzman.*T))-1)./L_h(a,c)).*(sinh(width_FB_IB
            (a,i)./L_h(a,c)))./(cosh(width_FB_IB(a,i)./L_h(a,c))))-(
            photo_current_W(a,i,c)+(J_0_diode_1_n_layer(a).*(exp(
            e_charge.*V_VC(i)./(k_Boltzman.*T))-1))+((ni_cell(a).*
            dep_width_n_i(a,i)./sqrt(tau_p_GaAs.*tau_n_GaAs)).*pi.*
            sinh(e_charge.*V_n(a,i)./(2.*k_Boltzman.*T))./((V_bi_n_i(a
            )-(V_n(a,i)))./(k_Boltzman.*T)))+(((1./cosh(width_FB_IB(a,
            i)./L_e(a,c))).*J_0_diode_1_p_layer(a)).*(exp(e_charge.*
            V_VC(i)./(k_Boltzman.*T))-1))+((1./cosh(width_FB_IB(a,i)./
            L_e(a,c))).*((ni_cell(a).*dep_width_p_i(a,i)./sqrt(
            tau_p_GaAs.*tau_n_GaAs)).*pi.*sinh(e_charge.*V_p(a,i)
            ./(2.*k_Boltzman.*T))./((V_bi_p_i(a)-(V_p(a,i)))./(
            k_Boltzman.*T))))+((e_charge.*diffusionconstant_e(a).*n_0(
            a).*(exp(e_charge.*(V_VC(i)-V_VI_mi)./(k_Boltzman.*T))-1)
            ./L_e(a,c)).*(sinh(width_FB_IB(a,i)./L_e(a,c)))./(cosh(
            width_FB_IB(a,i)./L_e(a,c))))),0,optimset('Display','off')
            );
577    end
578
579    if width_FB_IB(a,i)==0
580         V_VI_mi=0;
581    end
582
583     V_VI(a,i,c)=V_VI_mi;
584         end
585     end
586 end
587
588 for i=1:antall
```

```
589     for c=1:energyvalues
590         for a=1:numberofdevices
591         V_IC(a,i,c)=V_VC(i)-V_VI(a,i,c);
592         end
593     end
594 end
595
596
597 total_current_1=zeros(numberofdevices,antall,energyvalues);
598 total_current_2=zeros(numberofdevices,antall,energyvalues);
599 total_current_0=zeros(numberofdevices,antall,energyvalues);
600 total_current_W=zeros(numberofdevices,antall,energyvalues);
601 J=zeros(numberofdevices,antall,energyvalues);
602 J_CV=zeros(numberofdevices,antall);
603 V_OC=zeros(numberofdevices,energyvalues);
604 J_SC=zeros(numberofdevices,energyvalues);
605
606 for a=1:numberofdevices
607     for c=1:energyvalues
608         for i=1:antall
609  if   width_FB_IB(a,i)~=0
610
611      total_current_0(a,i,c)=(1/concentration(a)).*(photo_current_0
            (a,i,c)+(J_0_diode_1_p_layer(a).*(exp(e_charge.*V_VC(i)./(
            k_Boltzman.*T))-1))+((ni_cell(a).* dep_width_p_i(a,i)./
            sqrt(tau_p_GaAs.*tau_n_GaAs)).*pi.*sinh(e_charge.*V_p(a,i)
            ./(2.*k_Boltzman.*T))./((V_bi_p_i(a)-(V_p(a,i)))./(
            k_Boltzman.*T)))+(((1./cosh(width_FB_IB(a,i)./L_h(a,c))).*
            J_0_diode_1_n_layer(a)).*(exp(e_charge.*V_VC(i)./(
            k_Boltzman.*T))-1))+((1./cosh(width_FB_IB(a,i)./L_h(a,c)))
            .*((ni_cell(a).*dep_width_n_i(a,i)./sqrt(tau_p_GaAs.*
            tau_n_GaAs)).*pi.*sinh(e_charge.*V_n(a,i)./(2.*k_Boltzman
            .*T))./((V_bi_n_i(a)-(V_n(a,i)))./(k_Boltzman.*T))))+((
            e_charge.*diffusionconstant_h(a).*p_0(a).*(exp(e_charge.*
            V_VI(a,i,c)./(k_Boltzman.*T))-1)./L_h(a,c)).*(sinh(
            width_FB_IB(a,i)./L_h(a,c)))./(cosh(width_FB_IB(a,i)./L_h(
            a,c)))));
612      total_current_W(a,i,c)=(1/concentration(a)).*(photo_current_W
            (a,i,c)+(J_0_diode_1_n_layer(a).*(exp(e_charge.*V_VC(i)./(
            k_Boltzman.*T))-1))+((ni_cell(a).* dep_width_n_i(a,i)./
            sqrt(tau_p_GaAs.*tau_n_GaAs)).*pi.*sinh(e_charge.*V_n(a,i)
            ./(2.*k_Boltzman.*T))./((V_bi_n_i(a)-(V_n(a,i)))./(
            k_Boltzman.*T)))+(((1./cosh(width_FB_IB(a,i)./L_e(a,c))).*
            J_0_diode_1_p_layer(a)).*(exp(e_charge.*V_VC(i)./(
            k_Boltzman.*T))-1))+((1./cosh(width_FB_IB(a,i)./L_e(a,c)))
            .*((ni_cell(a).*dep_width_p_i(a,i)./sqrt(tau_p_GaAs.*
            tau_n_GaAs)).*pi.*sinh(e_charge.*V_p(a,i)./(2.*k_Boltzman
            .*T))./((V_bi_p_i(a)-(V_p(a,i)))./(k_Boltzman.*T))))+((
            e_charge.*diffusionconstant_e(a).*n_0(a).*(exp(e_charge.*(
            V_VC(i)-V_VI(a,i,c))./(k_Boltzman.*T))-1)./L_e(a,c)).*(
            sinh(width_FB_IB(a,i)./L_e(a,c)))./(cosh(width_FB_IB(a,i)
            ./L_e(a,c)))));
613
```

```
614     J(a,i,c)=-total_current_W(a,i,c);
615
616  end
617  if width_FB_IB(a,i)==0
618
619     J_CV(a,i)=J_0_diode_1(a).*(exp((e_charge.*V_VC(i))./(
        k_Boltzman.*T))-1)+(J_0_diode_2_SCR(a).*sinh(e_charge.*V_VC
        (i)./(2.*k_Boltzman.*T))./(e_charge.*(V_bi(a)-V_VC(i))./(
        k_Boltzman.*T))); %recombination current
620     J(a,i,c)=(1/concentration(a)).*(-photo_current_W(a,i,c)-J_CV(a
        ,i)); %current-voltage characteristic from equivalent
        circuit
621
622  end
623     Voltage(a,i)=V_VC(i)-(J(a,i,c).*R_s(a).*area(a).*area(a));
624
625             if(abs(J(a,i,c))<=150)
626                 V_OC(a,c)=V_VC(i); %open-circuit voltage
627             end
628
629         end
630     end
631 end
632
633  for i=1:numberofdevices
634      for c=1:energyvalues
635      J_SC(i,c)=J(i,1,c);
636      end
637  end
638 %Efficiency of cells
639 efficiency=zeros(numberofdevices,antall,energyvalues);
640 P_in=1e+3; %Power incident for AM 1.5
641
642 for a=1:numberofdevices
643     for c=1:energyvalues
644         for i=1:antall
645             if J(a,i,c)>0
646                 efficiency(a,i,c) = abs(V_VC(i)*J(a,i,c)*100)/P_in
                    ;
647             else
648                 efficiency(a,i,c)=0;
649             end
650         end
651     end
652 end
653
654
655 efficiencymax=zeros(numberofdevices,energyvalues);
656 for i=1:numberofdevices
657     for c=1:energyvalues
658 efficiencymax(i,c)=max(efficiency(i,:,c));
659     end
660 end
```

```
661
662
663
664
665 energy_max=zeros(1,numberofdevices);
666 finalmaximumefficiency=zeros(numberofdevices);
667 loc=zeros(1,numberofdevices);
668
669 for i=1:numberofdevices
670     [finalmaximumefficiency(i),loc(i)]=max(efficiencymax(i,:))
671     energy_max(i)=E_H(loc(i))./eV;
672 end
673
674 width_intrinsic
675 J_withoutFB=IVflatband(minimum,maximum,step,width_intrinsic);
676 %
677 % sample A1681
678 figure(1)
679 %plot(V_VC,J_withoutFB(1,:),'b-','LineWidth',1.3);
680 plot(Voltage,J(1,:,loc(1)),'b-','LineWidth',1.3);
681 axis([minimum maximum 0 300])
682 hold on
683 plot(Voltage,J(2,:,loc(2)),'r:','LineWidth',1.3);
684 %plot(V_VC,J_withoutFB(3,:),'r-','LineWidth',1.3);
685 xlabel('Voltage␣(V)')
686 ylabel('Current␣density␣divided␣by␣concentration␣(A/m^2)')
687 legend('Radiative␣rec.','Radiative␣and␣non-radiative␣rec.','
      Location','SouthWest');
688 text(0.01,285,'Complete␣model,␣sample␣A1681','HorizontalAlignment'
      ,'left')
689 legend BOXOFF
690  hold off
691     exportfig(1, 'completespania', 'Color','rgb')
692     system('epstopdf␣completespania.eps')
693 %
694
695 V_OC(1,loc(1))
696 V_OC(2,loc(2))
697 V_OC(3,loc(3))
698 V_OC(4,loc(4))
699
700 %
701 J_SC(1,loc(1))
702 J_SC(2,loc(2))
703 J_SC(3,loc(3))
704 J_SC(4,loc(4))
```

Listing B.9: currentvoltage2